Dissertations   UMSL Graduate Works

5-3-2013

Microglial Activation by Amyloid-Beta

Geeta Subhash Paranjape

University of Missouri-St. Louis, geetaparanjape@umsl.edu

Follow this and additional works at: https://irl.umsl.edu/dissertation

Part of the Chemistry Commons

MICROGLIAL ACTIVATION BY AMYLOID-β

By

Geeta S. Paranjape

M.S., Chemistry, University of Missouri-St Louis, 2008
M.S., Biotechnology, University of Mumbai-India, 2005
B.S., Biochemistry, Ramnarain Ruia College-India, 2003

A Dissertation

Submitted to the Graduate School of the

UNIVERSITY OF MISSOURI-ST. LOUIS

In Partial fulfillment of the Requirements for the Degree

Doctor of Philosophy

in

CHEMISTRY

With an emphasis in Biochemistry

May 2012

Advisory Committee
Michael R. Nichols, PhD
Chairperson
Wesley R. Harris, PhD
Cynthia M. Dupureur, PhD
Chung F. Wong, PhD

For my family

ACKNOWLEDGEMENTS

First and foremost, I would like to thank my advisor Dr. Michael R. Nichols for giving me an opportunity to work in his laboratory. I am grateful for all his guidance and support particularly during the challenging phases of my PhD. I learnt a lot about Science and Research from him. I would also like to thank the members of my Dissertation committee Dr. Wesley Harris, Dr. Cynthia M. Dupureur and Dr Wong for their valuable suggestions.

My dissertation would not be complete without thanking my awesome colleagues. I thank Drs. Deepa Ajit, Nikkilina Crouse, and Maria L.D. Udan for training me well during my initial years in the lab. I truly enjoyed working with Shana Terrill, Kelley Coalier and Lisa Gouwens. I am sincerely thankful to them for the excellent team-work, all the stimulating discussions and good times. I am grateful to you ladies for always being there for me. I extend my thanks to all the previous and present members of Nicholslab for their help and support. I would also like to thank David C. Osborn for his help with electron microscopy studies.

I would like to extend my thanks to Drs. Charulata Prasannan and Supratik Datta for all the brainstorming discussions and valuable suggestions. My sincere gratitude goes to Drs. Charulata Prasannan and Rashmi Sharma for their unconditional love and warm friendship during some of the most challenging times of my PhD life. I thank my

iii

TABLE OF CONTENTS

LIST OF TABLES

LIST OF FIGURES

LIST OF ABBREVIATIONS

Aβ   Amyloid beta

AD   Alzheimer's Disease

ADDL   Aβ-derived diffusible ligands

AFM   Atomic force microscopy

APP   Amyloid precursor protein

BACE1   Beta-site APP-cleaving enzyme

CD   Cluster of differentiation

CNS   Central nervous system

CSF   Cerebrospinal fluid

DMSO   Dimethyl sulfoxide

DS   Down's syndrome

DLS   Dynamic light scattering

ELISA   Enzyme-linked immunosorbent assay

EM   Electron microscopy

FAD   Familial Alzheimer's disease

FBS   Fetal bovine serum

FTIR   Fourier transform infrared spectroscopy

GM-CSF   Granulocyte macrophage-colony stimulating factor

HFIP   Hexafluoroisopropanol

IgG   Immunoglobulin G

iNOS   Inducible nitric oxide synthase

IL	Interleukin
LMW	Low molecular weight
LPS	Lipopolysaccharide
LTP	Long Term Potentiation
MAC	Membrane Attack Complex
MS	Mass spectrometry
NFT	Neurofibrillary tangles
NMR	Nuclear magnetic resonance
NO	Nitric oxide
NSAID	Non-steroidal anti-inflammatory drug
PAMP	Pathogen-associated molecular pattern
PBS	Phosphate buffered saline
PBS/T	Phosphate buffered saline in Tween
PMS	Phenazine methosulfate
PMX-B	Polymyxin-B sulfate
PRR	Pattern recognition receptor
PS1	Presennilin 1
PS2	Presennilin 2
QLS	Quasielastic light scattering spectroscopy
RAGE	Receptor for advanced glycation end products
R_H	Hydrodynamic radius
ROS	Reactive oxygen species
sAPPα	soluble APP cleaved by α secretase

sAPPβ	soluble APP cleaved by β secretase
SD	Standard deviation
SDS	Sodium dodecyl sulfate
SE	Standard error
SEC	Size exclusion chromatography
SPR	Surface plasmon responance
SR	Scavenger receptors
TEM	Transmission electron microscopy
Tg	Transgenic
ThT	Thioflavin-T
TLR	Toll-like receptor
TNFα	Tumor necrosis factor alpha
WT	Wildtype
XTT	2,3-bis(2-methoxy-4-nitro-5-sulfophenyl)-2H-tetrazolium-5-carboxanilide

ABSTRACT

Paranjape, Geeta S.,Ph.D.,University of Missouri-Saint Louis, May 2012. Aβ(1-42) Protofibrils But Not Fibrils Activate Microglia. Major Professor: Michael R. Nichols.

One of the hallmark features of the Alzheimer's disease (AD) brain is the extracellular deposition of amyloid-β protein (Aβ) in both fibrillar (senile plaques) and diffuse forms. Significant proinflammatory markers including activated microglia and cytokines have been detected surrounding the plaques but are absent in diffuse areas suggesting that microglial activation is sensitive to Aβ structure. Since Aβ displays structural polymorphism *in vitro*, we sought to determine the relationship between Aβ aggregation state and microglial proinflammatory response. Size exclusion chromatography (SEC) purification of freshly reconstituted Aβ(1-42) in NaOH/F12 cell culture medium isolated classical 100 nm long curvilinear protofibrils which stimulated a robust production of microglial TNFα. The Aβ(1-42) protofibrils produced a concentration-dependent response in the low micromolar range. In contrast to Aβ(1-42), Aβ(1-40) required a pre-incubation of 24h at 25°C in order to produce protofibrils. Although both preparations were similar in morphology, Aβ(1-42) protofibrils were a much better stimulator of microglia than Aβ(1-40) protofibrils. Aβ(1-40) containing the Arctic mutation (E22G) formed protofibrils as soon as 3h after reconstitution , yet they were largely ineffective in

stimulating microglia. None of the Aβ protofibril preparations were toxic to microglia suggesting that Aβ(1-42) protofibrils activate microglia in a manner independent of toxicity. As expected, freshly-purified Aβ(1-42) or Aβ(1-40) monomer were not effective in stimulating microglia, but surprisingly, neither were Aβ(1-42) fibrils even though they exhibited extensive Thioflavin-T fluorescence compared to protofibrils. These findings suggest that Aβ(1-42) protofibrils are the most effective inducers of a proinflammatory response in mouse microglia.

Isolated Amyloid-β(1−42) Protofibrils, But Not Isolated Fibrils, Are Robust Stimulators of Microglia

Geeta S. Paranjape, Lisa K. Gouwens, David C. Osborn, and Michael R. Nichols*

Department of Chemistry and Biochemistry and Center for Nanoscience, University of Missouri—St. Louis, St. Louis, Missouri 63121, United States

ABSTRACT: Senile plaques composed of amyloid-β protein (Aβ) are an unshakable feature of the Alzheimer's disease (AD) brain. Although there is significant debate on the role of the plaques in AD progression, there is little disagreement on their role in stimulating a robust inflammatory response within the context of the disease. Significant inflammatory markers such as activated microglia and cytokines are observed almost exclusively surrounding the plaques. However, recent evidence suggests that the plaque exterior may contain a measurable level of soluble Aβ aggregates. The observations that microglia activation in vivo is selectively stimulated by distinct Aβ deposits led us to examine what specific form of Aβ is the most effective proinflammatory mediator in vitro. We report here that soluble prefibrillar species of Aβ(1−42) were better than fibrils at inducing microglial tumor necrosis factor α (TNFα) production in either BV-2 and primary murine microglia. Reconstitution of Aβ(1−42) in NaOH followed by dilution into F-12 media and isolation with size exclusion chromatography (SEC) revealed classic curvilinear β-sheet protofibrils 100 nm in length. The protofibrils, but not monomers, markedly activated BV-2 microglia. Comparisons were also made between freshly isolated protofibrils and Aβ(1−42) fibrils prepared from SEC-purified monomer. Surprisingly, while isolated fibrils had a much higher level of thioflavin T fluorescence per mole, they were not effective at stimulating either primary or BV-2 murine microglia compared to protofibrils. Furthermore, SEC-isolated Aβ(1−40) protofibrils exhibited significantly less activity than concentration-matched Aβ(1−42). This report is the first to demonstrate microglial activation by SEC-purified protofibrils, and the overall findings indicate that small, soluble Aβ(1−42) protofibrils induce much greater microglial activation than mature insoluble fibrils.

KEYWORDS: Alzheimer's disease, inflammation, amyloid-beta protein, tumor necrosis factor alpha, protofibrils, fibrils
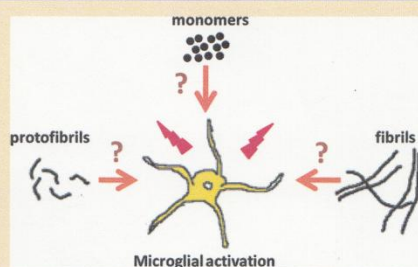
Alzheimer's disease (AD) is a complex neurodegenerative disease characterized by the accumulation of protein deposits in the affected brain and progressive dementia. The two classic forms of deposits are neurofibrillary tangles composed of tau protein and dense core neuritic plaques composed of amyloid-β protein (Aβ).[1] Both lesions are believed to contribute to disease onset and progression although the initial event appears to be Aβ accumulation.[2] Aβ is commonly produced as an unstructured 40- or 42-residue peptide fragment by proteolytic cleavage of the amyloid-β precursor protein.[3] The monomeric form of Aβ circulates ubiquitously in plasma and cerebrospinal fluid yet an aggregated fibrillar form comprises the characteristic Aβ plaques.[1] The mechanistic complexity of AD is increased by the growing number of reports demonstrating a variety of Aβ structures morphologically distinct from plaques that possess greater solubility and neuronal toxicity.[4]

It has been well documented that inflammatory markers such as activated microglia[5,6] stained with proinflammatory cytokines[7] have been observed surrounding the neuritic Aβ plaques in the human AD brain. In fact, studies in an AD transgenic mouse model have shown rapid microglial accumulation around newly formed plaques.[6] A chronic inflammatory state induced by accumulated Aβ has been suggested as one of the underlying mechanisms of progressive neurodegeneration in AD[8] and may in fact exacerbate Aβ deposition.[9] Multiple studies suggest that small Aβ(1−42) oligomers may cause early and significant alterations in synaptic function and then as fibrillar structures are produced, concomitant inflammatory responses appear (reviewed in ref 4).

In vitro Aβ aggregation studies have contributed significantly to the understanding of fibrillogenesis mechanisms and the structural properties of monomers, soluble intermediates, and mature fibrils. These studies have identified a continuum of Aβ species in the assembly process which vary in their size, length, solubility, and morphology.[10−14] In solution, Aβ monomers will undergo noncovalent self-assembly[15] to form soluble oligomers,[16] protofibrils[12] that are enriched in β-sheet structure,[13] and insoluble fibrils.[17] The types of intermediates formed during fibrillogenesis are dependent on the solution conditions.[12,16]
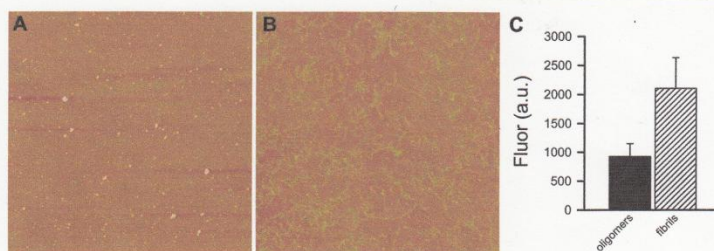
Figure 1. Aβ(1−42) structures formed in oligomer- or fibril-forming conditions are morphologically distinct. Aliquots of lyophyllized Aβ(1−42) were reconstituted to 100 μM as described in the Methods to generate oligomers or fibrils. After 24 h incubation at the given temperatures, aliquots of the solutions were diluted to 10 μM, applied to mica, and imaged by AFM. Representative images are shown for oligomers (panel A, 5 μm × 5 μm) and fibrils (panel B, 10 μm × 10 μm). ThT fluorescence measurements (n = 8 for oligomers and n = 10 for fibrils) were obtained for each preparation at a final concentration of 10 μM Aβ(1−42) (Panel C).

In addition to significant Aβ polymorphism exhibited in the AD brain, the structural diversity may even extend to the Aβ senile plaques based on recent observations indicating a significant level of oligomeric Aβ surrounding the plaques in an AD mouse model.[18]

In concert with in vitro aggregation studies, cellular studies have shown that monomeric, oligomeric, protofibrillar, fibrillar, and amorphous Aβ species possess distinct toxic and biological activities and potencies.[16,19−22] This is also the case with Aβ as a proinflammatory stimulus. It is generally felt that soluble Aβ oligomers and protofibrils contribute to early dendritic and synaptic injury in AD models (reviewed in ref 23) while fibrillar Aβ acts as a proinflammatory stimulus. However, many groups have reported induction of proinflammatory cytokines and signaling pathways by soluble prefibrillar species in glial cells. In some cases, the type and extent of proinflammatory response differed between Aβ fibrils and soluble oligomeric species.[24,25] The prevailing view is still that while small soluble Aβ species display greater cellular toxicity, fibrillar structures are the primary mediators of inflammation. Our own studies have indicated that soluble Aβ(1−42) fibrillar precursors were much more effective than fibrils at stimulating tumor necrosis factor α (TNFα) production in human monocytes.[26] In many reports, Aβ solutions were used that likely contained a high degree of polydispersity with respect to size and aggregation state. In this study, multiple aggregation conditions were evaluated in conjunction with separation and rigorous characterization of the isolates in order to identify the optimal Aβ species for microglia activation.

■ RESULTS AND DISCUSSION

Microglial TNFα Production Induced by Aβ(1−42) Prepared in Oligomer-Forming and Fibril-Forming Conditions. LaDu and colleagues previously compared the inflammatory response in rat astrocyte cultures induced by Aβ incubated in oligomer- or fibril-forming conditions.[25] We utilized their preparation methods and conditions to prepare Aβ(1−42) solutions that contain species of distinct morphology for evaluation of the inflammatory response in isolated murine microglia. The preparation of the Aβ species entailed reconstitution in DMSO followed by dilution into either cold F12 media (oligomer-forming) or 10 mM HCl (fibril-forming). A 24 h incubation of the Aβ(1−42) solutions at either 4 °C (oligomer-forming) or 37 °C (fibril-forming) produced the anticipated morphologies for both conditions as assessed by

atomic force microscopy (AFM) (Figure 1A). The images were similar to those of Stine et al.[14] Small punctate globular species were observed in the oligomer preparations (heights 3.1 ± 1.2 nm for n = 100 measurements) while long flexible fibers (heights 2.7 ± 0.9 nm for n = 100 measurements) were observed in the fibril preparations. ThT binding and fluorescence levels were significantly higher in the solutions containing fibrils compared to those containing oligomers (Figure 1B). This was consistent with the general understanding of fibrils as they are expected to have increased β-sheet character and a higher number of ThT binding sites. However, the observation that the oligomer preparations exhibited a considerable level of ThT fluorescence was somewhat surprising and suggested a significant level of β-structure.

The Aβ(1−42) oligomer and fibril preparations were evaluated for their ability to stimulate TNFα production by microglia. TNFα is an important product of the MyD88-dependent proinflammatory innate immune response[35] and is measurably increased in post-mortem AD brain sections,[7] and microvessels[36] and cerebrospinal fluid[37] of clinically diagnosed AD patients. Although most studies show similar responses between BV-2 and primary microglia, concerns have been raised that in some cases immortalized BV-2 microglia may not fully model primary microglia[38] and caution should be exercised when interpreting BV-2 results until direct comparison with primary cells can be made.[39] Therefore, it has become commonplace to utilize both microglial cell types for experimental testing which was the case in these studies. A 6 h incubation of 15 μM Aβ(1−42) oligomers or fibrils with murine microglia revealed significant differences in TNFα production between the two Aβ aggregation states (Figure 2). Similar trends of inflammatory activity were observed in both primary (Figure 2A) and BV-2 (Figure 2B) microglia. Despite the lesser ThT fluorescence, the Aβ(1−42) solutions prepared and incubated in oligomer-forming conditions were markedly better at inducing TNFα from murine microglia consistent with previous findings in rat astrocytes.[25]

Characterization of SEC-Isolated Aβ(1−42) Protofibrils Prepared and Eluted in Supplemented F12. Regardless of the conditions used to study Aβ(1−42) aggregation there is always a degree of polydispersity present in the solutions which likely include monomers, soluble aggregates of many sizes, and some fibril structures. In order to better define and characterize the soluble Aβ(1−42) aggregation species, SEC was used for separation and purification. SEC has been used in numerous studies to separate protofibrils from monomeric Aβ.[11,40] In this
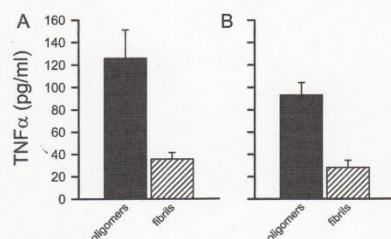
Figure 2. $A\beta(1-42)$ oligomers stimulate microglia more effectively than fibrils. Solutions of $A\beta(1-42)$ oligomers and fibrils prepared as in Figure 1 legend were incubated with microglia at a final concentration of 15 μM for 6 h. Secreted TNFα was measured by ELISA in the conditioned medium collected from treated primary murine microglia (panel A) and (panel B) BV-2 murine microglia. Data bars represent the average $\pm$ standard (std) error of n = 30 trials (oligomers and fibrils) for primary microglia and n = 32 trials (oligomers) and n = 33 trials (fibrils) for BV-2 microglia. Control treatments in the presence of 0.3% DMSO in F-12 media or 1.5 mM HCl produced 40 and 15 pg/mL TNFα, respectively, for primary and BV-2 microglia and were subtracted from $A\beta$-stimulated samples. Primary and BV-2 microglia were stimulated in serum-free and 2% FBS medium, respectively. Statistical differences between oligomers and fibrils for both sets of data had p values < 0.001.

set of experiments, a Superdex 75 column was used for separation. Using a modified version of the NaOH method,[41] lyophilized $A\beta(1-42)$ was reconstituted in NaOH followed by dilution in antibiotic-supplemented F-12 to prevent microbial growth. The use of F-12 media was retained from the oligomer-forming conditions in Figure 1 due to the physiological nature of the solution and the compatibility with microglial cell treatment. The $A\beta(1-42)$ solution (250 μM) was centrifuged at 18 000g and the supernatant was eluted in supplemented F-12 media as described in the Methods. The $A\beta(1-42)$ elution profile was monitored by UV absorbance (280 nm) and exhibited characteristic protofibril (void) and monomer (included) peaks (Figure 3).
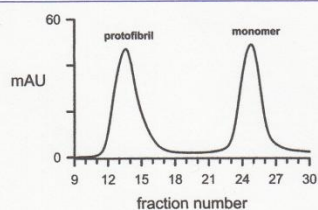
Figure 3. Dual peaks are observed following SEC elution of $A\beta(1-42)$ reconstituted in NaOH/F-12. Lyophilization $A\beta(1-42)$ (1 mg) was brought into solution with NaOH followed by supplemented F-12 media to a final concentration of 200 μM. The supernatant after centrifugation was eluted from a Superdex 75 column, and 0.5 mL fractions were collected. UV absorbance at 280 nm was monitored during the elution (solid line).

The significant $A\beta(1-42)$ void peak was observed without prolonged incubation of the reconstitution solution confirming that $A\beta(1-42)$ forms protofibrils rapidly under these conditions.[42]

SEC-purified monomer fractions did not exhibit ThT fluorescence while protofibril fractions at equivalent concentrations showed significant fluorescence (Figure 4A). Although
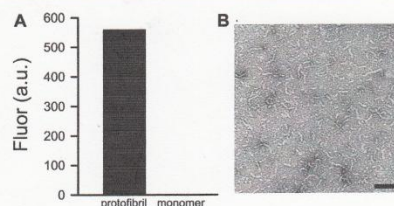
Figure 4. Structure and morphology of $A\beta(1-42)$ protofibrils. (A) Freshly isolated $A\beta(1-42)$ protofibrils and monomers after elution from Superdex 75 in supplemented F-12 were diluted to 5 μM respectively in supplemented F-12 containing 5 μM ThT, and fluorescence emission was measured as described in the Methods. (B) Protofibrils were diluted to 20 μM, applied to a copper formwar grid, and imaged by TEM at a magnification of 43 000×. The scale bar represents 100 nm.

F-12 media is not a common Superdex 75 elution buffer such as Tris or PBS, transmission electron microscopy (TEM) imaging of the F-12-eluted void peak showed classic short curvilinear protofibrils[11,43] < 100 nm in length (Figure 4B). Dynamic light scattering (DLS) measurements of the protofibril peak from seven separate SEC purifications produced an average R_H value of 21 nm with a standard deviation (std dev) of 6 nm (data not shown). Deconvolution of the average R_H values into histograms by data regularization revealed two predominant peaks of 4.5 $\pm$ 0.9 nm and 20.6 $\pm$ 6.5 nm. Peak 1 with the smaller R_H value was observed in 4 of 7 protofibril isolations, while peak 2 was always observed. Even within isolated $A\beta(1-42)$ protofibrils, a degree of polydispersity was present as the peak 2 histogram widths varied from narrow (e.g., 15–20 nm) to broad (e.g., 8–41 nm) in different experiments.

Microglial TNFα Production by SEC-Isolated $A\beta(1-42)$ Protofibrils, But Not Monomer. BV-2 murine microglia were treated with fresh SEC-isolated protofibril and monomer fractions and examined for their ability to stimulate an inflammatory response. Fraction concentrations were calculated based on UV absorbance and were used to determine final cellular treatment concentrations. Protofibrils (15 μM) induced a substantial level of secreted TNFα while monomers (15 μM) were much less effective (Figure 5). The presence of contaminating lipopolysaccharide (LPS) in SEC fractions was assessed in two ways, (1) a cell-free XTT assay in which the presence of any bacteria in the $A\beta$ samples would be expected to catalyze reduction of XTT and (2) TNFα production was monitored in the absence or presence of polymyxin B (PMX-B), a neutralizer of LPS signaling. The former method revealed no XTT reduction in the presence of $A\beta$ samples and in the latter method it was observed that PMX-B (100 ng/mL) had no effect on the $A\beta$ response yet blocked >99% of the LPS (3 ng/mL) response (data not shown). Thus, neither method showed any indication of bacterial or LPS presence. The findings demonstrated that isolated $A\beta(1-42)$ protofibrils were significant stimulators of BV-2 microglia whereas little stimulation was observed with purified monomeric $A\beta(1-42)$. The response to $A\beta(1-42)$ protofibrils was also tested in primary microglia isolated from newborn (3–4 day old) C57BL/6 mouse pups. Freshly isolated protofibrils were tested at multiple concentrations (5, 10, 15, and 20 μM) and exhibited a dose-dependent ability to induce TNFα production in both primary and BV-2 microglia (Figure 6). Typically primary microglia were more responsive to $A\beta(1-42)$
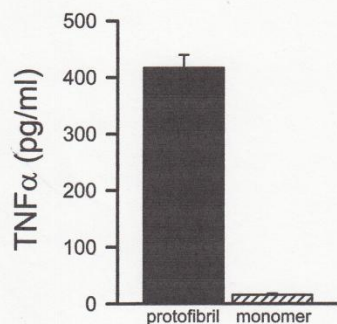
Figure 5. Protofibrils are significant stimulators of BV-2 microglia. SEC-isolated $A\beta(1-42)$ protofibrils and monomers in supplemented F-12 were incubated with BV-2 microglia at a final concentration of 15 μM for 6 h in medium containing 2% FBS. Secreted TNFα was measured by ELISA in the conditioned medium. Data bars represent the average $\pm$ std error of $n = 6$ trials. Control treatments with an equal volume of supplemented F-12 media produced 23 pg/mL TNFα and were subtracted from $A\beta$-stimulated samples.
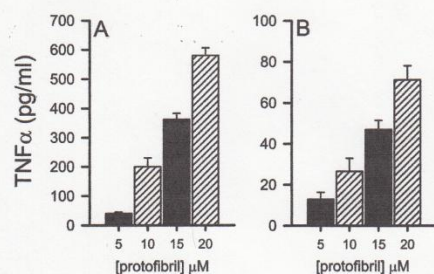
Figure 6. Protofibrils display a dose-dependent effect in their ability to induce TNFα production in microglia. SEC-isolated $A\beta(1-42)$ protofibrils in supplemented F-12 were incubated with primary microglia (panel A) or BV-2 microglia (panel B) for 6 h at final concentrations of 5, 10, 15, and 20 μM. Secreted TNFα was measured by ELISA in the conditioned medium. Data bars represent the average $\pm$ std error of $n = 4-6$ trials at each concentration for primary microglia and $n = 6$ trials at each concentration for BV-2 microglia. Control treatments with supplemented F-12 media produced 6 and 17 pg/mL TNFα respectively for primary and BV-2 microglia and were subtracted from $A\beta$-stimulated samples. Primary and BV-2 microglia were stimulated by $A\beta$ in serum-free conditions.

protofibrils than BV-2 microglia, but this disparity was dependent on the age and number of harvests of the primary cells as well as the BV-2 passage number. In some experiments, BV-2 cells secreted higher levels in response to $A\beta(1-42)$ protofibrils.

Comparison of Microglial TNFα Production between $A\beta(1-42)$ Protofibrils and Fibrils Prepared from SEC-Purified Monomer. We then sought to compare the microglial-activating ability of protofibrils and fibrils. SEC-purified $A\beta(1-42)$ monomer in supplemented F-12 was moved to 25 °C and subjected to gentle agitation for approximately 72 h. Fibrils were isolated by centrifugation, supernatant removal, and resuspension

of the pellet as described in the Methods. In all cases, >98% of the ThT fluorescence of the total solution was removed from the supernatant after centrifugation. ThT fluorescence comparisons of equivalent concentrations of $A\beta(1-42)$ fibrils and SEC-purified $A\beta(1-42)$ protofibrils and monomers immediately following elution showed fibrils with by far the best ThT binding ability (Figure 7A). Protofibrils displayed significantly lower ThT fluorescence and monomers were at background levels. TEM images of the isolated $A\beta(1-42)$ fibrils revealed long fibers with lengths exceeding 1 μm and typical widths of 5–10 nm (Figure 7B). The neutral pH and higher ionic strength of the F-12 media encouraged a considerable degree of lateral association between the fibrils. Surprisingly, fibrils were very poor in their ability to stimulate TNFα production in primary (Figure 7C) and BV-2 (data not shown) microglia. $A\beta(1-42)$ protofibrils invoked a dramatically higher microglial response compared to fibrils and monomers (Figure 7C). A cell-free XTT cell proliferation assay again showed no evidence of contamination in any of the preparations (data not shown). Our typical BV-2 and primary microglial preparations contained cells with both round and ramified morphologies with defined boundaries. After exposure to $A\beta$, the cells became clustered with rough boundaries and a less ramified morphology. These observations are consistent with those made by Garcao et al in rat microglia.[44] Primary microglia underwent more pronounced alterations in morphology compared to BV-2 cells. Even with these exterior changes to the cells after treatment with $A\beta$, no significant toxicity was observed using an XTT cell viability assay. Exposure of the microglia to $A\beta(1-42)$ fibrils, protofibrils, or monomer for 6 h did not inhibit mitochondrial-mediated reduction of XTT in either BV-2 or primary microglia (data not shown). The preparation of $A\beta$ protofibrils, fibrils, and monomers in the supplemented F-12, which is similar in pH and ionic strength to the microglial cell culture medium, likely helped prevent dramatic structural changes in the isolated $A\beta$ species when introduced to the microglia cells. Although this was not verified, very different microglial responses were clearly able to be observed between the distinct $A\beta$ species.

Comparison of Microglial TNFα Production between $A\beta(1-42)$ Protofibrils and $A\beta(1-40)$ Protofibrils. In order to compare $A\beta(1-40)$ protofibrils with those formed from $A\beta(1-42)$, a longer incubation was needed after NaOH reconstitution and dilution into supplemented F-12 medium. While $A\beta(1-42)$ protofibrils formed rapidly within minutes, $A\beta(1-40)$ required a 24 h incubation at 25 °C before significant amounts of protofibrils were generated (Figure 8). The $A\beta(1-40)$ protofibril fraction was assessed by TEM which revealed similar structures as observed for $A\beta(1-42)$ although the lengths appeared somewhat smaller (Figure 9A). Manual measurements of the images confirmed that the $A\beta(1-40)$ and $A\beta(1-42)$ protofibril fractions had statistically different ($p < 0.001$) lengths as $A\beta(1-40)$ protofibrils averaged 27 $\pm$ 11 nm while $A\beta(1-42)$ protofibrils averaged 50 $\pm$ 16 nm for $n = 50$ measurements. The length analysis only included unambiguous protofibril structures and excluded the smaller species (<15 nm). Despite morphological similarities, cellular studies demonstrated that $A\beta(1-40)$ protofibrils were much less effective in stimulating TNFα in primary microglia compared to $A\beta(1-42)$ protofibrils (Figure 9B). The concentration used in the microglial treatment for both $A\beta(1-40)$ and $A\beta(1-42)$ protofibrils was 15 μM.

The current report demonstrates the substantial activation of murine microglia by soluble $A\beta(1-42)$ aggregates. We observed
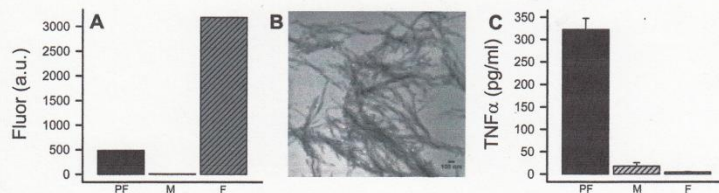
Figure 7. Protofibrils display less ThT fluorescence but stimulate microglia more effectively than fibrils. (A) Aliquots of SEC-purified $A\beta(1-42)$ protofibrils (PF), monomer (M), and $A\beta(1-42)$ fibrils formed from purified monomer (F) were diluted to 5 μM in 50 mM Tris-HCl pH 8.0 containing 5 μM ThT and fluorescence emission was measured and plotted as described in the Methods. Fibrils were isolated as described after gentle agitation for 72 h at 25 °C. One fluorescence measurement was obtained from each solution. (B) TEM images of isolated $A\beta(1-42)$ fibril pellets (74 μM) at a magnification of 25,000. (C) Aliquots of the solutions described in panel (A) were incubated with primary murine microglia for 6 h at a final concentration of 15 μM $A\beta(1-42)$. Secreted TNFα was measured by ELISA in the conditioned medium. Error bars represent the average ± std error of n = 6. Control treatments with supplemented F-12 media produced 15 pg/mL TNFα for primary microglia and were subtracted from $A\beta$-stimulated samples.
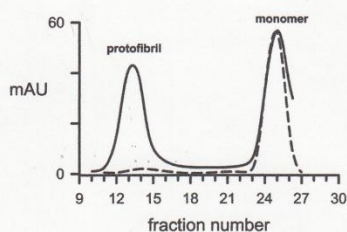
Figure 8. $A\beta(1-40)$ protofibrils require longer incubation for formation. $A\beta(1-40)$ was reconstituted and prepared for SEC as described in the Methods. $A\beta(1-40)$ solutions were eluted on Superdex 75 immediately (dashed line) or after a 24 h incubation at 25 °C (solid line). Fractions containing protofibrils and monomers were immediately placed on ice for further characterization. Concentrations were determined by UV absorbance.
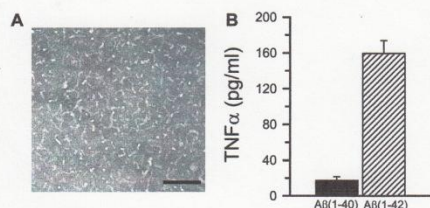
Figure 9. $A\beta(1-40)$ protofibrils do not stimulate microglia as well as $A\beta(1-42)$ protofibrils. (A) TEM image of a sample taken from the $A\beta(1-40)$ protofibril peak in Figure 8 (solid line). Sample was diluted to 20 μM $A\beta$, applied to a copper formwar grid as described in the Methods, and imaged at a magnification of 43 000X. The scale bar represents 100 nm. (B) Primary microglia were incubated with $A\beta(1-40)$ or $A\beta(1-42)$ protofibrils isolated by SEC in supplemented F-12 at a final concentration of 15 μM each for 6 h. Secreted TNFα was measured by ELISA in the conditioned medium. Data bars represent the average ± std error of n = 12 ($A\beta40$) and n = 9 ($A\beta42$) trials over two separate protofibril preparations for each protofibril type. Protofibrils were directly compared within each cell treatment experiment. Control treatments with an equal volume of supplemented F-12 media produced 31 pg/mL TNFα and were subtracted from $A\beta$-stimulated samples.

that an enriched fraction of SEC-isolated protofibrils elicited the greatest production of the proinflammatory cytokine TNFα compared to monomers and fibrils. The current results have similarities to our previous findings in THP-1 human monocytes in which soluble fibrillar precursors were optimal for inducing a proinflammatory response.[26] While many studies have shown that monocytes and microglia have similar responses to $A\beta$, microglial cells provide a more relevant model system for investigating $A\beta$ neuroinflammatory mechanisms. Furthermore, this report is the first to provide a direct comparison between SEC-purified $A\beta(1-42)$ protofibrils and isolated $A\beta(1-42)$ fibrils prepared from SEC-purified monomer in their ability to induce microglial activation.

An array of $A\beta$ aggregate morphologies ranging from dense core neuritic plaques to granular diffuse wispy $A\beta$ deposits are observed in the AD brain.[1] It has been known for some time that the plaques serve as a focal point for inflammation.[5] The rapid response of microglia to a site of new plaque formation has been revealed using multiphoton microscopy in a transgenic mouse model outfitted with a cranial window.[6] In this case, as well as others, microglia were not associated with diffuse $A\beta$ deposits. Although it is not a straightforward extrapolation from in vitro results to in vivo mechanisms, the findings from our current study may be relevant to recent findings in transgenic mouse models. Hyman and colleagues observed a halo of oligomeric $A\beta$ surrounding $A\beta$ plaques based on immunostaining with NAB61 antibody.[18] Although the plaques contain fibrillar $A\beta$ at the core,[45] these data suggest that the plaque composition is more complex than originally thought. There may be dynamic aggregation processes occurring in the plaque environment and the microglial cells may interact with multiple $A\beta$ species.

Much of the recent emphasis on soluble $A\beta$ aggregates has been on oligomers yet much more structural information is known about protofibrils. The first observation and characterization of protofibrils more than a decade ago identified these small soluble species with significant β-sheet structure[13] as precursors to fibrils.[10,11] Centrifugation followed by SEC on Superdex 75 was instrumental in isolating protofibrils for further characterization.[11] Previous size analysis of protofibrils identified a range of R_H values from 10 to 50 nm and lengths of typically <200 nm.[11] The $A\beta(1-42)$ protofibrils characterized in the current study were within these ranges but on the smaller end. The observation of bimodal R_H peaks in protofibril DLS

regularization histograms suggests that further separation and characterization may be possible. Structurally, protofibrils have similarities to fibrils based on thioflavin T binding, circular dichroism,[13] and hydrogen exchange,[43] but have not yet developed the full stability of fibrillar $A\beta$.[13,43] Protofibril diameters are typically smaller than fibrils and range from 4 to 6 nm although the protofibril to fibril transition can occur without a change in diameter.[10] The transition to fibrils can occur via mechanisms that incorporate monomer deposition on protofibril ends, end-to-end annealing of protofibrils, and lateral association of protofibrils.[12,34] Protofibrils display toxicity to neurons,[13] disrupt ion channels,[46] inhibit hippocampal long-term potentiation,[47] and are likely to possess other detrimental biological activities. Their solubility and diffusible nature quite possibly render them more effective in cellular interactions and engaging microglial receptors compared to mature insoluble fibrils.

The mechanism by which $A\beta$ fibrils evoke a proinflammatory response appears to involve multiple cell-surface receptors. A multireceptor complex comprising the SR-B receptor CD36, $\alpha_6\beta_1$-integrin, and the integrin-associated protein CD47 has been shown to mediate fibrillar $A\beta$ initiation of murine microglial activation.[48] Furthermore, receptor components of the innate immune system including CD14,[49] toll-like receptor (TLR) 2, and TLR 4 have also been identified as proinflammatory-linked receptors in microglial cells for $A\beta$ fibrils.[31] Moreover, a TLR4-TLR6-CD36 complex was recently shown to mediate cellular inflammatory responses to $A\beta(1-42)$ fibrils.[50] A cell-surface receptor that is selective for $A\beta$ protofibrils has not been identified although the known fibril receptors may recognize similar structural elements between the two species.

For many years, it has been accepted that fibrillar $A\beta$ is the primary trigger for inducing a glial inflammatory response in AD and in cell culture models. Many studies established and utilized solution conditions that were optimal for $A\beta$ fibril formation but may have contained other $A\beta$ species. Nevertheless, it was generally interpreted as microglial activation by $A\beta$ fibrils. Numerous studies have demonstrated cytokine production by fibrillar $A\beta$,[30,51] interaction of fibrillar $A\beta$ with proinflammatory receptors,[48-50] and initiation of proinflammatory signaling pathways by fibrillar $A\beta$.[52,53] More recently, studies have shown that a fibrillar state for $A\beta$ may not be required for microglial activation. These findings have been based on a lack of correlation between ThT binding and cell stimulation[54] or modulation of aggregation solution conditions to encourage formation of oligomers that display significant proinflammatory activity in microglia.[24,25] A recent study altered the $A\beta$ aggregation solution conditions to encourage formation of smaller or larger oligomers and fibrils. Stimulation of primary mouse microglia with these solutions revealed that, while polydisperse in $A\beta$ species, those solutions containing smaller oligomers were able to induce more $TNF\alpha$ mRNA than those containing larger oligomers and fibrils.[55] Less has been published regarding $A\beta$ protofibrils and their role in AD-linked inflammation. In one study, Parvathy et al. found that $A\beta$ protofibrils were not effective at inducing IL-1α mRNA expression in primary murine microglia compared to oligomers and fibrils.[56] This finding indicates that perhaps not all microglial proinflammatory products are upregulated to the same extent by $A\beta$ protofibrils. Interestingly, a new report suggests that soluble $A\beta$ aggregates may be one of the targets of the central nervous system glial cell response which includes both microglia and astrocytes. DaRocha-Souto et al. demonstrated in double-transgenic APP^{sw}-tau^{vlw} mice that the correlation between oligomeric $A\beta$ burden in the brain

(based on NAB61 antibody binding) and the number of reactive astrocytes was better than the correlation between total $A\beta$ plaque burden and reactive astrocytes.[57]

Given the polydispersity observed in $A\beta$ aggregation, there is a good possibility that many preparations are not homogeneous. In fact, many studies focusing on a particular biological activity of $A\beta$ utilize $A\beta$ solutions that have not been rigorously characterized. These solutions likely contain mixtures of $A\beta$ aggregated species including oligomers, protofibrils, and fibrils. The conditions can dictate which species is more highly populated, but the mixture prevents the identification of the most active species. In fact, the $A\beta(1-42)$ solutions prepared in fibril-forming conditions (Figures 1 and 2) may have contained a small population of protofibrils which might help to explain why a moderate amount of microglial $TNF\alpha$ production was observed. The formation of these fibrils at very low ionic strength precluded the ability to utilize centrifugation to separate the fibrils from any contaminating protofibrils. However, the $A\beta(1-42)$ fibrils prepared from SEC-purified monomer at physiological pH and ionic strength (Figure 7) were very poor at stimulating $TNF\alpha$ production from microglia. This observation was possible due to the additional isolation step whereby fibrils were separated from the remaining $A\beta$ solution by centrifugation and resuspended before application to the cells. This procedure likely removed any soluble aggregated species that may have been present in the initial solution thus allowing isolated fibrils to be evaluated. Looking back on previous studies, the persistent use of $A\beta$ solutions containing a polydisperse population of aggregated species when evaluating $A\beta$ biological activity may help to explain significant fluctuations in cell response and irreproducibility between experiments. Furthermore, the $A\beta(1-42)$ fibrils described in Figures 1 and 2 were prepared under nonphysiological solution conditions (e.g., 10 mM HCl), and while the acidic conditions may have enhanced fibril formation, the internal structure may be quite different from the fibrils formed under more physiological conditions in Figure 7. Petkova et al. found that parallel β-sheet $A\beta(1-40)$ fibrils prepared under different conditions had distinct hydrogen-bond registries and marked differences in neuronal toxicity.[58] The same phenomenon has been observed for soluble aggregates. Chiti and co-workers demonstrated that oligomers grown under different solution conditions can have identical morphologies yet show different internal structures and toxicities.[59] There remain potential concerns with in vitro preparation of aggregated $A\beta$ species for cellular studies as their structure may have important differences from those formed in vivo. In the current study, the preparation, isolation, and characterization of $A\beta(1-42)$ protofibrils under close to physiological solution conditions may help avoid some of the concerns. The significant and consistent microglial response to an enriched SEC fraction of $A\beta(1-42)$ protofibrils demonstrates that these soluble fibrillar precursors are potent proinflammatory mediators. The much weaker microglial response to an equal concentration of $A\beta(1-40)$ protofibrils suggests that even though the two protofibril species appear morphologically similar, there are distinct properties between the two types of protofibrils that influence their inflammatory activity.

■ METHODS

Cell Culture and Primary Microglia Isolation. BV-2 cells are primary mouse microglial cells immortalized by stable transfection with the c-myc oncogene[27] and are functionally identical to native primary microglia.[28] BV-2 cells were provided by Dr. Gary Landreth,

Case Western Reserve University, and were maintained in Dulbecco's modified Eagle's medium (DMEM, 4.5 g/L glucose) (Hyclone) containing 50 U/mL penicillin, 50 μg/mL streptomycin, 50 μM β-mercaptoethanol, and 5% fetal bovine serum (FBS, Hyclone). BV-2 cells were used for their ease of culture, initial observations, optimization of microglia/Aβ interactions, and to reduce the usage of mice for primary cells. Primary murine microglia were obtained from newborn C57BL/6 mouse pups as previously described.[29] Care and breeding of the C57BL/6 parent mice (Harlan Laboratories) was done at the University of Missouri—St. Louis Animal Facility. Briefly, 3–4 day old mouse pups were euthanized with an overdose of inhaled isoflurane (Fisher Scientific). The brains were isolated and meninges were removed under sterile conditions. Brain tissue was minced using sharp edged forceps, resuspended in 0.5% trypsin (Hyclone), and incubated at 37 °C for 20 min to allow further dissociation of the tissue. Subsequently, tissue was resuspended in complete DMEM containing 10% fetal bovine serum, 4 mM L-glutamine, 100 U/mL penicillin, 0.1 mg/mL streptomycin and 0.25 μg/mL amphotericin-B (Fisher Scientific), OPI medium supplement (oxalocetate, pyruvate, insulin, Sigma-Aldrich), and 0.5 ng/mL recombinant mouse granulocyte-macrophage colony-stimulating factor (GM-CSF) (Invitrogen). The cell suspension was further triturated using a pipet and filtered through a 70 μm cell strainer to remove debris. The resulting cell suspension was centrifuged at 200g for 5 min at 25 °C, resuspended in complete medium, and seeded into 150 cm² flasks (Corning). Cells were cultured at 37 °C in 5% CO₂ until confluent (1–2 weeks), and microglia were selectively harvested from the adherent astrocyte layer by overnight shaking of the flask at 37 °C in 5% CO₂ and collection of the medium. The flasks were replenished with fresh medium and then incubated further to obtain additional microglia. Typically, this procedure was repeated 3–4 times for one flask without removal of the astrocyte layer.

Cell Stimulation Assay. For cellular studies, BV-2 microglia were removed from culture flasks with 0.25% trypsin and seeded in a sterile 96-well cell culture plate overnight at a density of 5×10^5 cells/mL in growth medium described above. Prior to cell treatment, medium was replaced with fresh medium containing either 0 or 2% FBS followed by Aβ stimulation at a final concentration of 15 μM. The inclusion of 2% FBS initially was adapted from an established THP-1 monocyte protocol.[30] Treatment of BV-2 without serum has been reported elsewhere[31] and the absence of serum during BV-2 cell stimulation did not dramatically alter the results. The cells were incubated at 37 °C for 6 h in 5% CO₂, and the medium was collected and stored at −20 °C for subsequent analysis by enzyme-linked immunosorbent assay (ELISA). Primary microglia were collected after shaking flasks overnight and then centrifuged at 200g for 10 min at 25 °C. The cells were resuspended in complete microglial medium without GM-CSF or FBS and plated at a density of 5×10^5 cells/ml in a sterile 96-well cell culture plate for either 2 h or overnight. The longer preincubation, which has been used previously[31] and was done to allow greater adherence of the microglia, had no deleterious effects on the cells. Prior to treatment, the medium was replaced again and lipopolysaccharide (3 ng/mL) or Aβ (15 μM) was added to the cells. The medium was collected after 6 h and stored at −20 °C for subsequent determination of secreted TNFα levels by ELISA. The background cellular response was assessed using the particular buffer vehicle for the Aβ.

ELISA. Measurement of secreted TNFα in the supernatants was determined by ELISA as previously detailed.[32] Briefly, 96-well plates were coated overnight with monoclonal antimouse TNFα capture antibody, washed with phosphate-buffered saline (PBS) containing 0.05% Tween-20, and blocked with PBS containing 1% BSA, 5% sucrose, and 0.05% NaN₃ following by a wash step. Successive treatments with washing in between were done with samples or standards, biotinylated polyclonal antimouse TNFα detection antibody in 20 mM Tris with 150 mM NaCl and 0.1% BSA, streptavidin-horseradish peroxidase (HRP) conjugate, and equal volumes of HRP substrates 3,3′,5,5′-tetramethylbenzidine and hydrogen peroxide. The reaction was stopped by the addition of 1% H₂SO₄ solution. The optical density of each sample was analyzed at 450 nm with a reference reading at 630 nm using a SpectraMax 340 absorbance plate reader (Molecular Devices, Union City, CA). The concentration of TNFα in the

experimental samples was calculated from a mouse TNFα standard curve of 15–2000 pg/mL. When necessary, samples were diluted to fall within the standard curve. TNFα concentrations for absorbance values below the lowest 15 pg/mL standard were determined by extrapolation of the standard curve regression line.

Preparation of Aβ Peptides. Aβ(1–42) was obtained from W.M. Keck Biotechnology Resource Laboratory (Yale School of Medicine, New Haven, CT) in lyophilized form and stored at −20 °C. Aβ(1–40) was obtained from rPeptide (Bogarth, GA) or prepared by solid phase synthesis in the Structural Biology Core at the University of Missouri—Columbia as described previously.[33] Aβ peptides were typically dissolved in 100% hexafluoroisopropanol (HFIP) (Sigma-Aldrich, St. Louis, MO) at 1 mM, aliquoted into sterile microcentrifuge tubes, and evaporated uncovered at room temperature overnight in a fume hood. The following day, the aliquots were vacuum-centrifuged to remove any residual HFIP and stored in desiccant at −20 °C. Some Aβ peptides were treated with 100% trifluoroacetic acid and vacuum-centrifuged prior to HFIP treatment. Aβ oligomers and fibrils obtained directly from lyzophilized aliquots were prepared as previously described.[14] Briefly, lyophilized Aβ42 aliquots were resuspended in sterile anhydrous dimethyl sulfoxide (DMSO) (Sigma-Aldrich, St. Louis, MO) at 5 mM. For oligomer preparation the sample was diluted to 100 μM in sterile ice-cold Ham's F-12 cell culture medium with L-glutamine but without phenol red (F-12, Bioworld, Dublin, OH) and incubated for 24 h at 4 °C. For fibril preparation, the sample was diluted to 100 μM in 10 mM HCl and incubated for 24 h at 37 °C. Aβ concentrations in these preparations were based on dry peptide weight.

Size Exclusion Chromatography. An amount of 1–1.5 mg of lyophilized Aβ peptide was dissolved in 50 mM NaOH to yield a 2.5 mM Aβ solution. The solution was then diluted to 250 μM Aβ in sterile prefiltered (0.22 μm) Ham's F-12 cell culture medium (described above) with additional supplementation of 100 U/mL penicillin, 0.1 mg/mL streptomycin, and 0.25 μg/mL amphotericin-B (heretofore referred to as supplemented F-12). Aβ(1–42) solutions were centrifuged immediately at 18 000g for 10 min with a Beckman-Coulter Microfuge18 instrument while Aβ(1–40) solutions were incubated for 24 h at 25 °C prior to size-exclusion chromatography (SEC). The centrifugation supernatant was eluted from a Superdex 75 HR 10/30 column (GE Healthcare) in supplemented F-12 medium. Prior to injection of Aβ, Superdex 75 column was coated with 2 mg bovine serum albumin (BSA, Sigma) to prevent any nonspecific binding of Aβ to the column matrix. Following a 1 mL loading of the sample, Aβ was eluted at 0.5 mL/min and 0.5 mL fractions were collected and immediately placed on ice. Fractions 13, 14 eluting in the void volume were pooled together and designated as protofibrils while fractions 24–25 eluting in the included peak were pooled and designated as monomer. UV absorbance at 280 nm was monitored continuously in milliabsorbance units (mAU) during the elution, and concentrations of both protofibrils and monomers were determined directly from the absorbance trace using an extinction coefficient of 1450 cm⁻¹ M⁻¹ at 280 nm. The delay volume between the absorbance detector and fraction collector was minimal, and this was verified in initial experiments by measuring Aβ concentrations in the fractions on a Cary Bio 50 UV absorbance spectrophotometer and comparing those concentration values to those determined from the chromatography absorbance trace. Aβ(1–42) fibrils were prepared from SEC-purified Aβ(1–42) monomer in supplemented F-12 by incubation at room temperature under gentle agitation for ∼72 h. The aggregated Aβ(1–42) solution was then centrifuged at 18 000g for 10 min, supernatant was removed, and the pellet was resuspended in the same volume of supplemented F-12. The concentration of fibrils was assumed to match the original starting concentration of the Aβ(1–42) monomer. Thioflavin-T (ThT) fluorescence measurements were done on the total Aβ(1–42) solution, the 18 000 g supernatant, and the resuspended pellet in order to monitor the conversion of Aβ monomer into fibrils.

Thioflavin T Fluorescence Measurements. Aβ(1–42) monomer, protofibril and fibril solutions were assessed by ThT fluorescence as described previously.[34] Aβ aliquots were removed and diluted 10-fold into 50 mM Tris-HCl pH 8.0 containing 5 μM ThT. Fluorescence

xxiv

emission scans (460−520 nm) were acquired on a Cary Eclipse fluorescence spectrophotometer using an excitation wavelength of 450 nm and integrated from 470 to 500 nm to obtain ThT relative fluorescence values. F-12 medium, supplemented or not, did not show any significant ThT fluorescence in the absence of $A\beta$. All ThT fluorescence numbers are reported in relative fluorescence units denoted arbitrary units (a.u.) in the figures.

Atomic Force Microscopy. $A\beta$(1−42) aggregation solutions (100 μM) were diluted to 10 μM in water. Grade V1 mica (Ted Pella, Inc., Redding, CA) was cut into 11 mm circles and affixed to 12 mm metal discs. Aliquots (50 μL) were applied to freshly cleaved mica, allowed to adsorb for 15 min, washed twice with water, air-dried, and stored in a container with desiccant. Images were obtained with a Nanoscope III multimode atomic force microscope (Digital Instruments, Santa Barbara, CA) in TappingMode. Height analysis was performed using Nanoscope III software on flattened height mode images.

Transmission Electron Microscopy. SEC-purified $A\beta$(1−42) protofibril and aggregation solutions were diluted to 20 μmol/L in water unless otherwise stated and applied (10 μL) to a 200-mesh Formvar-coated copper grid (Ted Pella, Inc.). Samples were allowed to adsorb for 10 min at 25 °C, followed by removal of excess sample solution. Grids were washed three times by placing the sample side down on a droplet of water. Heavy metal staining was done by incubation of the grid on a droplet of 2% uranyl acetate (Electron Microscopy Sciences, Hatfield, PA) for 5 min, removal of excess solution, and air drying. Affixed samples were visualized with a JEOL JEM-2000 FX transmission electron microscope operated at 200k eV.

Dynamic Light Scattering. Hydrodynamic radius (R_H) measurements were made at room temperature with a DynaPro Titan instrument (Wyatt Technology, Santa Barbara, CA). Samples (30 μL) were placed directly into a quartz cuvette and light scattering intensity was collected at a 90° angle using a 10 s acquisition time. Particle diffusion coefficients were calculated from autocorrelated light intensity data and converted to R_H with the Stokes−Einstein equation. Average R_H values were obtained with Dynamics software (version 6.7.1). Histograms of percent intensity vs R_H were generated by Dynamics data regularization and intensity-weighted mean R_H values were derived from the regularized histograms.

XTT Cell Viability and Proliferation Assay. Viability of $A\beta$-treated microglia was determined by using an XTT [2, 3-bis (2-methoxy-4-nitro-5-sulfophenyl)-2H-tetrazolium-5-carboxanilide] assay. Cellular metabolic activity was monitored by mitochondria-mediated reduction of XTT (Sigma). XTT assay was also used in a cell-free manner to rule out the possibility of any bacterial contamination of $A\beta$(1−42) and $A\beta$(1−40) samples. In cellular XTT assay, cells exposed to $A\beta$ for 6 h were further incubated with 0.33 mg/mL XTT and 8.3 μM phenazine methosulfate (PMS) (Acros, Morris Plains, NJ) for 2 h at 37 °C. The extent of XTT reduction was measured by absorbance of reduced form of XTT at 467 nm. The cell-free XTT assay was done in parallel to the cell stimulation studies, in a similar manner as above except the $A\beta$ sample was incubated with XTT and PMS without any cells at the same final concentration of 15 μM for 6 h.

Statistical Analysis. Cellular responses and protofibril length measurements were evaluated for statistical differences by paired t test analysis in SigmaPlot 10.0 software.

■ AUTHOR INFORMATION

Corresponding Author
*Mailing address: Department of Chemistry and Biochemistry, University of Missouri—St. Louis, One University Boulevard, St. Louis, Missouri 63121. Telephone: (314) 516-7345. Fax: (314) 516-5342. E-mail: nicholsmic@umsl.edu.

Author Contributions
M.N. conceived the project. G.P. performed the following: preparation and purification of protofibril, monomer, and fibril samples, cell culture and primary microglia isolation, microglial activation studies, toxicity assays, ELISA, and fluorescence measurements. L.G. did the AFM imaging and analysis. D.O. did the TEM imaging. M.N. performed the DLS studies. M.N. and G.P. wrote the paper.

■ ACKNOWLEDGMENTS

■ ABBREVIATIONS

AD, Alzheimer's disease; $A\beta$, amyloid-β protein; HFIP, hexafluoroisopropanol; SEC, size exclusion chromatography; ThT, thioflavin T; TEM, transmission electron microscopy; AFM, atomic force microscopy; DLS, dynamic light scattering

■ REFERENCES

(1) Selkoe, D. J. (2004) Cell biology of protein misfolding: The examples of Alzheimer's and Parkinson's diseases. *Nat. Cell Biol. 6*, 1054−1061.

(2) Fagan, A. M., and Holtzman, D. M. (2010) Cerebrospinal fluid biomarkers of Alzheimer's disease. *Biomarkers Med. 4*, 51−63.

(3) Suzuki, N., Cheung, T. T., Cai, X. D., Odaka, A., Otvos, L. Jr., Eckman, C., Golde, T. E., and Younkin, S. G. (1994) An increased percentage of long amyloid β protein secreted by familial amyloid β protein precursor (βAPP$_{717}$) mutants. *Science 264*, 1336−1340.

(4) Haass, C., and Selkoe, D. J. (2007) Soluble protein oligomers in neurodegeneration: lessons from the Alzheimer's amyloid β-peptide. *Nat. Rev. Mol. Cell Biol. 8*, 101−112.

(5) McGeer, P. L., Itagaki, S., Tago, H., and McGeer, E. G. (1987) Reactive microglia in patients with senile dementia of the Alzheimer type are positive for the histocompatibility glycoprotein HLA-DR. *Neurosci. Lett. 79*, 195−200.

(6) Meyer-Luehmann, M., Spires-Jones, T. L., Prada, C., Garcia-Alloza, M., de Calignon, A., Rozkalne, A., Koenigsknecht-Talboo, J., Holtzman, D. M., Bacskai, B. J., and Hyman, B. T. (2008) Rapid appearance and local toxicity of amyloid-β plaques in a mouse model of Alzheimer's disease. *Nature 451*, 720−724.

(7) Dickson, D. W., Lee, S. C., Mattiace, L. A., Yen, S. H. C., and Brosnan, C. (1993) Microglia and cytokines in neurological disease, with special reference to AIDS and Alzheimer disease. *Glia 7*, 75−83.

(8) McGeer, E. G., and McGeer, P. L. (1998) The importance of inflammatory mechanisms in Alzheimer disease. *Exp. Gerontol. 33*, 371−378.

(9) Golde, T. E. (2002) Inflammation takes on Alzheimer disease. *Nat. Med. 8*, 936−938.

(10) Harper, J. D., Wong, S. S., Lieber, C. M., and Lansbury, P. T. Jr. (1997) Observation of metastable $A\beta$ amyloid protofibrils by atomic force microscopy. *Chem. Biol. 4*, 119−125.

(11) Walsh, D. M., Lomakin, A., Benedek, G. B., Condron, M. M., and Teplow, D. B. (1997) Amyloid β-protein fibrillogenesis: Detection of a protofibrillar intermediate. *J. Biol. Chem. 272*, 22364−22372.

(12) Harper, J. D., Wong, S. S., Lieber, C. M., and Lansbury, P. T. Jr. (1999) Assembly of $A\beta$ amyloid peptides: an *in vitro* model for a possible early event in Alzheimer's disease. *Biochemistry 38*, 8972−8980.

(13) Walsh, D. M., Hartley, D. M., Kusumoto, Y., Fezoui, Y., Condron, M. M., Lomakin, A., Benedek, G. B., Selkoe, D. J., and Teplow, D. B. (1999) Amyloid β-protein fibrillogenesis: Structure and

biological activity of protofibrillar intermediates. *J. Biol. Chem.* 274, 25945−25952.

(14) Stine, W. B. J., Dahlgren, K. N., Krafft, G. A., and LaDu, M. J. (2003) *In vitro* characterization of conditions for amyloid-β peptide oligomerization and fibrillogenesis. *J. Biol. Chem.* 278, 11612−11622.

(15) Jarrett, J. T., Berger, E. P., and Lansbury, P. T. Jr. (1993) The carboxy terminus of the β amyloid protein is critical for the seeding of amyloid formation: Implications for the pathogenesis of Alzheimer's disease. *Biochemistry* 32, 4693−4697.

(16) Dahlgren, K. N., Manelli, A. M., Stine, W. B. Jr., Baker, L. K., Krafft, G. A., and LaDu, M. J. (2002) Oligomeric and fibrillar species of amyloid-β peptides differentially affect neuronal viability. *J. Biol. Chem.* 277, 32046−32053.

(17) Harper, J. D., Lieber, C. M., and Lansbury, P. T. Jr. (1997) Atomic force microscopic imaging of seeded fibril formation and fibril branching by the Alzheimer's disease amyloid-β protein. *Chem. Biol.* 4, 951−959.

(18) Koffie, R. M., Meyer-Luehmann, M., Hashimoto, T., Adams, K. W., Mielke, M. L., Garcia-Alloza, M., Micheva, K. D., Smith, S. J., Kim, M. L., Lee, V. M., Hyman, B. T., and Spires-Jones, T. L. (2009) Oligomeric amyloid β associates with postsynaptic densities and correlates with excitatory synapse loss near senile plaques. *Proc. Natl. Acad. Sci. U.S.A.* 106, 4012−4017.

(19) Deshpande, A., Mina, E., Glabe, C., and Busciglio, J. (2006) Different conformations of amyloid β induce neurotoxicity by distinct mechanisms in human cortical neurons. *J. Neurosci.* 26, 6011−6018.

(20) Lorenzo, A., and Yankner, B. A. (1994) β-amyloid neurotoxicity requires fibril formation and is inhibited by Congo red. *Proc. Natl. Acad. Sci. U.S.A.* 91, 12243−12247.

(21) Pike, C. J., Walencewicz, A. J., Glabe, C. G., and Cotman, C. W. (1991) *In vitro* aging of β-amyloid protein causes peptide aggregation and neurotoxicity. *Brain Res.* 563, 311−314.

(22) Walsh, D. M., Klyubin, I., Fadeeva, J. V., Cullen, W. K., Anwyl, R., Wolfe, M. S., Rowan, M. J., and Selkoe, D. J. (2002) Naturally secreted oligomers of amyloid β protein potently inhibit hippocampal long-term potentiation *in vivo*. *Nature* 416, 535−539.

(23) Heneka, M. T., and O'Banion, M. K. (2007) Inflammatory processes in Alzheimer's disease. *J Neuroimmunology* 184, 69−91.

(24) Sondag, C. M., Dhawan, G., and Combs, C. K. (2009) Beta amyloid oligomers and fibrils stimulate differential activation of primary microglia. *J. Neuroinflammation* 6, 1.

(25) White, J. A., Manelli, A. M., Holmberg, K. H., Van Eldik, L. J., and Ladu, M. J. (2005) Differential effects of oligomeric and fibrillar amyloid-β1−42 on astrocyte-mediated inflammation. *Neurobiol. Dis.* 18, 459−465.

(26) Ajit, D., Udan, M. L., Paranjape, G., and Nichols, M. R. (2009) Amyloid-β(1−42) fibrillar precursors are optimal for inducing tumor necrosis factor-α production in the THP-1 human monocytic cell line. *Biochemistry* 48, 9011−9021.

(27) Banati, R. B., and Graeber, M. B. (1994) Surveillance, intervention and cytotoxicity: is there a protective role of microglia? *Dev. Neurosci.* 16, 114−127.

(28) Lehrmann, E., Kiefer, R., Christensen, T., Toyka, K. V., Zimmer, J., Diemer, N. H., Hartung, H. P., and Finsen, B. (1998) Microglia and macrophages are major sources of locally produced transforming growth factor-β_1 after transient middle cerebral artery occlusion in rats. *Glia* 24, 437−448.

(29) Esen, N., and Kielian, T. (2007) Effects of low dose GM-CSF on microglial inflammatory profiles to diverse pathogen-associated molecular patterns (PAMPs). *J. Neuroinflammation* 4, 10.

(30) Yates, S. L., Burgess, L. H., Kocsis-Angle, J., Antal, J. M., Dority, M. D., Embury, P. B., Piotrkowski, A. M., and Brunden, K. R. (2000) Amyloid beta and amylin fibrils induce increases in proinflammatory cytokine and chemokine production by THP-1 cells and murine microglia. *J. Neurochem.* 74, 1017−1025.

(31) Reed-Geaghan, E. G., Savage, J. C., Hise, A. G., and Landreth, G. E. (2009) CD14 and Toll-like receptors 2 and 4 are required for fibrillar Aβ-stimulated microglial activation. *J. Neurosci.* 29, 11982−11992.

(32) Udan, M. L., Ajit, D., Crouse, N. R., and Nichols, M. R. (2008) Toll-like receptors 2 and 4 mediate Aβ(1−42) activation of the innate immune response in a human monocytic cell line. *J. Neurochem.* 104, 524−533.

(33) McDonough, R. T., Paranjape, G., Gallazzi, F., and Nichols, M. R. (2011) Substituted tryptophans at amyloid-β(1−40) residues 19 and 20 experience different environments after fibril formation. *Arch. Biochem. Biophys.* 514, 27−32.

(34) Nichols, M. R., Moss, M. A., Reed, D. K., Lin, W. L., Mukhopadhyay, R., Hoh, J. H., and Rosenberry, T. L. (2002) Growth of β-amyloid(1−40) protofibrils by monomer elongation and lateral association. Characterization of distinct products by light scattering and atomic force microscopy. *Biochemistry* 41, 6115−6127.

(35) Kielian, T. (2006) Toll-like receptors in central nervous system glial inflammation and homeostasis. *J. Neurosci. Res.* 83, 711−730.

(36) Grammas, P., and Ovase, R. (2001) Inflammatory factors are elevated in brain microvessels in Alzheimer's disease. *Neurobiol. Aging* 22, 837−842.

(37) Tarkowski, E., Andreasen, N., Tarkowski, A., and Blennow, K. (2003) Intrathecal inflammation precedes development of Alzheimer's disease. *J. Neurol., Neurosurg. Psychiatry* 74, 1200−1205.

(38) Horvath, R. J., Nutile-McMenemy, N., Alkaitis, M. S., and Deleo, J. A. (2008) Differential migration, LPS-induced cytokine, chemokine, and NO expression in immortalized BV-2 and HAPI cell lines and primary microglial cultures. *J. Neurochem.* 107, 557−569.

(39) Romero-Sandoval, E. A., Horvath, R., Landry, R. P., and DeLeo, J. A. (2009) Cannabinoid receptor type 2 activation induces a microglial anti-inflammatory phenotype and reduces migration via MKP induction and ERK dephosphorylation. *Mol. Pain* 5, 25.

(40) Jan, A., Hartley, D. M., and Lashuel, H. A. (2010) Preparation and characterization of toxic Aβ aggregates for structural and functional studies in Alzheimer's disease research. *Nat. Protoc.* 5, 1186−1209.

(41) Teplow, D. B. (2006) Preparation of amyloid β-protein for structural and functional studies. *Methods Enzymol.* 413, 20−33.

(42) Jan, A., Adolfsson, O., Allaman, I., Buccarello, A. L., Magistretti, P. J., Pfeifer, A., Muhs, A., and Lashuel, H. A. (2011) Aβ42 neuro-toxicity is mediated by ongoing nucleated polymerization process rather than by discrete Aβ42 species. *J. Biol. Chem.* 286, 8585−8596.

(43) Kheterpal, I., Lashuel, H. A., Hartley, D. M., Walz, T., Lansbury, P. T. Jr., and Wetzel, R. (2003) Aβ protofibrils possess a stable core structure resistant to hydrogen exchange. *Biochemistry* 42, 14092−14098.

(44) Garcao, P., Oliveira, C. R., and Agostinho, P. (2006) Comparative study of microglia activation induced by amyloid-beta and prion peptides: role in neurodegeneration. *J. Neurosci. Res.* 84, 182−93.

(45) Terry, R. D., Gonatas, N. K., and Weiss, M. (1964) Ultrastructural studies in Alzheimer's presenile dementia. *Am. J. Pathol.* 44, 269−297.

(46) Ye, C. P., Selkoe, D. J., and Hartley, D. M. (2003) Protofibrils of amyloid β-protein inhibit specific K+ currents in neocortical cultures. *Neurobiol. Dis.* 13, 177−190.

(47) O'Nuallain, B., Freir, D. B., Nicoll, A. J., Risse, E., Ferguson, N., Herron, C. E., Collinge, J., and Walsh, D. M. (2010) Amyloid β-protein dimers rapidly form stable synaptotoxic protofibrils. *J. Neurosci.* 30, 14411−14419.

(48) Bamberger, M. E., Harris, M. E., McDonald, D. R., Husemann, J., and Landreth, G. E. (2003) A cell surface receptor complex for fibrillar β-amyloid mediates microglial activation. *J. Neurosci.* 23, 2665−2674.

(49) Fassbender, K., Walter, S., Kuhl, S., Landmann, R., Ishii, K., Bertsch, T., Stalder, A. K., Muehlhauser, F., Liu, Y., Ulmer, A. J., Rivest, S., Lentschat, A., Gulbins, E., Jucker, M., Staufenbiel, M., Brechtel, K., Walter, J., Multhaup, G., Penke, B., Adachi, Y., Hartmann, T., and Beyreuther, K. (2004) The LPS receptor (CD14) links innate immunity with Alzheimer's disease. *FASEB J.* 18, 203−205.

(50) Stewart, C. R., Stuart, L. M., Wilkinson, K., van Gils, J. M., Deng, J., Halle, A., Rayner, K. J., Boyer, L., Zhong, R., Frazier, W. A., Lacy-Hulbert, A., Khoury, J. E., Golenbock, D. T., and Moore, K. J. (2010)

CD36 ligands promote sterile inflammation through assembly of a Toll-like receptor 4 and 6 heterodimer. *Nat. Immunol. 11*, 155−161.

(51) Meda, L., Cassatella, M. A., Szendrei, G. I., Otvos, L. Jr., Baron, P., Villalba, M., Ferrari, D., and Rossi, F. (1995) Activation of microglial cells by β-amyloid protein and interferon-γ. *Nature 374*, 647−50.

(52) McDonald, D. R., Bamberger, M. E., Combs, C. K., and Landreth, G. E. (1998) β-Amyloid fibrils activate parallel mitogen-activated protein kinase pathways in microglia and THP1 monocytes. *J. Neurosci. 18*, 4451−4460.

(53) Della Bianca, V., Dusi, S., Bianchini, E., Dal Pra, I., and Rossi, F. (1999) β-amyloid activates the O_2 forming NADPH oxidase in microglia, monocytes, and neutrophils - A possible inflammatory mechanism of neuronal damage in Alzheimer's disease. *J. Biol. Chem. 274*, 15493−15499.

(54) Hashioka, S., Monji, A., Ueda, T., Kanba, S., and Nakanishi, H. (2005) Amyloid-β fibril formation is not necessarily required for microglial activation by the peptides. *Neurochem. Int. 47*, 369−76.

(55) Heurtaux, T., Michelucci, A., Losciuto, S., Gallotti, C., Felten, P., Dorban, G., Grandbarbe, L., Morga, E., and Heuschling, P. (2010) Microglial activation depends on beta-amyloid conformation: role of the formylpeptide receptor 2. *J. Neurochem. 114*, 576−586.

(56) Parvathy, S., Rajadas, J., Ryan, H., Vaziri, S., Anderson, L., and Murphy, G. M. Jr. (2009) Aβ peptide conformation determines uptake and interleukin-1α expression by primary microglial cells. *Neurobiol. Aging 30*, 1792−1804.

(57) DaRocha-Souto, B., Scotton, T. C., Coma, M., Serrano-Pozo, A., Hashimoto, T., Sereno, L., Rodriguez, M., Sanchez, B., Hyman, B. T., and Gomez-Isla, T. (2011) Brain oligomeric β-amyloid but not total amyloid plaque burden correlates with neuronal loss and astrocyte inflammatory response in amyloid precursor protein/tau transgenic mice. *J. Neuropathol. Exp. Neurol. 70*, 360−376.

(58) Petkova, A. T., Leapman, R. D., Guo, Z., Yau, W. M., Mattson, M. P., and Tycko, R. (2005) Self-propagating, molecular-level polymorphism in Alzheimer's β-amyloid fibrils. *Science 307*, 262−265.

(59) Campioni, S., Mannini, B., Zampagni, M., Pensalfini, A., Parrini, C., Evangelisti, E., Relini, A., Stefani, M., Dobson, C. M., Cecchi, C., and Chiti, F. (2010) A causative link between the structure of aberrant protein oligomers and their toxicity. *Nat. Chem. Biol. 6*, 140−147.

CHAPTER 1

INTRODUCTION

1.1 Protein misfolding and amyloids

Protein folding represents one of the most fundamental and ubiquitous self-assembly processes in biological systems by which proteins adopt native, three-dimensional structure. Since only correctly folded protein can perform its normal biological function, this process requires precision and fidelity (Dobson, 2003). Therefore, biological systems have evolved the mechanisms involving chaperones and proteasomal systems. Chaperones involve a set of proteins which assist the folding process by directing the nascent proteins towards the correct pathway of folding, and if such mechanisms fail, proteasomal proteins degrade the misfolded proteins before causing further damage to the living organism (Sherman and Goldberg, 2001).

One of the major consequences of failure of a protein to fold correctly or retain its correct structure is its aggregation into insoluble filamentous polymers, rich in β-sheet

structure (Selkoe, 2003). When normally soluble proteins get deposited in the extracellular tissue (typically 10 nm in diameter fibrils) the condition is referred to as amyloids (Selkoe, 2003). Examples include amylin protein in diabetic pancreas and immunoglobulins in multiple myeloma (Selkoe, 2003). The term amyloid was first used by German pathologist Rudolf Virchow in 1854 to describe waxy tissue deposits for their resemblance to starch (Kyle, 2001). Later, amyloids were found to be proteinaceous rather than starchy, but the term amyloid is still widely used to describe extracellular protein aggregates (Kyle, 2001). Although some amyloids have been reported to carry out a functional role in bacteria, fungi, and mammals, most of the amyloids have been commonly associated with disease. The examples of functional amyloids include *Escherichia coli* protein curlin (Chapman, et al., 2002), spider silk, and mammalian protein Pmel17 (Fowler, et al., 2006). These benefit the host in processes like cell adhesion, propagation, and biosynthesis of melanin, pigment deposition and release of hormones. The formation of functional amyloids is under tight regulation, emphasizing the importance for balancing their formation and clearance (Fowler, et al., 2007).
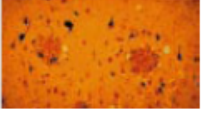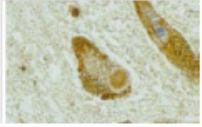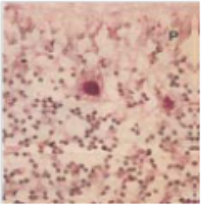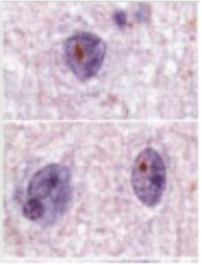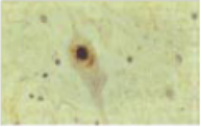
There is a class of emerging diseases in which intracellular proteins accumulate within the cells. Such aggregates resemble extracellular amyloids in their characterstic β-sheet rich structure, birefringence with aniline dyes like congo-red and insolubility. These diseases are broadly categorized as conformational diseases (Carrell and Lomas, 1997). Some of the well studied examples include Prion diseases, Huntington disease, Alzheimer's disease (AD), Parkinson's disease and Lewy body dementia. Table 1.1 lists some of the examples of such diseases and underlying protein pathology. Among these

diseases, AD is particularly different in that it shows accumulation of amyloid-forming protein both extracellularly and intracellularly (Selkoe, 2003).

All these amyloidogenic proteins listed in Table 1.1 are diverse in their size, structure, location, function and sequence, yet they can form β-sheet rich aggregates with a distinct cross-beta X-ray diffraction pattern. Interestingly, a series of studies from the Dobson laboratory have demonstrated that diverse and structurally unrelated proteins can be manipulated to form amyloids under a set of specific environmental conditions. Such amyloids are not only morphologically indistinguishable from those associated with the disease but can also exhibit cytotoxicity. These studies suggest that widely different amyloids might share a common mechanism of pathogenicity (Chiti, et al., 1999; Bucciantini, et al., 2002). This accentuates the need to understand the structural basis of aggregation on protein folding to make the disease amenable to intervention.

1.2 Alzheimer's disease

Alzheimer's disease (AD) is a debilitating progressive neurodegenerative disorder characterized by severe loss of memory and disruption of an individual's ability to think and co-ordinate different behavioral processes including speech and task performance (Thies and Bleiler, 2011). Extensive neuronal loss is observed particularly in the basal forebrain and hippocampus, resulting into significant shrinkage of brain as compared to normal age matched controls. This pathology is believed to contribute towards cognitive decline in AD (Selkoe, 2011).

Disease	Protein	Locus	Pathology
Alzheimer's disease	Amyloid-β Tau	Extracellular plaques Tangles in neuronal cytoplasm	
Fontotemporal dementia with parkinsonism	Tau	Tangles in neuronal cytoplasm	
Parkinson's disease, dementia with Lewy-bodies	α-Synuclein	Neuronal cytoplasm	
Creutzfeldt-Jacob disease; 'mad cow disease'	Prion protein (PrP^{sc})	Extracellular plaques Oligomers, inside and outside neurons	
Polyglutamine expansion diseases (Huntington's disease, spinocerebellar ataxias etc)	Long glutamine stretches within certain proteins	Neuronal nuclei and cytoplasm	
Amyotrophic lateral sclerosis	Superoxide dismutase	Neuronal cytoplasm	

Table 1.1 Some human brain diseases that are characterized by misfolding and aggregation of proteins.

AD is the most frequent cause of dementia in the aging population. It has been reported that worldwide, there were 26.6 million cases of AD in 2006, which are projected to increase by almost four times by the year 2050 without further development of a potential therapy (Hampel, et al., 2010). It is the sixth leading cause of death in the United States alone with currently 5.2 million Americans afflicted with AD. The total cost of healthcare and other related services spent towards AD is estimated to be $183 billion in the year 2011, reflecting the huge socioeconomic impact of AD (Thies and Bleiler, 2011). Since the onset of AD is age-dependent and the general population is aging, significant efforts are currently being directed toward a basic understanding of AD.

1.3 AD Pathology

Alzheimer's disease was first diagnosed in 1906 by Bavarian psychiatrist Alois Alzheimer (Selkoe and Podlisny, 2002). During the postmortem analysis of brain slices, he found two distinctive microscopic lesions, namely senile plaques (SP) and neurofibrillary tangles (NFT) in the cerebral cortex. Amyloid β protein (Aβ) was found to be a major constituent protein of senile plaques (Glenner and Wong, 1984) while hyperphosphorylated Tau protein constitutes neurofibrillary tangles (Grundke-Iqbal, et al., 1986). Apart from the senile plaques, Aβ is also found in variable amounts in the walls of arterioles, arteries, capillaries, venuoles of meninges and parenchyma in AD patients.

Long after their discovery, these lesions still form the basis of a definitive diagnosis of AD postmortem (Selkoe, 1994). The progressive development of neurofibrillary tangles and abnormal dendritic structures (neuropil threads) follows a predictable course of occurrence within the AD brain, forming the basis for Braak and Braak staging of AD brain. Braak staging involves six stages; Braak stage I-II represents entorhinal NFTs with no dementia, III-IV represents limbic NFTs with mild cognitive impairement. Further progression to neocortical NFTs in the stage V-VI is concluded as end stage severe dementia with significant neuronal loss. However, the neuronal alterations are observed even before Braak I (Braak and Braak, 1991, 1995).

1.3.1 Neurofibrillary tangles

Neurofibrillary tangles are intraneuronal fibrils of hyperphosphorylated tau protein (Grundke-Iqbal, et al., 1986). These 10 nm in diameter fibrils are typically observed as paired helical filaments (PHF) mixed with some straight filaments. Tau tangles are observed in AD brains particularly in the entorhinal cortex, hippocampal formation, amygdale and association cortices of the frontal, temporal, and parietal lobes. Intracellularly, NFTs were found not only in the neurons but also in dystrophic neurites (swollen axons and dendrites) present within and outside of the amyloid plaque (Braak and Braak, 1995).

Under normal conditions, tau is a heat stable, soluble, microtubule-associated protein, and plays an important role in the assembly and stabilization of microtubules *in vitro*. Microtubules form an important unit of the cytoskeleton, and in the central nervous

system play an important role in axonal transport and neurotransmission (Weingarten, et al., 1975). Hyperphosphorylated tau forms oligomers, which are believed to convert later into highly insoluble fibrils (Maeda, et al., 2006; Maeda, et al., 2007). It is not clear whether phosphorylation induces fibril formation, but it does reduce the affinity of tau for microtubules. As a consequence, microtubules destabilize and promote degeneration of affected neurons in AD. (Bramblett, et al., 1993). Within the tangles, hyperphosphorylated tau is shown to be associated with ubiquitin, which is a major component of the proteasomal system. Complexation with ubiquitin is regarded as an unsuccessful attempt of proteasomal system to clear tau aggregates from the brain (Selkoe, 2011). Formation of tau tangles can occur independently of amyloid plaques in other tauopathies like progressive supranuclear palsy cortico-basal ganglionic degeneration, Guam Parkinsonism dementia complex, Niemann–Pick type C, pugilistic dementia, and Pick's diseases, and in some cases leads to dementia as well (Sanchez, et al., 2001; Binder, et al., 2005; Guillozet-Bongaarts, et al., 2007; Alonso, et al., 2008).

1.3.2 Senile plaques

Senile or neuritic plaques consist of extracellular deposits of the Aβ protein and are associated with dystrophic neurites (axons and dendrites) and activated immune cells including astrocytes, and microglia (Wisniewski, et al., 1989). The dystrophic neurites located in the proximity of senile plaques display cytoplasmic inclusions as dense bodies, which show immunoreactivity for the amyloid precursor protein (APP) and ubiquitin, suggesting the presence of abnormal ubiquitination process. Several studies have shown

the presence of heparin sulfate, glycoproteins, carbohydrate residues, advanced glycation end products (Vitek, et al., 1994), racemic amino acids and isopeptide bonds in addition to Aβ within the senile plaques (Glabe, 2001). This indicates that senile plaques display an array of different molecules along with activated immune cells. Several of these molecules represent long lived proteins and components of the proteasome (Glabe, 2001).

Protein sequencing studies showed that senile plaques contains Aβ protein that can exist as 40- or 42- amino acid variants differing only at their carboxy terminus (Glenner and Wong, 1984; Iwatsubo, et al., 1994). Although insoluble Aβ fibrils form the core of a mature neuritic plaque, several immunological studies have detected the presence of other forms of Aβ within and surrrounding other plaque-like deposits (Tagliavini, et al., 1988). These Aβ species are poorly characterized but are believed to be largely amorphous. Collection of such species gives rise to diffuse plaques, which in contrast to the classical plaque, lack the presence of swollen neurites and altered glia giving it an undefined appearance. Extensive studies now support that diffuse and compact plaques are not the two extremes of Aβ morphologies within the AD brain but, in fact, they represent a continnum in which Aβ species of varying size and structure exist in a complex equillibrium (Selkoe, 1994). These species display varying degrees of altered neuritis and gliosis associated with them. It is believed that the diffuse plaques are "preamyloid", which ultimately evolve into mature senile plaques (Lemere, et al., 1996).

1.4 Generation of Aβ from amyloid precursor protein (APP)

Aβ peptide is a product of a sequential proteolytic cleavage of a larger precursor protein called amyloid precursor protein (APP) (Kang, et al., 1987) (Figure 1.1). APP is a single membrane-spanning glycoprotein containing 695 amino acid residues. The single gene encoding APP is located on chromosome 21, which provides an explanation for AD-like pathology seen in individuals with Down's syndrome having trisomy 21 (three copies) in terms of gene dosage effect (Kang, et al., 1987; Goate, et al., 1989). While glia can produce APP, neurons are the major source of APP within the brain (Selkoe, 1994).

APP belongs to an evolutionarily conserved protein family, which shares similarity with the NOTCH family of receptors. Notch proteins are important determinants of cell fate during early development. A mouse deficient in APP did not show any adverse phenotypes. However, a double knockout (KO) mice with a combined deficiency of both APP and its homolog resulted in a lethal phenotype (von Koch, et al., 1997; Heber, et al., 2000). Different "loss of function" and "gain of function" mutants of APP in a variety of model systems including mouse, zebrafish, *Caenorhabditis elegans*, *Drosophila melanogaster* have indicated a role for APP in cell adhesion, neuron migration, synaptogenesis and early neuronal development (Selkoe and Podlisny, 2002; Guo, et al., 2011). APP KO mice not only showed behavioral defects in locomotor activity and passive avoidance learning, but also displayed defective long term potentiation (LTP) and increase in gliosis (Dawson, et al., 1999; Phinney, et al., 1999; Seabrook, et al., 1999; Senechal, et al., 2008).
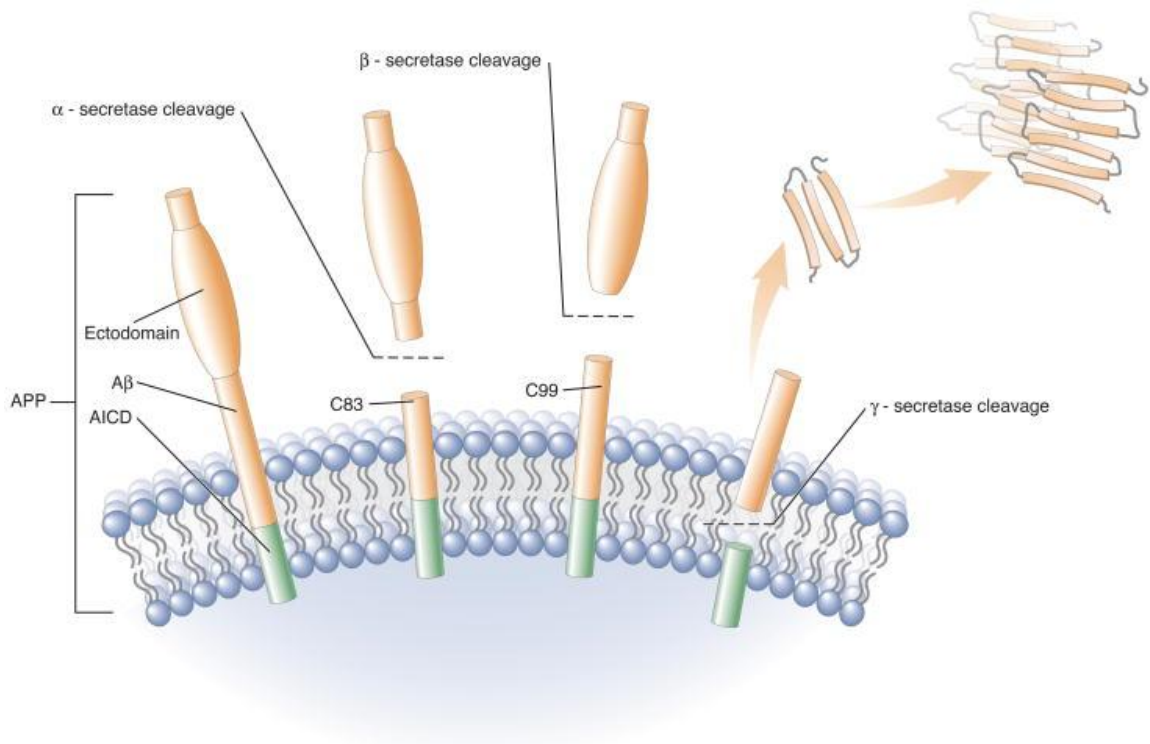
Figure 1.1 Generation of Aβ from APP by proteolytic processing (reproduced from (Li, et al., 2009a). Stepwise proteolytic processing of APP by α-, β-, and γ-secretases. Major cleavage sites of the three secretases in APP are indicated by dashed horizontal lines. The transmembrane domain is shown as a cylinder. The Aβ-domain is shown in orange, and the APP intracellular domain (AICD) in green. Aβ, amyloid β peptide; AICD, APP intracellular domain; APP, amyloid precursor protein; C83, 83-residue APP C-terminal fragment; C99, 99-residue APP C-terminal fragment.

The APP gene undergoes alternative splicing to generate multiple isoforms of different amino acid lengths (Kang, et al., 1987). APP processing also involves post translational modifications like O- and N-linked glycosylation, sulfation and phosphorylation in addition to its cleavage by a number of proteolytic enzymes called secretases to release various fragments of APP (Selkoe, 1994). One of the noteworthy features of APP is its constitutive processing by regulated intramembrane proteolysis (RIP). APP is acted upon by α- or β-secretase to release the soluble ectodomain α-sCTF or β-sCTF respectively. The remaining membrane bound CTF (c83 or c95) is then cleaved by γ-secretase to give rise to p3 or Aβ respectively. With α-, γ-secretase, Aβ domain is cleaved in the middle, preventing the formation of intact Aβ (Sisodia, et al., 1990). On the other hand, β-secretase, also known as β-site APP-cleaving enzyme (BACE-1), acts near the N-terminus of the Aβ domain, followed by γ-secretase cleavage in an intramembrane fashion. Thus, resulting intact Aβ peptide contains 28 residues from outside the membrane and 12-14 residues of transmembrane domain. Since γ-secretase cleavage is heterogeneous, it produces Aβ of 37-43 amino acid in length (Seubert, et al., 1993). Aβ(1-40) is the predominant variant produced as a result of amyloidogenic pathway followed by Aβ(1-42). γ-secretase is a multiprotein complex consisting of 4 proteins. These include presinilin 1 (PS-1), an aspartyl protease which carries out the catalysis along with Nicastrin, APH-1 and Presinilin 2 (PS-2). Together they form an active enzyme complex (De Strooper, et al., 1998; Edbauer, et al., 2003).

Both Aβ (1-40) and (1-42) are found to be constitutively present in CSF of normal individuals in nanomolar concentrations. Due to the presence of Aβ in CSF, other biologic fluids and conditioned cell culture media under normal circumstances of APP

processing, it is believed that AD represents an impairment in the balance between Aβ

production and clearance (Seubert, et al., 1992; Shoji, et al., 1992; Haass, et al., 1994;

Walsh, et al., 2000). Therefore, proteins that are a part of amyloidogenic processing of

APP, including BACE-1, γ-secretase, make obvious and major drug targets against AD.

1.5 Genetic basis of AD

Although, most of the AD cases are typically late onset (LOAD) and sporadic in

nature, familial forms of the disease were identified after the discovery of APP (Selkoe

and Podlisny, 2002). AD is categorized to be of a familial form based on the history of

an AD type-demented individual in the family. Approximately 10% of the AD cases are

familial, which follow the autosomal dominant, Mendelian pattern of inheritance. The

rest of the cases display a more complex pattern of inheritance. 50% of early onset AD

(EOAD) cases are linked to mutations in three genes namely APP, PS1 and PS2, which

have a role in the processing of APP as discussed earlier in section 1.4, and generate

amyloidogenic Aβ(1-42) peptide to a greater extent (Selkoe and Podlisny, 2002). So far,

33 mutations in APP, 194 mutations in PS1 and 20 mutations in PS2 are reported to exist

worldwide based on the AD and frontotemporal dementia (FTD) mutation database

(http://www.molgen.ua.ac.be/ADMutations).

APP mutations are less common and their carriers are heterozygotes. Most of the

APP missense mutations leading to AD are located within or near α, β or λ-secretase

cleavage sites, external to the Aβ sequence, and appear to operate via gain of toxic

amyloidogenic function mechanism (Selkoe and Podlisny, 2002; Selkoe, 2011). Typically mutations in β-secretase lead to increased levels of total Aβ. α-secretase mutants generate Aβ, which in turn accelerates amyloidosis, and γ-secretase mutants increase the ratio of Aβ(1-42) to Aβ(1-40) by increasing the production of longer Aβ peptide, which is more prone to aggregation (Mullan, et al., 1992; Citron, et al., 1994; Suzuki, et al., 1994; Scheuner, et al., 1996; Selkoe, 2011).

Intra-Aβ mutant phenotypes differ in the distribution of deposits, levels of Aβ and other AD related cognitive symptoms. E22Q (Dutch), A21G (Flemish), E22K (Italian), E22G (Arctic), and D23N (Iowa) are some of the well studied intra Aβ mutations. These mutant peptides appear to affect the biochemistry of Aβ aggregation and fibrillization kinetics during *in vitro* studies. E22Q (Dutch) and A21G (Flemish) mutants result in the intracerebral haemorrhage whereas the E22G (Arctic) mutation leads to rapid formation of protofibrils *in vitro* (Levy, et al., 1990; Hendriks, et al., 1992; Nilsberth, et al., 2001).

The identification of genetic mutations causing AD have led to the development of a number of animal model systems, especially in mice, which display differential degrees of amyloid plaque burden and have provided important insights into the mechanism of AD and development of therapeutic strategies (Duyckaerts, et al., 2008). A transgenic mice bearing a mutant human PS1 showed an increase in Aβ production, behavioral deficits, impaired calcium homeostasis, altered axonal transport and tau phosphorylation (Mattson, et al., 2001; Lazarov, et al., 2007). Double transgenic mice harboring both APP and BACE1 mutations showed an increased number of diffuse deposits and resulted in decreased Aβ levels accompanied by severe neurodegeneration. BACE-1 knockout (KO) mice not only ameliorated amyloid pathology by decreasing Aβ

production, but also were able to rescue the behavioral and neurodegenerative deficits in several studies underscoring the importance of BACE-1 in AD pathogenesis. APP and PS1 double transgenic mice harboring 5 different FAD mutations (5XFAD) can develop lesions as early as two months of age. APP/PS1 double KO mice were not viable or had severe cognitive deficiency with large quantities of C99 fragments. These and several other studies strongly support a causal role of Aβ in AD pathogenesis via impairment of normal APP processing.

In late onset familial and sporadic cases, the prevalence of apolipoprotein A4 (ApoE4) allele is linked to the predisposition of AD, which accounts for more than 95% of AD cases (Mahley, 1988; Corder, et al., 1993; Saunders, et al., 1993; Strittmatter, et al., 1993). The Apo E protein plays an important role in lipid metabolism and cholesterol homeostasis in the brain (Mahley, 1988). Apo E gene occurs in 4 different isoforms E1, E2, E3 and E4. Apo E4 allele-bearing individuals tend to develop AD in a manner that is dependent of dose of ApoE4 allele, although the presence of Apo E4 is neither necessary nor sufficient to cause AD (Daw, et al., 2000; Kowalska, 2004). Tumor necrosis factor α (TNFα), interlekin 1 (IL-1) and α2-macroglobulin are also considered to be susceptibility genes for AD (Daw, et al., 2000). ApoE isoform-dependent predisposition to AD can be explained by a variety of mechanisms, including modulation in total Aβ levels, formation of plaques and their clearance, tau tangle formation and impairment of neuronal signaling pathways (LaDu, et al., 1994; Beffert and Poirier, 1996; Herz and Beffert, 2000; Holtzman, et al., 2000; Raber, et al., 2000; Huang, et al., 2001; Buttini, et al., 2002; Huang, 2011). However, the exact contribution of ApoE isoform to AD pathogenesis remains unclear. Altogether, both *in vitro* and *in vivo* genetic studies of AD have

implicated an important role for Aβ in AD pathogenesis via a number of diverse mechanisms, and in combination with different susceptibility genes, provide a basis for a potential combinatorial therapeutic approach.

1.6 Central role of Aβ in the AD pathogenesis

In AD, accumulation of Aβ preceeds the appearance of tau tangles, but taupathies do not induce secondary deposition of Aβ. The most solid support for a causal role of Aβ came from the fact that EOAD occurs due to mutations in the genes primarily involved in the processing of Aβ, which give rise to clinically similar AD phenotypes as in LOAD cases. Moreover, intra-Aβ mutations develop AD pathology by altering the aggregation kinetics of Aβ. In contrast, mutations in tau cause tauopathy and dementia, but do not display amyloid plaques (Spillantini, et al., 1998). Thus, tauopathies can be regarded as a result of different neurologic insults rather than being specifically an outcome of AD (Hardy and Selkoe, 2002; Selkoe, 2011).

When mice expressing mutant tau were crossed with Tg2576 transgenic mice bearing a mutated APP, the tau tangle formation was enhanced as compared to single Tg mice with tau mutation (Lewis, et al., 2001). Aβ alone induced phosphorylation of tau and loss of cholinergic neurons in rat primary septal culture but caused neurotoxicity in hippocampal cultured neurons only in the presence of tau (Rapoport, et al., 2002; Zheng, et al., 2002).

Even though development of animal models which perfectly reproduce the full phenotype of AD has been elusive, several models of AD carrying FAD mutations have shown an increase in amyloid plaques in the absence of NFTs (Games, et al., 1995; Duff, et al., 1996; Hsiao, et al., 1996; Chen, et al., 2000; Lewis, et al., 2001) and still have some memory and learning deficiency (Wong, et al., 2002). The fact that Down's syndrome patients develop diffuse amyloid plaques very early in their lifetime, followed by classic neuritic plaque and tangles in their thirties and forties accompanied by AD-like dementia, strongly favors the hypothesis that Aβ deposition precedes AD pathogenesis (Lemere, et al., 1996). Some normal aged individuals and AD patients display the presence of diffuse plaques without any cognitive dysfunction, which in part is believed to be due to lack of transition of diffuse plaques into neuritic plaques (Selkoe, 2000).

Also, both active immunization studies using synthetic Aβ and passive immunization studies using anti-Aβ antibodies of AD transgenic mice prevented not only amyloid deposition but also reduced related neuritic dystrophy and astrogliosis. This indicates the potential of Aβ as an effective target for preventing AD (Schenk, et al., 1999; Bard, et al., 2000; Janus, et al., 2000). Collectively, these observations suggest that Aβ deposition might be the primary event in AD pathogenesis, followed by interaction of tau and other risk factors like ApoE with Aβ to display a complete phenotype of AD (Hardy, et al., 1998).

1.7 Aggregation of Aβ

Aβ protein has a high propensity to self aggregate in an orderly manner to form long fibrils 4-10 nm in diameter. Under normal conditions, monomeric Aβ is highly soluble. By some yet unknown mechanism, Aβ starts to self aggregate forming amyloids which get deposited in the brain. Between the two carboxy terminal variants of Aβ, Aβ (1-42) has a much higher propensity to aggregate than Aβ (1-40) (Jarrett, et al., 1993). This difference is attributed to the presence of two additional amino acids on carboxy terminal namely, Isoleucine and Valine, making Aβ (1-42) slightly more hydrophobic than Aβ (1-40). Moreover, Aβ (1-42) is resistant to degradation by proteases like collagenase and pepsin (Glenner and Wong, 1984; Masters, et al., 1985a).

Interestingly when Down's syndrome brains were used as model system to gain insights into the initiation and progression of AD, Aβ(1-42) was the first form to get deposited in the diffuse plaques in the earlier stages while Aβ (1-40) was predominant variant in vascular tissue and neuritic plaques during later stages (Lemere, et al., 1996). Also, FAD cases display elevated Aβ(1-42) levels (Hsiao, et al., 1996), and higher Aβ(1-42) plasma concentration is a susceptibility factor for AD (Mayeux, et al., 1999). All these observation suggests a critical role for Aβ(1-42), which is believed to be a result of its higher aggregation propensity (Jarrett, et al., 1993).

Synthetic Aβ peptides readily form fibrils *in vitro* that are indistinguishable from those directly isolated from AD brains (Kirschner, et al., 1987; Halverson, et al., 1990; Barrow and Zagorski, 1991; Hilbich, et al., 1991). This work had a huge impact on the Aβ field since it further led to a number of studies to understand the structure,

mechanism, kinetics, and intermediates of the fibril assembly process at the molecular level which are still under active investigation. The Aβ sequence has 14 consecutive hydrophobic residues at the C-terminus with a prevalence of valine and isoleucine, which are β-branched residues, and the presence of glycine every fourth residue (Jarrett and Lansbury, 1992). Consequently, peptides with a longer carboxy terminus are less soluble in aqueous media than the shorter fragments containing N-terminal residues, particularly at physiologic pH. Despite the differences in the solubility, they retain the ability to form amyloid fibrils. The central part containing residues 19-28 was found to be crucial for fibril formation, and the length of the carboxy terminal was found to contribute towards the stability of fibrils by stabilizing β-sheets. Accordingly, Aβ (1-42) fibrils are more stable and less soluble than other shorter carboxy variants (Gorevic, et al., 1987; Hilbich, et al., 1991; Burdick, et al., 1992). The KLVFF motif at position 16-20 has been shown to be crucial for fibrillogenesis (Tjernberg, et al., 1996).

Aβ-fibrillization displays a nucleation-dependent polymerization mechanism (Jarrett and Lansbury, 1992). The formation of a nucleus or seed is the first step followed by addition of monomers to the already formed nucleus, which results in fibril elongation and growth. After the linear growth phase, fibril formation reaches a plateau where the monomer and fibrils are in equillibrium. Formation of the nucleus is a comparatively slower phase and represents a lag before linear growth into fibrils. The extent of lag time is influenced by the concentration of monomer. Nucleation represents the rate-limiting step of Aβ-fibrillization (Burdick, et al., 1992; Jarrett and Lansbury, 1992). The driving force for fibril formation was proposed to be entropy driven based largely on the hydrophobic effect (Hilbich, et al., 1991). Multiple lines of evidence for oligomeric

18

intermediates make the fibrilization process less straightforward than once thought (Bitan, et al., 2003)

Aβ aggregation is influenced by a number of parameters *in vitro* including pH, concentration, temperature, length of the hydrophobic carboxy terminus, and time of incubation after solubilization of Aβ (Burdick, et al., 1992). The rate and extent of aggregation is higher at acidic pH as compared to neutral pH. In fact, pH 5-6 was found to increase the rate of formation of plaque-like insoluble aggregates due to the insolubility of Aβ around its isoelectric point (5.5) (Barrow and Zagorski, 1991; Burdick, et al., 1992). The pH dependence of Aβ-aggregation has several important biological implications. It is postulated that fibril formation might take place in the low pH environment of lysosomes during APP processing, and its leakage outside the cells can nucleate extracellular fibril formation (LaFerla, et al., 2007).

1.8 Kinetics of Aβ aggregation

Understanding the kinetics of Aβ fibrillization in terms of rate constants is valuable for the development of pharmacological agents which can interfere with plaque formation. In nucleation-dependent polymerization, a certain critical concentration of monomer is required, above which the formation of polymer ensues (Harper and Lansbury, 1997). Two pathways are proposed for Aβ-fibrillogenesis based on the aggregation reactions monitored by quasielastic light scattering (QLS) spectroscopy also known as dynamic light scattering (DLS), which is sensitive to the light scattered by

aggregation species of different sizes. QLS thus determines the hydrodynamic radius (R_H) of the particles based on their average diffusion coefficients.

In one pathway of fibrillogenesis, when the concentration of monomer exceeds critical concentration, Aβ form micelles, which are in equilibrium with monomer. Micelles increase the local concentration of Aβ monomer, which in turn favors the formation of a nucleus (Lomakin, et al., 1997) (Figure 1.2). In fact, surface tension measurements showed that Aβ forms miceller structures by reducing the surface tension of water in a manner similar to that of amphipathic detergents (Soreghan, et al., 1994). The nucleus then acts as a site for elongation by further addition of monomers resulting in fibrillization. Therefore, in such a case, the rate of initial elongation is independent of initial monomer concentration. When monomer concentration is below the critical concentration, the fibrillization can be influenced by the number of pre-existing heterogeneous or non-Aβ nuclei (Hartley, et al., 2008). Thus, Aβ fibrillization is proposed to be governed by three main parameters, namely rate constant of nucleation k_n, rate constant of elongation k_e and critical concentration c*. However, in a dynamic biological environment, various other parameters might influence the fibrillization of Aβ in a complex manner, for example by complexation of Aβ monomers with a protein to form a nucleus for fibril elongation (Lomakin, et al., 1996; Lomakin, et al., 1997; Hartley, et al., 2008).

Aβ (1-40) has an almost 5-fold higher critical concentration than Aβ (1-42) (Harper and Lansbury, 1997). *In vivo* concentrations of Aβ are in the nanomolar range, which is much lower than the critical concentration. It is believed that local supersaturation is achieved and conserved for a timescale, which allows the
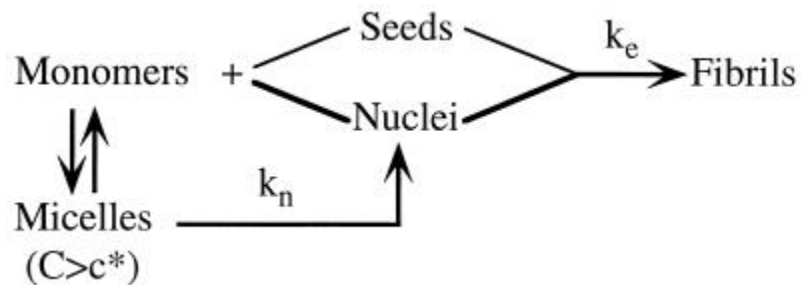
Figure 1.2 Kinetic model of Aβ fibrillogenesis (reproduced from Lomakin 1997).
Aβ monomers can form fibrils in a nucleation-dependent polymerization via two different
mechanisms. In one mechanism,nucleation takes place on the pre-existing seeds. In
other mechanism, formation of micelles take place when monomer concentration C
exceeds the critical concentration c*. Micelles are formed in a rapid equilibrium with
monomers, and spontaneously nucleate with a rate k_n. The seeds or nuclei are further
elongated by addition of free monomers.   The rate constant of elongation (k_e) is
proportional to the concentration of free monomer.

nucleation and further polymerization within cellular compartments (Jarrett and Lansbury, 1992; Harper and Lansbury, 1997; Lomakin, et al., 1997).

1.9 Structure of Aβ fibrils

Cross-β motif is the major motif found in amyloid fibril structure (Eanes and Glenner, 1968). A number of studies including X-ray diffraction (Sunde and Blake, 1997), electron diffraction (Serpell, et al., 2000), cryogenic EM (cryo-EM) (Serpell and Smith, 2000), proteolysis, chemical cross linking and mutagenesis supported the existence of cross-β structure in amyloid fibrils. Cross-β structure represents a pattern where β-sheets run nearly perpendicular to long fibril axis and backbone hydrogen bonds linking individual β-strands together run parallel to the long fibril axis (Eanes and Glenner, 1968).

Solid state NMR structural studies are particularly useful in assigning structural constraints in the amyloid fibrils due to the fact that the non-crystalline and largely insoluble nature of fibrils make them less amenable to molecular level structural determination by X-ray diffraction and liquid state nuclear magnetic resonanace (NMR). Earlier solid state NMR studies using a nine-residue fragment Aβ (34-42) predicted the presence of antiparallel β-sheets with alternating hydrogen bond registries (Lansbury, et al., 1995). Solid state NMR study using a longer fragment Aβ (10-35) showed the nature of β-sheets to be parallel (Benzinger, et al., 1998; Antzutkin, et al., 2000), which was found to be the most common orientation in Aβ (1-40) and Aβ (1-42) fibrils in a number

of studies (Antzutkin, et al., 2000; Antzutkin, et al., 2002; Balbach, et al., 2002). This was further supported by several independent studies employing EM, XRD, electron paramagnetic resonance and Hydrogen/deuterium exchange. Antiparallel β-sheet structure was found to be adopted by shorter Aβ fragments including Aβ (16-22), (34-42), (11-25) (Balbach, et al., 2000; Petkova, et al., 2004) and also in Aβ mutant peptide carrying D23N (Iowa) mutation (Tycko, et al., 2009).

The most widely accepted model of amyloid fibrils is based on solid state NMR studies on Aβ(1-40) fibril (Petkova, et al., 2002). It shows residues 10-22 and 30-40 forming β-strands flanked by a loop between residues 23-29 with residues 1-8 being disordered as shown (Figure 1.3). Thus, hydrophobic residues make the core, which is stabilized by extensive hydrophobic interactions, whereas the polar side chains are exposed to the outer surface of fibrils. Oppositely charged D23 and K28 form a salt bridge inside the core which along with in-register parallel β-sheet alignment contributes to the stability of hydrophobic interactions.

Interestingly Aβ fibrils were shown to display subtle structural differences at the molecular level based on a solid state NMR study (Petkova, et al., 2005). Moreover, these differences were dependent on the physical conditions employed during fibril growth. More importantly, subtle differences in the molecular structure were shown to have a significant effect on their toxicity to neuronal culture. Furthermore, addition of preformed fibril seeds to unaggregated solution formed fibrils structurally identical to the seeds. This study further implicated that subtleties in the structure of Aβ fibrils were governed by mechanism of its nucleation rather than primary sequence of the peptide or thermodynamic stability of the
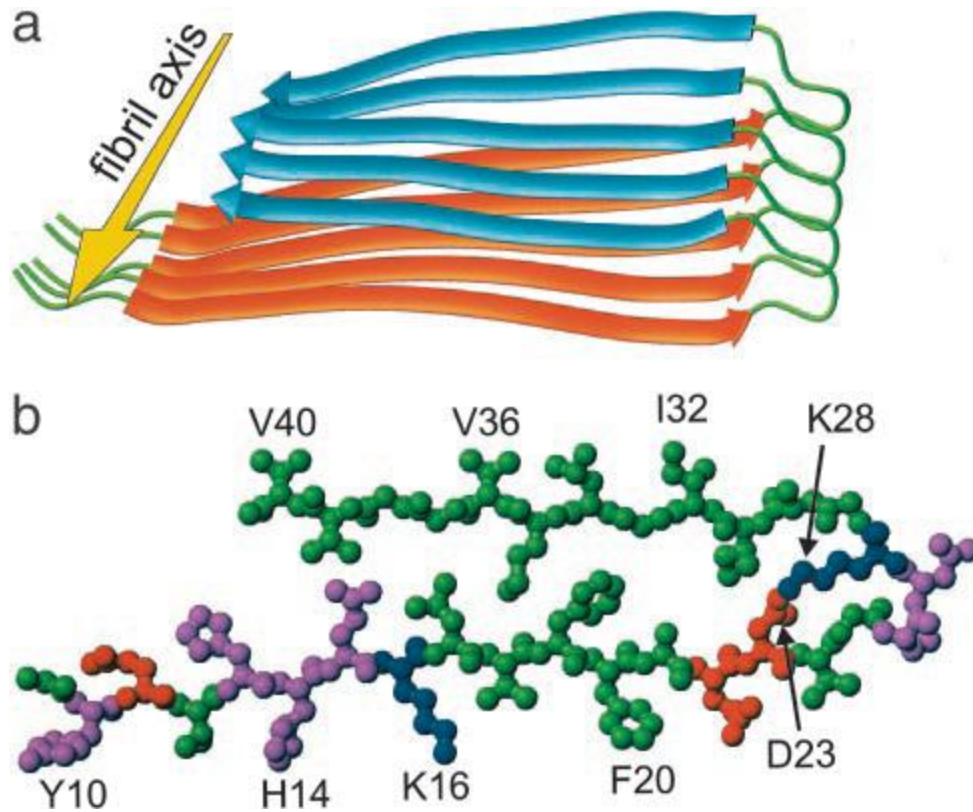
Figure 1.3 Structural model for Aβ(1-40) fibrils based on the solid state NMR constraints. (reproduced from (Petkova, et al., 2002)). a. Schematic representation of a single cross-β unit. The yellow arrow indicates the direction of long fibril axis, which is parallel to the intermolecular backbone hydrogen bonds. Cross-β unit has double molecular layer, with in-register parallel β-sheet by residues 12-24 (orange ribbons) and 30-40 (blue ribbons). b. Central Aβ(1-40) molecule from energy minimization of five-shain system, viewed down the long axis of fibril. Color coded residues depicts the nature of side chains hydrophobic (green), magenta (polar), positive (blue) and negative (red).

structure (Stine, et al., 2003; Petkova, et al., 2005; Shivaprasad and Wetzel, 2006; Tycko, 2011).

1.10 Amyloid cascade hypothesis

The amyloid cascade hypothesis was put forth by Hardy and Higgins in 1992 to describe the possible sequence of events which leads to development of AD. The amyloid hypothesis proposed a causal role for Aβ in AD. Aβ peptide itself or products of APP processing can be neurotoxic. Aβ deposition into senile plaques was thought to be the primary event, which is followed by a number of secondary events, culminating in neuronal cell death and dementia. In sporadic AD cases, which are more common than the familial cases, AD might be a result of one or more factors that initiate Aβ deposition (Hardy and Higgins 1992).

Amyloid hypothesis is further supported by the *in vitro* observations that suggested that Aβ fibril formation is needed to exert its neurotoxicity (Mattson, et al., 1993; Pike, et al., 1993; Lorenzo and Yankner, 1994). One of the mechanisms of Aβ-induced neurotoxicity is shown to be mediated by destabilization of calcium homeostasis. Moreover, impaired calcium metabolism resulted into hyperphosphorylation of tau and subsequent formation of NFTs (Mattson, et al., 1992; Mattson, et al., 1993). This study suggests that tau pathology can be a seconday consequence of Aβ-accumulation. Moreover clinically Aβ deposition is known to preceed tangle formation (Braak and Braak, 1991).

1.11 Challenges of amyloid cascade hypothesis

Recent developments in the AD field have led to some challenges for the amyloid cascade hypothesis. The most significant of the challenges is that no correlation was observed between amyloid plaque burden and cognitive decline (Lue, et al., 1999; Naslund, et al., 2000). Different parameters representing the plaque burden, including total Aβ, total insoluble Aβ, Aβ immunereactive plaques or thioflavin-T positive Aβ deposits, do not seem to correlate with synaptic loss. In contrast to insoluble Aβ, the disease severity is found to be well correlated to soluble Aβ levels (Naslund 2000, Lue 1999, McLean 1999). Genetic mutations which lead to AD display variation not only in the age of disease onset but also in the AD symptoms (Hardy and Selkoe 2002).

Also, several sensitive biophysical and immunological methods have detected the presence of soluble, metastable, and oligomeric intermediates. It is not yet clear if these structures represent a single pathway of fibril formation or are merely the products of several other aggregation pathways not necessarily leading to fibril formation. Although less knowledge is available on the formation and abundance of these intermediate species, there is fairly solid evidence for their existence and role in synaptotoxicity. Thus, there is emerging support for the role of oligomers as the main culprits causing neuronal damage well before plaque formation. In this view, the plaques are regarded as the inactive sink or reservoir, where Aβ species are in equilibrium with smaller, potentially neurotoxic species (Koffie, et al., 2009). This in turn might partially explain the failure of drugs clearing amyloid plaques in clinical trials

(http://newsroom.lilly.com/releasedetail.cfm?releaseID=499794). It is speculated that plaque clearing drugs in fact might lead to release of toxic oligomeric species from the plaques, worsening the disease.

According to recent clinical reports, a significant number of human subjects were found to be cognitively normal despite the presence of amyloid plaques in their brains (Morris, et al., 2009; Rentz, et al., 2010). On similar lines, cognitive impairment and inhibition of LTP was observed well before or completely independent of plaque formation in transgenic animal models of AD. (Moechars, et al., 1999; Mucke, et al., 2000). While these new findings do not quite fit within the framework of the amyloid hypothesis, there is still significant support for the role of Aβ as a primary causal agent in AD.

1.12 Aβ oligomers

Aβ oligomers are comprised of Aβ species which are soluble and remain in the supernatant even under the influence of high centrifugal force. Aβ oligomers are shown to display a wide range of sizes and structures as evidenced by a number of biophysical and imaging techniques. So far, the nomenclature of oligomers is elusive and mostly has been based loosely on either the actual morphology as detected by imaging techniques such as atomic force microscopy (AFM), EM, or in some cases, their apparent size on a SDS-PAGE gel. There are a variety of reasons that complicate a standard analysis of oligomers. It is now well established that a number of physical factors like pH, ionic

strength, temperature and time of incubation largely dictate the aggregation of Aβ, which in turn influences the nature of oligomers it can form. In some cases, the Aβ solutions were supplemented with small amounts of either some protein factors (ADDLs) or organic solvents (Oda, et al., 1995; Lambert, et al., 1998; Stine, et al., 2003; Kayed, et al., 2009) in addition to the medium in which Aβ was resuspended. Interestingly, most of these oligomers were found to be present in the AD brain samples or transgenic mouse models with the help of specific antibodies, underscoring the relevance of *in vitro* oligomer studies in the context of actual disease pathology.

There is mounting evidence that Aβ oligomers are responsible for synaptotoxicity, which provides an explanation for the observed neuronal loss well before the detection of plaques. Recently, oligomeric Aβ was found to form a halo around the dense plaques by multiphoton *in vivo* imaging using an oligomer-specific NAB1 antibody, making the plaque composition look more complex than just a deposition of fibrillar Aβ. Interestingly, neuronal loss was observed in the immediate vicinity of this oligomeric halo (Koffie, et al., 2009). The studies on preparation and analysis of Aβ oligomers started in the late nineties. In the past couple of decades, a number of oligomeric species were reported, which includes protofibrils, ADDLs, annular protofibrils, prefibrillar and fibrillar oligomers, globulomers, paranuclei, and Aβ56*. It is still not clear if all these oligomers signify the same structure or represent a unique species in its own sense.

1.12.1 Protofibrils

In 1997, Harper *et al*, observed metastable protofibrils by AFM while studying fibrillization of both Aβ (1-40) and Aβ (1-42). The diameter of Aβ (1-42) protofibril was 4.2 nm while the diameter of Aβ (1-40) protofibril was 3.1 nm. The lengths were reported to be in the range of 70-100 nm, and over the time protofibrils disappeared to form < 1μm long fibrils of 7-8 nm diameter. Protofibrils of both Aβ variants exhibited periodicity of 22 nm (Harper, et al., 1997).

Walsh, *et al* (1997), independently reported the detection of small, soluble, and curvilinear structures, which they also called protofibrils to distinguish them from mature fibrils. TEM analysis revealed protofibrils to be 100-200 nm long consistent with Harper, *et al* (1997), and 6-10 nm in diameter and had morphology similar to small fibrils (Walsh, et al., 1997). Rotatory shadowing of protofibrils essentially complemented the morphological analysis by TEM except a large number of <10 nm protofibrils could be observed, and a beaded pattern of 3-6 nm periodicity was revealed within protofibrils (Walsh, et al., 1999).

Protofibrils have an average R_H between the range 10-50 nm based on QLS. The determination of molecular weights of protofibrils is not quite straightforward because of the non-ideal chromatographic behavior on a size exclusion column and disaggregation into monomers and low molecular weight oligomers upon separation on SDS-PAGE. Using dialysis, radiolabeled SEC purified protofibrils were found to be in equilibrium with low molecular weight Aβ (Walsh, et al., 1999).

Walsh and colleagues (1997) used a Superdex 75 size exclusion column to separate protofibrils from low molecular weight Aβ. During separation, protofibrils typically eluted out in the void volume. Protofibrils are formed at physiological pH in a solution of considerable ionic strength. Ionic strength influences the length and rate of protofibril growth (Harper, et al., 1999). Aβ (1-42) formed the protofibrils within 1 day of incubation, while Aβ (1-40) required a longer incubation before it formed the protofibrils. The size exclusion chromatography (SEC) protofibril peak increased in size over time with a concomitant decrease in monomer peak, and eventually both the peaks declined, indicating that protofibrils are intermediates during fibrillogenesis.

A significant amount of β-sheet content was suggested both by a significant thioflavin −T/Congo red binding and circular dichroism. Although a decent amount of random coil and some α-helical content was observed, the CD spectrum was similar to fibrils. Furthermore, substitution of residues within the hydrophobic core by glycine or proline, which destabilizes β-sheets, resulted in very little or no protofibril formation, suggesting the importance of the hydrophobic core in protofibril formation (Walsh, et al., 1997; Walsh, et al., 1999; Kheterpal, et al., 2003). Subsequently, HDX-MS confirmed that 40% of the amide protons comprising the core of protofibrils are highly protected. Additionally, the degree of protective structure increases from monomers to protofibrils to fibrils (Kheterpal, et al., 2003).

Protofibrils displayed a significant biological activity, as they stimulated acute electrophysiological changes, altered metabolism and caused neurotoxicity in primary rat cortical neurons in contrast to LMW Aβ (Hartley, et al., 1999; Walsh, et al., 1999). The direct support for biological relevance of protofibrils came from the discovery that a

familial APP mutation, E693G (Arctic) from a family in northern Sweden displayed a high propensity to form protofibrils rapidly as compared to WT. Interestingly, Arctic mutation is the only mutation among other intra-Aβ mutations which produces a classical AD phenotype (Nilsberth, et al., 2001).

When Aβ (1-40) WT and arctic protofibrils eluting in the void volume of Superdex 75 column were further subjected to a Superose 6 SEC column, different fractions contained protofibrils of different size (160 kDa-800 kDa) and morphology. Among other structures, one of the notable structures observed using EM and single particle averaging was annular protofibrils having an average diameter of 6-9 nm with a central cavity of 1.5-2 nm diameter filled with the negative stain. These structures were named amyloid pores, and are believed to disrupt the membrane integrity in a fashion similar to bacterial pore forming toxins (Lashuel, et al., 2003). Recently, protofibrils generated by aggregation of disulfide bond stabilized dimers of (AβS26C)$_2$ inhibited LTP while freshly prepared (AβS26C)$_2$ did not have any effect (O'Nuallain, et al., 2010). Transgenic mice harboring both Arctic and Swedish mutations formed substantial protofibrils well before plaque formation, and their amount was inversely correlated to spatial learning and memory deficits (Lord, et al., 2009). However, in some studies, the biological activity of protofibrils was attributed to the ongoing polymerization process in the presence of monomers in addition to protofibrils (Wogulis, et al., 2005).

Elongation of protofibrils can follow end to end annealing or addition of monomers to the ends (Harper, et al., 1999). Nichols et al (2002) showed that protofibril growth can also occur via lateral association (Nichols, et al., 2002). Elongation of protofibrils is shown to be dependent on pH, ionic strength, temperature and

31

concentration of Aβ (Harper, et al., 1999), while the dissociation into monomers was seen mainly after dilution. Interestingly, some lipids are shown to disassemble fibrils backward into protofibrils, which are indistinguishable from those formed during forward assembly and also are neurotoxic (Martins, et al., 2008).

1.12.2 Aβ-derived diffusible ligands (ADDLs)

ADDLs are reported as small, slowly sedimenting, globular Aβ (1-42) species of mass between 17-42 kDa and having a diameter 4.8-5.7 nm as measured by AFM (Oda, et al., 1995). ADDLs were originally prepared in the presence of clusterin (Apo J), a protein upregulated in the AD brain. Clusterin slows down the aggregation of Aβ into fibrils, instead forming soluble, globular species (Oda, et al., 1995). ADDLs could also be prepared in the absence of clusterin by either incubating Aβ (1-42) in phenol red-free F12 cell culture medium at 4°C for 24 h or at 37°C in brain slice culture medium for 24h (Lambert, et al., 1998).

ADDLs rapidly block hippocampal LTP and act as potent neurotoxins effective at nanomolar concentration. ADDL toxicity is found to be dependent on expression of Fyn, a tyrosine kinase of the Src family, the levels of which are upregulated in the neurons isolated from AD brain (Lambert, et al., 1998). Soluble oligomers in the AD brain were found to be 70-fold in excess of that in age matched control brain. Moreover, they shared the epitopes with ADDLs as shown by immunoreactivity to oligomer selective antibodies

M93 and M94 (Gong 2003) and also were able to bind synaptic terminals (Lacor, et al., 2004).

SEC analysis of ADDLs yielded two distinct peaks, an early eluting peak near the void volume of a Superdex 75 column followed by an included peak (Chromy, et al., 2003; Hepler, et al., 2006). Further rigorous biophysical analyses using non-denaturing methods like SEC-Multi-angle laser light scattering (MALLS) and analytical ultracentrifugation (AU) showed that the high molecular weight peak of ADDLs in fact consists of a polydisperse population of relatively high molecular weight oligomers (150-1000 kDa) instead of a single molecular weight species as observed by PAGE. SEC-MALLS and AU definitively showed that the lower molecular weight peak represents a significant amount of monomer (~90%) in a total ADDL preparation. This study emphasizes the dynamic nature of equilibria in an ADDL formulation, which is highly sensitive to type of buffer, nature of excipient, storage temperature, and time. Interestingly, only the high molecular weight SEC fraction exhibits the property to bind to neuronal axonal processes, while the monomers do not show any binding. $A\beta(1-40)$ failed to form high molecular weight ADDL species, and instead exclusively eluted out in a low molecular weight peak. $A\beta(1-40)$ LMW peak instead represented an equilibrium between monomers and dimers based on SEC-MALLS indicating the difference in the aggregation properties of two $A\beta$ alloforms (Hepler, et al., 2006). Under the supramicellar concentrations of SDS, both ADDLs and fibrils produce the same electrophoretic profile, suggesting the contribution of harsh detergent towards formation and stabilization of certain oligomers. This makes the SDS-PAGE analysis of oligomers less clear (Bitan, et al., 2005; Hepler, et al., 2006).

1.12.3 Pre-fibrillar and fibrillar Aβ-oligomers

Structural classification between different oligomeric species has become possible by conformation-specific antibodies in the absence of high resolution structures (Glabe, 2008). These antibodies can recognize specific conformations across a broad range of amyloid-forming proteins regardless of their primary sequence (Kayed, et al., 2003; Glabe, 2008). The epitopes recognized by these antibodies represent distinct aggregation states of the amyloidogenic peptides. Specifically, A11 antibody developed against molecular mimetic of soluble oligomers is reported to recognize soluble pre-fibrillar oligomers (Kayed, et al., 2003). Moreover these pre-fibrillar oligomers are transient intermediates that ultimately result into the formation of fibrils. Interestingly, A11-antibody neither stains thioflavin-S positive plaques from AD brain nor other low molecular weight forms or fibrils prepared *in vitro* (Kayed, et al., 2003). OC-antibody, developed in 2007, recognizes species over a wide range of size distribution that contain an element of fibril structure. OC-antibody is reported to recognize structures with sizes corresponding to dimer to >500 kDa on a western-blot. A11 and OC-antibodies have been reported to recognize mutually exclusive epitopes (Kayed, et al., 2007). However, there is a broad overlap between the sizes of soluble fibrillar oligomers and prefibrillar oligomers. This evidence suggests that size may not be the best criteria to distinguish between different oligomers. In fact, Aβ species of same apparent size can have distinct conformations as shown by A11 and OC-anibodies (Glabe, 2008).

1.12.4 Aβ*56

The Tg2576 mouse model of AD overexpresses a Swedish double mutation (K670N/M671L) in APP and develops significant memory deficits at 6 months of age, which remain stable for 7-8 months. Since abundant Aβ plaque morphology appears between 9-14 months, well after the initiation of cognitive dysfunction, Lesné *et al* (2006) sought to identify an early Aβ species which would be a possible candidate for such a dysfunction. They found an Aβ species in extracellular soluble brain extracts of 6-month old Tg2576 mice. This species migrates at an apparent size of 56 kD on SDS-PAGE and correlates well with the development of memory deficits in Tg2576. These species were designated as Aβ*56 (Lesne, et al., 2006). Furthermore, when injected in normal young rats at lower nanomolar concentrations, the rats developed deficits in long term spatial memory in the Morris water maze. Based on apparent molecular weight, Aβ*56 is considered a dodecamer, and it also shows immunoreactivity to A11-antioligomer conformation specific antibody developed by Kayed and colleagues (2003) (Lesne, et al., 2006). Interestingly, in a recent comparative study, only Aβ*56 among other cell derived and synthetic oligomers positively correlated to cognitive dysfunction in a concentration dependent manner in rats (Reed, et al., 2011). However, in Tg2576 mice, forms of memory other than spatial memory are also affected, as evidenced by impaired performance in hippocampal dependent contextual fear conditioning assay, decreased spine density in the dentate gyrus, and disruption in long-term potentiation (LTP), long before the detectable appearance of Aβ*56 (Dineley, et al., 2002; Jacobsen,

et al., 2006). Thus it supports the possibility that more than one oligomeric species can be a candidate for causing overall neuronal dysfunction (Walsh and Selkoe, 2007).

1.12.5 Annular protofibrils

Annular protofibrils were observed as ring like structures when SEC isolated Aβ-Arctic protofibrils were incubated for longer times. TEM analysis revealed a diameter of 7–10 nm; inner diameter 1.5–2.0 nm and relative molecular mass of 150K–250K equivalent to 40–60 Aβ-Arctic (E22G) molecules. Annular protofibrils are thought to represent a distinct species that shares similarity with bacterial pore forming toxins (Lashuel, et al., 2002; Lashuel, et al., 2003). The β-Barrel is suggested as an underlying motif for this similarity.

Kayed et al (2009) prepared homogenous populations of annular protofibrils *in vitro* by exposing pre-fibrillar oligomers (PFOs) to an air/water interface or a hydrophobic /hydrophilic interface. EM analysis of these APFs revealed a stain-filled cavity in the middle. Moreover, the diameter of these APFs range between 8-25 nm. APFs appear to undergo a rough beaded to a rather smooth morphological transition during prolonged incubation. In fact, PFOs were reported to act as precursors for APFs upon interaction with amphipathic membranes and increased the conductance of lipid bilayer in a concentration dependent manner (Kayed, et al., 2009; Lasagna-Reeves, et al., 2011). Furthermore, APFs did not convert to fibrils even after prolonged incubation in

the presence of fibril seeds. Thus APFs are believed to represent species formed independent of fibril formation.

The conformation specific antibody α-APF designed to specifically recognize the APF epitope showed immunoreactivity to extracellular diffuse plaques and intracellularly around the nucleus in AD brain sections but not in age matched control brain sections. The immunoreactivity to α-APF was also found near membranes and vesicles within cellular processes and synapses in a transgenic mouse model expressing mutant APP (Kokubo, et al., 2009). Recently, double immunofluorescence studies have shown the colocalization of activated astrocytes from AD brains with α-APF, further suggesting that APFs could be formed intracellularly after astrocytic uptake of soluble oligomers, which in turn can become detrimental by causing inactivation of glutamine synthase (Lasagna-Reeves and Kayed, 2011).

1.12.6 Paranuclei

To capture early oligomers formed immediately after the preparation of Aβ(1-40) and (1-42) peptide, Bitan and colleagues used photo-induced crosslinking of unmodified proteins (PICUP), followed by their separation by SDS-PAGE to determine size distribution across the range of oligomers (Bitan, et al., 2001; Bitan, et al., 2003).

Aβ(1-42), immediately after elution through SEC, rapidly formed different assembly states including dimers, trimers, pentamers and hexamers along with some higher order structures. Based on DLS, EM and PICUP results, Bitan et al (2003)

proposed that Aβ(1-42) pentamers and hexamers act as paranuclei, since these species represent the initial, minimal structural unit for Aβ assembly into larger oligomers without causing significant change in the secondary structure. In contrast to Aβ(1-42), Aβ(1-40) shows a completely different oligomeric distribution consisting mainly of monomers, dimers and trimers. The difference in oligomer distribution was found to be dependent on the peptide length; Ile-41 was shown to be key determinant of paranuclei formation. Moreover, inclusion of residues Ala-42 and Thr-43 increases the propensity of these paranuclei to assemble together to form higher order beaded structures (Bitan, et al., 2003). The inability of Aβ40 to form paranuclei under similar conditions as Aβ42 is proposed to provide an explanation for discrepancies in alloform-specific biological activity.

1.12.7 Cell-derived low-n oligomers

Different low-n oligomers which separate at 8 (dimers) and 12 kDa (trimers) on SDS-PAGE have been detected in buffer-soluble fractions of AD brain tissue lysates and CSF (Walsh and Selkoe, 2007). A variety of cultured cells are shown to secrete similar SDS stable low-n oligomers in their conditioned medium at nanomolar concentrations, which are physiologically relevant concentrations (Podlisny, et al., 1995; Podlisny, et al., 1998; Walsh, et al., 2000; Walsh, et al., 2002; Cleary, et al., 2005; Shankar, et al., 2008). In fact, the origin of these oligomers was found to be endogenous, and traced back to the intracellular microsomal compartments (Walsh, et al., 2000).

Furthermore, these oligomers are shown to act as potent synaptoxins by causing loss of dendritic spines and modulation in calcium influx via NMDA receptors both *in vitro* and *in vivo* (Walsh, et al., 2002; Walsh, et al., 2005; Shankar, et al., 2007; Walsh and Selkoe, 2007). These oligomers not only blocked long term potentiation (LTP) but also altered short term memory; the earliest symptoms of AD. Moreover, these effects could be rescued by anti Aβ antibodies indicating the reversible nature of effects (Cleary, et al., 2005; Walsh and Selkoe, 2007).

Further support came when Aβ dimers directly isolated from AD brain were able to disrupt memory in rats. It was noteworthy in this study that plaques exerted toxicity only when solubilized to release dimers, supporting the idea that plaques might represent an inert reservoir of potentially toxic species (Shankar, et al., 2008). Further structural investigation of dimers was achieved by specifically stabilizing Aβ dimers via formation of a disulfide bond between Aβ S26C monomers. These $(AβS26C)_2$ when aggregated, rapidly formed thioflavin-T positive, β-sheet rich protofibrils and were able to block LTP in contrast to freshly isolated $(AβS26C)_2$. Dimer formation strongly influenced the rate of PF formation, which further suggests that dimers can induce toxicity by forming relatively stable PFs (O'Nuallain, et al., 2010).

1.12.8 β-amy balls

β-amy balls were detected by light and electron microscopy as clearly defined spheres of 20-200 μm in diameter (Westlind-Danielsson and Arnerup, 2001). These structures were reported when Aβ(1-40) was incubated at excessive concentrations like

300-600 μM under physiological conditions for 20 h up to 2 weeks. Aβ(1-42) did not form these structures by itself but enhanced the formation of Aβ(1-40) β-amy balls. However, the physiological occurrence of these structures is not very clear (Westlind-Danielsson and Arnerup, 2001; Rahimi, et al., 2008).

1.12.9 Globulomers

Globulomers are highly water-soluble globular oligomeric species of 38-60 kDa formed when Aβ(1-42) was incubated in phosphate buffered saline at 400 μM in the presence of 0.2 % SDS or fatty acid micelles at 37°C (Barghorn, et al., 2005). Size determination under native conditions estimated globulomer to consist of 12 monomer subunits. It is proposed to represent a pathway independent of fibril formation. Aβ(1-42) globulomer-specific antibodies stained the tissues from AD brain and transgenic animals carrying APP mutation. Abeta(1-42) globulomers bind dendritic processes of neurons in cell cultures and are potent inhibitors of long-term potentiation in rat hippocampal slices (Barghorn, et al., 2005; Rahimi, et al., 2008).

1.12.10 Emerging model of Aβ(1-42) fibril assembly inclusive of oligomeric species

The process of Aβ(1-42) fibrillogenesis is believed to be more complex based on the recent progress in the field of Aβ oligomers (Bitan, et al., 2003). As discussed in section 1.12, a number of oligomeric structures with distinct structural and biological

properties have been detected both *in vitro* and *in vivo*. The current understanding of Aβ(1-42) assembly includes some of these oligomeric structures, which ultimately result into fibril formation. However, for some of the oligomeric structures it is not yet clear if they lie in the same pathway of fibril formation or exist as independent entities as a part of other aggregation pathways (Bitan, et al., 2003). Based on the current understanding, multiple aggregation pathways may exist for Aβ(1-42) (Bitan, et al., 2003).

According to a model described by Bitan and colleagues (Bitan, et al., 2003) (Figure 1.4), Aβ(1-42) monomer rapidly assembles to form paranuclei immediately after its dissolution. Paranuclei are described as the intial, and minimal, structural unit for fibril evolution, which can oligomerize to form larger oligomeric structures. Monomer, paranuclei and oligomers are predominantly believed to be unstructured (U), but might contain some degree of α-helix and β-sheet structure. Moreover, these structures are believed to be in a complex dynamic equilibrium with each other. Further maturation of these oligomers results into structural rearrangement to produce β-sheet rich protofibrils. Protofibrils further give rise to fibrils by a number of mechanisms including end to end annealing, lateral association and monomer addition to the protofibril ends (Harper, et al., 1999; Nichols, et al., 2002).

1.13 Modified amyloid hypothesis

In the last couple of decades, extensive progress has been made to understand the role of Aβ oligomers in synaptic dysfunction seen in AD, as discussed before in section 1.12. Aβ oligomers seem to be more potent synaptotoxins than fibrils. Multiphoton

41

imaging studies revealed co-localization of oligomeric Aβ and severe neuronal loss surrounding the periphery of senile plaques (Koffie, et al., 2009). Aβ induced neuronal toxicity is also mediated by tau protein (Zempel, et al., 2011). Dementia correlated with the extent of tangle formation, gliosis, and neuronal loss, but amyloid accumulation reached a plateau independent of disease severity (Ingelsson, et al., 2004). This evidence suggests that AD represents a complex process, and although Aβ could be the initial trigger, it might act in combination with other factors like inflammatory processes during further progression.

Recently Hyman proposed some modifications to the existing amyloid hypothesis (Hyman, 2011). According to Hyman, AD could be considered to be composed of two stages; Aβ dependent and Aβ independent stage. In the first stage of AD, deposition of soluble oligomers and fibrillar Aβ results in the local changes in the neuropil, loss of dendritic spines, remodeling of synapses and initiation of inflammatory processes. Second phase could be characterized by development of NFTs, continued neuronal loss and glial inflammation, which culminate in neurodegeneration and full development of AD phenotype. According to this proposition, the amyloid-induced neurodegenerative changes initiate during the first phase of Aβ accumulation. In the second phase, the amyloid deposition seems to reach a plateau. However, the secondary consequences of amyloid deposition such as inflammation and neurodegeneration continue to worsen, resulting into the final stage of the disease. Therefore, although the second stage is initiated by amyloid, treatments targeting amyloid depositions are less likely to be effective. The second phase could be regarded as not completely dependent on Aβ (Hyman, 2011).
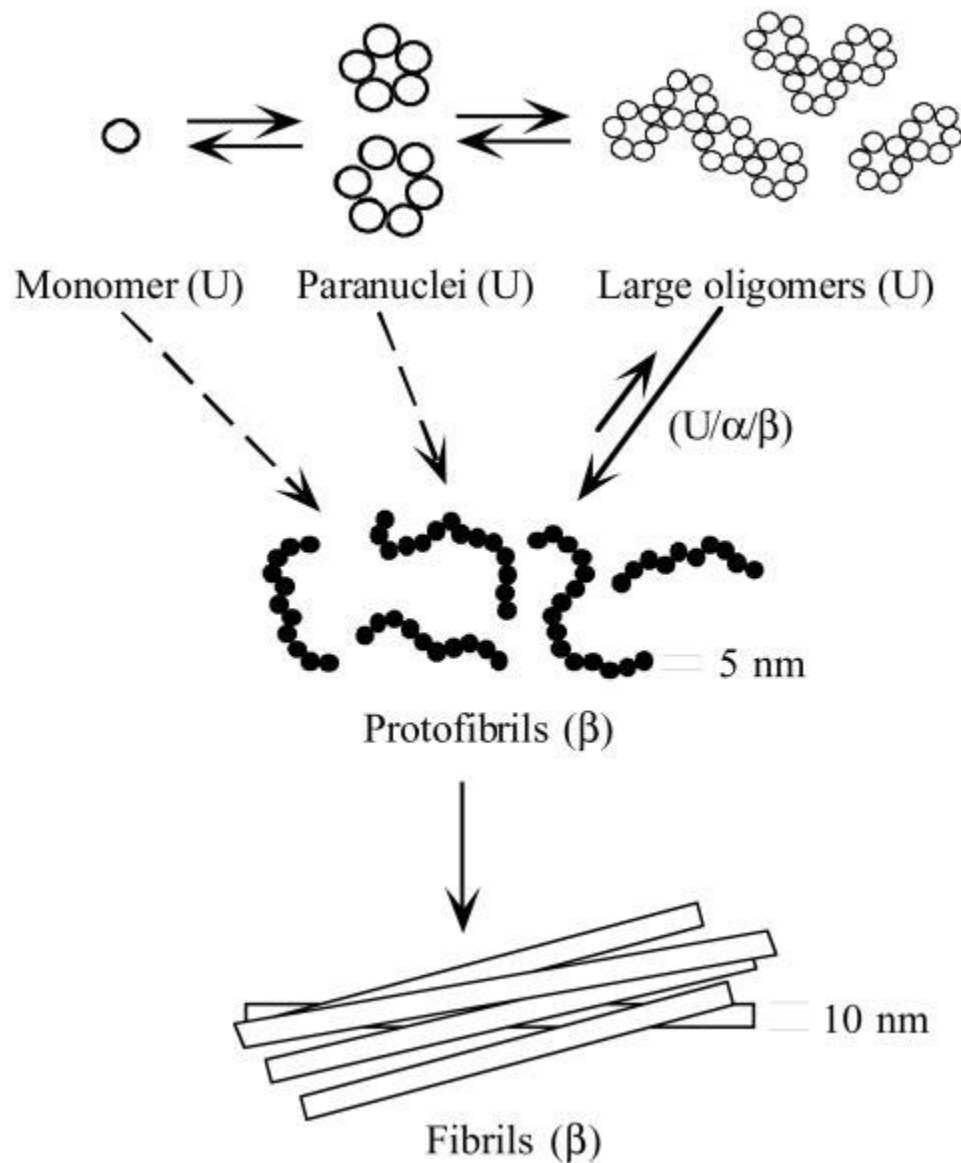
Figure 1.4. Model of Aβ(1-42) assembly (reproduced from (Bitan, et al., 2003)). Aβ(1-42) monomer forms paranuclei, which further oligomerize to form larger oligomers. Monomer, paranuclei and oligomers are usually unstructured (U) which rearrange structurally to mature into β-sheet rich protofibrils (β). Protofibrils mature to form fibrils which have a high degree of β-sheet. U, α and β represents unstructured, alpha helix or beta-sheet structure. 5 nm and 10 nm represent the diameters of protofibril or fibrils respectively.

This proposition can partially explain the failure of drugs targeting Aβ in the AD patients who have already developed mild cognitive impairement during the clinical trial. So it might be useful to devise therapeutic targets based on the stage of disease progression. However, targeting AD in early stages is currently limited by early detection based on biomarkers. Alternative therapeutic targets like proteins associated with neuroinflammatory pathways such as caspases could be explored (Hyman, 2011).

1.14 Inflammation in AD

The presence of a large number of senile plaques, NFTs and related cognitive dysfunction may be necessary for AD, yet it is not sufficient to develop a full neurodegenerative phenotype of AD in transgenic animals (Rogers, et al., 1996). It has been suggested that inflammation is one of the key contributing factors to the development of full AD phenotype (Rogers, et al., 1996). Inflammation is normally an act of the immune system to mount a non-specific response against any type of bodily injury. Inflammation include a wide variety of processes that not only involve removal of detritus but also healing of an insult (Ferrero-Miliani, et al., 2007) using a variety of immune effector cells and soluble molecular mediators. Usually inflammation is self-limiting (acute), but under certain circumstances it continues to exist resulting into chonic inflammation. Such an unregulated chronic inflammatory state becomes detrimental rather than beneficial to the host. AD brain displays a state of chronic inflammation as reflected in Braak staging (Braak and Braak, 1991).

The first evidence of involvement of inflammation in AD came from the studies where senile plaques of AD cortical samples were found to be associated with immune related elements like immunoglobulins and complements using light and electron microscopy (Eikelenboom and Stam, 1982; Ishii and Haga, 1984), although the presence of immune elements was less prominent in the plaques having a component of NFTs (Ishii and Haga, 1984).

AD brain displays characteristics features of classical inflammation, which include activated immune cells like microglia (Dickson, 1997), astrocytes, leukocytes (Itagaki, et al., 1989), and activation of complement system ,both within and surrounding the senile plaques, along with significantly elevated levels of a variety of inflammatory proteins as compared to non demented brains (Rogers, et al., 1996). A number of such proteins are listed in table 1.2. *In situ* mRNA expression studies confirmed that most of the inflammatory mediators are endogenously produced by local astrocytes and microglia (Finch and Marchalonis, 1996). The blood-brain barrier restricts the passage of peripheral immune proteins such as immunoglobulins and soluble inflammatory molecules into the brain. Therefore, brain was thought to be an immunologically privileged organ. However, increasing evidence for the existence of complex inflammatory processes in the AD brain suggests that brain might have unique immunological properties (Akiyama, et al., 2000).

Class of proteins elevated in Alzheimer's brain	Examples
Cytokines	Interleukin-1α (IL-1α), Interleukin-1β (IL-1β), Interlekin-6 (IL-6), tumor necrosis factor α (TNFα)
Acute Phase Reactants	α-1 -antichymotrypsin α-2-macroglobulin Serum Amyloid P α-1-antitrypsin C-reactive protein
Classical Complement Proteins	Clq, C4 ,C4d, C3,C3b,C3c, C3d, C7, C9, C5b-9 (MAC)
Complement Defense Proteins	Clusterin (Apo J), Vitronectin,
Leukocyte Common Antigen	CD-45
MHC-I	
MHC-II	HLA-DR, HLA-DP, HLA-DQ

Table 1.2 Inflammatory markers in the AD brain (adopted from (Rogers, et al., 1996))

1.15 Involvement of immune effector cells in causing inflammation

1.15.1 Neurons

Neurons were not conventionally regarded as immune cells, however there is emerging evidence for their role in the production of inflammatory proteins. Neurons are capable of producing complement proteins, interleukins (IL-1 and IL-6), TNFα and M-CSF (Akiyama, et al., 2000). Since these inflammatory proteins are elevated in AD, it is thought that neurons might contribute to exacerbate AD pathology in concert with microglia and astrocytes (Akiyama 2000).

1.15.2 Glia

Glia represents the most abundant cells of the nervous system. Glia are further categorized into astrocytes, microglia and oligodendrocytes, which together are responsible for neuronal homeostasis, synaptic plasticity and repair (Haydon, 2001).

1.15.2.1 Astrocytes

Astrocytes are primarily responsible for maintaining the homeostasis in the brain (Haydon, 2001). Earlier, glia were considered non-excitatory, which is recently

challenged by a number of studies on astroglia (Winship, et al., 2007; Schummers, et al., 2008). In fact, astrocytes play an important regulatory role in glutamatergic neurotransmission by preventing glutamate excitotoxicity via a glutamate-glutamine shuttle system. These processes are important for maintenance of synaptic plasticity linked to cognitive processes (Mattson and Rychlik, 1990; Fields and Stevens-Graham, 2002; McKenna, 2007). In the light of recent findings, the synapse has been redefined as a tripartite synapse, inclusive of not only pre and post synaptic nerve ending but astroglia as well (Araque, et al., 1999; Perea, et al., 2009).

Astrocytes are interconnected by connexin gap junctions to facilitate redistribution of metabolites and are also known to contribute towards the blood brain barrier (Rawunduzy et al., 1997; Siushansian et al., 2001; Frantseva et al., 2002; Nakase et al., 2003). Upregulation of intermediate filament proteins, particularly glial fibrillary acidic protein (GFAP), Vimentin, hypertrophic cellular processes along with altered expression of many proteins, are some of the classic features of reactive astroglia (Eddleston and Mucke, 1993; Bushong, et al., 2002; Bushong, et al., 2004). Reactive astrocytes protect neurons from oxidative stress via a glutathione-dependent scavenging mechanism (Iwata-Ichikawa, et al., 1999).

Activation of astrocytes leads to upregulation of a number of inflammatory molecules like cytokines, interleukins, growth factors, proteases and protease inhibitors. Area number of these molecules are known to be involved in AD pathogenesis (Eddleston and Mucke, 1993). In transgenic mouse models of AD, overexpression of molecules like TGF-β and IL-6 in astrocytes caused increased deposition of Aβ, astrocytosis and behavioral decline (Wyss-Coray, et al., 1997). In another study, Aβ

induced astroglial activation and subsequent release of chemokines to promote chemotaxis of microglia and infiltration of monocytes/macrophages towards Aβ (Johnstone, et al., 1999). These chemokines are believed to further amplify the inflammatory response in an autocrine or paracrine manner, leading to evolution of lesions in several neurodegenerative disorders including AD (Aloisi, et al., 1992). In a very recent study by DaRocha Souto et al (2011), brain oligomeric Aβ was correlated particularly to astrocytic inflammatory response and neuronal loss in APP/tau double transgenic mice suggesting that astrocytes may be activated in the earlier stages of AD and contribute to AD progression (DaRocha-Souto, et al., 2011).

1.15.2.2 Microglia

Microglia are the resident immune cells of the CNS, constituting 12% of the total glial population (Gonzalez-Scarano and Baltuch, 1999). As opposed to astrocytes and oligodendrocytes, microglia have mesodermal origin, and display molecular markers representative of both monocyte and macrophage line. Microglial progenitors were known to cross the blood brain barrier (BBB) during early embryonic stages and populate within the brain. However, recent observations suggest that peripheral monocytes can infiltrate the blood-brain barrier in response to various insults including Aβ deposition, and differentiate into brain macrophages, which are indistinguishable from microglia immunologically (Simard and Rivest, 2004; Malm, et al., 2005). Certain cytokines can also alter the expression of specific cell surface receptors in a microglial subtype dependent manner, and thereby exert different immunomodulatory effects in response to

Aβ (Shimizu, et al., 2008). The idea of structural, functional, and location-dependent subsets of microglial population has been proposed but lacks evidence for definitive markers that can distinguish between different subsets (Graeber and Streit, 2010).

Structurally, microglia can exhibit diverse morphologies, ranging from round, amoeboid to more ramified, depending on the environment (Graeber, 2010). Therefore, before the advent of specific microglial markers, the nature and identity of microglia were debated. It is now increasingly clear that microglia are extremely plastic both structurally and functionally (Graeber, 2010). They can adopt different phenotypes in response to their environment. In fact, time-lapse imaging experiments using *in vivo* two photon imaging revealed that microglia in normal, healthy brain continuously sample their micro-environment by their highly motile, labile processes, thus representing a constant dynamic state rather than a resting state (Nimmerjahn, et al., 2005). Microglia are the professional phagocytes of the brain. In addition to being principal immune effector cells, microglia are also capable of surveying the functional status of synapses intermittently and eliminating a defunct synapse to maintain synaptic integraity (Wake, et al., 2009).

1.16 Activation of microglia

Under an insult, microglia adopt an alternate phenotype, subsequently express or secrete a variety of pro and anti-inflammatory molecules, and become "activated" (Nimmerjahn, et al., 2005). It is a non-specific process. Since the threshold for

microglial activation is less, they can respond to a slightest perturbation rapidly, however, if uncontrolled, can last as long as a lifetime as exemplified by chronic inflammation in AD (Graeber, 2010). Some of the most common markers used to assess microglial activation include HLA-DR (MHCII), CD11b, CD-45, and peripheral benzodiazepine receptors (PDZ or translocator protein 18 kDa) (Colton and Wilcock, 2010).

Upon exposure to an antigen, microglia undergo classical activation, which is typically proinflammatory in nature and is mediated by pro-inflammatory cytokines like tumor necrosis factor-α (TNFα), interleukin-6 (IL-6), interleukin 1β (IL-1β)), proteases (e.g., matrix metalloproteinase-9), superoxide anion, nitric oxide (NO) and reactive oxygen-nitrogen species. Classical activation results in tissue defense and removal of antigen. Another pathway called alternative activation exists, which is primarily involved in downregulation of the proinflammatory state after removal of antigen and ensuing tissue repair and homeostasis.

Alternative activation is reinforced by anti-inflammatory cytokines IL-4, IL-13, IL-10, TGF-β and upregulation of scavenger receptors for phagocytosis of apoptotic cells and harmful byproducts. Treatment of microglia with IL-4 resulted into expression of proteins such as arginase 1, YM1, YM2, FIZZ1 (RELMα), and the mannose receptor (CD206) (Colton, et al., 2006; Martinez, et al., 2009). Moreover, expression of these proteins influenced the microglial phenotype to transform into alternatively activated macrophages. Thus, microglia possess the ability to transform into multiple phenotypes with distinctive functions (Cameron and Landreth, 2010). The balance between the classical and alternative activation is achieved in a successful innate immune response. Although in chronic inflammatory neurodenerative diseases like AD, a heterogenous

population of activated microglia exists simultaneously and leads to a complex inflammatory process (Colton and Wilcock, 2010).

1.16.1 Relevance of microglial activation in AD

It is now well established that microglia get activated following the exposure to Aβ, and upregulate the expression of a variety of pro and anti-inflammatory cytokines and reactive oxygen species (Meda, et al., 1995; Lorton, 1997; Yates, et al., 2000; Cameron and Landreth, 2010). Particularly activated microglia were found to be abundant in the cortex of AD patients (Edison, et al., 2008). Moreover, this increase in activated microglia did not correlate well with the total amyloid plaque buden but rather to the cognitive decline (Edison, et al., 2008). Microglial activation pathways, their products and the relation to AD pathology have been extensively studied either using a variety of *in vitro* cell culture models like primary murine microglia, BV2 microglial cell line, primary human microglia cultured from AD brain or *in vivo* animal models of AD.

Recent developments in "*in vivo*" imaging techniques have led to increased understanding of the dynamic nature of microglial interactions with plaques. *In vivo* multiphoton microscopy of a transgenic mice model of AD detected recruitment of microglia to plaques within one day of plaque formation, which coincided with dystrophic neurites. However, Aβ clearance by these microglia was not observed (Meyer-Luehmann, et al., 2008). In another study, microglial recruitment to plaque was followed by uptake of amyloid specific dye, albeit with less efficiency. Importantly,

plaque size was correlated to the number and size of plaque associated microglia (Bolmont, et al., 2008). Bolmont *et al* also hypothesized that smaller protofibrils might form along the periphery of plaque, which can stimulate microglial activation and clearance mechanisms. Cagnin, et al, used positron emission tomography (PET) to image carbon 11-labeled compound that recognizes peripheral benzodiazepine receptor (TP-18), which is a marker of activated microglial cells, and showed the correlation of microglial activation with cognitive decline and AD neuropathology (Cagnin, et al., 2001). These studies strongly support that activation of microglia is one of the earliest events in the AD pathogenesis. Furthermore, the activation process could be monitored as an indicator of disease severity by PET-based imaging as one of the biomarkers of AD progression.

Activation of microglia needs to be under tight regulation in order to avoid bystander damage to the surrounding tissue. Microglia have evolved different mechanisms to prevent unwanted activation. In one of the mechanisms, microglia exhibit fractalkine receptors (CX3CR1), which interact with fractalkine (CX3CL1) ligand on the neurons and astroglia during microglial surveillance (Cardona, et al., 2006). Similarly CD200 ligand on the microglial surface interacts with CD200 receptor on neurons. These cell-cell interactions signal microglia to downregulate unwanted activation in a healthy brain. Such receptor-ligand interactions are impaired during neurodegeneration, leading to chronic inflammation (Cardona, et al., 2006; Walker, et al., 2009).

1.16.2 Evidence for the role of microglia in plaque evolution

Numerous studies have shown that upon exposure to Aβ, microglia become activated, rapidly move towards plaque by extending their processes and cluster around the plaques (Dickson, et al., 1988; Itagaki, et al., 1989; Perlmutter, et al., 1990). Aβ also stimulates microglial proliferation in the vicinity of plaques, allowing their further accumulation in senile plaques (Bornemann, et al., 2001). Microglia can facilitate the aggregation of soluble Aβ species into fibrillar species upon failure of microglial Aβ-clearance mechanisms (Nagele, et al., 2004). In fact,the extensive inflammation mediated by activated microglia accelerated plaque deposition in the PDAPP transgenic mice model of AD, when coexpressed with ApoE (Qiao, et al., 2001).

Frautchy and colleagues observed increase in the density and size of microglia in entorhinal, occipital cortex and hippocampus, which are the primary brain regions showing maximum deposition of Aβ (Frautschy, et al., 1998). They also demonstrated quantitatively that microglia are more concentrated within the senile plaques (Frautschy, et al., 1998), which is further supported by colocalization of microglia immunoreactive for TNFα, IL-1β with thioflavin-positive plaques (Benzing, et al., 1999). In contrast to dense core plaques, diffuse plaques showed no detectable association with microglia in APP23 mice harboring a double Swedish mutation (Stalder, et al., 1999). This finding is consistent with studies carried out on brain sections from AD patients and non-demented controls, which suggest that microglial association and activation increases significantly during transition of diffuse plaques into neuritic plaques (Mackenzie, et al., 1995; Cotman, et al., 1996; Sasaki, et al., 1997).

Interestingly, microglia showed immunereactivity to Aβ(1-40) antibodies but not to Aβ(1-42) antibodies, which is in agreement with a previous study using brain samples

from AD patients that demonstrated the association of microglia only with the plaques containing Aβ(1-40) (Fukumoto, et al., 1996). This observation is also supported indirectly by detection of fewer microglia in a PDAPP mouse model of AD, that expresses high levels of Aβ(1-42) (Masliah, et al., 1996). Since Aβ(1-42) is the first form to get deposited in the diffuse plaques followed by Aβ(1-40) as the plaque matures (Iwatsubo, et al., 1994), the above studies together suggest a role for microglia in plaque evolution. A number of studies have shown that microglia not only recruit themeselves to the Aβ deposits but also engulf Aβ using a variety of phagocytic mechanisms Simard *et al* (2006) demonstrated that bone marrow derived microglia showed efficient chemotaxis towards Aβ deposits and subsequent phagocytosis in transgenic mice model system, while resident microglia lacked this ability (Simard, et al., 2006). It is possible that different microglial subsets contribute to plaque development in a differential manner. Interestingly, in a P301S mutant human tau transgenic (Tg) mice, significant microglial activation preceded the development of tau tangles, suggesting that microglial activation might play an important role in tau pathology in addition to plaque developement (Yoshiyama, et al., 2007).

1.17 Microglial receptors for Aβ

Since microglia lack gap junctions unlike astroglia, they have to rely mostly on the autocrine and paracrine mechanisms for communication with each other (Graeber, 2010). To enable effective communication, microglia display a repertoire of diverse

receptors, which upon interaction with a ligand initiate a downstream signaling cascade. The signaling pathways represent both activating and dampening loops. Most of these pathways are involved either in the production of pro-and anti-inflammatory cytokines or clearance of Aβ. In fact, sometimes these pathways seem to be interdependent. Aβ is shown to interact with multiple microglial receptors, affecting the functional phenotype of not only microglia themselves but also of the surrounding cells via secreted immunomodulators (Figure 1.5) (Salminen, et al., 2009).

1.17.1 Toll-like receptors (TLRs)

TLRs are pattern recognition receptors, which recognize pathogen associated molecular patterns (PAMPs). Since they are capable of recognizing and responding to patterns common to many different pathogens rather than a specific pathogen, they are principal to the innate immune system. TLRs can form homogeneous or heterogeneous complexes for interaction with ligand. Multiple costimulatory molecules and small glycosylphosphatidyl-inositol (GPI) anchored proteins like CD14 are known to complex with TLRs to initiate downstream signaling (Kielian, 2006; Salminen, et al., 2009). The downstream signaling involves a change in proinflammatory gene expression via activation of nuclear factor kappa B (NF-κB) transcription factor (Kielian, 2006).

Aβ induced microglial activation by binding to CD14 coreceptor, which could be blocked by the use of antibodies against CD-14 or genetic deficiency of CD-14. Moreover, microglial activation was dependent on the aggregation state of Aβ in

56
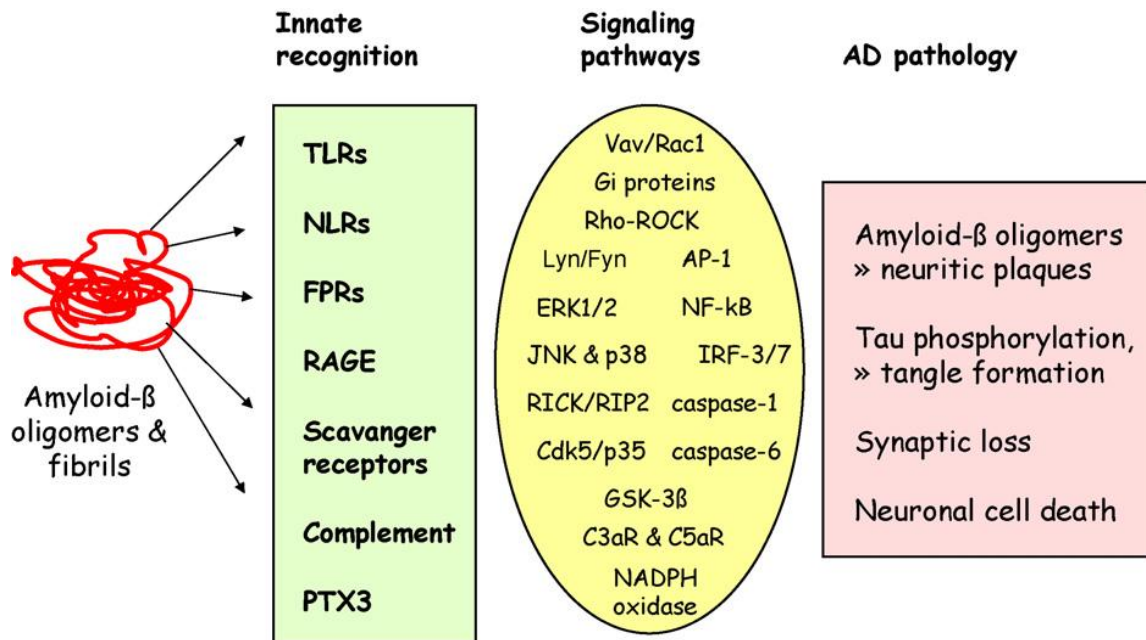
Figure 1.5 Schematic representation of different signaling components involved in AD pathogenesis. (reproduced from (Salminen, et al., 2009)). Aβ oligomers and fibrils activate overlapping signaling pathways via interaction with different innate receptors

such a way that only fibrillar Aβ was an effective activator, while non fibrillar Aβ had no effect (Fassbender, et al., 2004). (Fassbender, et al., 2004). Aggregated Aβ(1-42) also caused TLR-4 mediated release of proinflammatory mediators in murine microglia Aβ(1-42). This study was futher supported by the increased expression of TLR4 observed in the brains of transgenic mice and AD patients (Walter, et al., 2007). In another study, TLR2 along with TLR4 and CD14 resulted into fibrillar Aβ-induced microglial activation via Src-Vav-Rac and p38MAPK, and generation of reactive oxygen species (Reed-Geaghan, et al., 2009). Moreover, in a transgenic AD mouse model, deficiency of CD14 reduced plaque burden and was accompanied by alteration in both microglial activation phenotype and inflammatory milieu (Reed-Geaghan, et al., 2010). Aβ(1-40) is also reported to enhance the pro-inflammatory cytokine production by TLR2 and TLR4 agonists but antagonizes TLR9-induced inflammation in primary murine microglia, indicating that different TLR members can both activate and dampen inflammatory pathways in response to Aβ (Lotz, et al., 2005). In a recent study, CD36 (a class B scavenger receptor highly expressed on microglia in AD brains), has been shown to interact with fibrillar Aβ(1-42) to produce reactive oxygen species and NF-κB dependent upregulation of cytokines via complexation with TLR4 and TLR6 heterodimer (Stewart, et al., 2010). Interestingly, this signaling was independent of MD-2 and CD14, the well established coreceptors for Aβ-induced signaling, and instead activated MyD88 and TRIF-dependent pathways (Coraci, et al., 2002; Stewart, et al., 2010). Furthermore, this study did not observe involvement of TLR2 in Aβ(1-42) fibril-induced inflammation. However, in another study, fibrillar Aβ stimulated MyD88-dependent production of proinflammatory cytokines via TLR2 in primary murine microglia (Jana, et al., 2008).

Recently, TLR2 was shown to be a primary receptor for oligomeric Aβ (Liu, et al., 2011). In addition to a role as proinflammatory mediator, TLRs are known to contribute towards microglia-mediated neuronal degeneration (Lehnardt, et al., 2003) and Aβ-uptake (Chen, et al., 2006). TLRs are reported to be regulated by TREMs (triggering receptors expressed on myeloid cell). TREM-1 and TREM-2 proteins form complexes with the DAP12 adapter proteins and trigger a signaling pathway. TREM-1 acts to amplify TLR mediated inflammation, while TREM-2 downregulates cytokine release in macrophages and activates phagocytosis in microglia (Klesney-Tait, et al., 2006). Interestingly, TREM-2 expression is upregulated in microglia associated with amyloid plaques in transgenic AD mice. TREMs can modulate TLR-associated inflammation and phagocytosis by a feedback system (Frank, et al., 2008).

1.17.2 Receptors for advanced glycation end products (RAGE)

RAGE belongs to an immunoglobulin superfamily. It is believed that RAGE recognize a particular structural determinant, rather than a specific molecule, similar to pattern recognition receptors. It recognizes multiple ligands, such as β-sheet rich fibrils of amyloidogenic proteins such as Aβ, amylin and prions (Schmidt, et al., 2000). Expression of RAGE is significantly elevated in Alzheimer's disease brain, especially in neurons and microglia proximal to amyloid plaques. Aβ displays affinity for RAGE in nanomolar range. RAGE plays an important role in microglial chemotaxis, cytokine

production, and also represents a major source of oxidative stress in neurons, which is believed to contribute towards AD pathogenesis (Yan, et al., 1996).

The importance of RAGE in AD was observed in a study using primary human microglia (Lue, et al., 2001). When microglia from human AD brains were cultured with focal deposits of Aβ(1-42), the expression of growth factor, M-CSF, was significantly elevated compared to microglia cultured from non-demented brains.   M-CSF is a macrophage-colony stimulating factor which promotes microglial activation and chemotaxis. This effect could be blocked by anti-RAGE antibodies in primary human microglia from AD brains. Also, M-CSF led to further increase in RAGE expression suggesting a feedback mechanism for RAGE expression (Lue, et al., 2001). Circulating Aβ binds to RAGE on endothelial cells, which facilitates the transfer of Aβ across BBB. Once across the BBB, Aβ acculumates in the brain in the absence of efficient elimination mechanisms (Li, et al., 2009b). In a transgenic AD mouse model inhibition of RAGE was able to reduce neurovascular stress caused by reactive oxygen species downstream of RAGE-Aβ interaction (Deane, et al., 2003).   The involvement of RAGE in AD pathogenesis was further potentiated when a double transgenic mouse model displaying mutant APP and overexpression of neuronal RAGE led to altered synaptic plasticity and increased neuronal pathology (Arancio, et al., 2004). Recently, a transgenic mouse model expressing mutant APP in neurons was also manipulated to overexpress RAGE in microglia. This genetic manipulation led to a wide range of effects, including increased production of inflammatory cytokines, increased infiltration of microglia and astrocytes, accumulation of Aβ, reduced acetylcholine esterase (AChE) activity, and accelerated impairment in spatial memory. These deteriorating effects could be reduced significantly

by inhibiting RAGE-mediated signaling (Fang, et al., 2010). There appears to be an age-dependent decrease in RAGE expression in transgenic mice bearing Swedish mutation in APP, which is thought to be biologically relevant (Cui, et al., 2011).

1.17.3 Scavenger receptors (SR)

SR class is activated by a variety of diverse ligands, including modified lipoproteins, anionic polysaccharides and Aβ (Husemann, et al., 2002). Some of the SR family members include SR class A, SR class B, SR class C, macrophage receptor containing a collagenous domain (MARCO), and endothelial cell scavenger receptor (SR-EC), CD68 (Husemann, et al., 2002).

SRs mediate adhesion of microglia to Aβ fibrils (El Khoury, et al., 1996), chemotactic recruitment of microglia to amyloid deposits via the Src-kinase pathway (Moore, et al., 2002), and internalization of aggregated Aβ (Paresce, et al., 1996). Bamberger and colleagues also reported a role for B-class scavenger receptor CD36 in complex with integrin-associated protein CD47, and alpha(6)beta(1)-integrin in mediating the production of IL1-β and reactive oxygen species in murine microglia stimulated with Aβ fibrils (Bamberger, et al., 2003). Engagement of this receptor complex also results in the phagocytosis of fibrillar Aβ (Koenigsknecht-Talboo and Landreth, 2005). Interestingly, CD36 is found to be overexpressed on microglia in human AD brains, suggesting its biological relevance (Coraci, et al., 2002; Moore, et al., 2002). Recently, MARCO (SR-A) has been shown to physically interact with formyl

peptide like receptors to activate glial signal transduction pathways in response to Aβ (Brandenburg, et al., 2010).

1.17.4 Peroxisome proliferator-activated receptor (PPAR)

PPARs is a family of three (α/γ/δ) nuclear receptors that act as whole body lipid sensors, and have been used widely for Type II diabetes mellitus treatments and recently have displayed potential as an anti-AD target (Landreth, et al., 2008).

PPARγ enhances anti-inflammatory signaling by downregulating NF-κB dependent expression of proinflammatory genes like matrix metalloproteinase (MMP), cycloxtgenase 2 (COX-2), and inducible nitric oxide synthase (iNOS) (Combs, et al., 2000). In fact, acute 7 day oral treatment with the PPARγ agonist not only reduced the number of activated microglia and reactive astrocytes in the hippocampus and cortex but also reduced the plaque burden in 10-month-old APPV717I mice (Heneka, et al., 2005). PPARγ enhances Aβ clearance by stimulating a cellular metalloprotease, which acts independently of insulin degrading enzyme (IDE) (Camacho, et al., 2004; Espuny-Camacho, et al., 2010)

1.17.5 N-Formyl peptide receptors (FPR)

FPRL-1 and FPRL-2 belong to FPRs, which are seven-transmembrane, G protein-coupled receptors that are activated by chemotactic peptides including Aβ (Le, et al.,

2001). Microglial FPRs are capable of both inducing phagocytosis and inflammation via an increase in oxidative stress against Aβ (Tiffany, et al., 2001). Like some other receptors, FPRL-1 was highly expressed on the CD11b positive microglia, which were in close proximity to senile plaques in the brain tissue of AD patients (Paresce, et al., 1996; Le, et al., 2001), .

FPRL-1 facilitated rapid internalization of Aβ(1-42), followed by its intracellular degradation in mononuclear phagocytes. Moreover, FPRL-1 receptors were able to recycle back to the cell surface under a lower concentration of Aβ. However, continued exposure of Aβ seems to result in the intracellular formation of Congo Red-positive fibrillar aggregates, possibly by overburdening the FPRL-1 mediated clearance of Aβ (Yazawa, et al., 2001). Prior treatment with FPR agonist resulted in the desensitization of FPRs for mediating Aβ-induced effects, indicating the saturable nature of the receptor (Tiffany, et al., 2001). Interferon-γ (IFNγ) and CD40 ligand synergistically increase the expression of FPRL-2, a mouse homolog of human FPRL-1 via activation of MAPK and IkappaB-alpha in mouse microglia (Chen, et al., 2007). Recently FPRL-2 activation in mouse microglia is shown to be dependent on the conformation of Aβ in such a way that smaller oligomers (trimers and tetramers as detected by native and denaturing gel electrophoresis) were better stimulators than larger oligomers and fibrils(Heurtaux, et al., 2010). All these inflammatory responses taking place downstream of Aβ-FPRL-1 interaction are mediated by Gi- protein, as demonstrated by its sensitivity to pertussis toxin (Lorton, 1997; Tiffany, et al., 2001)

1.17.6 NOD-like receptors (NLRs) and inflammasome

NLRs are expressed mainly on microglia and human astrocytes and play a pivotal role in the regulation of IL-1β and other pro-inflammtory cytokine production in response to a number of PAMPs and DAMPs (danger-associated molecular patterns), which includes Aβ (Halle, et al., 2008). IL-1β is strongly elevated in response to Aβ based on a number of *in vitro* and *in vivo* studies. IL-1β is synthesized as a 35 kDa pro-IL-1β precursor, which is then cleaved by inflammasome to generate a mature 17 kDa IL-1β subunit. Inflammasome is a complex of proteins comprising of a NLR protein, caspase and the adaptor protein ASC (apoptosis-associated speck-like protein containing a CARD). NLRs act as sensors of IL-1β concentration, which after reaching a critical concentration, in turn increases the expression and generation of active IL-1β. However, NLRs require a primary signal from other PRRs like TLRs (Masters and O'Neill, 2011).

Aβ(1-42) fibrils were shown to stimulate the production of IL-1β in murine microglia via activation of NALP-3 inflammasome (Halle, et al., 2008). NALP-3 dependent release of IL-1β not only resulted into chemotaxis and activation of microglia but also induced production of other inflammatory mediators like nitric oxide and TNFα via autocrine and paracrine mechanisms. However, the activation of the NALP-3 pathway required cathepsin-B mediated internalization of Aβ, and subsequent impairment in lysosomal function upstream of NALP-3 inflammasome (Halle, et al., 2008).

White *et al* (2005) showed that Aβ(1-42) oligomers were more effective in inducing IL-1β than fibrillar Aβ(1-42). Interestingly, oligomer-induced IL-1β release decreased while fibril-induced IL-1β release increased over time although, underlying

receptors mediating these effects were not studied in this particular study(White, et al., 2005).

1.18 Molecular mediators

1.18.1 Cytokines

Among a plethora of inflammatory mediator molecules involved in AD, some of the most prominent molecules include proteins of complement pathway and proinflammtory cytokines. The pro-inflammatory cytokines, including TNFα, IL-1, and TGF-β, are upregulated in microglia near senile plaques (Griffin et al1995, Dickson et al 1993) (Table 1.2). These cytokines have the ability to coordinate and amplify most of the inflammatory pathways by altering the gene expression of APP, complement and acute phase proteins in astrocytes, neurons and microglia themselves (Potter, et al., 1992; Barnum, et al., 1993).

1.18.1.1 TNFα

TNFα is produced as a type II transmembrane homotrimer, which is cleaved by a metalloprotease, TNF α converting enzyme (TACE) to release 51 kDa, soluble trimer (Wajant, et al., 2003). Each subunit is composed of an antiparallel β-sandwich (Arai, et al., 1990). TNFα production is one of the earliest events upon exposure to Aβ (Medeiros,

et al., 2007), and its levels are significantly elevated in AD serum, CSF, cortex and glial cells. Microglia and astroglia are the primary sources of TNFα in the CNS.

Both neurotrophic and neurotoxic effects of TNFα on AD pathology could be explained by the presence of two distinct TNF receptors; TNF receptor type 1 (TNF-R1; CD120a; p55/60) and TNF receptor type 2 (TNF-R2; CD120b; p75/80). Membrane bound TNF can activate both the receptor types whereas soluble TNF only activates type 2 receptor. TNF-R1 has a death domain, which can interact with death domains from other proteins, resulting into the activation of caspases and apoptotic pathway. TNF-R2 lack a death domain but can alter gene expression via members of TNF receptor-associated factor (TRAF) family. TNF induces activation of NF-κB transcription factor, which in turn regulates the expression of a large number of proinflammatory cytokines including IL1, IL8, IL6 and GM-CSF and survival factors like manganese superoxide dismutase (MnSOD). Crosstalk between both the receptors leads to further amplification of the signal. As the name suggests, TNFα is known to cause cell death by necrosis, which is different from apoptotic cell death both morphologically and mechanistically. Necrosis does not require caspases or ATP and is linked to inflammation *in vivo*. Most commonly, TNFα indirectly triggers apoptosis or necrosis via generation of ROS.

TNFα protects neurons from Aβ-induced damage by decreasing oxidative stress and glutamate toxicity via NF-κB dependent transcriptional regulation (Barger, et al., 1995), upregulating receptors involved in microglial chemotaxis towards Aβ for clearance (Cui, et al., 2002), and expressing anti-apoptotic factor (bcl-1). Intrathecal TNFα negatively correlated with levels of apoptotic markers and tau protein in the AD brain as compared to non demented controls (Tarkowski, et al., 1999). Deficiency of

TNF receptors (TNFR) suppressed microglial activation and led to greater neuronal loss *in vivo* (Bruce, et al., 1996). On the other hand, TNFα mediate Aβ-induced inhibition of LTP *in vivo* (Wang, et al., 2005) and iNOS- dependent apoptosis of neurons (Combs, et al., 2001). In fact, blockage of TNFα action by pharmacological inhibitors or genetic deficiency reduced cognitive dysfunction caused by Aβ (Medeiros, et al., 2007). TNFα can exacerbate AD by stimulating the expression of APOE (Bales, et al., 2000) and Aβ (Blasko, et al., 1999). Moreover, genetic linkage analysis revealed an association between the TNF, TNFR1 and TNFR2 genes and the occurrence of late onset AD (Perry, et al., 2001).

1.18.1.2 TGF

TGFs are a family of peptide growth factors and play a key role in tissue development, homeostasis, repair, promote microglial chemotaxis and are potent modulators of inflammatory responses induced by both astrocytes and microglia, (Yao, et al., 1990). TGF-β on one hand enhances microglial clearance of Aβ, reduces plaque burden and neuronal degeneration (Wyss-Coray, et al., 2001; Tesseur, et al., 2006), but on the other hand its overexpression is linked to amyloid deposition in AD brain tissue and cerebral amyloid angiopathy (CAA) (Wyss-Coray, et al., 1997). All three different isoforms of TGF-β are implicated in AD, however they affect the cellular distribution and degradation of Aβ in an isoform specific manner (Harris-White, et al., 1998).

1.18.1.3 IL-1

IL-1 exists as two different forms; IL-1α and IL-1β. Extracellular 17.5 kDa secreted IL-1 is produced from a membrane bound form by proteolytic cleavge. Both the isoforms can activate the only receptor (IL1R1) to produce inflammatory molecules like prostaglandin E2, collagenase, and phospholipase-A2. IL-1 mainly acts in concert with IL-6 and TNFα in a multifunctional way (Arai, et al., 1990). IL-1β immunostaining was seen both in microglia and astrocytes surrounding both diffuse and senile plaques in a Tg 2576 mouse model of AD and AD brain tissue and is believed to contribute to plaque formation (Benzing, et al., 1999; Apelt and Schliebs, 2001). IL-1 also upregulates expression of APP by almost 6-fold in primary human astrocytes (Rogers, et al., 1999).

1.18.1.4 Interleukin-6

IL-6 is believed to amplify the inflammatory signaling pathways mediated by IL-1, and involves the Janus kinase/signal trasducer and activator of transcription (JAK-STAT) pathway (Cacquevel, et al., 2004). Significant upregulation of IL-6 mRNA was observed in the entorhinal cortex and superior temporal gyrus in AD brain compared to non demented controls (Luterman, et al., 2000).

1.18.2 Complement proteins

Complement proteins are a set of heat labile serum proteins which complement the cytotoxicity of antibodies and bridge the humoral immune system with the innate immune system. In a classical complement pathway, antigen-antibody interaction triggers the binding of the first complement component C1q. The binding initiates a cascade of sequential proteolysis. The products serve as local inflammatory mediators, chemotactic agents and opsonins. Also it generates membrane attack complex (MAC) on the target cell which disturbs ion homeostasis by pore formation in the membrane, ultimately causing cell lysis. Two other complement pathways exist, namely alternate and lectin, which slightly differ in the protein products they utilize, but parallel the classical pathway (Akiyama, et al., 2000). Complement proteins of both classical and alternative pathways, including C1q, C4, C3, are upregulated in the AD brain as compared to controls (Shen 1997), and colocalize with compact, thioflavin positive plaques in AD brains as opposed to diffuse, thioflavin negative plaques (Eikelenboom and Stam, 1982; Stoltzner, et al., 2000; Strohmeyer, et al., 2000). Synthesis of C1q was stimulated in hippocampal organotypic slice cultures stimulated with Aβ (Fan and Tenner, 2004). C1q can activate the classical pathway by direct binding to fibrillar Aβ aggregates within the senile plaque but not to monomeric Aβ, independent of an antibody in vitro (Rogers, et al., 1992; Afagh, et al., 1996) and the alternative pathway via interactions with C3. The activation of complement was highly specific by Aβ since other proteins similar in size and charge, in both monomeric and aggregated form, failed to do so (Bradt, et al., 1998). *In situ* hybridization studies in culture and AD brain

showed microglia and astrocytes in the vicinity of plaques to be the source of complement proteins (Veerhuis, et al., 1999; Fonseca, et al., 2011). Complement C3a and C5a also recruit microglia and astrocytes to the fibrillar Aβ and further prompts a robust inflammatory response (Fonseca, et al., 2004; Fonseca, et al., 2011). Cellular or pharmacological inactivation of complement pathways and related downstream signaling using transgenic murine models of AD proposed a detrimental role of complement towards AD pathogenesis (Maier 2008, Fonseca 2009). On the other hand, *in vivo* studies on transgenic mouse employing complement C3 inhibitor reduced neuropathology, indicating a neuroprotective role of complement system in AD pathology. C1q in the absence of other complement components protects neurons against Aβ-induced neurotoxicity both *in vitro* and *in vivo*, and the mechanisms might involve induction of neurite outgrowth, increased clearance of apoptotic cells and inhibition of inflammatory cytokines (Wyss-Coray *et al.*2002; Mukherjee and Pasinetti 2000 Zhou 2008, Pisalyaput and Tenner, 2008 Fraser 2010 Benoit 2011). The role of complement in AD pathogenesis thus appears to be more complex.

1.19 Role of microglia in AD: Concluding remarks

Ample evidence corroborates the involvement of microglia in AD pathogenesis, yet it is not very clear if microglia act to cause protection or toxicity to neurons (Cameron and Landreth, 2010). In fact, considering evidence for both functionalities, it is proposed that microglia represent a dynamic phenotype, and are capable of alternating between

different states. This idea is supported by a study that showed that hippocampal microglia switch from a phagocytic (alternative) phenotype during early stage to an inflammatory (classical) phenotype in later stage during aging of APP/PS1 transgenic mice (Jimenez, et al., 2008).

As discussed in earlier sections microglia seem to act to clear Aβ deposits during earlier stages of AD, but upon continued exposure the microglial phagocytic machinery gets overburdened and microglia instead become pro-inflammatory. Unregulated production of pro-inflammatory mediators results in chronic inflammation which is believed to exacerbate the AD pathology and related neurodegeneration (Perry, et al., 2010).

The potential of anti-inflammatory therapy against AD has been explored. Several epidemiological studies involving populations from different countries found that use of non steroidal anti-inflammatory drugs (NSAIDs) was linked to decreased prevalence of AD (McGeer, et al., 1996; McGeer and McGeer, 2007). In fact, postmortem analysis of AD-type pathology from non-demented patients using NSAID revealed fewer activated microglia than the NSAID non-users, supporting that microglial activation is a key factor contributing to AD pathology (Mackenzie, 2000). NSAIDs have also been observed to reduce plaque burden and cognitive deficiencies in transgenic animal models of AD, although subsequent clinical trials have been disappointing (McGeer and McGeer, 2007). The efforts have been directed in identifying specific targets of inflammatory pathways as both biomarkers for early diagnosis of AD as well as treatment for AD (Akiyama, et al., 2000; Weggen, et al., 2001).

There is ample *in vitro* evidence for clustering of activated microglia around senile plaques (Dickson, et al., 1988; Cameron and Landreth, 2010). Moreover, gliosis correlated linearly with disease severity while plaque burden remained unchanged (Serrano-Pozo, et al., 2011). Recently, sensitive antibodies have detected a halo of oligomeric Aβ surrounding senile plaques, supporting the idea that plaques are not only comprised of fibrillar Aβ but exhibit a complex composition. It is not very clear which exact species of Aβ is responsible for microglial activation (DaRocha-Souto, et al., 2011). This is particularly important since burgeoning evidence indicates that smaller, soluble oligomers are potent neurotoxins, while fibrils are not as effective (Koffie, et al., 2011). Although microglial activation has been a subject of intense research, a clear correlation between Aβ-aggregation state and microglial activation is not yet established.

One of the main reasons could be the lack of homogeneity of Aβ preparations. Many *in vitro* studies investigating Aβ-induced activation of microglia have utilized aggregated solutions of Aβ, which represent a polydisperse mixture of soluble and insoluble Aβ species. In such cases, it might not be possible to attribute the biological activity to one particular species.

In this study, we have carefully prepared homogeneous solutions of Aβ(1-42) protofibrils, fibrils, monomers and confirmed the aggregation states of Aβ using a variety of biophysical and imaging techniques. Subsequently the optimal aggregation state of Aβ involved in mouse microglial activation *in vitro* was identified. This finding may be biologically relevant if translated *in vivo* and will open up avenues for development of new drug targets against AD.

CHAPTER 2

METHODS

2.1 Cell culture

2.1.1 Primary murine microglia isolation and culture

Primary mixed glial culture was obtained from neonatal C57BL/6 mice (Harlan laboratories Inc). Briefly 3-4 days old post natal mice were euthanized with an overdose of inhaled isoflurane (Fisher). The brains were isolated and meninges were removed by rolling the brains over gauze under sterile conditions. The isolated brains were collected in a 50 mL sterile conical tube containing 20 ml of phosphate buffered saline (PBS) supplemented with antibiotics and kept on ice. After all the brains were collected, brain tissue was transferred to a 100 mm cell-culture dish, minced using sharp edged forceps in a scissor action, and resuspended in 5.0 ml of 0.5% trypsin (Hyclone) followed by

incubation at 37$^{\mathbf{o}}$C for 20 min to allow further dissociation of the tissue. Subsequently, cells were resuspended in 10 ml complete Dulbecco's modified Eagle's medium (DMEM, 4.5 g/l glucose, Hyclone) containing 10% heat-inactivated fetal bovine serum (FBS) (Hyclone), 4 mM L-glutamine, 100 U/ml penicillin, 0.1 mg/ml streptomycin and 0.25 μg/mL amphotericin-B (P/S/A triple antibiotic mixture, Fisher), OPI medium supplement (oxaloacetic acid-pyruvate-insulin, Sigma-Aldrich), and 0.5 ng/ml recombinant mouse granulocyte macrophage- colony stimulating factor (GM–CSF) (Invitrogen). The cell suspension was further triturated using a 10 ml pipette and filtered through a 70-μm cell strainer to remove tissue debris (Fisher Scientific). The resulting cell suspension was centrifuged at 200 x g for 5 min at 25$^{\mathbf{o}}$C, resuspended in complete medium and seeded into 150-cm^2 flasks (Corning). Each 150-cm^2 flask contained 30 ml of total cells. The number of flasks generated out of a single batch of mouse pups was dependent on the size of the litter. Cells were cultured at 37$^{\mathbf{o}}$C in 5% CO_2 until confluency (1-2 weeks). Microglia typically looked like round cells resting on top of the granular astrocytic layer. Microglia were selectively harvested by overnight shaking of the flask at 37$^{\mathbf{o}}$C in 5% CO_2 (at a speed between 5 and 6 on the shaker in the cell culture laboratory) and the medium was collected. The flasks were replenished with fresh growth medium, and incubated further to obtain subsequent batches of microglia. Typically, this procedure was repeated 3-4 times for one flask (Esen and Kielian, 2007) before the flasks were discarded.

74

2.1.2 BV-2 murine microglial culture

BV-2 mouse microglial cell line was a gift from Dr Landreth (Case Western Reserve University). The cells were maintained in Dulbecco's modified Eagle's medium (DMEM, 4.5 g/l glucose) (Hyclone) containing 50 U/ml penicillin, 50 μg/ml streptomycin, 50 μM β-mercaptoethanol, and 5% fetal bovine serum. BV-2 cells were typically passaged twice a week. For passaging, the confluent cells were washed 1 x with phosphate buffered saline (PBS) (Hyclone) and 1 ml of 0.25% trypsin was added. After incubating the cells for 10 min at 37°C and 5% CO_2, 9 ml of growth medium was added to inactivate trypsin. 1 ml of resuspended cells were then centrifuged for 7 min at 100 x g and resupended in 10 ml of fresh growth medium, added to 75 cm^2 flask and incubated further until next passage. BV-2 cells were used until passage #50. After that the cells were discarded and a new frozen aliquot (frozen in the year 2008 by M.L.D. Udan at passage #37-38) was thawed and cultured in the fresh growth medium as described above. However, one washing step was added before the culturing of cells which involved centrifugation for 7 min at 100 x g to remove any residual DMSO present in the cryopreservation medium.

2.1.3 TNFα measurements using ELISA

Measurement of secreted TNFα in the cellular conditioned medium was determined by ELISA as previously detailed (Udan, et al., 2008) except that the assay

was modified for the measurement of mouse TNFα. Briefly, 96-well plates were coated overnight with 100 μl of 0.4 μg /ml monoclonal anti-mouse TNFα capture antibody (stock aliquot stored at -20°C at 200 μg/ml in PBS), washed with phosphate-buffered saline (PBS) containing 0.05% Tween-20 and blocked with PBS containing 1% BSA, 5% Sucrose and 0.05% NaN$_3$ following by a wash step. Successive treatments with washing in between were done with samples or standards, 0.2 μg /ml biotinylated polyclonal anti-mouse TNFα detection antibody (stock aliquot stored at -20°C at 50 μg/ml in detection antibody diluent) in 20 mM Tris with 150 mM NaCl and 0.1% BSA, streptavidin-horseradish peroxidase (HRP) conjugate, and equal volumes of HRP substrates 3,3',5,5'-tetramethylbenzidine and hydrogen peroxide. The reaction was stopped by the addition of 1% H$_2$SO$_4$ solution. The optical density of each sample was analyzed at 450 nm with a reference reading at 630 nm using a SpectraMax 340 absorbance plate reader (Molecular Devices, Union City, CA). The concentration of TNFα in the experimental samples was calculated from a TNFα standard curve of 15-2000 pg/ml. When necessary, samples were diluted to fall within the standard curve. TNFα concentrations for absorbance values below the lowest 15 pg/ml standard were determined by extrapolation of the standard curve regression line.

2.1.4 Characterization of primary murine microglia proinflammatory response

Microglia are known to express a variety of toll-like receptors (TLRs) (Cameron and Landreth, 2010). In order to get an estimate of microglial sensitivity for various TLR

ligands, we carried out dose-response experiments for TLR-ligands such as lipopolysaccharaide (LPS, TLR4 ligand), Pam_3CSK_4 (TLR 1 and 2 ligand) and FSL-1 (TLR 2 and 6 ligand). LPS (600 µg/ml, Pam_3CSK_4 (600 µg/ml) and FSL-1 (60 µg/ml) were aliquotted, stored at -20°C and were further used to make appropriate dilutions for addition to the cells. Primary microglia were harvested by shaking the culture flask as described above and medium containing microglia was centrifuged at 200 g for 10 min at 25°C. Microglia (100 µl) were then plated into 96-well culture plates in a medium devoid of GM-CSF for 2 h at 37°C in 5% CO_2. The medium was replaced with fresh medium without GM-CSF and ligands were added. After 6 or 24 h incubation at 37°C, the cellular medium was collected and analyzed using ELISA for the production of TNFα as described in 2.1.3. Appropriate dilution of the sample was carried out in order to allow the sample values to fall within the standard curve ranging between 15-2000 pg/ml. The final concentrations of TLR-ligands (LPS, Pam3CSK4 and FSL-1) used in these dose-dependence studies were 100, 30, 10, 3 and 1 ng/ml.

LPS produced a concentration-dependent TNFα response between the range 1-10 ng/ml above which the response appeared to plateau (Figure 2.1). $Pam_3CSK_4$and FSL-1 also produced a concentration dependence response over the range of concentrations selected in this study (Figure 2.2 and Figure 2.3). The extent of TNFα production was dramatically altered between 6 and 24 h treatment with ligands, 6 h displaying maximum response. Therefore, the experiments were optimized for 6 h treatment time for subsequent studies unless stated otherwise.
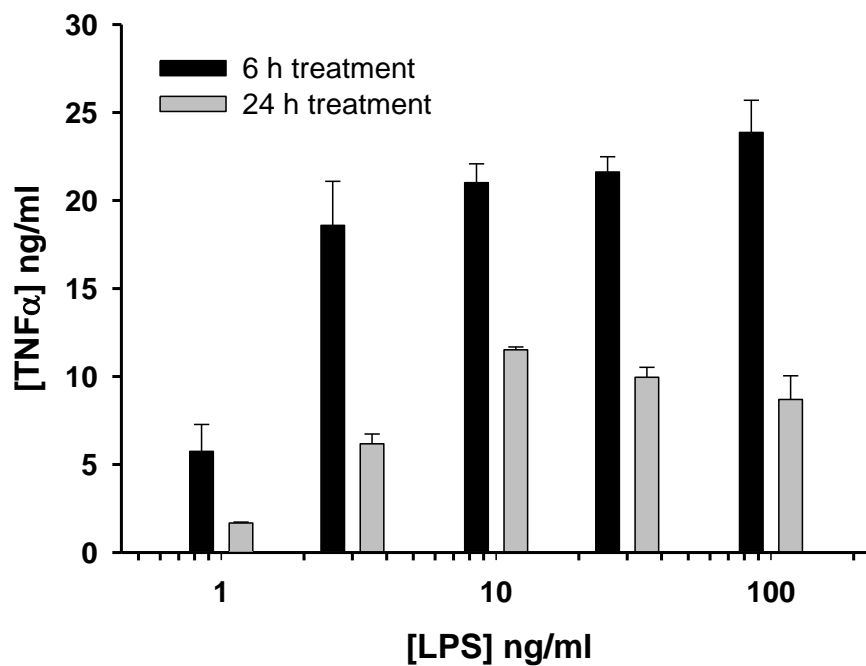
Figure 2.1   Concentration-dependence of LPS-induced TNFα production by primary murine microglia. Primary murine microglia in complete microglial medium without GM-CSF were treated with LPS at a final concentration of 1, 3, 10, 30 and 100 ng/ml for 6 or 24 h at 37°C. The conditioned medium was collected and analyzed using ELISA.
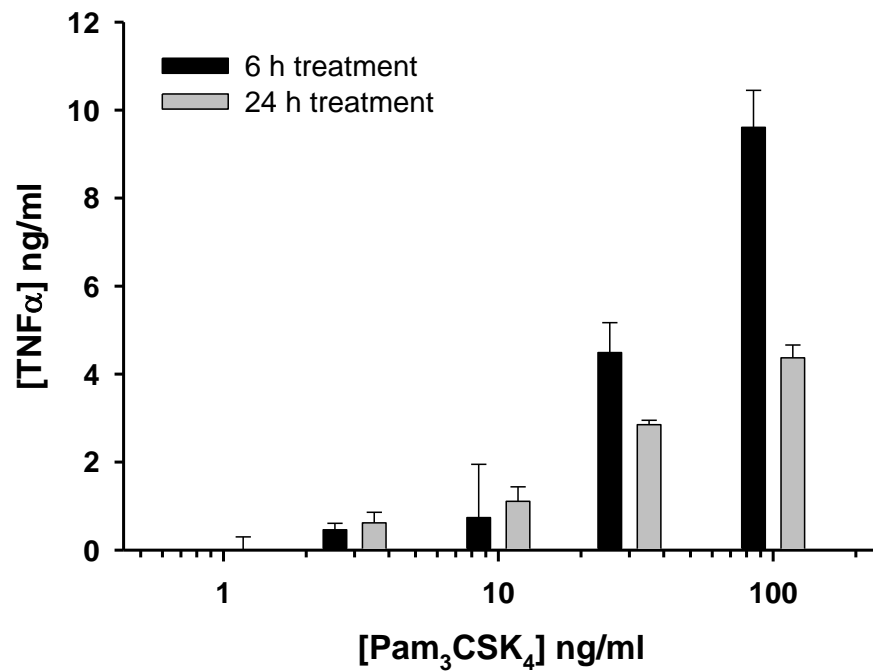
Figure 2.2 Concentration-dependence of Pam₃CSK₄-induced TNFα production by primary murine microglia. Primary murine microglia in complete microglial medium without GM-CSF were treated with Pam₃CSK₄ at a final concentration of 1, 3, 10, 30 and 100 ng/ml for 6 or 24 h at 37°C. The conditioned medium was collected and analyzed using ELISA.
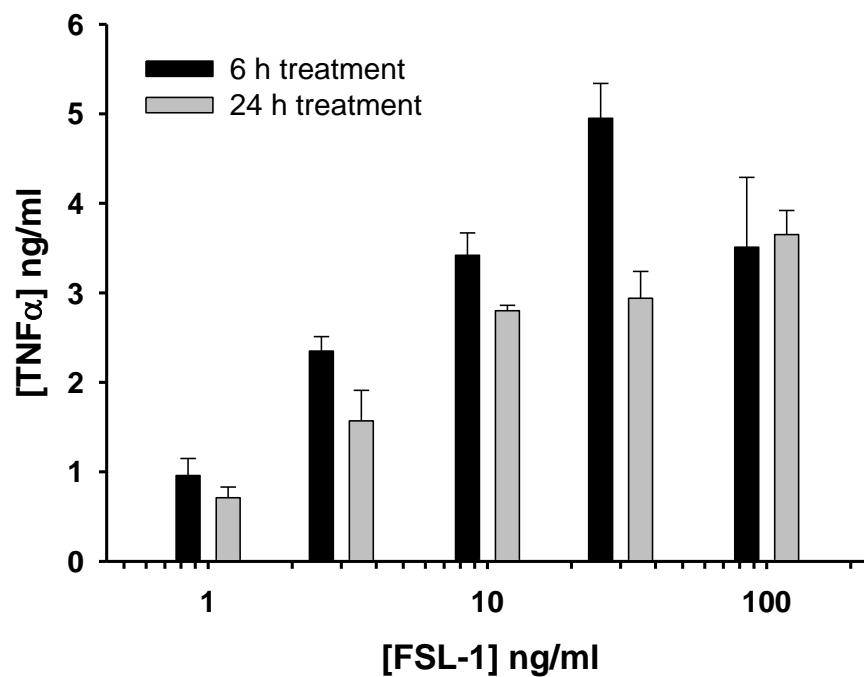
Figure 2.3   Concentration-dependence of FSL1-induced TNFα production by primary murine microglia. Primary murine microglia in complete microglial medium without GM-CSF were treated with FSL-1 at a final concentration of 1, 3, 10, 30 and 100 ng/ml for 6 or 24 h at 37°C. The conditioned medium was collected and analyzed using ELISA.

2.1.5 Characterization of BV-2 microglia proinflammatory response

Dose-response studies for LPS were also carried out for BV-2 microglia. BV-2 microglia (300 μl) were plated at a concentration of 1 x 10^5 cells/well overnight in a 48-well plate in the growth medium. Next day, the medium was replaced with medium containing 2% FBS and LPS was added for 6 or 24 h at 37°C. Serial dilutions of LPS stock solution (600 μg/ml in sterile water) were prepared to give the final concentrations of LPS as 1, 10 and 100 ng/ml for the cellular treatment. Cellular medium was analyzed by ELISA (as described in section 2.1.3). LPS produced a dose-dependent TNFα response at both 6 and 24 h of incubation (Figure 2.4). Since both 6 and 24 h produced a comparable TNFα response for each concentration of LPS, cellular treatment time was optimized to 6 h. LPS at 10 ng/ml and 3 ng/ml were used as positive controls for all the cell stimulation studies.

2.2 Preparation of Aβ

Aβ peptide has a high propensity for aggregation. Any seeds present in the Aβ solution affects the kinetics of Aβ aggregation (Evans, et al., 1995) as well as the molecular structure of aggregation species like fibrils (Petkova, et al., 2005) and oligomeric intermediates. Therefore, it is important to remove any-preformed seeds in order to obtain a homogenous solution of Aβ. The treatment of Aβ peptide with 100% hexafluoroisopropanol destabilizes the intermolecular hydrogen bonds. Synthetic
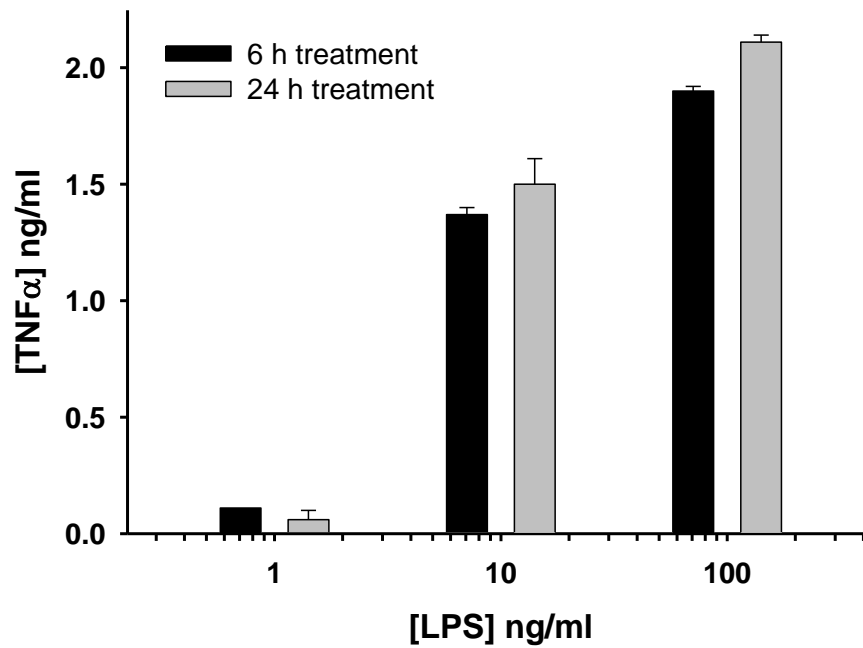
Figure 2.4 Concentration-dependence of LPS-induced TNFα response in BV-2 mouse microglia. BV-2 microglia were plated overnight in the growth medium containing 5% FBS followed by incubation with LPS at a final concentration 1, 10 and 100 ng/ml for 6 or 24 h. The conditioned medium was analyzed by ELISA for quantifying TNFα production

Aβ(1-42) peptides (Keck Center, Yale University) were dissolved in 100% hexafluoroisopropanol (HFIP) (Sigma) for 1 h at room temperature. The resulting 1 mM Aβ(1-42) stock solution was aliquoted into sterile microcentrifuge tubes, evaporated overnight under the fume hood, uncovered, at room temperature. Subsequently, the aliquots were vacuum-centrifuged to remove any residual HFIP, and stored at -20°C.

Our studies also utilized crude Aβ(1-42) and Aβ(1-40) peptides synthesized by Dr. Fabio Gallazi, University of Missouri-Columbia. We treated these peptides with trifluoroacetic acid (TFA) at a concentration of 1 mM followed by bath sonication for 10 minutes and its subsequent removal by speed-vacuum centrifugation. The TFA-pretreated peptide was further treated with 100% HFIP (final [Aβ] 1 mM) at 37°C for 1 h to facilitate further disaggregation of peptide as well as removal of residual TFA. Speed-vacuum centrifugation was employed to allow evaporation of HFIP. The lyophilized aliquots were then stored at -20°C in a container with dessicant.

1.5 mg Aβ(1-40) E22G mutant peptide was a gift from Dr Wetzel, University of Pittsburg and lyophilized in an identical manner as synthetic Aβ(1-42) peptide purchased from Keck center, Yale University and 0.75 mg aliquots were prepared and stored -20°C in a container with dessicant.

2.2.1 Size exclusion chromatography

We used AKTA-fast protein liquid chromatography (FPLC) along with a size-exclusion column for isolation of Aβ monomer and protofibrils. Size exclusion chromatography (SEC) separates the protein on the basis of its shape and size in such a

way that bigger molecules elute out first followed by the smaller molecules. AKTA-FPLC$_{TM}$ is particularly useful for efficient protein purification since it enables a constant flow rate for solvent elution via two high-precision pumps (www.gelifesciences.com).

For experiments, 1.14 mg of lyophilized Aβ(1-42) peptide was dissolved in 50 mM sodium hydroxide (NaOH, Fisher Scientific) to give a 2.5 mM Aβ solution, and further diluted to 250 μM using sterile F-12 cell culture medium (BioWorld, Dublin, OH). F-12 cell culture medium was supplemented with 100 U/ml penicillin, 0.1 mg/ml streptomycin and 0.25 μg/mL amphotericin-B (Triple antibiotic mixture, Fisher) and filtered through 0.22 μm syringe filter (Fisherbrand) to prevent any bacterial contamination in Aβ solutions (called as supplemented F-12). The Aβ solution was centrifuged at 18000 x g for 10 min with a Beckman-Coulter Microfuge®18 and immediately subjected to SEC. The centrifugation supernatant was eluted from a Superdex 75 HR 10/30 column (GE Healthcare) in supplemented F-12 medium. Prior to injection of Aβ, Superdex 75 column was coated with 2 mg bovine serum albumin (BSA, Sigma) to prevent any non-specific binding of Aβ to the column matrix. Aβ was then eluted at 0.5 ml/min and elution of Aβ was continuously monitored using UV absorbance at 280 nm. 0.5 ml fractions were collected and immediately placed on ice. The fractions eluted in void volume were pooled together and labeled as protofibrils and the fractions eluted in the included peak were pooled and labeled as monomer. Sometimes, the individual protofibril fractions were added to the cells separately to compare the TNFα production between different fractions within the Aβ(1-42) protofibril peak. Concentrations of both protofibrils and monomers were determined directly from the absorbance trace using an extinction coefficient of 1450 cm^{-1} M^{-1} at 280 nm. Isolation of

protofibrils and monomers was also carried out in artificial cerebrospinal fluid (aCSF) containing 130 mM sodium chloride (NaCl, Fisher Scientific), 3 mM potassium chloride (KCl, Fisher Scientific), 1 mM sodium phosphate dibasic (Na_2HPO_4 $7H_2O$, Fisher Scientific) and 15 mM sodium bicarbonate ($NaHCO_3$, Fisher Scientific) adjusted to pH 7.8 in a similar manner as described above. aCSF composition was modified from a protocol described in Tzounopoulos et al (Tzounopoulos, et al., 2004).

For preparation of Aβ(1-40) protofibrils, 1.2 mg Aβ(1-40) crude peptide was resuspended in 50 mM NaOH and further diluted in supplemented F-12 medium in the similar manner as described before for Aβ(1-42). Aβ solution was then subjected to SEC either immediately or after 24 hour incubation at 25°C as described before. Aβ(1-40) E22G (Arctic) mutant protofibrils were prepared using NaOH/supplemeted F-12 in a similar manner except that the Aβ solution was incubated for either 3 h or 24 h at room temperature prior to SEC.

Aβ(1-42) monomer was also obtained using an alternative method for Aβ-aggregation age studies. For these experiments, 2.2 mg crude Aβ(1-42) peptide was resuspended in 6 M guanidium hydrochloride (GuHCl, Fisher Scientific) and 10 mM ammonium hydroxide (NH_4OH, Fisher Scientific) to give a total volume of 1.0 ml. Aβ solution was then subjected to SEC and eluted using either 1x PBS (Hyclone) or 50 mM HEPES buffer (pH 8.0) or 50 mM Tris-Cl buffer (pH 8.0). Monomer fractions eluted in the included peak were sometimes pooled or used individually. Sometimes, the purified monomer was flash-frozen using dry-ice/ethanol mixture and stored at -80°C. Aggregation reactions were carried out either using freshly purified or flash-frozen SEC-purified monomer at different temperatures in a time dependent manner as described in

chapter 5. Aliquots were drawn from the Aβ aggregation reactions at 0, 48, 96 and 216 hours and flash frozen using dry-ice/ethanol mixture and stored at -80°C until the experiment. Chaotropic nature of the GuHCl/NH$_4$OH treatment yielded more monomer, which was desired for carrying out aggregation studies on SEC-purified Aβ(1-42) monomer.

2.2.2 Aβ(1-42) oligomer and fibril preparation

Aβ oligomers and fibrils obtained directly from lyophilized aliquots were prepared as previously described (Stine, et al., 2003). Briefly, lyophilized Aβ(1-42) aliquots were resuspended in sterile anhydrous dimethyl sulfoxide (DMSO) (Sigma-Aldrich, St. Louis) at 5 mM. For oligomer preparation the sample was diluted to 100 μM in sterile ice-cold F-12 cell culture medium without phenol red (Bioworld, Dublin, OH) and incubated for 24 h at 4°C. For fibril preparation the sample was diluted to 100 μM in 10 mM HCl and incubated for 24 h at 37°C.

2.2.3 Aβ(1-42) fibril preparation using SEC-purified monomer

SEC purified Aβ(1-42) monomer eluted in supplemented F-12 or aCSF (the concentration of Aβ monomer fraction differed slightly between experiments but generally 56 μM monomer was used) was incubated at room temperature, with gentle agitation for ≤72h. The aggregated Aβ(1-42) solution was centrifuged at 18000 x *g* for

10 min. The supernatant was removed and the pellet was resuspended into supplemented F-12 or aCSF to match the original starting concentration based on the Aβ(1-42) monomer. The resulting solution was labeled as Aβ(1-42) fibrils. The total Aβ(1-42) solution, 18000 x g supernatant and resuspended pellet was assessed for Thioflavin-T (ThT) fluorescence as described in section 2.3 in order to monitor conversion of monomer into ThT-positive fibrils.

2.3 Microglia stimulation experiment with Aβ

TLRs particularly TLR 2, 4 and 6 have been previously shown to play a role in Aβ-induced proinflammatory response (Fassbender, et al., 2004; Walter, et al., 2007; Udan, et al., 2008; Stewart, et al., 2010; Liu, et al., 2011). Therefore, predetermined optimal TLR ligand concentrations were utilized as positive controls for our Aβ-cell stimulation experiments (Figure 2.1-2.4). For experiment involving Aβ, medium containing primary microglia was centrifuged at 200 g for 10 min at 25°C. We resuspended and plated the microglia in complete microglial assay medium without GM-CSF or FBS overnight before the addition of freshly purified monomer, protofibrils or pre-formed fibrils. For cell stimulation studies involving Aβ(1-42) oligomers prepared in DMSO/F-12 medium and fibrils prepared in DMSO/ 10 mM HCl (Chapter 4), primary microglia were resuspended and plated in medium without serum for 2 h before the addition of Aβ and actual Aβ-treatment was also carried out in the medium devoid of serum. Serum-free conditions were adopted from the literature (Reed-Geaghan, et al.,

2009). In the experiments investigating the dependence of microglial TNFα response on the aggregation age of SEC-purified Aβ(1-42), primary microglia were resuspended and plated in a medium without GM-CSF for 2 h followed by incubation of Aβ in a medium without GM-CSF but in the presence of 10% heat-inactivated serum as in complete microglial growth medium. For all the cell stimulation experiments primary murine microglia (100 μl) were plated at a density of 5 x 10^5 cells/ml in a sterile 96-well cell culture plate. Prior to addition of Aβ to the cells, medium was always replaced with fresh assay medium as described previously. Freshly purified Aβ (1-42) monomer, protofibrils, or preformed fibrils prepared from SEC-isolated monomer were added to the cells at a final concentration of 15 μM. The concentration of monomer and protofibril fractions varied slightly from experiment to experiment. Therefore, the volume of Aβ added to achieve a final concentration of 15 μM was slightly different. Consequently, the assay medium was added in such a way that the total volume of cellular treatment was 100 μl. The negative control in each experiment consisted of addition of equal volume of buffer and assay medium to match the Aβ treatment. For example, in a typical experiment involving 56 μM of Aβ fraction, 27 μl of Aβ was added to 73 μl of assay medium whereas for the negative control, 27 μl of buffer was added to 73 μl of assay medium. For experiments involving Aβ(1-42) oligomers prepared in DMSO/F-12 medium or Aβ(1-42) fibrils prepared in DMSO/ 10 mM HCl 15 μl of Aβ sample was added to 85 μl of assay medium to give a final concentration of 15 μM Aβ in cell stimulation assays. For experiments investigating the relationship between Aβ(1-42) aggregation age and microglial proinflammatory response, final concentration of Aβ was 11 μM. After the addition of 30 μl of Aβcells were incubated at 37°C in 5 % CO_2. The

medium was collected after 6 h and stored at -20°C until analyzed by ELISA. The vehicle containing Aβ was added at the same volume as Aβ and utilized as negative control to assess the background cellular response.

All the BV-2 cellular studies were carried out in identical manner with respect to the volume of Aβ and assay medium added to the adhered microglia. For cellular studies described in chapter 3, BV-2 cells were resuspended at a density of 5 x 10^5 cells/ml in the growth medium and seeded (100 μl). in a sterile 96-well cell culture plate overnight. Prior to the cellular treatment, medium was replaced with fresh medium without FBS for monomer, protofibril and fibril stimulation followed by Aβ stimulation at a final concentration of 15 μM for 6 h similar to that of primary microglia. For studies involving Aβ(1-42) oligomers prepared in DMSO/F-12 medium and fibrils prepared in DMSO/ 10 mM HCl (Chapter 4), the cellular treatment was carried out in the assay medium containing 2% FBS for 6 h. In Aβ(1-42) aggregation age studies (Chapter 5), BV-2 microglia were incubated at 37°C for 24 h in 5% CO_2 in the presence of Aβ. The cellular conditioned medium was collected after incubation with Aβ and stored at -20°C and TNFα production was measured using ELISA.

2.3.1 Polymyxin-B sulfate neutralization assay

Polymyxin-B sulfate (PMX-B) is a peptide antibiotic active against most gram negative bacteria, and was originally isolated from *Bacillus polymyxa*. Polymyxins are known to display bacetriocidal activities by disrupting the membrane structure due to

their amphipathic nature (Storm, et al., 1977). PMX-B has been used in order to check the contamination of Aβ solutions by either gram-negative bacteria or trace levels of endotoxins (Meda, et al., 1995; Udan, et al., 2008). This assay was fairly important particularly in the context of Aβ-induced inflammation since it ruled out the possibility of false positive inflammatory reactions to Aβ due to contaminating endotoxin.

This assay was implemented to exclude the presence of endotoxin in a number of Aβ-aggregation solutions as detailed before in Udan *et al* (Udan, et al., 2008). Both BV-2 and primary mouse microglia were plated as described before in section 2.1.1 and 2.1.2 for cell stimulation experiments. PMX-B was stored as 50 mg/ml stock at -20$^{\textbf{o}}$C, which was diluted to a working stock of 600 μg/ml with water. PMX-B was added to the cells at a final concentration of 100 ng/ml followed by addition of 10 ng/ml LPS or 15 μM Aβ sample. The cells were then incubated at 37$^{\textbf{o}}$C for 6 h and the conditioned medium was collected for the subsequent analysis using ELISA. LPS was always used as a positive control for PMX-B neutralization assays.

2.3.2 XTT cell viability and proliferation assay

Viability of Aβ-treated microglia was determined by using an XTT [2, 3-bis (2-methoxy-4-nitro-5-sulfophenyl)-2H-tetrazolium-5-carboxanilide] assay. XTT is a tetrazolium dye (Figure 2.5) that can be reduced via mitochondrial electron transport chain in the presence of phenazine methosulfate (PMS) to form a water-soluble formazan product. which in turn is an indicator of cellular health (Scudiero, et al., 1988).
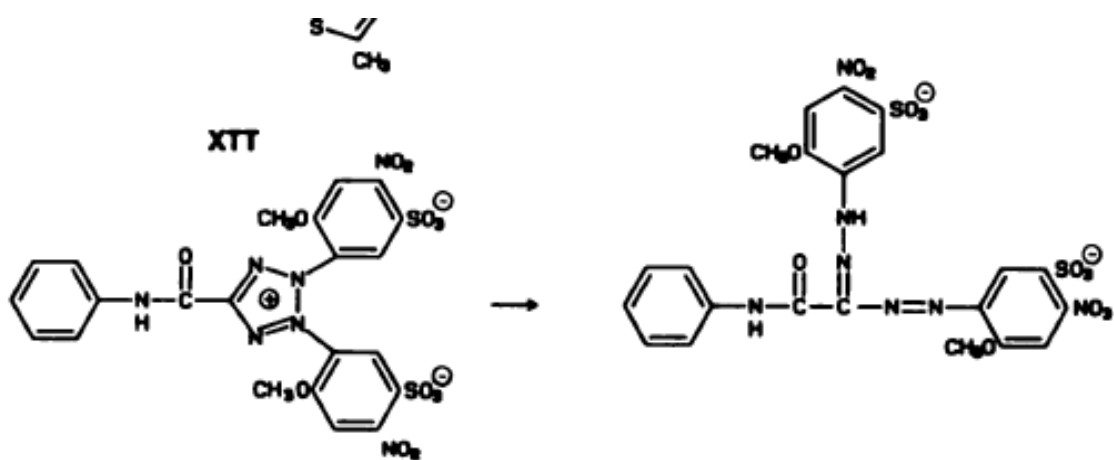
Figure 2.5 Reduction of XTT to form a formazan derivative. XTT gets reduced via mitochondrial electron transport chain to form a formazan derivative, which absorbs at 467 nm.

XTT assay was also used in a cell free manner to rule out the possibility of any bacterial contamination of Aβ(1-42) samples. XTT is obtained as a yellow color solid. After receipt, XTT solid is divided into ~15 mg aliquots and stored in 15 ml conical tubes at -20°C. For the use, solid in one conical tube is brought up in sterile RPMI-1640 medium without phenol red to give 1 mg/ml solution of XTT under aseptic conditions. The solution (1 mg/ml) is then aliquoted in 0.5 ml aliquots and stored in -20°C. PMS was stored in 5 mM (prepared in sterile water) aliquots at -20°C. The aliquoting in the solid form was carried out to prevent the bacterial contamination of working stock of XTT. In cellular XTT assay, cells exposed to Aβ for 6 h were further incubated with 0.33 mg/ml XTT (diluted in RPMI 1640 medium without phenol red) and 8.3 μM phenazine methosulfate (PMS) (Acros, Morris Plains, NJ) for 2 h at 37°C in 5% CO_2. The extent of XTT reduction was measured by absorbance of reduced form of XTT at 467 nm. The cell free XTT assay was done in parallel to the cell stimulation studies, in the similar manner as above except Aβ sample was incubated with a solution containing 0.33 mg/ml XTT and 8.3 μM PMS without any cells at the same final concentration of 15 μM for 6 h before the absorbance measurements.

2.4 Thioflavin-T fluorescence measurements

ThT is a benzathiazole dye as shown in Figure 2.6. Freshly purified solutions of Aβ(1-42), Aβ (1-40) as well as Aβ (1-40) E22G (Arctic) monomer and protofibril solutions were monitored by ThT-fluorescence. Aβ solution was diluted 10-fold into a 5

μM ThT solution prepared in 50 mM Tris-HCl buffer (pH 8.0) to make a total volume of 70 μl. ThT fluorescence emission scans (460-520 nm) were carried out using a Cary Eclipse Fluorescence spectrophotometer at an excitation wavelength of 450 nm. ThT fluorescence values were obtained by integration of emission scan between 470-500 nm. The vehicle buffer for Aβ did not show any significant ThT fluorescence when used as a negative control in the absence of Aβ.

2.5 Transmission electron microscopy (TEM)

SEC-purified Aβ(1-42) as well as Aβ(1-40) protofibrils, Aβ(1-42) fibrils formed using SEC-purified monomer, Aβ(1-42) oligomers and fibrils prepared in DMSO/10 mM HCl were diluted to 20 μmol/ L in water and 10 μl was applied to 200-mesh formvar coated copper grid (Ted Pella Inc.). Samples were allowed to incubate at room temperature for 10 min. The excess solution was wicked using a tissue wipe. Grids were washed two to three times by being placed sample side down on a droplet of water. Heavy metal staining was performed by incubation of grid in 2% uranyl acetate (Electron MicroscopySciences, Hatfield, PA) for 5 min in a similar manner followed by removal of excess solution and air drying. Affixed samples were visualized with a Philips EM 430 TEM at 300kev (Courtesy David C. Osborn).
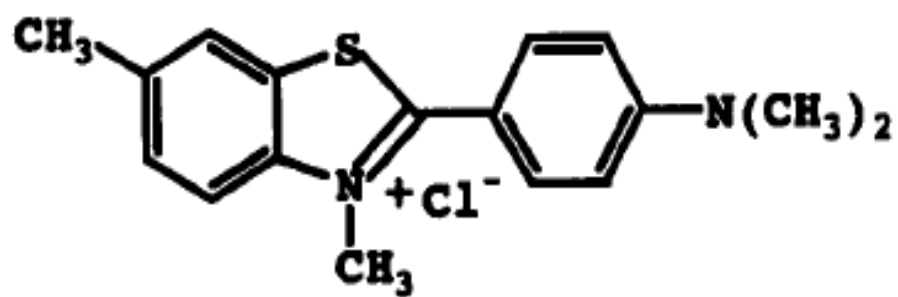
Figure 2.6 Structure of Thioflavin-T dye

2.6 Atomic Force Microscopy (AFM)

Aβ(1-42) aggregation solutions (100 μM) were diluted to 10 μM in water. Grade V1 mica (Ted Pella, Inc, Redding, CA) was cut into 11 mm circles and affixed to 12 mm metal discs. Aliquots (50 μl) were applied to freshly cleaved mica, allowed to adsorb for 15 min, washed twice with water, air dried, and stored in a container with desiccant. Images were obtained with a Nanoscope III multimode atomic force microscope (Digital Instruments, Santa Barbara, CA) in TappingMode^{TM}. Height analysis was performed using Nanoscope III software on flattened height mode images. AFM sample preparation and imaging was carried out by Lisa K. Gouwens.

2.7 Dynamic light scattering (DLS)

Hydrodynamic radius (R_H) measurements were made at room temperature with a DynaPro Titan instrument (Wyatt Technology, Santa Barbara, CA). Samples (30 μl) were placed directly into a quartz cuvette and light scattering intensity was collected at a 90º angle using a 10-second acquisition time. Particle diffusion coefficients were calculated from auto-correlated light intensity data and converted to R_H with the Stokes-Einstein equation. Average R_H values were obtained with Dynamics software (version 6.7.1). Histograms of percent intensity vs. R_H were generated by Dynamics data regularization and intensity-weighted mean R_H values were derived from the regularized histograms. DLS measurements were carried out and analyzed by Dr. Michael R. Nichols.

2.8 Dot-blot assays

Dot-blot assays make use of the specificity of antigen-antibody interaction. Dot-blot assays can be regarded as a more qualitative assay to detect the presence of antigen in a particular sample under investigation. Dot-blot assays are very similar to western blot assays except that the sample is directly adsorbed on the nitrocellulose membrane instead of electrophoretic transfer from polyacrylamide gel electrophoresis (PAGE) to the membrane. Therefore, dot-blots are relatively more straightforward and require less time than western blots. The following dot-blot protocol was adopted from Ajit et al (Ajit, et al., 2009).

Nitrocellulose membrane was moistened by immersing in water for 2 minutes. The membrane was then allowed to dry for 20 minutes. 2 μl of Aβ sample was spotted onto the membrane and allowed to adsorb for 15-20 minutes. The membrane was then blocked for any non-specific binding by incubation in 5.0 ml blocking buffer consisting of 10% dried milk in phosphate buffered saline containing 0.2% Tween-20 (called as PBST) for 1 h at 25°C with gentle agitation. The membrane was then transferred to 5.0 ml of primary antibody solution which consists of primary antibody diluted 1:5000 in PBST containing 5% dried milk. Two different primary antibodies were utilized in our dot-blot assays. Ab9 antibody (obtained from Mayo Clinic) recognizes 1-16 residues of N-terminus and thereby is capable of recognizing Aβ irrespective of its conformational state. On the other hand, OC-antibody is a conformation-specific antibody developed by Charles Glabes laboratory from University of California, Irvine that recognizes fibrillar oligomers of Aβ (Kayed, et al., 2007). The membrane was washed three times (for 5

96

minutes each) with PBST to remove non-specifically bound primary antibody and then incubated with secondary antibody diluted 1:1000 in 5.0 ml of PBST containing 5% dried milk for 1 h with gentle shaking at 25°C. Separate secondary antibodies were used for two different primary antibodies because of their species compatibility. Anti-mouse IgG (HAF007, R&D systems) was used as a secondary antibody for Ab9 whereas anti-rabbit IgG (HAF008, R&D systems) was used as secondary antibody for OC. Washing step was repeated three times as described above and membrane was incubated for 1 minute in 6 ml of ECL-western blotting substrate (Pierce, Thermo Scientific) with vigorous shaking. ECL-western blotting substrate was prepared by mixing equal volumes of detection reagent 1 with detection reagent 2. Excess ECL substrate was removed by blotting the membrane on Whatman paper. The dot blot was developed by exposing the film for 20 seconds.

CHAPTER 3

MICROGLIAL ACTIVATION BY Aβ PROTOFIBRILS

3.1 Introduction

Alzheimer's disease (AD) is a neurodegenerative disease more prevalent in the elderly population (Thies and Bleiler, 2011). Extracellular senile plaques and intracellular tau tangles represent the two classical hallmarks of the AD brain (Selkoe, 2011). Clustering of activated microglia and significant level of endogenous inflammatory markers associated with the senile plaques depicts the characteristic inflammatory component associated with AD pathology (Finch and Marchalonis, 1996). Moreover, such a state of chronic inflammation is believed to contribute towards neuronal degeneration observed in AD (McGeer and McGeer, 1998). Amyloid-β (Aβ) protein is a major constituent of senile plaques (Glenner and Wong, 1984). It is ubiquitously generated as a product of sequential proteolytic cleavage of a larger precursor protein known as amyloid precursor protein (APP) (Kang, et al., 1987). Three

different proteases such as α, β and γ secretase are involved in the APP cleavage (Sisodia, et al., 1990). Since γ-secretase cleaves APP in a heterogeneous fashion, it give rise to carboxy-terminal variants of Aβ protein with varying amino acid length (Edbauer, et al., 2003). Aβ(1-42) and Aβ(1-40) are the most common variants, which in their unaggregated monomeric form circulates normally in the body at nanomolar concentrations (Seubert, et al., 1992; Shoji, et al., 1992). By some yet unknown event, monomeric Aβ starts to aggregate into long fibers, rich in β-sheet structure, forming the core of the plaques (Glenner and Wong, 1984). The aggregation propensity is significantly higher for the Aβ variants with longer carboxy terminus (Jarrett, et al., 1993). Genetic evidence has shown that mutations in APP alter normal Aβ metabolism, thereby causing familial AD (Scheuner, et al., 1996; Selkoe and Podlisny, 2002). Also, active immunization studies using synthetic Aβ and passive immunization studies using anti-Aβ antibodies in AD transgenic mice not only prevented amyloid deposition but also reduced related neuritic dystrophy and astrogliosis (Schenk, et al., 1999; Janus, et al., 2000). These and several other lines of evidence support the amyloid hypothesis, which proposes a primary role for Aβ accumulation in the AD pathogenesis (Hardy and Higgins, 1992).

In vitro aggregation studies on Aβ have been particularly useful in understanding the mechanistic details of Aβ aggregation. Starting from its monomeric form, Aβ is reported to form a variety of species including dimers, protofibrils, and oligomers during fibrillogenesis. These species differ significantly in their size, morphology, structure and solubility (Walsh and Selkoe, 2007). Interestingly, these species were shown to be present in the AD brain by means of specific antibodies (Gong, et al., 2003; Kayed, et al.,

2003; Shankar, et al., 2008). Furthermore, they exhibited significant toxicity to neuronal cultures *in vitro* (Hartley, et al., 1999; Dahlgren, et al., 2002; Lacor, et al., 2004; O'Nuallain, et al., 2010). In fact, recent evidence has shown that a significant amount of oligomeric Aβ exists within and around the periphery of senile plaques in the AD brain (Koffie, et al., 2009; DaRocha-Souto, et al., 2011). Moreover, oligomeric Aβ appears to correlate better with clinical disease severity than total amyloid plaque burden (DaRocha-Souto, et al., 2011). Although there is increasing support for the role of oligomers in early synaptotoxicity, Aβ fibrils are generally believed to act as a stimulus for microglia-mediated inflammation *in vitro*. In light of the recent detection of oligomeric species in the periphery of senile plaques, investigating the nature of stimulus for microglial activation needs a revisit, particularly since microglia are found to be clustered around the plaques.

In a study by White et al (2005), oligomeric Aβ(1-42) was found to be more effective than fibrils in provoking a proinflammatory response (White, et al., 2005). In fact, both fibrils and oligomers have been shown to produce a qualitatively distinct activation profile in microglia when probed using antibodies against different tyrosine kinases (Sondag, et al., 2009).

A number of studies have been carried out on Aβ protofibrils to better understand their structure and neurotoxic properties after their original identification in 1997 by Walsh and colleagues (Walsh, et al., 1997). Moreover, the biological relevance of Aβ protofibrils became more apparent after identification of their role in a familial AD case. In this familial case, a family from northern Sweden was found to harbor an intra-Aβ mutation E22G (Arctic), which resulted in the rapid formation and stabilization of

protofibrils (Nilsberth, et al., 2001). However, the role of Aβ protofibrils in microglial activation has not been investigated.

In this study, we prepared Aβ(1-42) protofibrils and investigated their ability to provoke a proinflammatory response in murine microglia. Furthermore, we isolated insoluble Aβ(1-42) fibrils, Aβ(1-40) wild type (WT) and Aβ(1-40) E22G (Arctic) protofibrils to compare their ability to activate microglia with that of the Aβ(1-42) protofibrils. In our study, we rigorously characterized Aβ preparations to be able to correlate aggregation state to microglial proinflammatory response.

3.2 SEC isolation of Aβ(1-42) protofibrils and monomers

SEC has been extremely helpful in separating Aβ protofibrils from low molecular weight Aβ (Walsh, et al., 1997; Lashuel, et al., 2003). Walsh and colleagues prepared Aβ protofibrils by resuspending Aβ peptide in sodium hydroxide (NaOH) followed by dilution using phosphate-buffered saline (PBS) and subjecting the solution to SEC. Curvilinear 100-200 nm long protofibrils eluted out in the void volume (Walsh, et al., 1997). Use of NaOH allows rapid transition to basic pH preventing the aggregation of Aβ around its isoelectric pH (5.5) (Jan, et al., 2010). We slightly modified the original method of Walsh *et al* to prepare Aβ(1-42) protofibrils. We resuspended 1.14 mg Aβ(1-42) peptide in NaOH (concentration of Aβ 2.5 mM), followed by dilution into F-12 cell culture medium supplemented with antibiotics (supplemented F-12) to give a 250 μM Aβ(1-42) solution. This solution was centrifuged at 18000 *g* for 10 minutes and

immediately loaded onto Superdex 75 SEC-column and eluted in supplemented F-12 as described in the methods. An elution profile was obtained by monitoring absorbance at 280 nm and the concentrations of Aβ in various fractions were calculated using an extinction coefficient of 1450 $M^{-1}cm^{-1}$. The elution profile typically showed two peaks as shown in Figure 3.1. Protofibrils eluted in the void peak followed by monomers in the included peak. The void peak fractions were pooled and designated as Aβ(1-42) protofibrils whereas included peak fractions were pooled and designated as Aβ(1-42) monomer for the experiments. Usually the distribution of protofibrils to monomers was equivalent, but the equilibrium was found to be shifted towards increased formation of protofibrils with increasing incubation time between resuspension of Aβ(1-42) peptide and its loading on the SEC (data not shown). This shift is in agreement with kinetics of Aβ(1-40) protofibril formation reported by Walsh et al (Walsh, et al., 1997).

F-12 medium has comparable ionic strength (16 mS/cm as estimated by conductivity measurements) to PBS (21 mS/cm) used in the original preparation of Aβ protofibrils by Walsh *et al* (Walsh, et al., 1997). Moreover, the use of cell culture medium is physiologically compatible for the subsequent cellular studies yet there were some shortcomings for the use of F-12 medium. Firstly, F-12 medium is slightly pink in color and gives a noticeable background absorbance. This background absorbance interfered with the bicinchoninic acid (BCA) assay for estimating protein concentration in SEC-isolated protofibril or monomer fractions in F-12 medium. Secondly, the high glucose content in the F-12 medium made it susceptible to bacterial contamination after prolonged incubation. We prevented contamination by incorporating antibiotics in the F-
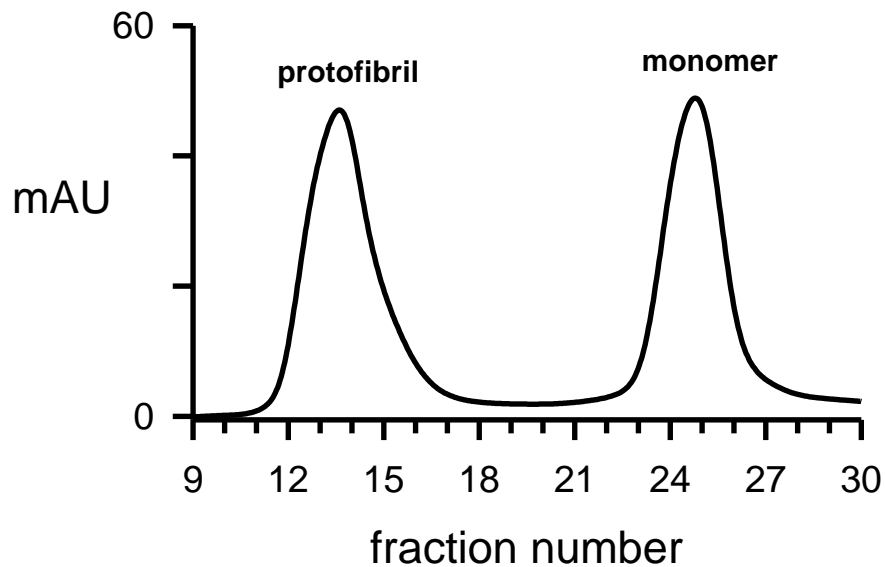
Figure 3.1 Isolation of Aβ(1-42) protofibrils and monomers using size exclusion chromatography. Dual peaks are observed following SEC elution of Aβ(1-42) reconstituted in NaOH/F-12. Lyophylized Aβ(1-42) (1.1 mg) was brought into solution with NaOH followed by supplemented F-12 media (250 μM). The supernatant after centrifugation was eluted from a Superdex 75 column and 0.5 ml fractions were collected. UV absorbance at 280 nm was monitored during the elution (solid line).

12 medium as described before in the methods and also carefully analyzed all of our experiments for any traces of bacterial contamination. However, to avoid these potential caveats, the use of artificial cerebrospinal fluid (aCSF) was explored for the isolation of Aβ(1-42) protofibrils. Isolation of Aβ(1-42) protofibrils was carried out in an identical manner except that aCSF was used to dilute Aβ(1-42) reconstituted in NaOH as well as to elute Aβ from SEC. Our aCSF composition was modified from the compositions described in the literature and contained 130 mM sodium chloride (NaCl), 3 mM potassium chloride (KCl), 1 mM sodium phosphate dibasic (NaH_2PO_4) and 15 mM sodium bicarbonate ($NaHCO_3$). Our aCSF preparation had comparable ionic strength (15 mS/cm based on conductivity measurements) with F-12 medium although was devoid of glucose for preventing the likelihood of contamination. Using aCSF we were able isolate Aβ(1-42) protofibrils and monomer, and the SEC-elution profile was identical to that with F-12 medium (data not shown).

Aβ protofibrils are typically high molecular weight species, and therefore, scatter a substantial amount of light. Scattering interferes with accurate concentration measurements based on UV in such a way that the concentrations are overestimated. We were able to complement UV concentration measurements of protofibrils and monomers in aCSF by the BCA assay (carried out by Ben Ruck), which exhibited little to no background absorbance unlike F-12 medium (data not shown). Furthermore, use of aCSF as elution buffer made the concentration estimation by quantitative amino acid analysis (QAAA) feasible, since F-12 medium contains a number of amino acids which would interfere with QAAA. QAAA was carried out on our samples by Keck center, Yale University, and revealed that the monomer concentration closely matched the

concentration based on UV but the protofibril concentrations were overestimated as expected by almost 3 times the actual concentration (data not shown).

3.3 Preparation of Aβ(1-42) fibrils from SEC-isolated monomer

Our next goal was to prepare homogeneous solutions of Aβ(1-42) fibrils. Many studies have utilized fibrils that are formed by incubating Aβ(1-42) solutions at higher temperatures or for longer time. These solutions can exhibit some degree of polydispersity, and the presence of soluble species cannot be completely ruled out. Some fibrillar preparations described in the literature used non-physiological conditions to form fibrils, which include acidic pH, low ionic strength and an absence of buffer (Stine, et al., 2003). Also, these solutions were prepared using HFIP-treated, lyophilized Aβ(1-42) peptide as a starting material. In this case, the presence of pre-existing seeds or rapid formation of seeds cannot be ruled out owing to the high propensity of Aβ(1-42) for aggregation (Chapter 5). So we wanted to take an extra step using SEC to obtain highly monomeric Aβ(1-42) solutions for fibril formation. The monomer fraction obtained during protofibril separation using physiologically compatible F-12 medium was further subjected to gentle agitation for 72 h at 25°C. After 72 h, the Aβ solution was centrifuged at 18000 g for 10 mins to pellet out the insoluble fibrils, and the supernatant was removed. The pellet was resuspended in fresh F-12 cell culture medium to match the original monomeric concentration. Conversion of SEC-isolated monomer to fibrils was monitored using ThT-fluorescence. ThT is a benzothiazole dye which exhibits enhanced emission fluorescence at 482 nm when excited at 450 nm upon binding to amyloids

(LeVine, 1993). The presence of β-sheet structure in the aggregates is an important element of the amyloid-ThT interaction. ThT fluorescence thus offers a common and relatively easy method to monitor the formation of β-sheet-containing aggregates in a particular Aβ solution (LeVine, 1993). However, ThT is also shown to bind nucleic acids by intercalation (Canete, et al., 1987). Khurana *et al* have shown that ThT can form micelles above critical micelle concentration of 4 μM in aqueous solutions (Khurana, et al., 2005). Moreover, they suggested that the benzothiazole group is exposed at the surface of micelles, which can form a hydrogen bond with amyloid fibrils via the positively charged nitrogen on the thiazole group. Thus they suggest that the interaction between Aβ fibrils and ThT can be both electrostatic and hydrophobic (Khurana, et al., 2005). The enhancement of ThT emission fluorescence decreases with decreasing pH of the amyloid solution. Khurana and colleagues suggest that pH modulates the ionic interaction that forms ThT micelles, so at lower pH, the micelles are dissolved based on AFM analysis (Khurana, et al., 2005).

ThT measurements of 72 h aggregation solution revaled that >98% ThT-fluorescence was spun down as a pellet confirming the conversion of monomer into fibrils (Figure 3.2). Furthermore, the fluorescence was recovered after reconstitution of the pellet. Also, this isolation step was able to remove any soluble species from the fibril preparation, yielding a homogeneous fibril solution for our experiments.
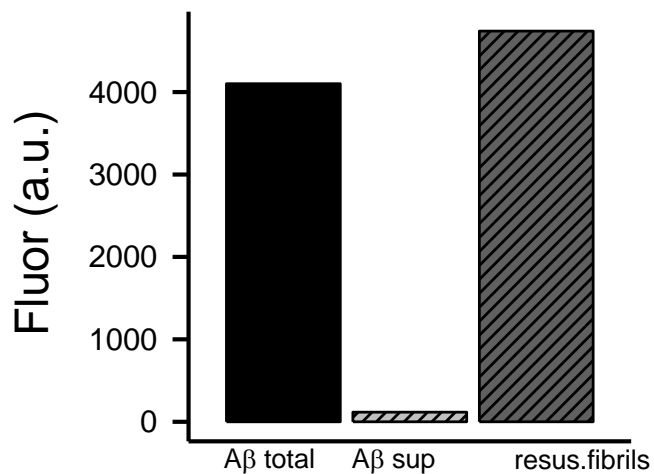
Figure 3.2 Preparation of Aβ(1-42) fibrils using SEC-isolated Aβ(1-42) monomer.
SEC-isolated Aβ(1-42) monomer in F-12 cell culture medium was gently agitated for
approximately 72 h at 25°C. Resulting Aβ solution was then centrifuged at 18000 g for
10 min, supernatant was removed and the insoluble pellet was resuspended in F-12 cell
culture medium to match the original concentration of monomer. Aβ total solution before
centrifugation, 18000 g supernatant and the resuspended fibril pellet were diluted 10-fold
in 5 μM ThT in 50 mM tris buffer (pH 8.0). ThT-fluorescence scans were carried out as
described in methods. These data are representative of four different experiments.

3.4 Morphological analysis of Aβ(1-42) protofibrils and fibrils prepared from SEC-isolated monomer by transmission electron microscopy

We wanted to confirm the isolation of Aβ(1-42) protofibrils and fibrils morphologically using TEM. TEM images of negatively stained protofibrils revealed classic curvilinear structures of <100 nm length (Figure 3.3 panel A). These images are consistent with that reported by Walsh et al (Walsh, et al., 1997). Estimated Aβ(1-42) protofibril length was 50 ± 16 nm (standard deviation, std dev) for n=50 measurements based on manual length measurements of unambiguous protofibril structures in the TEM image.

Dynamic light scattering (DLS) measurements were carried out on peak protofibril fractions from seven separate SEC purifications (measurements carried out and analyzed by Dr. Michael R. Nichols). The average hydrodynamic radius (R_H) was 21 ± 6 nm (std dev). Deconvolution of the average R_H values into histograms by data regularization revealed two predominant peaks of 4.5 ± 0.9 nm and 20.6 ± 6.5 nm. Peak 1 with the smaller R_H value was observed in 4 of 7 protofibril isolations while peak 2 was always observed. Even within isolated Aβ(1-42) protofibrils, a degree of polydispersity was present as the peak 2 histogram widths varied from narrow (e.g. 15-20 nm) to broad (e.g. 8-41 nm) in different experiments.

TEM images of negatively stained Aβ(1-42) fibrils revealed long fibers of > 1 μm length and 5-10 nm width (Figure 3.3 panel B). Moreover, these fibrils were found to be laterally associated with each other, which might be due to the physiological ionic strength and pH of the F-12 cell culture medium.
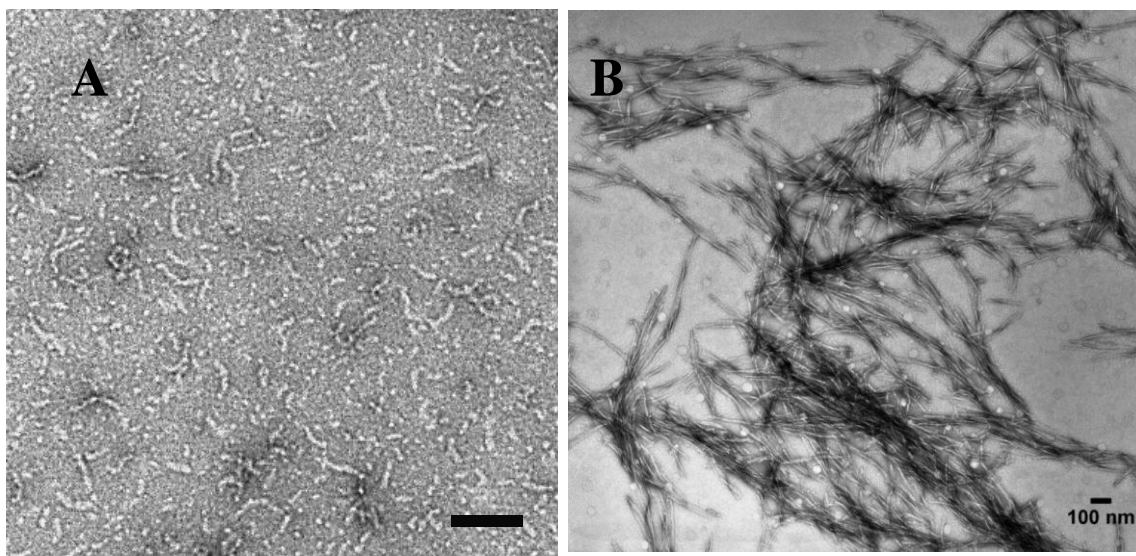
Figure 3.3 Morphological analysis of Aβ(1-42) protofibrils and Aβ(1-42) fibrils prepared in F-12 medium. Panel A. Protofibrils were diluted to 20 μM, applied to a copper formvar grid, and imaged by TEM at a magnification of 43,000. The scale bar represents 100 nm **Panel B.** TEM images of Aβ(1-42) fibril pellets (74 μM) (prepared as detailed in methods) at a magnification of 25,000.

TEM images of Aβ(1-42) protofibrils and fibrils isolated in aCSF looked similar to those isolated in F-12 medium (data not shown).

3.5 Thioflavin-T fluorescence studies on different aggregation states of Aβ(1-42)

The utility of ThT fluorescence was discussed earlier in section 3.3 and it was used here to study different aggregation states s of Aβ(1-42) peptide including SEC-isolated monomer, protofibrils and isolated fibrils. Fibrils displayed the maximum ThT-fluorescence/mole, which is consistent with their high β-sheet content (Figure. 3.4). Protofibrils displayed relatively less yet considerable ThT-fluorescence, whereas monomer showed very little to no ThT-fluorescence. We have observed previously that freshly reconstituted Aβ(1-42) peptide possessed considerable ThT fluorescence, which suggests against its highly monomeric nature (data shown in chapter 5, figure 5.2). By SEC, we were able to get highly monomeric solutions of Aβ(1-42) based on lack of ThT-fluorescence (Figure 3.4). Aβ(1-42) protofibrils and fibrils isolated in aCSF showed similar ThT-binding profile (data not shown).
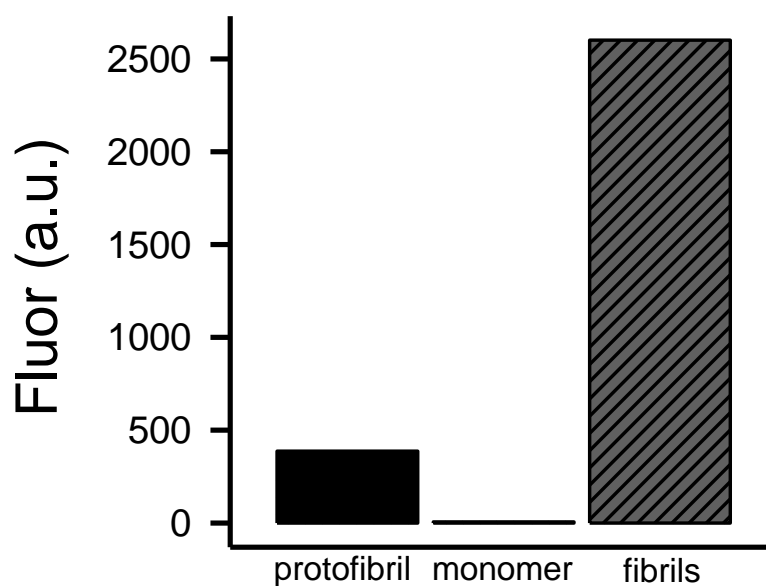
Figure 3.4 ThT fluorescence measurements of Aβ(1-42) protofibrils, monomer and preformed fibrils Freshly isolated Aβ(1-42) protofibrils, monomers after elution from Superdex 75 in supplemented F-12 and preformed fibrils prepared using SEC-isolated monomer were diluted 10-fold in 5 μM ThT in tris buffer (pH 8.0) and fluorescence emission was measured as described in the Methods.

3.6 Aβ(1-42) protofibrils activated microglia but Aβ(1-42) fibrils or monomer did not

Next, we wanted to investigate the ability of different aggregation states of Aβ(1-42) namely, protofibrils, monomers and fibrils, to cause microglial activation. Production of proinflammatory molecules is one of the important outcomes of microglial activation (Cacquevel, et al., 2004). Moreover, AD brain is found to have elevated levels of tumor necrosis factor α (TNFα), which is a proinflammatory cytokine (Dickson, et al., 1993). Homogeneous solutions of freshly isolated protofibrils, monomers and pre-formed fibrils were added to the primary or BV-2 mouse microglial cells at a concentration of 15 μM under serum-free conditions as detailed in methods. The cellular conditioned medium was collected after 6 h incubation at 37°C in 5% CO_2 for further analysis using ELISA for TNFα production. Surprisingly, fibrils failed to stimulate microglial TNFα production despite their maximum β-sheet content (Figure 3.5). In fact, Aβ(1-42) protofibrils were the most effective inducers of microglial TNFα response, whereas Aβ(1-42) monomer was largely ineffective. BV-2 microglia showed similar results (data not shown). Most of the cell-stimulation experiments utilized freshly isolated protofibrils and monomers, yet we have observed that protofibrils continue to activate microglia even after continued incubation at 4°C after their isolation by SEC (data not shown). However, we have not investigated this systematically.

Moreover, freshly purified Aβ(1-42) protofibrils induced a dose-dependent pro-inflammatory response when added at 5, 10, 15 and 20 μM concentration to the primary murine microglia (Figure 3.6 panel A) and BV-2 microglia (Figure 3.6 panel B).
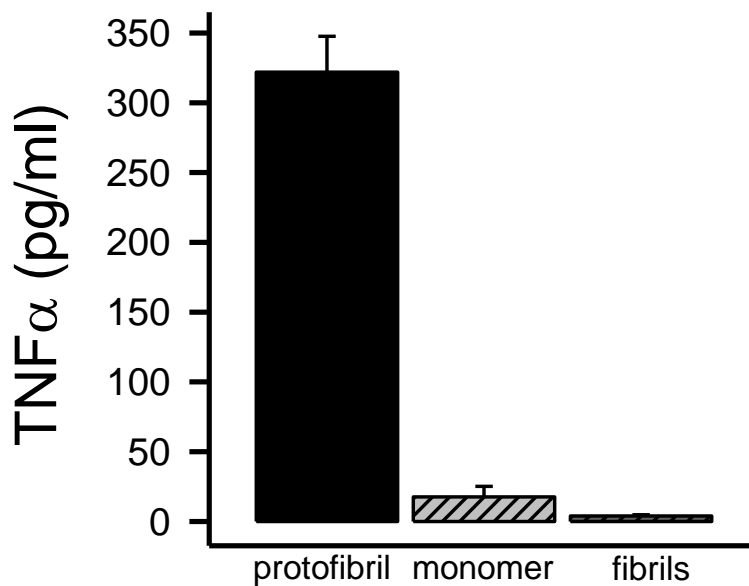
Figure 3.5 Aβ(1-42) protofibrils are significant stimulators of primary mouse microglia while monomer and fibrils fail to stimulate microglia. Primary mouse microglia were plated in a medium without serum for 24 h. Freshly purified Aβ(1-42) protofibrils, monomers and preformed fibrils were added to the cells at a final concentration of 15 μM for 6 h at 37ºC under serum-free conditions. The conditioned medium was analyzed for TNFα production using ELISA. Error bars represent the average ± std error of n=6. Control treatments with supplemented F-12 media produced 15 pg/ml TNFα for primary microglia and were subtracted from Aβ-stimulated samples.
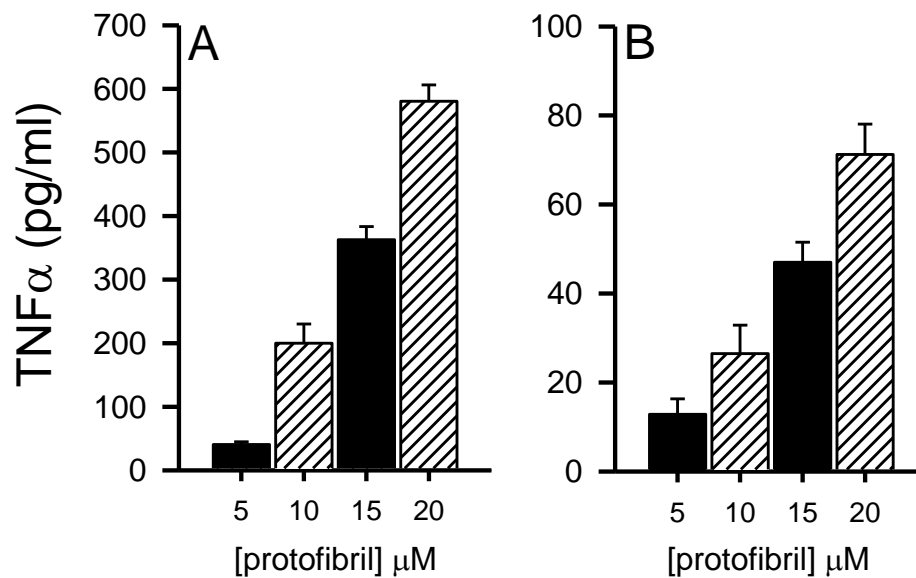
Figure 3.6 Concentration dependence of Aβ(1-42) protofibril-induced microglial TNFα response SEC-isolated Aβ(1-42) protofibrils in supplemented F-12 were incubated with primary microglia (Panel A) or BV-2 microglia (Panel B) for 6 h at final concentrations of 5, 10, 15, and 20 μM. Secreted TNFα was measured by ELISA in the conditioned medium. Data bars represent the average ± std error of n=4-6 trials at each concentration for primary microglia and n=6 trials at each concentration for BV-2 microglia. Control treatments with supplemented F-12 media produced 6 and 17 pg/ml TNFα respectively for primary and BV-2 microglia and were subtracted from Aβ-stimulated samples. Primary and BV-2 microglia were stimulated by Aβ in serum-free conditions.

SEC-isolated Aβ(1-42) protofibrils in aCSF were not only morphologically similar to those in F-12 cell culture medium but also were able to invoke a microglial proinflammatory response at the same concentration (15μM) (data not shown). Also, the monomer isolated in aCSF did not activate microglia (data not shown). These observations in turn support our earlier observation that Aβ(1-42) protofibrils act as strong inflammatory stimuli (Figure 3.5). Also, it is likely that the actual protofibril concentration in the cellular treatment was much less than 15 μM based on QAAA for protofibrils in aCSF. For both experiments, the background TNFα response was found out to be very low as assessed using the buffer vehicle for Aβ and was subtracted from Aβ-induced response.

3.7 Aβ(1-42) protofibril induced TNFα production in non-toxic manner and was independent of trace levels of contaminating bacteria or endotoxins

3.7.1 Aβ(1-42) protofibril induced TNFα production in non-toxic manner

Aβ(1-42) protofibrils have been shown to be neurotoxic (Hartley, et al., 1999; O'Nuallain, et al., 2010). We wanted to ensure that Aβ(1-42) protofibril-induced TNFα production in murine microglia was solely the result of the Aβ-challenge, rather than any compromise in cellular health or cytotoxicity. Also, conditioned medium of microglial cells challenged with Aβ have been previously shown to confer neurotoxicity via TNFα (Floden, et al., 2005). Therefore, it was important to find out if Aβ(1-42) protofibrils are

115

exerting toxicity to microglia themselves. We made use of the XTT [2, 3-bis (2-methoxy-4-nitro-5-sulfophenyl)-2H-tetrazolium-5-carboxanilide] cell proliferation assay (Scudiero, et al., 1988) to assess microglial health after treatment with Aβ. As described in methods, XTT is a tetrazolium derivative that can be reduced by mitochondrial enzymes to a colored product which absorbs at 467 nm. The intensity of color is directly proportional to the mitochondrial metabolism, which in turn reflects the cellular health. We incubated BV-2 and primary mouse microglia pretreated for 6 h with Aβ(1-42) protofibrils, fibrils or monomer in the presence of XTT as detailed in the methods. After 2 h of incubation, the reduced form of XTT was read at 467 nm. The XTT cell proliferation assay showed high absorbance values for microglial cells treated with Aβ(1-42) protofibrils. Moreover, there was no significant difference in XTT reduction between cells treated with protofibrils and cells treated with buffer vehicle or lipopolysaccharide (LPS) (Figure 3.7). This observation suggests that Aβ(1-42) protofibrils activate microglia in a non-toxic manner. BV-2 microglia pretreated with Aβ(1-42) fibrils were non-toxic to microglia as well. Consequently, the possibility of fibrils being neurotoxic was also ruled out. Similar results were obtained for primary mouse microglia confirming the non-toxic nature of Aβ(1-42) protofibrils and fibrils to microglia.

3.7.2 Aβ(1-42) preparations were free of traces of endotoxin or bacterial contamination

Bacterial endotoxins such as LPS are known to elicit a TNFα response by microglia. To assess the presence of contaminating bacteria, the XTT assay was also
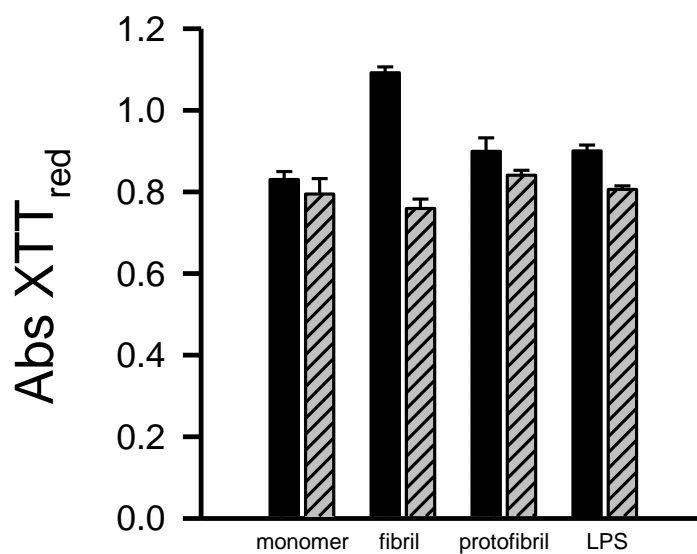
Figure 3.7 Aβ(1-42) protofibrils activated microglia in a non-toxic manner. BV-2 microglia pretreated with Aβ(1-42) protofibrils, monomer or fibrils were incubated with XTT and PMS for 2 h at 37°C as detailed in methods. The absorbance was read at 467 nm. LPS (3 ng/ml) and F-12 medium was used as control n=6 for samples (black bars), n=3 for controls (hatched bars)

employed in a cell-free manner. Different Aβ(1-42) preparations including monomer, protofibrils and fibrils were incubated at the same concentration of 15 μM in the presence of 0.33 mg/ml XTT and 8.3 μM PMS solution for 6 h as detailed in methods. In other words, the XTT assay was carried out in parallel to cellular treatment in the absence of microglia. So any bacterial presence was expected to reduce XTT which could be compared to control wells with sterile buffer vehicle. We did not see any significant reduction of XTT as compared to controls (Figure 3.8) suggesting that our Aβ(1-42) preparations are devoid of bacterial contamination.

The presence of trace levels of endotoxins was also assessed by utilizing a polymyxin B neutralization assay (Meda, et al., 1995; Udan, et al., 2008). Polymyxin B is an antibiotic, which neutralizes the endotoxin-induced proinflammatory response by binding to endotoxin (Storm, et al., 1977). Addition of polymyxin-B to the microglia (100 ng/ml) was able to block LPS (3 ng/ml)-induced TNFα production, while it had no effect on Aβ(1-42) protofibril (15 μM)-induced TNFα production (Figure 3.9).

3.8 Size-exclusion chromatography isolation of Aβ(1-40) and Aβ(1-40) E22G (Arctic) protofibrils

Aβ(1-42) was able to form classical curvilinear protofibrils immediately after reconstitution with NaOH/F-12. We wanted to examine if other variants of Aβ peptide such as Aβ(1-40) and Aβ(1-40) E22G (Arctic) can form protofibrils under similar conditions. Interestingly, Aβ(1-40) peptide (1.2 mg) did not form any protofibrils when
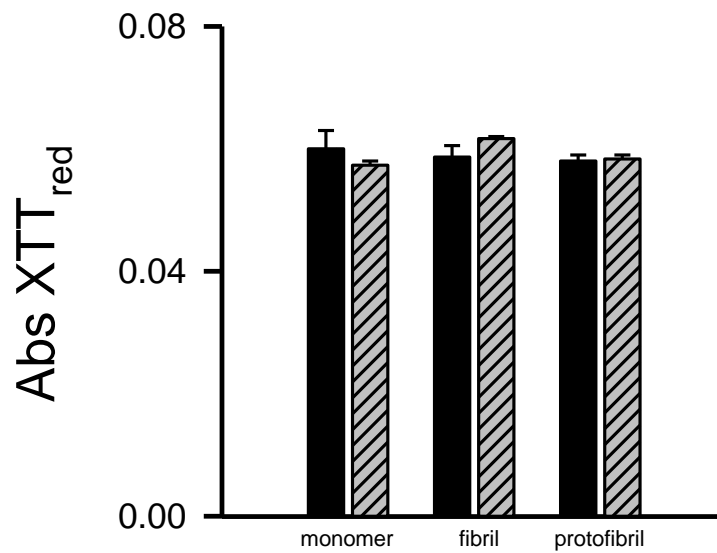
Figure 3.8 The preparations of Aβ(1-42) protofibrils, monomer and pre-formed fibrils are endotoxin-free. Freshly purified Aβ(1-42) protofibrils, monomers and fibrils prepared using SEC-isolated monomer were incubated with XTT and PMS for 6 h at 37°C. The final concentration of Aβ was 15 μM. For the negative control, F-12 cell culture medium was incubated with XTT and PMS at the same volume as Aβ sample. The reduction of XTT was read at 467 nm.
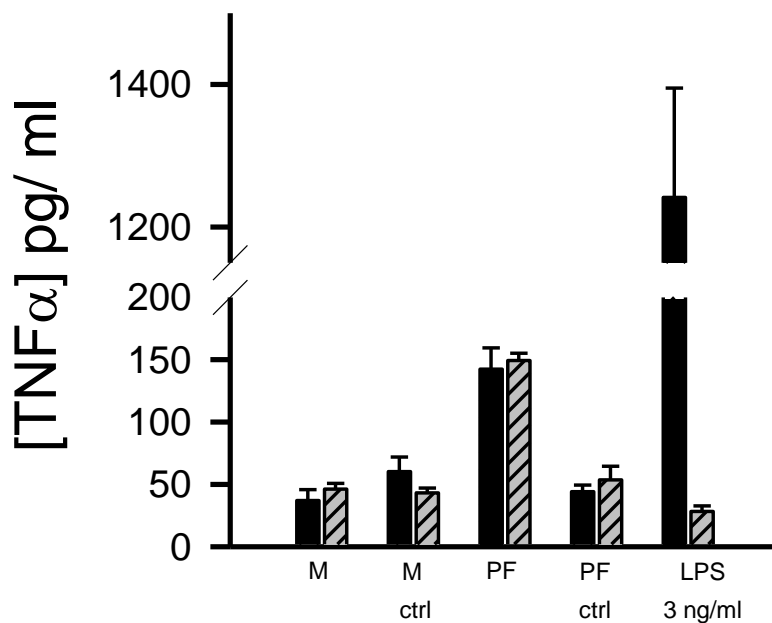
Figure 3.9 Polymyxin B did not affect Aβ(1-42) protofibril-induced TNFα response in primary murine microglia. Primary murine microglia were plated in serum-free medium for 24 h. Freshly purified Aβ(1-42) monomer (M) and protofibrils (PF) were added to the microglia at a final concentration of 15 μM. In some wells, PMX-B was added at a final concentration of 100 ng/ml. Lipopolysaccharide (LPS) (3 ng/ml) was used as a positive control. As negative control, F-12 medium was added at the same volume as each monomer and protofibril sample. The cells were incubated for 6 h at 37°C. The conditioned medium was analyzed using ELISA for TNFα production.

separated on SEC right after its reconstitution in NaOH/supplemented F-12 in an identical manner as Aβ(1-42). In fact, all of the Aβ(1-40) peptide eluted as monomer in the included peak (Figure 3.10, dashed line). Incubation of Aβ(1-40) for 24 h at 25°C was required to generate significant amount of protofibrils after reconstitution in NaOH/supplemented F-12 (Figure 3.10, solid line). Also, most of the ThT-fluorescence stayed in the 18000 g supernatant of Aβ(1-40) solution after 24 h (data not shown), which indicated the formation of protofibrils, consistent with ThT-binding nature of soluble protofibrils.

The intra-Aβ mutation E22G (Arctic mutation) was first found to be associated with AD in a family from Sweden (Nilsberth, et al., 2001). Interestingly, this mutation causes rapid formation of protofibrils (Nilsberth, et al., 2001). In our studies, Aβ(1-40) E22G (Arctic) mutant resuspended in NaOH/F-12 was able to form protofibrils as soon as 3 h after incubation at 25°C. However, prolonged incubation for 24 h did not significantly change the amount of protofibrils formed (Figure 3.11). In agreement with Lashuel et al, we observed that E22G mutation was able to accelerate the formation of protofibrils as compared to the wild type Aβ(1-40) (Lashuel, et al., 2003).

3.9 Biophysical and morphological characterization of Aβ(1-40) and Aβ(1-40) E22G (Arctic) protofibrils

Both Aβ(1-40) and Aβ(1-40) E22G protofibrils exhibited greater ThT fluorescence per mole than the monomers, similar to Aβ(1-42) protofibrils (Figure 3.12 Panel A and C).
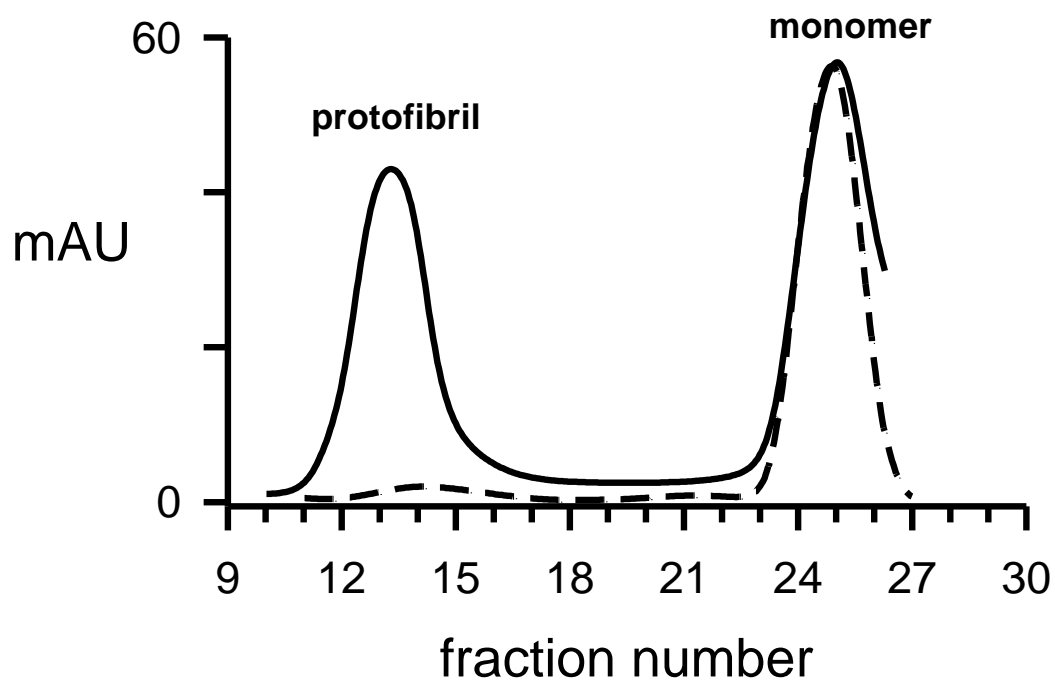
Figure 3.10 Aβ(1-40) protofibrils require longer incubation for formation. Aβ(1-40) was reconstituted and prepared for SEC as described in the Methods. Aβ(1-40) solutions were eluted on Superdex 75 immediately (dashed line) or after a 24 hr incubation at 25°C (solid line). Fractions containing protofibrils and monomers were immediately placed on ice for further characterization. Concentrations were determined by UV absorbance.
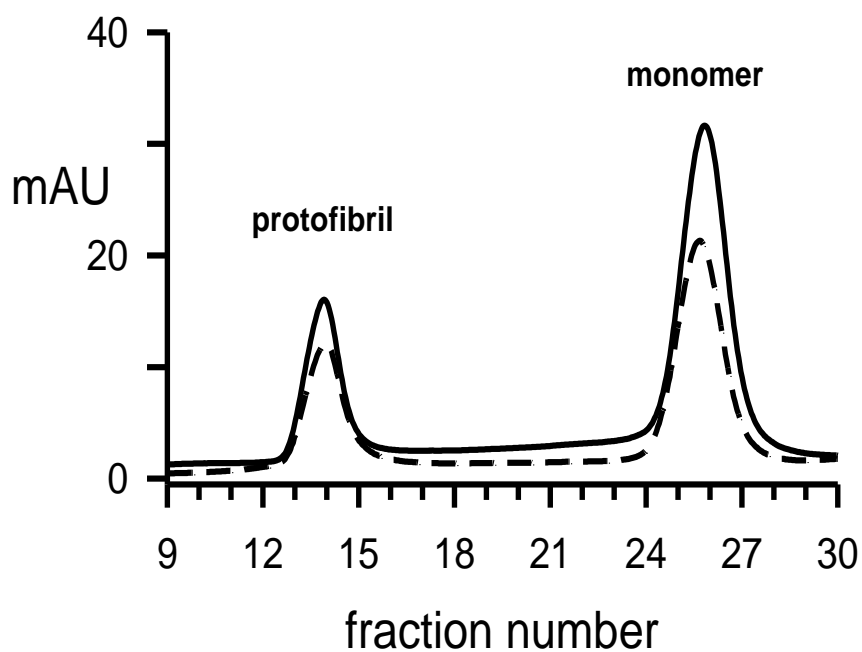
Figure 3.11 SEC-isolation of Aβ(1-40)E22G (Arctic) protofibrils. Aβ(1-40) E22G was reconstituted and prepared for SEC as described in the Methods. Aβ(1-40) solutions were eluted on Superdex 75 after 3 h incubation at 25°C (solid line) or after a 24 h incubation at 25°C (dashed line). Fractions containing protofibrils and monomers were immediately placed on ice for further characterization. Concentrations were determined by UV absorbance.
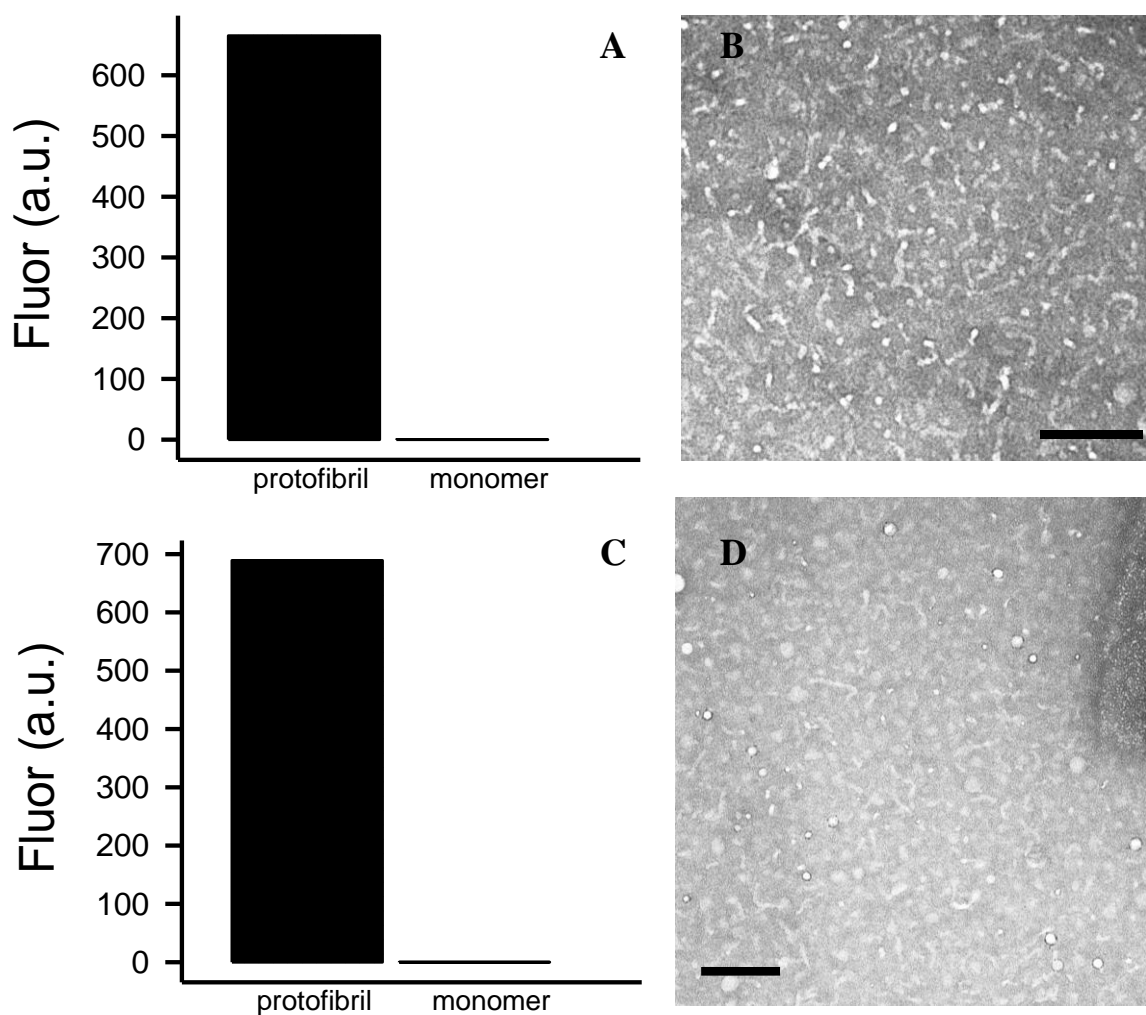
Figure 3.12 Structure and morphology of Aβ(1-40) and Aβ(1-40) E22G (Arctic) protofibrils. Panel A Freshly purified Aβ(1-40) protofibrils and monomers were diluted in 5 μM ThT in tris buffer (pH 8.0) and ThT fluorescence measurements were carried out as described in methods and normalized to 5 μM [Aβ]. Panel B. TEM image of a sample taken from the Aβ(1-40) protofibril peak. Sample was diluted to 20 μM Aβ, applied to a copper formvar grid as described in the Methods, and imaged at a magnification of 43,000. The scale bar represents 100 nm. Panel C. Freshly purified Aβ(1-40) E22G (Arctic) protofibrils and monomers were diluted in 5 μM ThT in tris buffer (pH 8.0) and ThT fluorescence measurements were carried out as described in methods and normalized to 5 μM [Aβ]. Panel D. TEM image of a sample taken from the Aβ(1-40) E22G (Arctic) protofibril peak. Sample (22 μM) applied to a copper formvar grid as described in the Methods, and imaged at a magnification of 43,000. The scale bar represents 100 nm.

Aβ(1-40) protofibrils displayed curvilinear structures < 100 nm in length when analyzed using TEM (Figure 3.12 Panel B). Estimated Aβ(1-40) protofibril length was 27 ± 11 nm (standard deviation, std dev) for n=50 measurements based on manual length measurements of unambiguous protofibril structures in the TEM image. Length measurements revealed that Aβ(1-40) protofibrils were significantly shorter than Aβ(1-42) protofibrils. Aβ(1-40) E22G (Arctic) protofibrils appeared to have similar curvilinear structure (Figure 3.12 Panel D) as both Aβ(1-42) and Aβ(1-40) protofibrils although the image quality was not good enough to carry out manual length measurements. Qualitatively, Aβ(1-40) E22G protofibrils appeared to have lengths between 50-100 nm.

3.10 Neither Aβ(1-40) nor Aβ(1-40) E22G (Arctic) protofibrils stimulated significant microglial proinflammatory response

Previously we have shown that Aβ(1-42) protofibrils are potent activators of microglia (Figure 3.5). Next, we wanted to investigate microglial activation by Aβ(1-40) and Aβ(1-40) E22G (Arctic) protofibrils. Both BV-2 and primary murine microglia were stimulated either with 15 μM Aβ(1-40) protofibrils or 15 μM Aβ(1-40) E22G protofibrils isolated by SEC. Conditioned medium after 6 h treatment was analyzed for TNFα production by ELISA.

Interestingly, both freshly purified Aβ(1-40) (Figure 3.13 Panel A) and Aβ(1-40) E22G (Arctic) protofibrils (Figure 3.13 Panel B) failed to stimulate primary murine

125
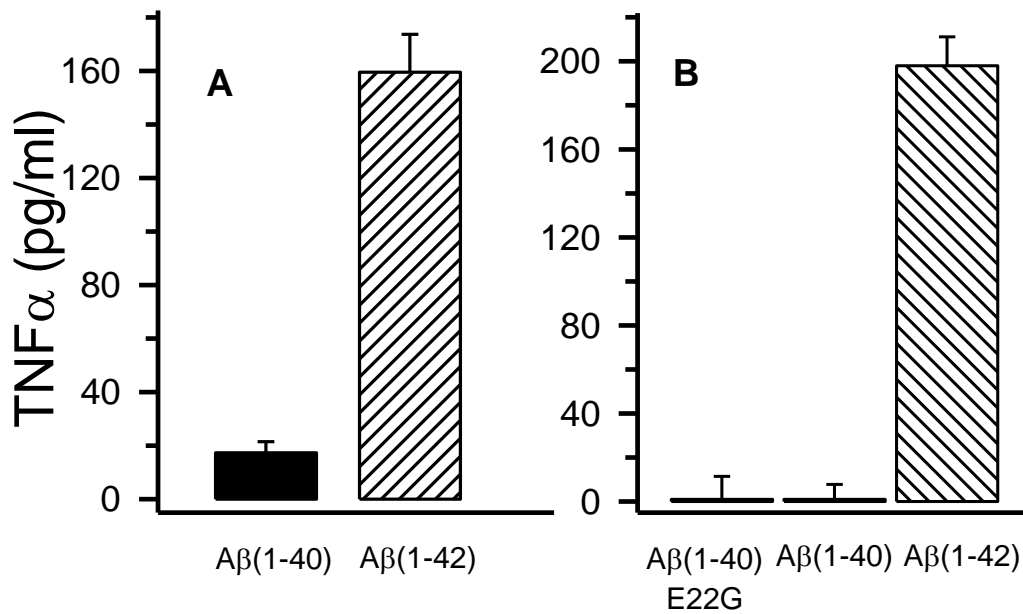
Figure 3.13 Neither Aβ(1-40) nor Aβ(1-40) E22G (Arctic) were potent activators of microglia. Panel A. Freshly purified Aβ(1-40) protofibrils or pre-isolated Aβ(1-42) protofibrils were added to the primary murine microglia at a final concentration of 15 μM for 6 h at 37°C under serum-free conditions. The conditioned medium was analyzed by ELISA for TNFα production. Panel B. Freshly purified Aβ(1-40) E22G (Arctic) protofibrils or pre-isolated Aβ(1-40) or Aβ(1-42) were added to the primary microglia at 15 μM for 6 h at 37°C under serum-free conditions. The conditioned medium is analyzed for TNFα production by ELISA.

microglia in comparison to Aβ(1-42) protofibrils. The only caveat is that the Aβ(1-42) protofibrils used in these studies were not freshly purified because of the logistics of the experimental span. We were still able to see a marked difference between Aβ(1-42) protofibrils and freshly purified Aβ(1-40) or Aβ(1-40) E22G (Arctic) protofibrils.

LPS (3 ng/ml) was used as a positive control and was able to stimulate microglial TNFα production. All the protofibril samples were carefully checked for any traces of bacterial contamination by means of cell-free XTT assay as described in methods. No significant difference in XTT reduction was observed between Aβ samples and their respective controls indicating that they are free of any bacterial contamination (Figure 3.14). A cellular XTT proliferation assay carried out in parallel to cellular stimulation studies showed that none of the protofibrils were toxic to the primary murine microglia (Figure 3.15).

3.11 Aβ(1-42) protofibril-induced microglial TNFα response was influenced by serum concentration in the assay medium

Microglial TNFα response to LPS is known to be influenced by the concentration of serum in the cellular medium during treatment (Cooper, et al., 2002). It was interesting to find out if serum concentration also has an effect on Aβ(1-42) protofibril-induced TNFα production. Serum is believed to have a complex composition with a variety of proteins. Some of the serum proteins like Apo E appear to have effects on Aβ-
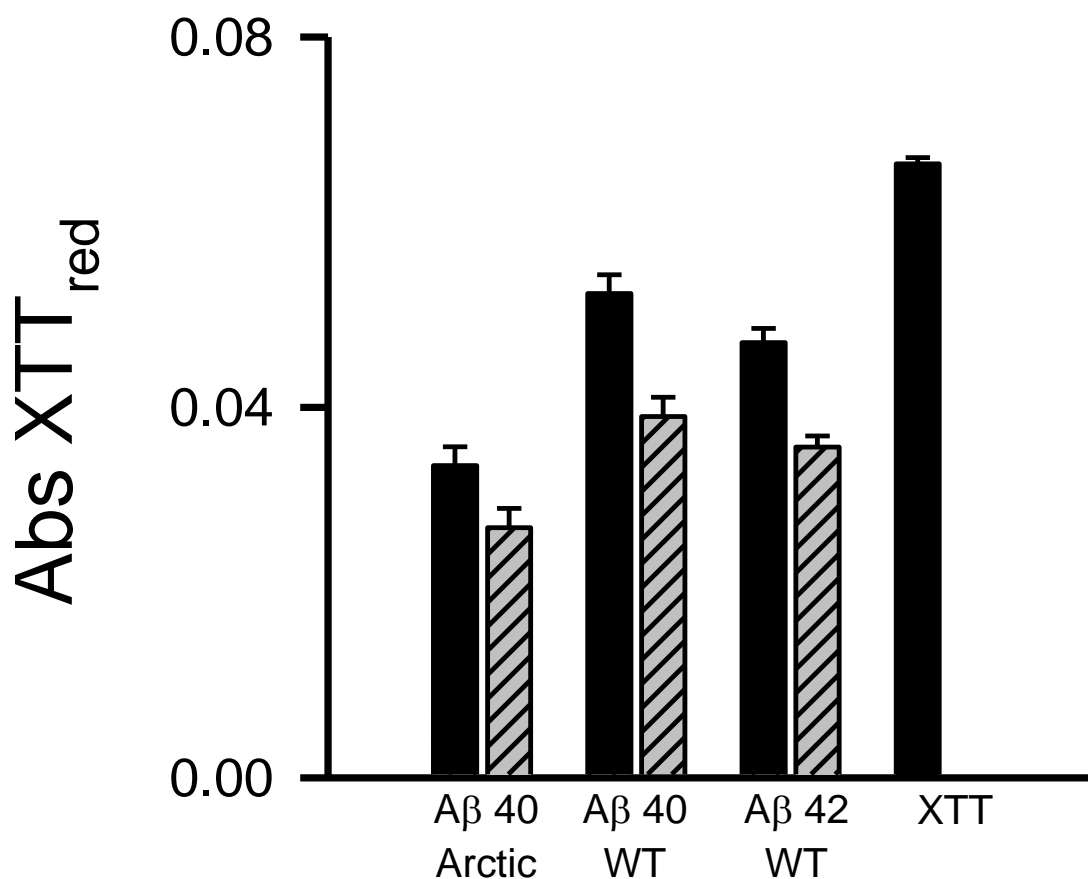
Figure 3.14 Aβ(1-40) and Aβ(1-40) E22G (Arctic) protofibrils are endotoxin-free. 15μM freshly purified Aβ(1-40) E22G (Arctic), pre-formed Aβ(1-40) WT, pre-formed Aβ(1-42) protofibrils) were incubated further with XTT and PMS for 6 h at 37°C. XTT solution was used to assess the background reduction. The reduction of XTT was monitored at 467 nm. Solid data bars represent Aβ samples and shaded bars represent respective buffer controls or XTT as labeled.
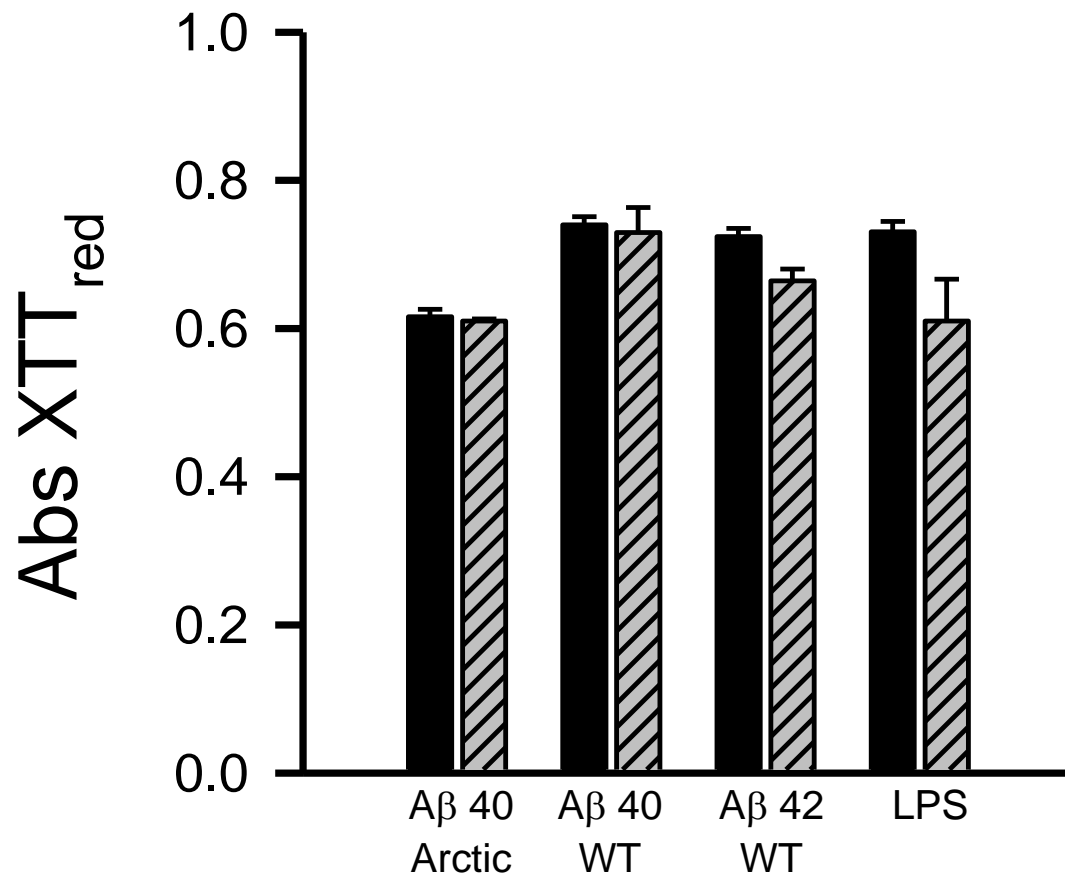
Figure 3.15 Aβ(1-40) and Aβ(1-40) E22G (Arctic) protofibrils are non-toxic to mouse microglia. Primary murine microglia pre-incubated with 15μM freshly purified Aβ(1-40) E22G (Arctic), pre-formed Aβ(1-40) WT, pre-formed Aβ(1-42) protofibrils, LPS(3 ng/ml) were incubated further with XTT and PMS for 2 h at 37°C. F-12 medium was used as negative control. The reduction of XTT was monitored at 467 nm. Solid data bars represent Aβ or LPS treated cells and shaded bars represent respective buffer controls

aggregation. It is commonplace to use serum-free or reduced serum medium during cell stimulation assays involving Aβ (Sondag, et al., 2009).

We plated BV-2 microglia in a medium containing 5% FBS (BV-2 microglial growth medium) overnight. Next day, the medium was removed and replenished with media containing 5% (same as growth medium), 2% or 0% FBS. These assay media were identical to the growth medium except for the serum content. Prior to replenishment, the microglial cells were washed 1X with the respective assay medium. Aβ(1-42) protofibrils were isolated in aCSF and added to the microglia at 15 μM final concentration for 6 h.

Subsequent analysis of conditioned medium by ELISA showed that serum concentration does influence Aβ(1-42) protofibril-induced TNFα production (Figure 3.16). We observed that the extent of TNFα response was maximum in the serum-free medium followed by medium containing 2% FBS. The extent of response was reduced under 5% serum conditions. Similar results were observed for primary murine microglia. Moreover, presence or absence of serum during plating of primary microglia did not seem to have any effect on the Aβ(1-42) protofibril-induced TNFα production. The exact reason for this discrepancy was not investigated in the current study.

3.12 Discussion

This study reports the robust activation of murine microglia by Aβ(1-42) protofibrils. SEC purified Aβ(1-42) protofibrils were able to cause a significant TNFα
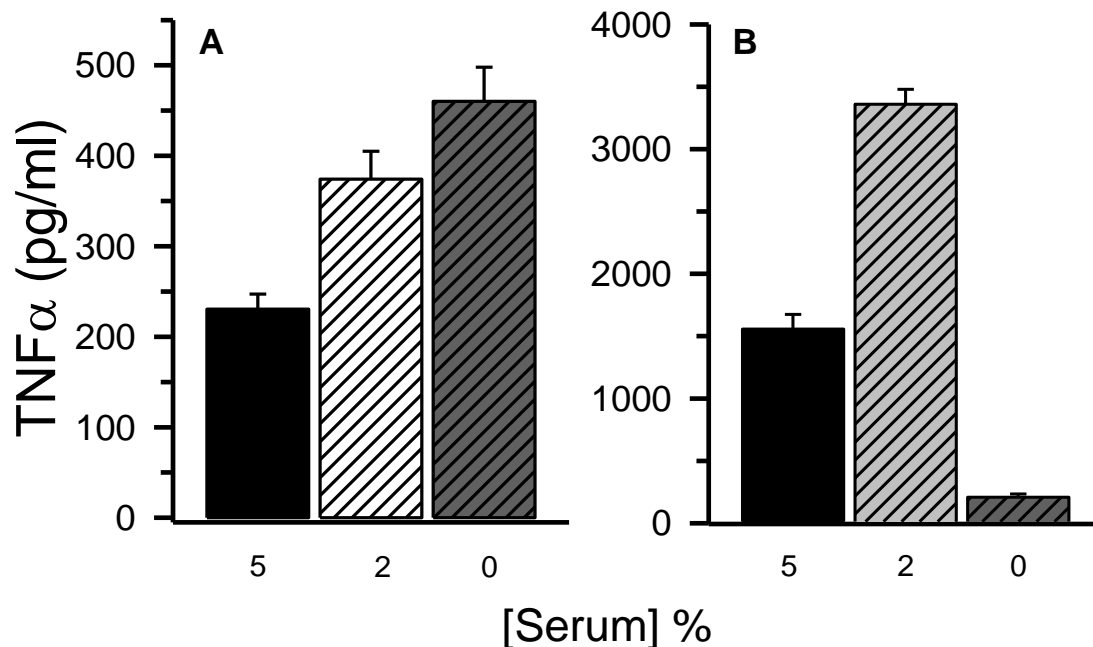
Figure 3.16 **Both Aβ(1-42) protofibril and LPS-induced microglial TNFα production is influenced by serum conditions during Aβ or LPS-stimulation.** Panel A. BV-2 microglia were plated overnight in a medium containing 5% serum. Freshly purified Aβ(1-42) protofibrils isolated in aCSF were added to the BV-2 microglia at a final concentration of 15 μM under 5, 2 or 0% serum conditions for 6 h at 37°C. The TNFα production was measured by ELISA. Panel B. BV-2 microglia were plated overnight in a medium containing 5% serum. LPS (3 ng/ml) was added to BV-2 microglia for 6 h under 5, 2 or 0% serum conditions. The conditioned medium was analyzed by ELISA for TNFα production.

production in murine microglia while Aβ(1-42) fibrils isolated from SEC-purified monomer were largely ineffective. Previously we have reported that soluble fibrillar precursors are optimal proinflammatory stimulus for THP-1 monocytes (Ajit, et al., 2009). Since protofibrils are considered as the latest precursor during fibril formation, the current study is in agreement with our findings in THP-1 monocytes.

Although THP-1 monocytes are regarded as a well-accepted model system for microglia (Combs, et al., 2001), the current investigation of Aβ-induced inflammation in microglial cell system is biologically more relevant in the context of Alzheimer's disease.

In vitro aggregation studies have identified different oligomeric intermediates of Aβ, which possess distinct structure and biological activity. Importantly, specific antibodies developed against these oligomers were able to react with Aβ deposits within the AD brain (Gong, et al., 2003; Kayed, et al., 2003; Lasagna-Reeves and Kayed, 2011). Thus amyloid plaques are no longer considered to be solely fibrillar, but in fact, are believed to represent an environment where multiple Aβ species are in complex dynamic equilibrium. Recent studies using multiphoton imaging have shown rapid recruitment of microglia to the nascent plaques in a mouse model of AD (Meyer-Luehmann, et al., 2008). Upon exposure to Aβ, microglia undergo activation and secrete significant amount of proinflammatory molecules resulting into a state of chronic inflammation in the AD brain (Dickson, et al., 1993). Several studies have indicated a close association of microglia with amyloid plaque (Dickson, et al., 1988; Eikelenboom, et al., 2011). Due to the complex plaque environment, it is possible that multiple Aβ species can cause microglial activation. In fact, oligomers and fibrils have been shown to cause differential activation of microglia (Parvathy, et al., 2009; Sondag, et al., 2009).

Our study demonstrates that SEC-isolated Aβ(1-42) protofibrils act as an effective stimulus for microglial proinflammatory response. Original Aβ protofibril preparation by Walsh et al consisted of the use of phosphate buffered saline (PBS) (Walsh, et al., 1997). We modified this procedure by replacing PBS with physiological F-12 cell culture medium having a higher ionic strength. This method resulted into classic curvilinear protofibrils, < 100 nm in length, consistent with those observed by Walsh et al. Our protofibril preparation showed considerable ThT-fluorescence in agreement with their β-sheet content as shown by hydrogen-deuterium exchange studies (Kheterpal, et al., 2003). Our isolated fibril preparation exhibited the maximum ThT-fluorescence, but it failed to produce any TNFα response in murine microglia. This finding is different from many other studies where fibrils were shown to activate microglia (McDonald, et al., 1997; Combs, et al., 2001; Stewart, et al., 2010). One explanation for this observation may lie in our fibril preparation, which involved centrifugation of the aggregation solution followed by resuspension of insoluble fibrils, and therefore was devoid of any soluble species (Figure 3.2). Many of the studies investigating Aβ-induced inflammation have used solution conditions which are likely to result in polydisperse Aβ solutions. Such polydisperse solutions may lead to inconsistencies in the experimental results, making it less straightforward to interpret the exact species responsible for the biological effect.

Previously, microglia have been shown to interact with Aβ via multiple receptors including scavenger receptors (El Khoury, et al., 1996) and toll-like receptors (TLRs) (Walter, et al., 2007; Udan, et al., 2008). CD36 forms a heterotrimeric complex with TLR4 and TLR6 and has been found to mediate an Aβ fibril-induced proinflammatory response (Stewart, et al., 2010). Moreover, this study did not observe an Aβ fibril-

133

mediated proinflammatory response via TLR2. However, more recently, TLR2 was shown to be a primary receptor for Aβ-oligomer induced inflammation (Liu, et al., 2011). It may be possible that different receptors mediate the interaction between Aβ and microglia at different stages of disease progression. The receptors mediating Aβ-protofibril induced signaling have not been investigated. It is possible that protofibrils share the same receptor molecules with fibrils for interaction with microglia due to similarity in their structures (Kheterpal, et al., 2006).

Interestingly, the current study also shows the difference between Aβ(1-42) protofibrils and Aβ(1-40) or Aβ(1-40) E22G (Arctic) protofibrils in their ability to stimulate microglia. Arctic mutation E22G is an intra-Aβ mutation that causes a familial form of AD. This mutant peptide displayed enhanced rate of formation of protofibrils as compared to Aβ(1-40)WT (Nilsberth, et al., 2001). Interestingly, the arctic mutation did not influence the ability of Aβ(1-40) protofibrils to evoke a TNFα response comparable to Aβ(1-42). In contrast to Aβ(1-42), both WT and Arctic Aβ(1-40) were ineffective in stimulating microglia at a concentration of 15 μM. Morphological analysis using TEM revealed that protofibrils of all Aβ variants used in this study were curvilinear structures, which were soluble at 18000 g. However, manual length measurements of unambiguous protofibrils in the TEM image have indicated that Aβ(1-40) protofibrils are significantly shorter than Aβ(1-42) protofibrils. One important caveat in such cellular stimulation studies is that the stability of the Aβ aggregation state is usually assumed over the course of stimulation. It is possible that in a complex cellular environment, the structure of Aβ added might change significantly over time. Therefore, one possibility for such a discrepancy might be related to the differences in their stability during the course of

cellular treatment. However, we observed differences in the kinetics of protofibril formation between different Aβ variants, and the findings were similar to a study by Lashuel et al (Lashuel, et al., 2003).

Together, the current study demonstrates that Aβ(1-42) protofibrils activate murine microglia significantly while the insoluble fibrils formed under physiological pH and higher ionic strength failed to do so. Furthermore, the ability to produce a substantial TNFα response was limited only to Aβ(1-42) protofibrils whereas protofibrils of Aβ(1-40) WT or Arctic mutant of Aβ(1-40) prepared in a similar manner did not stimulate microglia.

CHAPTER 4

MICROGLIAL ACTIVATION BY STINE ET AL Aβ(1-42) OLIGOMER-FORMING
AND FIBRIL-FORMING CONDITIONS

4.1 Introduction

Amyloid plaques and neurofibrillary tangles (NFTs) are signature proteinaceous
lesions found in the brain of Alzheimer's disease (AD) patients (Selkoe, 2004).
Amyloid-β (Aβ) protein is a major component of amyloid plaques (Glenner and Wong,
1984) whereas hyperphosphorylated tau protein constitutes NFTs (Grundke-Iqbal, et al.,
1986). Both of these constituent proteins are found in the human body in unaggregated
monomeric forms under normal conditions, yet it is their aggregated form that marks the
AD pathology (Grundke-Iqbal, et al., 1985; Seubert, et al., 1992; Shoji, et al., 1992).
Although the complete mechanism of how AD pathogenesis is initiated is not entirely
clear, genetic evidence points towards Aβ aggregation as a central event in the process
(Hardy and Higgins, 1992). Amyloid precursor protein (APP) undergoes sequential

proteolysis by three secretases named α,β and γ to form Aβ protein of varying amino acid length at the carboxy-terminus (Sisodia, et al., 1990). Aβ protein is a highly amphipathic molecule and has a propensity to aggregate into long fibrils. Based on *in vitro* aggregation studies, Aβ can form a variety of intermediate oligomeric species of a wide range of sizes and structures such as protofibrils, amyloid-derived diffusible ligands (ADDLs) and annular protofibrils (Walsh, et al., 1997; Lambert, et al., 1998; Dahlgren, et al., 2002; Kayed, et al., 2003; Stine, et al., 2003; Kayed, et al., 2009). It is not very clear if all the intermediate species results into fibril formation or they represent off-pathway end products. Many of these studies have modulated solution conditions to generate a particular Aβ species. Some of the solution conditions include non-physiological buffers and small quantities of organic solvents (Kayed, et al., 2003; Stine, et al., 2003; Kayed, et al., 2009). The contribution of such excipients towards Aβ aggregation is not very clear. However, antibodies developed against such intermediates were able to react with Aβ deposits in the AD brain indicating their biological relevance (Gong, et al., 2003; Kayed, et al., 2003; Lasagna-Reeves and Kayed, 2011). There is increasing evidence that although fibrillar Aβ forms the core of the plaque, oligomeric species are present within and surrounding the plaques, making the plaque environment more complex than once thought (DaRocha-Souto, et al., 2011). Although studies of Aβ oligomers have led to increased understanding of the mechanisms involved in AD pathogenesis, some caveats remain to be addressed. In the absence of high resolution structures of different oligomeric species, a lot of structural characterization is based on gel-based techniques (Bitan, et al., 2005). However, considerably more structural characterization is available for protofibrils based on hydrogen-deuterium exchange studies (Kheterpal, et al., 2003).

Moreover, there is discrepancy in the nomenclature of different oligomers. The current nomenclature of oligomers is loosely based on the morphology. The structural relationship between different oligomers is still quite unclear.

Apart from the fact that Aβ oligomers have been detected in the AD brain, they also exhibit biological activity *in vitro*. Aβ oligomers have been shown to be potent synaptotoxins, which inhibit long term potentiation, alter synaptic transmission(Lambert, et al., 1998; Hartley, et al., 1999; Dahlgren, et al., 2002). Other than being neurotoxic, Aβ also results in the activation of brain immune cells such as microglia and induces significant inflammatory processes (Meda, et al., 1995; McDonald, et al., 1997; Combs, et al., 2001). Extensive inflammation is another characteristic of AD pathology apart from the presence of proteinaceous lesions in the brain of an individual (Dickson, et al., 1988). Inflammation in AD is marked by activation of glial cells (astrocytes and microglia) to produce a plethora of inflammatory molecules, a condition referred to as gliosis (Akiyama, et al., 2000; Apelt and Schliebs, 2001). Some of these inflammatory molecules include tumor necrosis factor α (TNFα), interleukin 1β (IL-1β), and reactive oxygen species (ROS) (Akiyama, et al., 2000). Recently, oligomeric Aβ was found to be positively correlated with gliosis, while the total plaque burden reached a plateau (Serrano-Pozo, et al., 2011). Activated microglia are found in the close proximity of plaque periphery, which was recently shown to be immunoreactive to anti-oligomeric Aβ antibody (DaRocha-Souto, et al., 2011). Aβ(1-42)-oligomers were found to be more effective than fibrils in provoking a proinflammatory response in rat astrocytes *in vitro* (White, et al., 2005). Oligomers might provide an explanation to explain the early

synaptic and inflammatory changes even before the development of mature amyloid plaques (Rahimi, et al., 2008; Hyman, 2011).

In this study, we compared microglial activation between soluble Aβ(1-42) oligomers formed in F-12 cell culture medium and Aβ(1-42) fibrils formed under acidic conditions. We prepared the Aβ aggregation solutions based on the original protocol by LaDu and colleagues (Stine, et al., 2003). We have further extended the biophysical analysis of oligomers and fibrils by the use of thioflavin-T (ThT) fluorescence measurements, size-exclusion chromatography (SEC) and imaging techniques.

4.2 Preparation of Aβ(1-42) oligomers and fibrils based on Stine et al

Aβ aggregation is influenced by a variety of physical factors including pH, temperature, ionic strength, mechanical strength and nature of excipient. Lambert *et al* originally prepared amyloid-derived diffusible ligands (ADDLs) by resuspending Aβ(1-42) in dimethyl sulfoxide (DMSO) followed by further dilution using F-12 cell culture medium without phenol red in the presence or absence of ApoJ protein (Lambert, et al., 1998). F-12 medium is a common cell culture medium which has physiological pH and ionic strength (16 mS/cm as determined by conductivity measurement). This medium contains a variety of amino acids and co-factors like other cell culture media (www.invitrogen.com). LaDu and colleagues optimized the oligomer-forming and fibril forming conditions for Aβ(1-42). Their oligomeric preparation is similar to the ADDLs preparation but was devoid of ApoJ protein (Stine, et al., 2003). Moreover, they extensively characterized the oligomer and fibril forming conditions using various

biophysical techniques. We took advantage of Stine et al protocol to prepare Aβ(1-42)

oligomers and fibrils (Stine, et al., 2003).

Synthetic Aβ(1-42) peptide was dissolved in 100% hexafluoroisopropanol (HFIP)

to give 1 mM Aβ solution. The solution was incubated at 1 h at 25°C followed by

aliquotting. HFIP was allowed to evaporate overnight under the chemical fume hood.

Any residual HFIP was removed by vacuum-centrifuging for approximately 1 h, and the

aliquots were stored at -20°C. For making Aβ(1-42) oligomers, one aliquot was

resuspended in anhydrous DMSO to give 5 mM Aβ, followed by further dilution into ice-

cold F-12 cell culture medium without phenol red at a final concentration of 100 μM.

This solution was vortexed for 15 seconds and further incubated at 4°C for 24 h to form

Aβ(1-42) oligomers.

For preparation of Aβ(1-42) fibrils, a HFIP-pretreated and lyophilized Aβ aliquot

was resuspended at 5 mM concentration in DMSO as described above. The Aβ solution

was then diluted into 10 mM HCl (pH was determined to be 2.3 and ionic strength 4

mS/cm using conductivity measurements) to give a final concentration of 100 μM,

vortexed for 15 seconds and incubated at 37°C for 24 h to form fibrils.

4.3 Morphological analysis of Aβ(1-42) oligomers and fibrils using atomic force

microscopy (AFM)

We carried out morphological analysis of our oligomer and fibril preparation

using AFM. 10 μl of Aβ oligomers or fibrils (10 μM) was applied on freshly cleaved

mica and imaged by AFM (Sample preparation and subsequent imaging was done by Lisa K. Gouwens) (Figure 4.1). Aβ oligomer preparation contained small punctate globular species. Moreover, it was completely devoid of any fibrillar structures. Heights of oligomers were 3.1 ± 1.2 nm for n=100 measurements. The fibril preparation contained long flexible fibers (heights 2.7 ± 0.9 nm for n=100 measurements). The lengths of fibrils were > 1 μm.

4.4 ThT-fluorescence studies on Aβ(1-42) oligomers and fibrils

Thioflavin-T fluorescence studies (discussed previously in Chapter 3 Section 3.3) were carried out on both Aβ(1-42) oligomer and fibril preparations after 24 h (Figure 4.2). Fibril displayed maximum ThT-binding. Oligomers showed lesser yet considerable ThT fluorescence. Interestingly, we observed that Aβ solutions exhibited considerable ThT fluorescence right after their reconstitution into either oligomer forming medium or fibril forming medium. Particularly, the extent of ThT fluorescence for oligomer preparation did not change over the course of 24 h at 4°C. On the contrary, fibril preparation showed a significant change over 24 h.
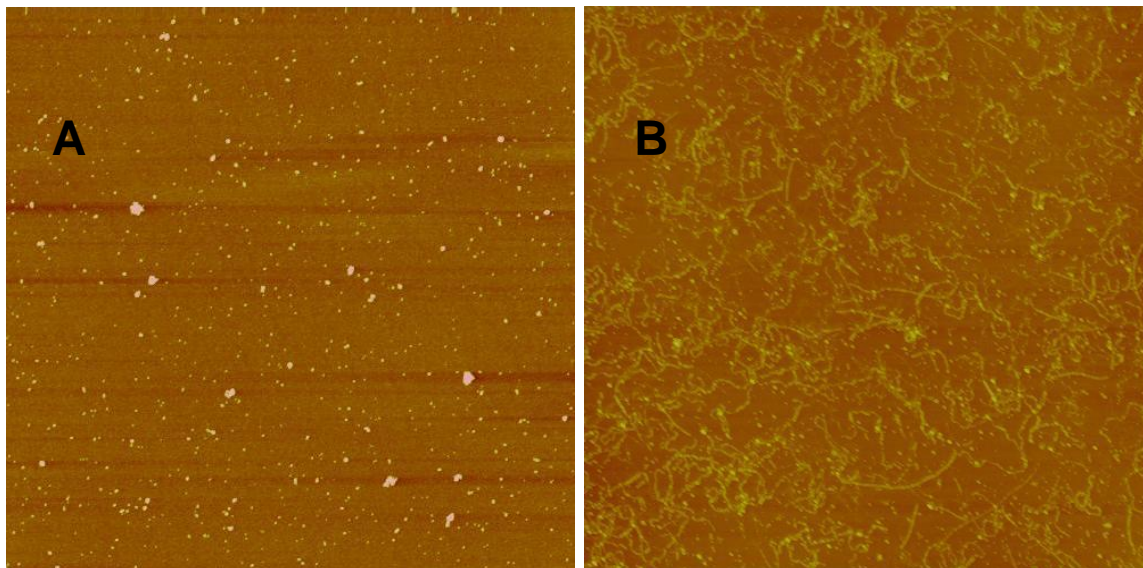
Figure 4.1 Aβ(1-42) structures formed in oligomer- or fibril-forming conditions are morphologically distinct. Aliquots of lyophyllized Aβ(1-42) were reconstituted to 100 μM as described in the Methods to generate oligomers or fibrils. After 24 hr incubation at the given temperatures, aliquots of the solutions were diluted to 10 μM, applied to mica and imaged by AFM. Representative images are shown for oligomers (Panel A, 5 μm x 5 μm) and fibrils (Panel B, 10 μm x 10 μm).
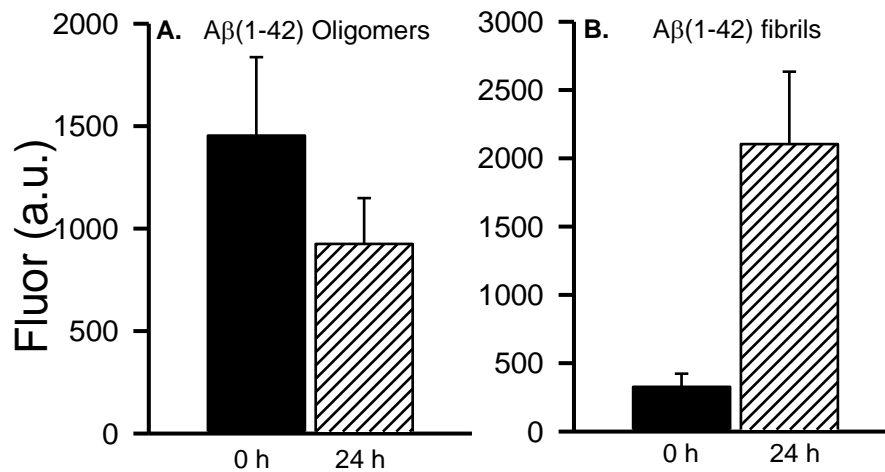
Figure 4.2 Aβ(1-42) Oligomers and fibril preparations are structurally different. ThT fluorescence measurements (n=8 for oligomers and n=10 for fibrils) were obtained for each preparation at a final concentration of 10 μM Aβ(1-42) right after reconstitution (0 h) or after 24 h incubation at 4°C for oligomers (Panel A) and 37°C for fibrils (Panel B)

4.5 Aβ(1-42) oligomers induced microglial TNFα response to a larger extent than Aβ(1-42) fibrils

Cell stimulation experiments were carried out using Aβ(1-42) oligomers and fibrils on BV-2 and primary mouse microglia. BV-2 microglia were plated in a 96-well cell culture plate in the growth medium containing 5% serum for overnight at 37°C. Aβ(1-42) oligomer or fibril solution was added at a final concentration of 15 μM for 6 h under reduced serum conditions (2% serum). Primary microglia were treated with oligomers and fibrils in the identical manner as BV-2 microglia except that primary murine microglia were plated in a serum-free medium for 2 h prior to the treatment with Aβ under serum-free conditions. When the conditioned medium for both BV-2 and primary microglia was analyzed using TNFα ELISA, we observed that Aβ(1-42) oligomers were more effective in stimulating microglial TNFα production than Aβ(1-42) fibrils (Figure 4.3). Despite possessing higher ThT-fluorescence, fibril preparations were significantly weaker in stimulating microglial proinflammatory response (Figure 4.2 and 4.3).

4.6 Aβ(1-42) oligomers were not toxic to microglia

TNFα response can be induced as a result of compromised cellular health associated with toxicity. We wanted to investigate if Aβ(1-42) oligomers are stimulating the release of microglial TNFα as a result of their toxicity. We made use of XTT [2, 3-

Figure 4.3 Aβ(1-42) oligomers stimulate microglia more effectively than fibrils.
Solutions of Aβ(1-42) oligomers and fibrils were incubated with microglia at a final
concentration of 15 μM for 6 hrs. Secreted TNFα was measured by ELISA in the
conditioned medium collected from treated primary murine microglia (Panel A) and
(Panel B) BV-2 murine microglia. Data bars represent the average ± standard (std) error
of n=30 trials (oligomers and fibrils) for primary microglia and n=32 trials (oligomers)
and n=33 trials (fibrils) for BV-2 microglia. Control treatments in the presence of 0.3 %
DMSO in F-12 media or 1.5 mM HCl produced 40 and 15 pg/ml TNFα respectively for
primary and BV-2 microglia and were subtracted from Aβ-stimulated samples. Primary
and BV-2 microglia were stimulated in serum-free and 2% FBS medium respectively.
Statistical differences between oligomers and fibrils for both sets of data had p values
<0.001.

bis (2-methoxy-4-nitro-5-sulfophenyl)-2H-tetrazolium-5-carboxanilide] cell proliferation

assay (Scudiero, et al., 1988) to assess microglial health after treatment with Aβ. As

described in methods, XTT is a tetrazolium derivative which can be reduced by

mitochondrial enzymes to a colored product which absorbs at 467 nm. The intensity of

color is directly proportional to the mitochondrial metabolism which in turn reflects the

cellular health. We incubated BV-2 and primary mouse microglia pretreated for 6 h with

Aβ(1-42) oligomers in the presence of XTT as detailed in methods. After 2 h of

incubation, the reduced form of XTT was read at 467 nm. We observed no significant

difference in XTT reduction between cells treated with oligomers and cells treated with

buffer vehicle (Figure 4.4). This observation suggests that Aβ(1-42) oligomers were not

toxic to the microglia. Primary murine microglia pretreated with Aβ(1-42) fibrils were

also able to metabolize XTT comparable to buffer control ruling out the possibility of

fibrils being toxic to microglia. Similar results were obtained for BV-2 mouse microglia.

This data supports our observation that microglial TNFα production is an outcome of

immune response stimulation with Aβ oligomers rather than a response from dying cells.

4.7 Characterization of Aβ(1-42) oligomers by size-exclusion chromatography (SEC) and
their morphological analysis by electron microscopy (EM)

Apart from the morphological analysis by atomic force microscopy (AFM), Stine

et al also characterized Aβ(1-42) oligomers formed in DMSO/F-12 medium by Western

Blot. They observed that Aβ(1-42) oligomer preparations at 0 h consisted mainly of
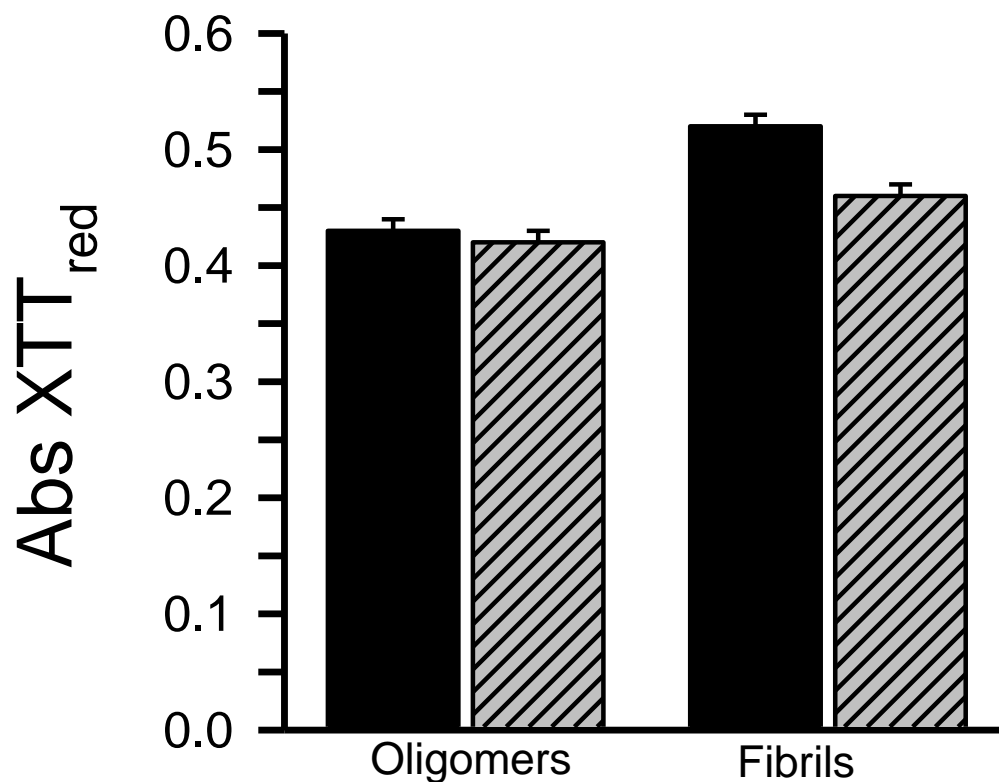
Figure 4.4 Both Aβ(1-42) oligomers and fibrils stimulated microglial proinflammatory response in a non-toxic manner. Primary murine microglia pretreated with Aβ(1-42) oligomers or fibrils were incubated with XTT and PMS for 2 h at 37°C as detailed in methods. The absorbance was read at 467 nm. The Aβ vehicle was used as control n=6 for samples (black bars), n=3 for controls (hatched bars)

monomer, trimer and tetramers, while after 24 h incubation the preparation showed

higher oligomers (30-60 kDa) and increased trimer and tetramer bands. The caveat in

getting full structural details like the state of oligomerization from SDS-PAGE

experiments is that Aβ forms SDS-resistant species due to its amphipathic nature (Bitan,

et al., 2005). Therefore, we further analyzed this oligomeric preparation by SEC under

non-denaturing conditions. Importantly, we wanted to compare the elution profile of

Aβ(1-42) protofibril preparation (discussed in Chapter 3) to that of the oligomer

preparation described in this study based on SEC. We wanted to get an idea about the

size distribution of Aβ(1-42) oligomers as compared to that of the protofibril preparation

based on the SEC-elution profile. We separated oligomers formed in F-12 medium with

a Superdex 75 SEC-column. The elution profile was monitored by absorbance at 280

nm. We observed that SEC of oligomers yielded an elution profile consisting of dual

peaks (Figure 4.5). The void peak containing higher molecular weight species (>70000

molecular weight) followed by the included peak, which contained mostly low molecular

weight species like monomer and dimer (Walsh, et al., 1997; Chromy, et al., 2003). This

elution profile was qualitatively identical to that of Aβ(1-42) protofibril preparation

containing NaOH/F-12. However, we also observed a small shoulder peak right next to

the void peak for the oligomer elution. When imaged using TEM, however, we did not

find any evidence of Aβ structure in the shoulder peak. We were not able to identify if

that was a ghost peak related to an SEC-artifact. Previously, Chromy *et al* carried out

SEC analysis of Aβ(1-42) oligomers using F-12 as a running buffer on a Superdex 75

column. They reported that the oligomers eluted in a single peak shortly after the void

volume, followed by a monomer peak. Although we observed a small hump next to the
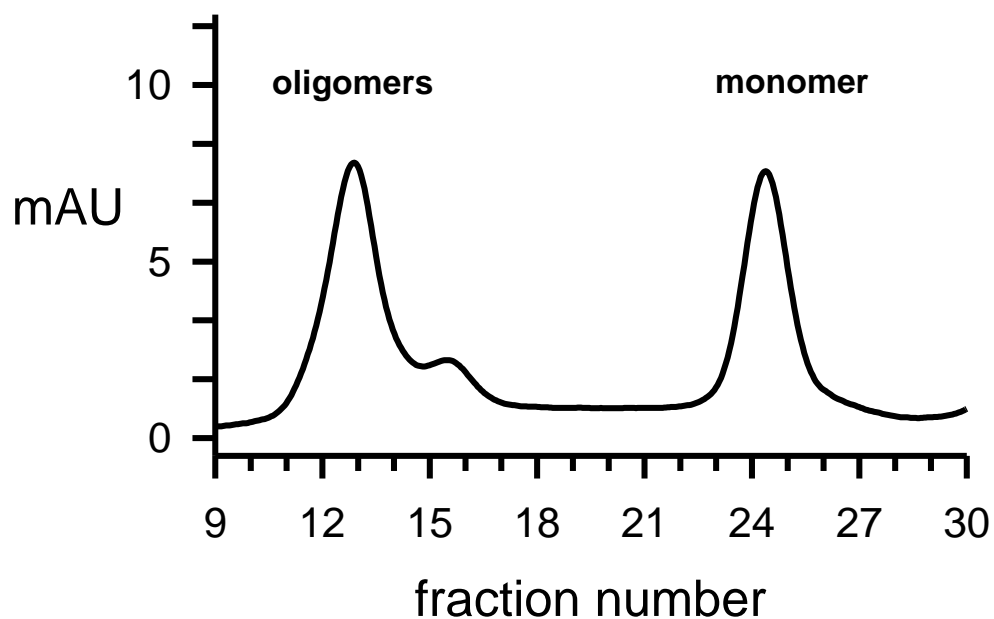
Figure 4.5 Size-exclusion chromatography separation of Aβ(1-42) oligomers formed using DMSO/F-12 medium. Dual peaks are observed following SEC elution of Aβ(1-42) reconstituted in DMSO/F-12. Lyophylized Aβ(1-42) was brought into solution with DMSO (5 mM) followed by supplemented F-12 media (100 μM). The supernatant after centrifugation was eluted from a Superdex 75 column and 0.5 ml fractions were collected. UV absorbance at 280 nm was monitored during the elution (solid line).

void volume, the majority of the high molecular weight Aβ species eluted out in the void volume peak, unlike that of Chromy *et al*. The Aβ(1-42) protofibril and oligomer preparations were similar in that both contained a significant amount of unaggregated LMW Aβ. However, there are some caveats which make the comparison between size distributions of oligomers and protofibrils less straightforward. Firstly, our protofibril preparation was 2.5-fold more concentrated than the oligomer preparation (100 μM). Secondly, the protofibril preparation was separated by SEC right after reconstitution and centrifugation, unlike the 24 h incubation in the case of oligomers. It is possible that both concentration and time of incubation governed the type of oligomers formed. Moreover, since both protofibrils and oligomers elute out in the void peak, it is not possible to further distinguish between those two peaks by a Superdex 75 column.

Although protofibrils were originally characterized morphologically by TEM (Walsh, et al., 1997; Walsh, et al., 1999), analysis of oligomers mostly relied on AFM (Stine, et al., 2003). We have observed that the mica surface used for AFM sample preparation may not allow adsorption of all Aβ species uniformly due to surface properties. We therefore took advantage of TEM to compare morphological differences between protofibrils and oligomers eluted in the void peak. We prepared TEM samples of void peak oligomers (10 μM) using negative staining (Figure 4.6, Imaging carried out by David C. Osborn). Based on TEM images, the oligomeric structures appear to resemble the curvilinear protofibrils. However, they looked significantly smaller than that of the protofibrils. Based on the TEM image showed in Figure 4.6, oligomer length was estimated to be less than 50 nm.
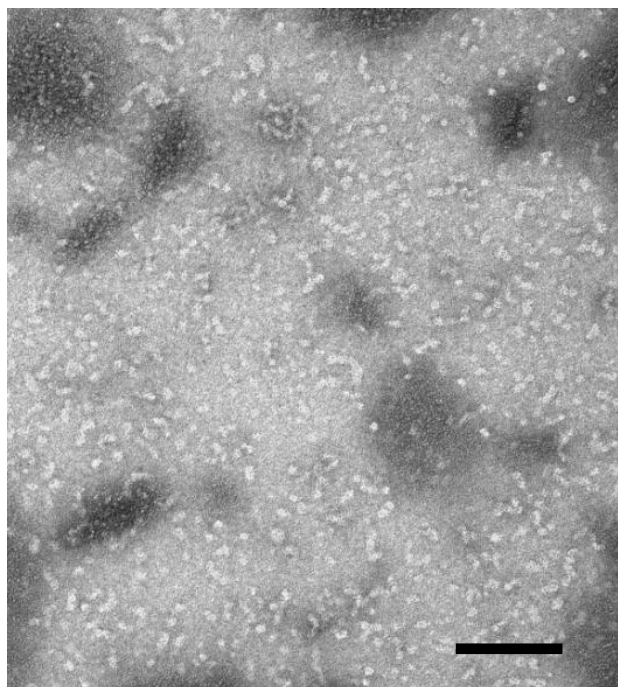
Figure 4.6 Morphological characterization of oligomers eluted in the void volume by TEM. Aβ(1-42) oligomers were subjected to SEC as shown in figure 4.5. Aβ oligomers (10 μM) eluted out in the void volume (Fraction 13) was adsorbed on formvar coated copper grids, negatively stained with 2% Uranyl acetate followed by imaging using Philips EM 430 TEM at 300kev. Scale bar is 100 nm.

<u>4.8 Characterization of Aβ(1-42) fibrils formed under Stine *et al* conditions</u>

Solid state nuclear magnetic resonance (NMR) studies have shown that Aβ fibrils formed under different conditions have subtle differences in their molecular structure (polymorphic). Moreover, slight structural differences can further translate into differential toxicity to neurons (Petkova, et al., 2005). As discussed previously in Chapter 3, we prepared Aβ(1-42) fibrils starting from a SEC-purified monomer eluted in F-12 medium by gentle agitation for approximately 72 h at room temperature. The resultant fibrils were isolated by centrifugation at 18000 *g*. These fibrils were > 1 μm long, and laterally associated with each other likely due to the higher ionic strength of F-12 medium (16 mS/cm) and agitation. The fibrils described in Chapter 3 failed to stimulate a microglial proinflammatory response when added to either BV-2 or primary mouse microglia at 15 μM (based on original monomer concentration). The extent of TNFα production was comparable to the background TNFα response in all the experiments. On the other hand, while TNFα production induced by fibrils prepared under acidic conditions (DMSO/dilute HCl) was lower than oligomers, it was considerably higher than the background response. From this data, it appeared that fibrils formed quiescently under low pH (pH 2.3) versus those formed at physiological pH with gentle agitation possessed differential ability to stimulate microglia. Moreover, 10 mM HCl displayed considerably lower ionic strength (4 mS/cm) than that of F-12 medium (16 mS/cm) as estimated by conductivity measurements. However, we did not compare these two fibril preparations side by side in the same experiment. Nevertheless it is possible

that changes at the structural level get translated into structure-specific activity (Petkova, et al., 2005).

We wanted to investigate additional differences between these two different fibril preparations. We already have shown that the fibrils formed in physiological pH and high ionic strength could readily spin down. We wanted to investigate if that holds true for fibrils formed under acidic conditions. Even after centrifugation at 18000 g, significant ThT fluorescence (79%) stayed in the supernatant suggesting that these fibrils were highly soluble (data not shown). We imaged the Aβ solution before and after centrifugation to determine whether the supernatant contained the fibrillar structures. Both the total and supernatant solution showed abundant long fibrils. Morphologically, these fibrils appeared different than those formed in F-12 medium (Figure 4.7 and Chapter 3, Figure 3.3 Panel B). First and the foremost, fibrils formed in low pH conditions appeared more flexible. Secondly, the degree of lateral association was minimal under acidic conditions and low ionic strength unlike fibrils formed in F-12 medium. Moreover, AFM images of the fibrils formed at low pH showed presence of some globular species along with long fibrillar structures (Figure 4.1 Panel B). Therefore, next we wanted to examine if the fibrils prepared in dilute HCl had residual soluble protofibrillar structures in the supernatant. To investigate this, we subjected 18000 g fibril supernatant to SEC separation. Interestingly, UV did not show any protein eluting out of the column (data not shown). This, in turn suggested that the long fibrils were not able to pass through the column but instead might have been trapped by the filter on top of the column. Thus, based on SEC results, this fibril preparation was devoid of any protofibrillar structures. The difference in the biological activities of two
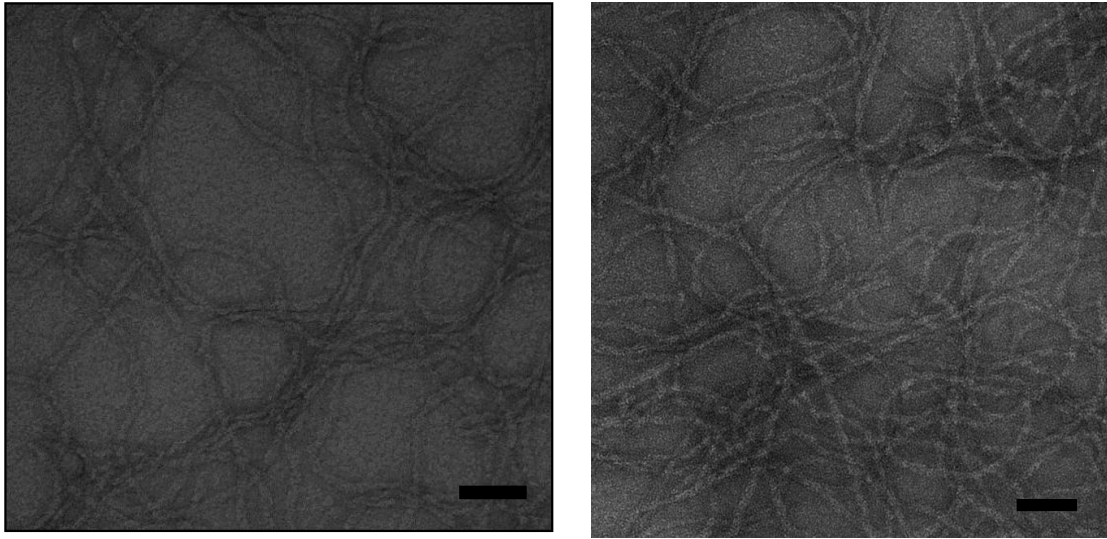
Figure 4.7 Morphological characterization of Aβ(1-42) fibrils prepared under acidic conditions. Aβ(1-42) was reconstituted using DMSO at 5 mM followed by its dilution into 10 mM HCl at 100 μM. The solution was further incubated at 37°C for 24 h. **Panel A.** After 24 h total fibril solution were diluted to 20 μM using water and 10 μl was adsorbed on formvar coated copper grids, negatively stained with 2% Uranyl acetate followed by imaging using TEM at a magnification of 59000 X. Scale bar is 50 nm. **Panel B.** The total Aβ(1-42 fibril solution was centrifuged at 18000 g for 10 min. The supernatant was diluted to 20 μM (The supernatant concentration was assumed to be 100 μM since very small amount of Aβ pelleted out). and adsorbed on the formvar-coated copper grids, negatively stained and imaged using TEM at a magnification of 59000 X. Scale bar is 50 nm.

different preparations of fibrils may be intrinsic to the molecular structure of fibrils rather than residual soluble protofibrils in fibril preparation formed under acidic conditions. These results in turn emphasize the effect of solution conditions on the structure and biological activity of fibrils.

4.9 Discussion

The current study demonstrates that soluble Aβ(1-42) oligomers were more effective than fibrils in inducing TNFα production in murine microglia. Our findings are consistent with a study by White et al (2005) in which oligomers were better than fibrils in stimulating a proinflammatory response in rat astrocyte culture. Both our study and that by White et al prepared Aβ(1-42) oligomer and fibrils solutions based on a protocol described by (Stine, et al., 2003). We further analyzed the oligomers and fibrils biophysically with ThT fluorescence, SEC and TEM imaging.

In this study, Aβ(1-42) was reconstituted in DMSO at 5 mM and the resulting Aβ solution was diluted to 100 μM with either F-12 medium or dilute HCl to form oligomers or fibrils respectively. Oligomers were formed at 4°C while the fibrils were generated at 37°C after incubation at 24 h. Thus, by modulating the solution and temperature conditions, Aβ(1-42) was able to form different species. These species not only possessed distinct morphologies as assessed by AFM but produced quantitatively different microglial TNFα response. Oligomer preparation was mostly globular and devoid of any fibrillar structures based on AFM in agreement with Stine et al. Moreover,

these oligomers exhibited substantial ThT fluorescence suggesting a considerable degree of β-sheet structure (Figure 4.2). Fibrils possessed maximum ThT fluorescence but were only weak activators of microglia as compared to oligomers. Our recent study discussed in Chapter 3 have demonstrated that Aβ(1-42) protofibrils are potent activators of murine microglia. Moreover, isolated fibrils formed using SEC-purified monomer in F-12 medium possessing maximum ThT binding were as ineffective as SEC-purified monomer possessing little to no ThT binding. Both these studies suggest that Aβ as an inflammatory stimulus might require an intermediate structure formed during fibrillogenesis. Such an intermediate species will likely have size and β-sheet character intermediate between monomer and fibril. Together, both these studies show a significant role for Aβ(1-42) protofibrils and oligomers in microglia-mediated inflammation. There is burgeoning evidence suggesting that smaller, soluble Aβ species have potent early synaptotoxic properties (Koffie, et al., 2011). In fact, oligomeric Aβ was found to be correlated to astroglial inflammatory response as well as clinical disease severity as compared to total Aβ burden in a mouse model of AD (DaRocha-Souto, et al., 2011; Serrano-Pozo, et al., 2011). Thus, intermediate Aβ species can offer a possible explanation for early neurodegeneration and inflammation observed well before the plaque formation in AD mouse models as well as AD patients (Rahimi, et al., 2008).

Most of the previous studies investigating Aβ-induced microglial activation utilized fibrillar preparations. Fibrils have been shown to induce a proinflammatory response via a number of receptors including heterotrimeric the TLR4-TLR6-CD36 complex, TLR2, 4 and CD14. Sondag et al (2009) showed that although both fibrils and oligomers can activate microglia, the activation profile is qualitatively distinct for each

156

stimulus with respect to tyrosine kinase signaling pathways. Fibrils have long been believed to act as inflammatory stimulus particularly due to the clustering of microglia and upregulation of inflammatory molecules surrounding the plaques. In the context of a recent study showing the presence of oligomeric Aβ in the plaque periphery (DaRocha-Souto, et al., 2011), our *in vitro* findings in murine microglia might be biologically relevant.

The isolated fibrils prepared from SEC-purified Aβ(1-42) monomer under physiological pH conditions (described in Chapter 3) failed to produce any TNFα response in murine microglia while the fibrils prepared under aqueous, non-buffered acidic conditions produced a small yet noticeable response. The difference in pH and ionic strength significantly affected the solubility of the fibrils. Fibrils formed at lower pH and little ionic strength were flexible and extremely soluble compared to the insoluble fibrils formed at physiological pH and high ionic strength. It is possible that solution conditions influenced the ability of fibrils to act as a proinflammatory stimulus by changing the structure at the molecular level required for interaction with microglial receptors. In fact, Petkova et al (2005) have shown that altering the solution conditions not only changed the structure of fibrils as assessed by solid state NMR but also influenced their ability to confer toxicity.

Oligomers described in the current study were analyzed previously by Western Blotting and contained higher oligomeric structures (30-60 kDa) along with trimers and tetramers (Stine, et al., 2003). Aβ forms SDS-resistant species and in some cases, SDS can lead to artificial oligomerization of amphipathic proteins limiting the use of western blot analysis for characterization of the oligomerization state (Bitan, et al., 2005). Native

gel electrophoresis is an alternative for SDS-PAGE. However, different oligomeric species can have identical mass to charge ratio, making the native gel data inferior to the SDS-PAGE resolution (Bitan, et al., 2005). AFM is another morphological technique that was extensively used to characterize oligomers. Commonly, AFM utilizes a mica surface for sample adsorption. It has been thought that not all Aβ species are capable of uniform adsorption on mica surface, and the adsorption is governed by surface properties of various Aβ species (Bitan, et al., 2005). To overcome these limitations, we extended the biophysical characterization of these oligomers by SEC and TEM. SEC showed an elution profile for oligomers which was qualitatively identical to our protofibril preparation. Both protofibrils and oligomers separated out in a void peak on a Superdex 75 SEC-column (>70000 molecular weight cut off). Chromy and colleagues observed a dual peak for Aβ(1-42) oligomers using Superdex 75 (Chromy, et al., 2003). However, in our hands, Aβ(1-42) oligomers eluted out in the void volume instead of shortly after the void volume as described by Chromy *et al.* We did observe a small shoulder peak after the void volume, but we could not detect any Aβ structures in the TEM images nor observe a significant DLS signal. Overall, DLS measurements carried out on the void peak showed smaller hydrodynamic radius values as compared to Aβ(1-42) protofibrils. Chromy and colleagues also described oligomers to be distinct from protofibrils at least for up to 24 h (Chromy, et al., 2003). Our dual SEC-profile was more comparable to that observed by Hepler *et al* (Hepler, et al., 2006). They used multi-angle light scattering (MALS) in-line with SEC to measure the molecular weight of the Aβ species and found out that the void peak in fact contained Aβ species of very high molecular weight (ranging between 100 kDa-150 kDa) (Hepler, et al., 2006) compare to that reported by

western blotting (Lambert, et al., 1998; Chromy, et al., 2003). Both protofibril and oligomer preparation have utilized solvents like NaOH or DMSO during the first step of Aβ reconstitution. NaOH being a strong base helps to cross the isoelectric pH of Aβ rapidly and thus results into highly monomeric solution (Jan, et al., 2010). Similarly, DMSO is a highly polar solvent to yield a highly soluble monomeric Aβ solution (Stine, et al., 2003). After the initial reconstitution, both preparations use the same F-12 medium without phenol red to get the final Aβ aggregation solution. One of the major differences in the preparation of protofibrils and oligomers is that protofibril preparation is 2.5-fold more concentrated than oligomer preparation. It is a well established fact that the Aβ concentration has a profound effect on the aggregation (Lomakin, et al., 1997; Harper, et al., 1999). So based on the current study, it is possible that the formation of Aβ oligomer or protofibrils is dependent on the concentration of aggregation solution. However, it is clear that both oligomers and protofibrils have early synaptotoxic (Hartley, et al., 1999; Dahlgren, et al., 2002; O'Nuallain, et al., 2010) as well as proinflammatory properties (Chapter 3) (White, et al., 2005). Investigating the concentration-dependence of Aβ(1-42) aggregation under protofibril and oligomer-forming conditions using non-denaturing techniques like SEC, native PAGE and imaging might provide mechanistic insight into the formation of these intermediates.

Together, this study shows that soluble, oligomeric Aβ(1-42) rather than fibrils act as effective proinflammatory stimulus in murine microglia. Moreover, this study emphasizes that solution conditions and concentration have significant effect on the Aβ aggregation in the context of soluble intermediates formed.

CHAPTER 5

DEPENDENCE OF Aβ(1-42)AGGREGATION AGE ON MICROGLIAL
PROINFLAMMATORY RESPONSE

5.1 Introduction

Alzheimer's disease is characterized by the presence of extracellular deposits of

amyloid-β (Aβ) protein known as senile plaques and intraneuronal tau tangles in the brain

of an individual (Selkoe, 2004). Although development of tau tangles correlates well

with the severity of AD, Aβ accumulation is considered to be the initial trigger for

neuronal degeneration during the earlier stages of AD (Selkoe, 1994; Koffie, et al., 2011).

Besides the signature proteinaceous lesions, AD neuropathology also involves innate

immune mechanisms as evident by the presence of activated microglia clustered around

the senile plaques along with a number of inflammatory proteins such as complements,

immunoglobulins and cytokines (Ishii and Haga, 1984; Dickson, et al., 1988). This

observation is further corroborated by upregulation of inflammatory cytokines and severe

glial inflammatory reactions (gliosis) surrounding Aβ-deposits (Akiyama, et al., 2000).

Furthermore, gliosis coincided with neuronal loss during *in vivo* studies using transgenic animal models of AD (Ingelsson, et al., 2004; DaRocha-Souto, et al., 2011) . *In vitro* studies have confirmed that Aβ acts as a potent inflammatory stimulus which causes overexpression of a number of proinflammatory markers, including tumor necrosis factor α (TNFα) and interleukin-1β (IL-1β) by the cells of monocytic/macrophage lineage including microglia and monocytes (Meda, et al., 1995; Combs, et al., 2001; Stewart, et al., 2010).

Aβ displays a high propensity to aggregate into fibrils. Aβ aggregation follows nucleation-dependent polymerization kinetics (Jarrett and Lansbury, 1992). In this type of kinetics, several monomer units form a nucleus which upon elongation ultimately gives rise to long fibrils (Jarrett and Lansbury, 1992). During fibrillogenesis, Aβ is known to adopt a variety of conformational states having different size, shape and a different degree of β-sheet structure (Bitan, et al., 2003). Markers of neuronal degeneration as well as inflammation were observed in the close vicinity of neuritic plaques (Dickson, et al., 1988; Tsai, et al., 2004). Since Aβ fibrils were found to be a major component of dense-core plaques (Glenner and Wong, 1984; Masters, et al., 1985b), fibrils were largely believed to be responsible for such a degenerating pathology (Hardy and Higgins, 1992). However, total amyloid plaque burden did neither correlated well with the neuronal loss nor with disease severity (Naslund, et al., 2000). Moreover, a number of cognitively normal individuals displayed significant amyloid plaque burden (Morris, et al., 2009). This evidence argues against the fibrils as important players in the AD related neurodegeneration (Hardy and Selkoe, 2002). Further support for this argument came from the recent studies employing highly sensitive, conformation-specific

antibodies against oligomeric Aβ revealing a complex plaque environment in which different species of Aβ are in a dynamic equilibrium within and around the periphery of the plaques in a mouse model of amyloid deposition (Koffie, et al., 2009). Moreover, oligomeric Aβ surrounding the plaques correlated with 60% of excitatory synaptic loss (Koffie, et al., 2009). This finding provided support to a number of *in vitro* studies in which small, soluble oligomers resulted in significant neuronal degeneration, as measured by inhibition of long-term potentiation (Lambert, et al., 1998; Walsh, et al., 2002), decrease in neuronal viability (Dahlgren, et al., 2002) and early alterations in electrical activity of neurons (Hartley, et al., 1999). In agreement with the above findings, oligomers were found to colocalize with markers of postsynaptic densities using hippocampal neuronal culture (Lacor, et al., 2004). In subsequent studies, Hyman and colleagues showed that oligomeric Aβ correlates not only with neuronal loss but also with the inflammatory reactions of brain immune cells such as astrocytes and microglia (astrocytosis and microgliosis) in a transgenic mouse model of AD (Koffie, et al., 2009; DaRocha-Souto, et al., 2011). Interestingly, they observed a linear increase in gliosis as the disease progressed, despite the total amyloid load reaching a plateau (Serrano-Pozo, et al., 2011). In fact, gliosis was found to be the best correlate of cognitive decline in a stereology based quantification study using a large number of AD and control brain samples (Serrano-Pozo, et al., 2011). Together, these studies suggest a role for astrocytes and microglia in the neurodegenerative pathology of AD rather than being innocent bystanders.

Structural polymorphism of Aβ is also believed to underlie its ability to act as an inflammatory stimulus (Ajit, et al., 2009). *In vitro* studies have shown that both fibrils

and oligomers can activate primary microglia (Sondag, et al., 2009). However, Sondag et al observed a qualitative difference in the activation profile of microglia depending on the aggregation state of Aβ (Sondag, et al., 2009). In a study by White *et al* oligomeric Aβ was more effective in inducing a proinflammatory response in rat astrocyte culture, while fibrils were not as effective (White, et al., 2005). Several *in vitro* studies investigating involvement of cell surface receptors and downstream signaling elements in Aβ-mediated proinflammatory response have provided evidence for fibrils as an effective inflammatory stimulus (McDonald, et al., 1997; Walter, et al., 2007; Stewart, et al., 2010). However, unlike Aβ-induced neurodegeneration, the neuroinflammation field still lacks a consensus regarding the structure-activity relationship in the context of Aβ-induced microglial inflammation. Knowledge of Aβ-induced inflammatory response is important in order to develop effective therapeutic targets against AD (Hyman, 2011).

Previously we have reported that soluble fibrillar precursors formed during fibrillogenesis of Aβ(1-42) were able to provoke maximum TNFα response in THP-1 monocytes (Ajit, et al., 2009). THP-1 cells belong to the same lineage as microglia, hence have been used as a model system for studying Aβ-induced microglial response (Klegeris and McGeer, 2001; Udan, et al., 2008; Ajit, et al., 2009). However, it has been argued that microglia, being the resident immune cells of the brain, is a more biologically relevant model system to study Aβ-induced inflammation. Therefore, we investigated the optimal aggregation state for Aβ(1-42)-induced microglial TNFα response.

5.2 Preparation of Aβ(1-42) for microglial cell stimulation experiments

The highly amphipathic character of Aβ peptide underlies its high propensity to form β-sheet rich aggregates (Broersen, et al., 2011). The process of aggregation is governed by a number of physical parameters that include pH, temperature, concentration, ionic strength, and time of incubation. The conditions used for preparation of Aβ are crucial to produce the desired structure or aggregation state of the peptide (Jan, et al., 2010). Highly fluorinated alcohol such as 100% hexafluoroisopropanol (HFIP) has been shown to dissociate preformed aggregates of Aβ by destabilizing the hydrogen bonds (Nichols, et al., 2005). However, low concentrations of HFIP have been reported to induce not only α-helical conformations but also turns and β-hairpins via intramolecular hydrogen bond formation in Aβ (Buck, 1998).

The aggregation state of Aβ can also influence its ability to induce a proinflammatory response (Ajit, et al., 2009). For my experiments using mouse microglia, I prepared aggregate-free solutions of Aβ by HFIP pretreatment of the purchased peptide followed by complete removal of HFIP using vacuum centrifugation as described in Ajit *et al* (Ajit, et al., 2009). The resulting lyophilized peptide was then reconstituted in water to give 100 μM solution of Aβ(1-42) (Ajit, et al., 2009). The solution was then aggregated at 4°C for 24, 48, 96 and 216 h. Aβ(1-42) aggregated in such a manner produces distinct morphologies described in Ajit et al (2009) using atomic force microscopy (AFM) images. In those studies Aβ exhibited punctate morphology right after its reconstitution and slowly progressed towards formation of fibrils by 48-96 h. There was a significant increase in the number of fibrils over time. At each

aggregation time point, including 0 h, an aliquot was drawn and flash frozen using a dry ice /ethanol mixture and stored at -80°C until used for the experiment. Flash-freezing of the Aβ aggregation solution was carried out due to the logistics of the microglia treatment as described in the Methods. Primary microglia need two days for their harvest and subsequent plating in order to be ready for the cell stimulation experiment. The Aβ aggregation age time points were separated by a two day period, making the microglial cell treatments difficult to manipulate. Moreover, the yield of microglia and the sensitivity of microglia to positive controls (for example lipopolysaccharide as described in the Methods) vary from batch to batch (data not shown). We thought that assessing different aggregation states of Aβ on the same batch of cells will minimize the variability in the cellular response and will also allow convenient manipulation of microglial cell culture. Thus, frozen aliquots were thawed rapidly and added to the primary murine microglia plated in a 96 well cell-culture plate at a final concentration of 15 μM for 6 and 24 h. When the conditioned medium of the cellular treatment was analyzed using ELISA for TNFα production, we observed that primary murine microglia produced TNFα response did not vary significantly over the time course of the Aβ-aggregation age (Figure 5.1). The magnitude of TNFα response remained essentially comparable irrespective of the aggregation age of Aβ. Moreover, the trend did not change significantly between 6 and 24 h treatment (6 or 24 h) (Figure 5.1). This observation was quite different from our previous studies on THP-1 monocytes (Ajit, et al., 2009). Aβ(1-42) prepared and aggregated in the identical manner produced a consistent trend in the monocyte proinflammatory response over the time course of Aβ aggregation. Ajit et al
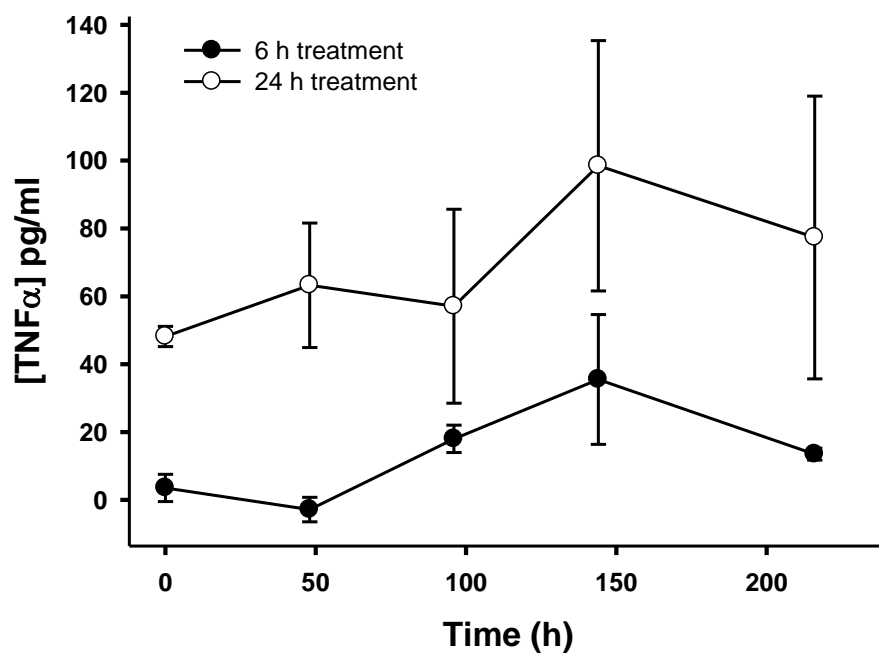
Figure 5.1 Dependence of primary microglial TNFα response on the aggregation age of Aβ(1-42). Aβ(1-42) was resuspended in sterile water at 100 μM and aggregated at 4°C. Aliquots were drawn at 0, 48, 96 and 216 h of aggregation and flash frozen with ethanol/dry-ice mixture. All the aliquots were thawed and treated at the same time with primary microglia plated in a 96-well plate for 6 or 24 h at a final concentration of 15 μM. Cellular medium was analyzed using TNFα ELISA.

observed that Aβ(1-42) corresponding to an intermediate aggregation state correlated with maximum proinflammatory response.

Aβ(1-42) preparation in water results into a low pH solution (pH 3). We wanted to compare our preparation under acidic conditions to that of physiological conditions. Aβ(1-42) was resuspended in NaOH, followed by dilution in phosphate buffered saline to give 100 μM solution and aggregated in a time dependent manner. Dissolution of Aβ in NaOH allows rapid transition to basic pH, followed by slow dilution in neutral buffer. This process minimizes the aggregation of Aβ at its isoelectric pH (pI 5.5). However, we did not see any correlation between Aβ-aggregation age and subsequent TNFα production by primary microglia by changing the aggregation conditions close to physiological conditions (data not shown).

Since Aβ-aggregation is temperature dependent, we boosted the temperature of Aβ(1-42)/water aggregation reaction to 37°C. The increase in temperature increased the extent of aggregation (as measured by ThT fluorescence) compared to aggregation reactions carried out at 4°C and also formed fibrils more rapidly (Ajit, et al., 2009). Aβ(1-42) fibrils are reported to act as a pro-inflammatory stimulus for microglia (McDonald, et al., 1997; Yates, et al., 2000; Combs, et al., 2001; Walter, et al., 2007). We thought if fibrils activate microglia, we would see an increase in microglia-stimulated TNFα response over the time course of Aβ-aggregation. We observed such an increase, which seemed to correlate with the age-dependent aggregation of Aβ(1-42) based on ThT fluorescence studies (Figure 5.2). However, there were two concerns. Firstly, we saw high ThT fluorescence values for the freshly reconstituted peptide. Ideally, freshly reconstituted peptide should be mostly monomeric hence should exhibit little to no ThT
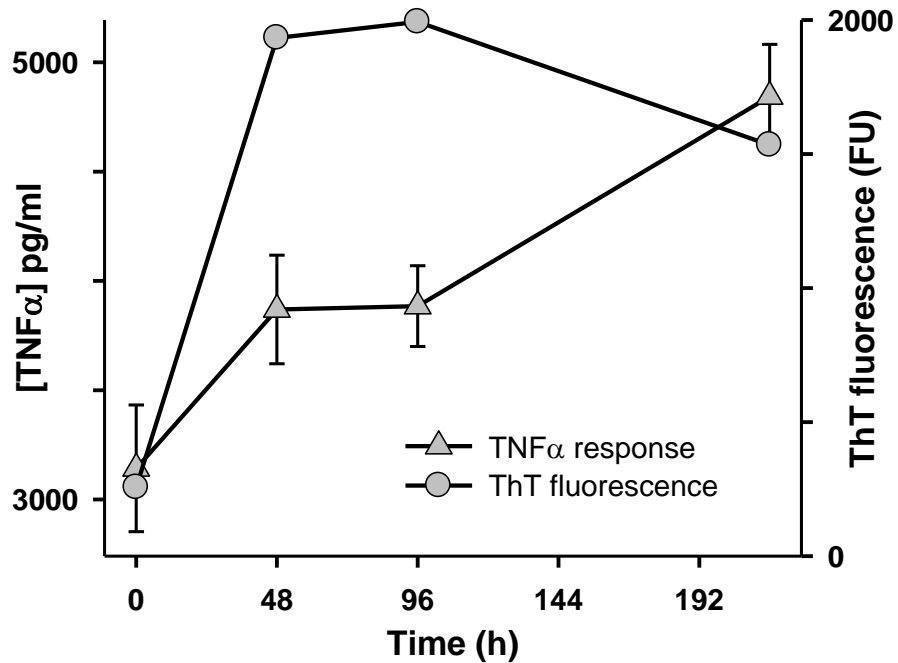
Figure 5.2 Dependence of primary microglial TNFα response and Thioflavin-T fluorescence of Aβ on the aggregation age of Aβ(1-42). Aβ(1-42) was resuspended in sterile water and incubated at 37°C. Aliquots were drawn at 0, 48, 96, and 216 h and flash-frozen using ethanol/dry-ice mixture. The aliquots were thawed at the same time and added to primary microglia plated in 96-well plate for 6 h at a final concentration of 15 μM. TNFα production was quantified by ELISA.

fluorescence. We thought that higher ThT values might suggest either the presence of preformed aggregates even after HFIP pretreatment or rapid formation of aggregates rich in β-sheet structure. Secondly, at any given time the aggregation reaction might represent a polydisperse mixture of different Aβ species in equilibrium. This makes the structure-activity correlation studies less straightforward to interpret. For these reasons we decided to further purify Aβ solutions in order to obtain highly-enriched monomeric samples using size-exclusion chromatography.

5.3 Isolation of Aβ(1-42) monomer using SEC

Size exclusion chromatography is a non-denaturing technique that separates the proteins on the basis of its size and shape. This technique is valuable in separating Aβ-monomers from aggregated Aβ species (Walsh, et al., 1997; Jan, et al., 2010). We expected that Aβ monomer solution obtained using SEC will be free of any pre-existing aggregates.

Previous studies have utilized guanidine hydrochloride (GuHCl) to denature the Aβ aggregates (Jan, et al., 2010). Crude synthetic Aβ(1-42) peptide (pretreated with trifluoroacetic acid/HFIP protocol as detailed in the methods) was resuspended in 6 M GuHCl and 10 mM NH$_4$OH to give 1.0 ml solution. The resultant solution was centrifuged at 18000 g followed by separation of monomer using SEC. The SEC-separation profile as shown in Figure 5.3 was obtained by monitoring UV absorbance at 280 nm. This treatment resulted in greater monomer yield and less yield of aggregated
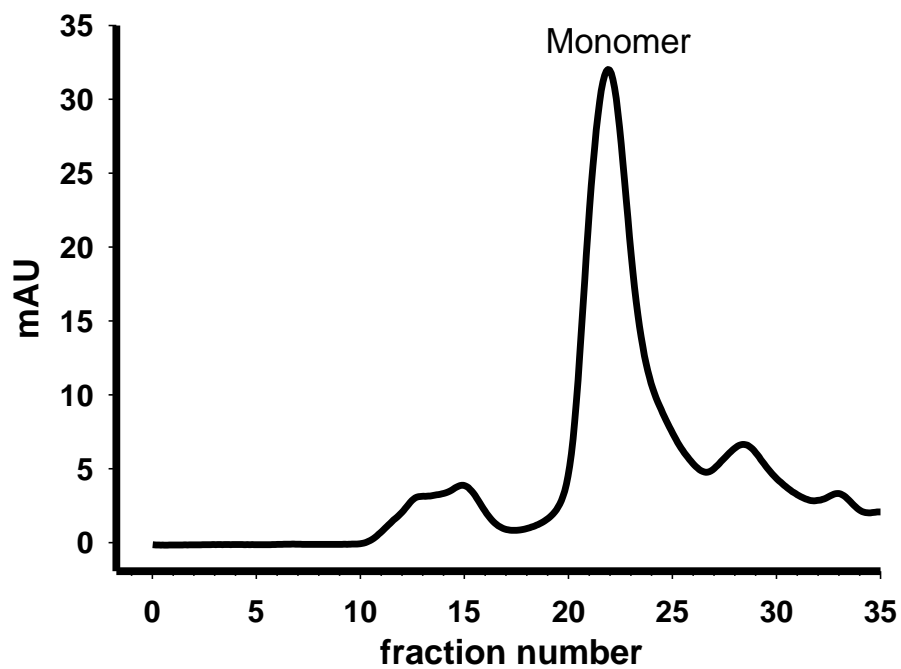
Figure 5.3   Size exclusion chromatography profile of Aβ(1-42).   Aβ(1-42) was resuspended in 6 M GuHCl and 10 mM NH₄OH at a concentration of 1 mg/ml. The peptide was immediately eluted at a flow rate of 0.5 ml/min using 50 mM Tris-HCl buffer (pH 8.0). SEC-profile was obtained by monitoring UV absorbance at 280 nm. Fractions 21-24 labeled as monomer were collected on ice and flash-frozen using ethanol/dry-ice mixture and stored -80°C.

Aβ in the void peak. Different elution buffers like 50 mM Tris-HCl (pH 8.0), 50 mM HEPES (pH 7.8) and 1x PBS were used for separation. Since the monomer yields were a little better with Tris-HCl buffer (data not shown), we optimized the SEC separation of Aβ(1-42) in Tris-HCl buffer. Moreover, a number of previous studies have studied aggregation of Aβ in Tris-HCl buffer (Nichols, et al., 2002; Nichols, et al., 2005).

5.4 Aggregation of SEC-isolated Aβ(1-42) monomer

As per our expectations, SEC-purified Aβ(1-42) monomer exhibited little to no ThT fluorescence values (Figure 5.4), confirming that SEC effectively separated the pre-existing aggregates to yield a highly pure monomeric solution. These monomeric fractions were collected, sometimes pooled together and aggregated as described before in section 5.2 in a time dependent manner. Aliquots were drawn at 0, 48, 96 and 216 h, flash frozen using dry ice/ethanol mixture and stored at -80°C until needed for cell treatment experiments. For the experiments, aliquots were thawed rapidly, used for microglial cell stimulation studies and also used to carry out ThT fluorescence scans.

5.5 Thioflavin-T fluorescence increases with Aβ(1-42) aggregation

ThT fluorescence measurement is used to estimate the amount of β-sheet structure present in a particular Aβ solution (as discussed previously in Chapter 3, Section 3.3).

We were able to monitor the progress of Aβ aggregation by carrying out ThT-fluorescence measurements at different time points during the course of aggregation. Since Aβ-aggregation is dependent on temperature, pH and concentration, it is possible that these parameters might influence the type and amount of intermediates that form during Aβ-aggregation process. So we determined the effects of modulating these conditions on Aβ-aggregation by using ThT fluorescence. Our objective for these experiments was to investigate if microglial pro-inflammatory response was susceptible to the changes in the aggregation kinetics of Aβ(1-42) monomer, which would provide more information about the optimal Aβ species.

5.5.1 Effect of temperature on aggregation of SEC-purified Aβ(1-42) monomer as monitored by ThT-fluorescence

Three separate aliquots from the same SEC-isolated Aβ(1-42) monomer fraction eluted in 50 mM Tris-HCl buffer (pH 8.0) were subjected to time-dependent aggregation at three different temperatures such as 4, 25 and 37°C. As discussed previously, the aliquots were drawn on 0, 48, 96 and 216 h and flash frozen using dry ice/ethanol mixture. Aliquots were thawed and diluted 10-fold in Tris-HCl buffer (pH 8.0) containing 5 μM ThT in a cuvette for ThT fluorescence measurements. Tris-HCl buffer did not show significant ThT fluorescence by itself. Aβ(1-42) aggregated in a temperature-dependent manner. The extent of ThT binding did not change significantly over time for the aggregation reactions carried out at 4 and 25°C. However, at 37°C Aβ(1-42) displayed a typical aggregation curve with a lag phase followed by a significant

increase in ThT-fluorescence (Figure 5.4). ThT-fluorescence appeared to reach a plateau towards the later time points of aggregation as reported before (Jarrett and Lansbury, 1992; Harper and Lansbury, 1997).

5.5.2 Effect of elution buffer on the aggregation of SEC-purified Aβ(1-42) monomer as monitored by ThT fluorescence

We wanted to use SEC isolated monomer for the aggregation studies followed by cellular stimulation studies. This required generation of a sufficient quantity of SEC-purified Aβ monomer. Therefore, it was essential to optimize SEC isolation of Aβ(1-42) peptide to get maximum recovery of monomer. Moreover, we wanted to make sure that the buffer, in which Aβ is eluted, does not interfere with the aggregation of Aβ.

Aβ(1-42) peptide was eluted in different buffers including PBS, 50 mM HEPES and 50 mM Tris-HCl buffer during SEC. The isolated monomer was subjected to aggregation at 37°C. Although all monomer solutions showed an increase in ThT fluorescence over time, the extent of ThT fluorescence was maximum for the monomer eluted in Tris-HCl buffer (Figure 5.5). Also Tris-HCl is a common buffer used for SEC-isolation of Aβ monomer (Nichols, et al., 2002; Nichols, et al., 2005). Furthermore, the recovery of Aβ(1-42) monomer was the highest in Tris-HCl buffer. Recovery was lower in HEPES buffer and therefore, we were not able to compare the aggregation reactions at equivalent concentrations of Aβ. This led us to use Tris-HCl buffer in all of our SEC experiments described in Chapter 5.
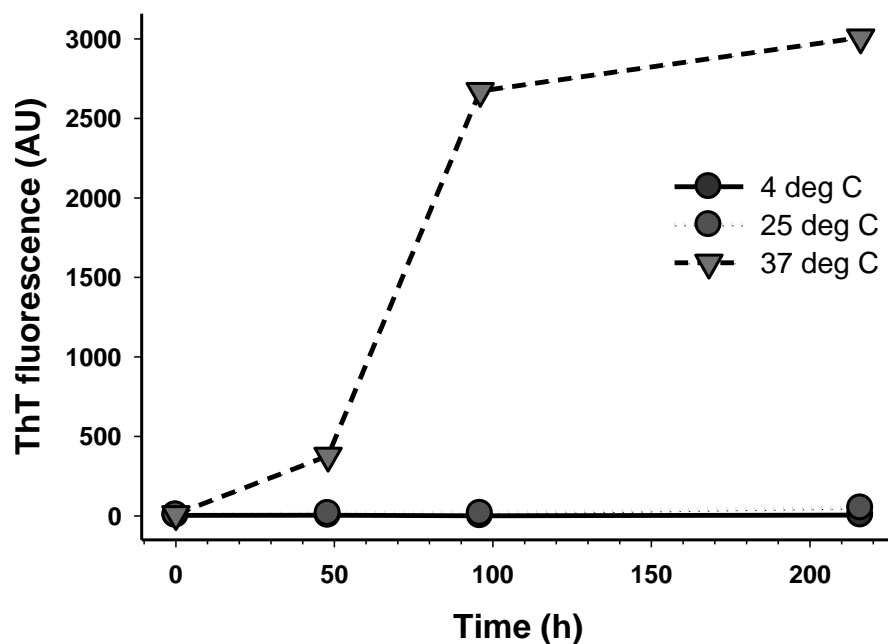
Figure 5.4 Effect of temperature on ThT-fluorescence of Aβ(1-42). SEC-purified Aβ(1-42) monomer (36 μM based on UV measurements) eluted in 50 mM Tris-HCl buffer (pH 8.0) was divided into 3 parts. The monomer was incubated at 4, 25 or 37°C and aliquots were drawn at 0, 48, 96 and 216 h, flash frozen using ethanol/dry-ice mixture. The aliquots were thawed and diluted 10-fold into 5 μM ThT in Tris-HCl buffer (pH 8.0) and fluorescence scans were carried out as described in methods.
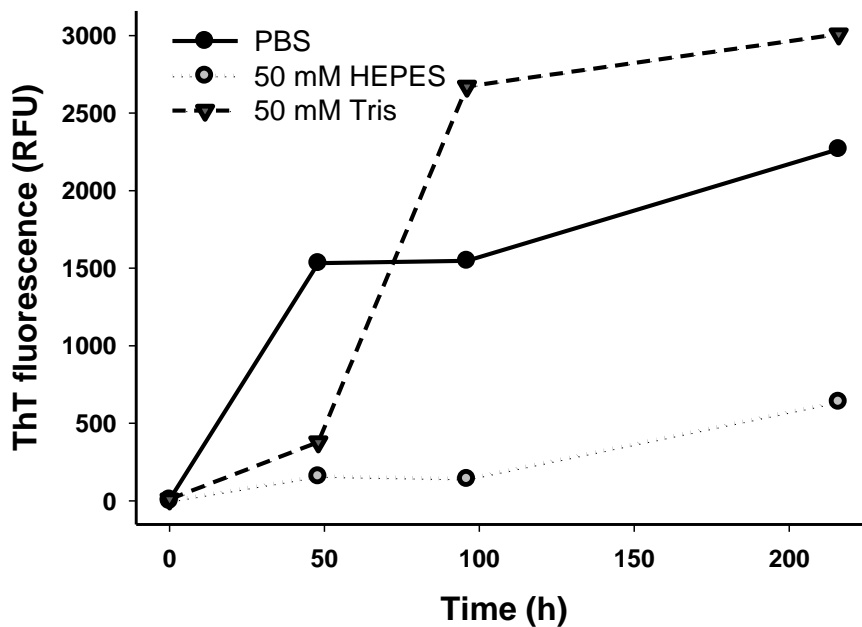
Figure 5.5 Effect of SEC-elution buffer on ThT-fluorescence of Aβ(1-42) aggregation. SEC-purified Aβ(1-42) monomer in three different buffers were aggregated at 37°C. Aliquots were drawn at different time points, flash-frozen with dry-ice/ethanol mixture and stored at -80°C. All the aliquots were thawed and ThT-fluorescence measurements were obtained as described in methods. The concentrations of Aβ(1-42) aggregation reactions were 36, 37 and 12 μM for Tris-HCl, PBS and HEPES respectively.

5.5.3 Dependence of the concentration of SEC-purified Aβ(1-42) monomeron its aggregation as monitored by ThT-fluorescence

One of the important factors which governs aggregation is the concentration of Aβ. Aβ is considered to exhibit properties similar to detergents due to its amphipathic nature. Like detergents, a critical concentration of Aβ monomer is required to form micellar aggregates, which act as nucleation sites for further elongation (Lomakin, et al., 1996; Lomakin, et al., 1997). Below its critical concentration, Aβ exists as monomer. Above its critical concentration, there is an equilibrium between monomer and fibrils. The critical concentration of Aβ(1-42) is in the lower micromolar range, which is five-fold less than that of its carboxy terminal variant Aβ(1-40) (Soreghan, et al., 1994; Harper and Lansbury, 1997).

We were interested in studying the concentration dependence of Aβ(1-42) aggregation using SEC isolated seed-free monomer at 37°C. We carried out a number of such aggregation experiments with varying Aβ(1-42) concentrations. In most of the experiments, ThT fluorescence showed an increase over time as described in Section 5.5.1. As the concentration of monomer increases, the lag time of aggregation should decrease (Harper and Lansbury, 1997), thereby decreasing the time required to attain half of maximal ThT fluorescence ($t_{1/2}$) (measure of lag time of aggregation). Therefore, we expected to see a negative correlation between $t_{1/2}$ and concentration of Aβ(1-42) monomer. However, we did not see any correlation (r^2=2.16 x 10^{-3} using Sigmaplot curve fitting parameters) between concentration of monomer and $t_{1/2}$, which was calculated manually by extrapolation using individual aggregation curves (Figure 5.6) (discussed further in section 5.8).
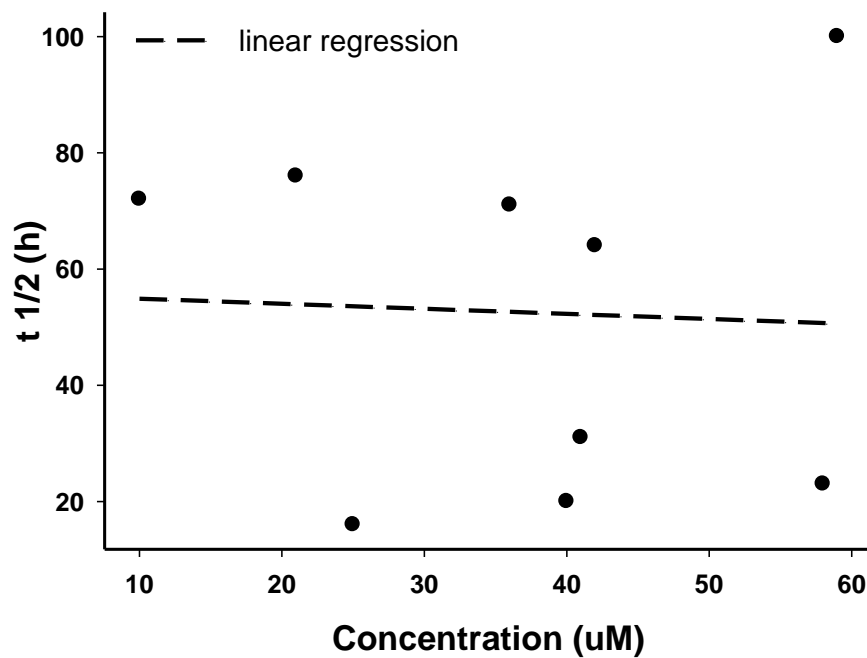
Figure 5.6 Dependence of ThT-fluorescence on the concentration of Aβ(1-42). SEC-purified Aβ(1-42) monomer in Tris-HCl buffer (pH 8.0) was aggregated at different concentrations at 37°C in a time dependent manner. The time corresponding to half of the maximum ThT fluorescence was designated as t1/2 and plotted against concentration of the aggregation reaction. (--) represents the linear fit for the data using SigmaPlot 10.0 software.

<u>5.6 Lack of correlation between Aβ(1-42) aggregation age as measured by ThT
fluorescence and Aβ-induced proinflammatory response</u>

30 μl of Aβ(1-42) aggregation solutions (36 μM) prepared as described in Section 5.4.1, were added to primary mouse microglia and BV-2 mouse microglia. The final concentration of Aβ was 11 μM in the cellular treatment. After 6 h incubation, the medium was collected and analyzed for the production of TNFα by ELISA to identify the Aβ(1-42) aggregation species which activates microglia most effectively.

5.6.1 Aβ(1-42)-induced proinflammatory response in primary murine microglia was dependent on the temperature at which Aβ was incubated

As described in section 5.5.1, SEC-isolated Aβ(1-42) monomer was aggregated in a time-dependent manner at 3 different temperatures 4, 25 and 37°C. The aggregation solutions were tested for their ability to produce TNFα in BV-2 mouse microglia for 24 h. Temperature not only influenced the aggregation of Aβ(1-42) monomer (Figure 5.7 and Figure 5.8) but also had a significant effect on the ability of Aβ to stimulate TNFα production.

5.6.2 Aβ(1-42)-induced proinflammatory response in primary murine microglia correlated with increased aggregation

SEC-purified Aβ(1-42) monomer in Tris buffer (pH 8.0) was aggregated at 37°C over time and ThT fluorescence was used to monitor progress of aggregation. Primary
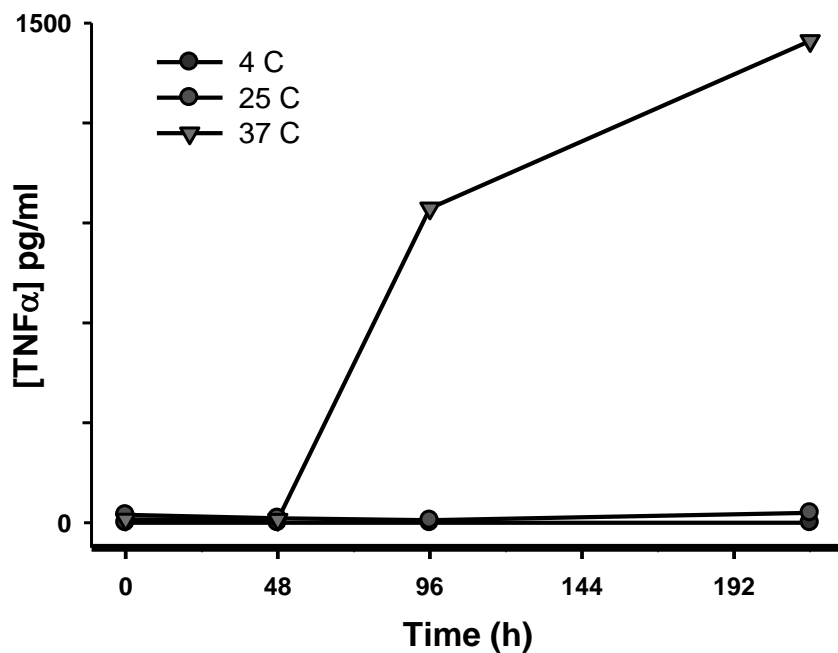
Figure 5.7 Dependence of microglial proinflammatory response on the aggregation age of Aβ(1-42). Aβ(1-42) monomer (36 µM) eluted in Tris-HCl buffer was incubated at 37°C for up to 216h. BV-2 microglia were exposed to a final Aβ(1-42) concentration of 10.6 µM for 24h. Cellular medium was analyzed for TNFα production using ELISA.
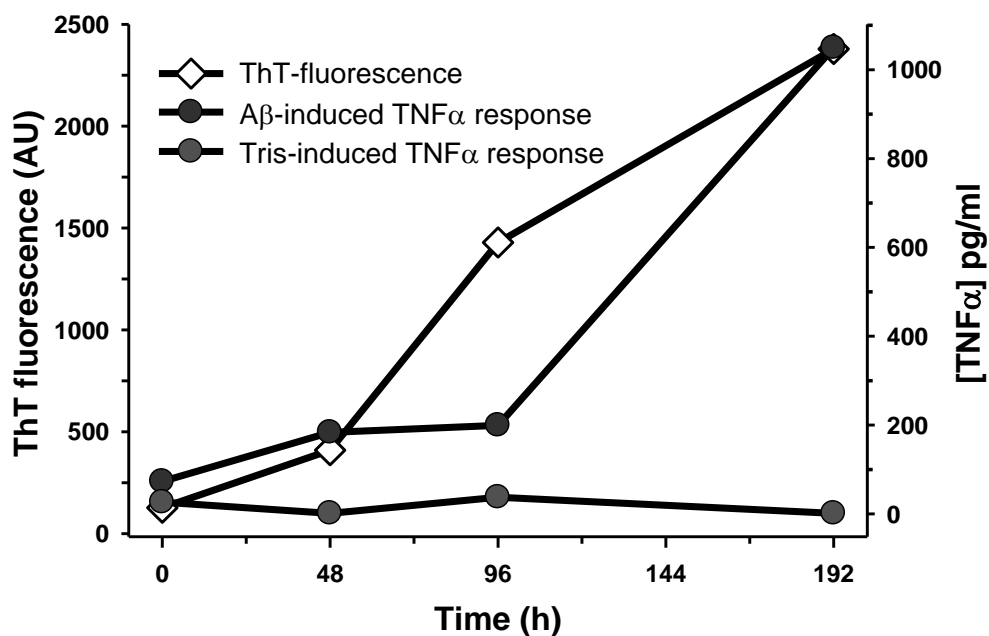
Figure 5.8 Correlation between Aβ-induced microglial proinflammatory response and ThT-fluorescence over time. Aβ(1-42) monomer (36 μM) was incubated at 37°C for up to 216 h. Aliquots were analyzed for ThT binding and proinflammatory activity in primary microglia. Cells were exposed to a final Aβ(1-42) concentration of 11 μM for 6 h and medium was analyzed using TNFα ELISA.

mouse microglia were treated with 11 µM of aggregated Aβ for 6 h. Freshly isolated Aβ(1-42) monomer was unable to stimulate TNFα production. Interestingly, the extent of TNFα production increased with increase in ThT-fluorescence over time. TNFα response was maximum when microglia were treated with 216 h aggregated Aβ(1-42) which correlated well with ThT-fluorescence (Figure 5.8). We have seen previously that freshly reconstituted Aβ(1-42) is essentially fibril-free based by AFM analysis, yet is able to transition to fibrillar structures by 96 h of aggregation at 37°C. Also AFM indicated that as time progressed further, the existing smaller punctuate species disappeared completely to give predominantly long fibrils (Ajit, et al., 2009). Based on this observation, we thought that Aβ(1-42) fibrils might be responsible for the microglial activation.

5.6.3 Aggregation of Aβ(1-42) as measured by ThT fluorescence was not sufficient to stimulate a consistent proinflammatory response in primary microglia

As described in previous section 5.6.2, we saw that Aβ(1-42)-induced TNFα production correlated with ThT-fluorescence over time, suggesting the role of aggregated Aβ(1-42) rather than unaggregated, monomeric Aβ(1-42) in inducing a microglial proinflammatory response. However, surprisingly, when we repeatedly studied the dependence of Aβ-aggregation age on microglial TNFα response under the same exact experimental conditions as described in 5.6.2, Aβ(1-42) failed to induce any TNFα response. Furthermore, we observed no correlation between the Aβ-aggregation age and microglial TNFα response despite the fact that ThT-fluorescence showed a time

dependent increase over time (Figure 5.9). We did not see a consistent, reproducible microglial response between different experiments. Another factor which made the analyses less straightforward is the variable microglial TNFα response to Tris-HCl buffer (pH 8.0). The background response in some cases was comparable to water treated cells, but in other experiments Tris background signal was very high, making the Aβ-induced microglial TNFα response hard to interpret (discussed further in section 5.8).

5.7 No correlation was found between Aβ(1-42) induced proinflammatory response and extent of reactivity to OC-antibody

OC-antibody is a conformation dependent antibody developed by Charles Glabes laboratory that specifically recognizes Aβ species that have an element of fibril structure (Kayed, et al., 2007). We have previously reported that SEC-purified Aβ(1-42) fraction, which is non-reactive to OC-antibody, failed to stimulate THP-1 monocytes (Ajit, et al., 2009). Moreover, Aβ(1-42)-induced TNFα response was diminished, when Aβ(1-42) solution was immunodepleted using OC-antibody (Ajit, et al., 2009). We wanted to investigate whether OC-reactivity is sufficient to produce TNFα response in a microglial cell system as well.

We made use of a dot blot technique to qualitatively detect the presence of OC-positive Aβ species in a particular aggregation solution of Aβ(1-42). The dot-blot technique is more useful for qualitative information, although the densitometry analysis of the dots developed by the use of chemiluminiscence can be used to get some idea into quantitative
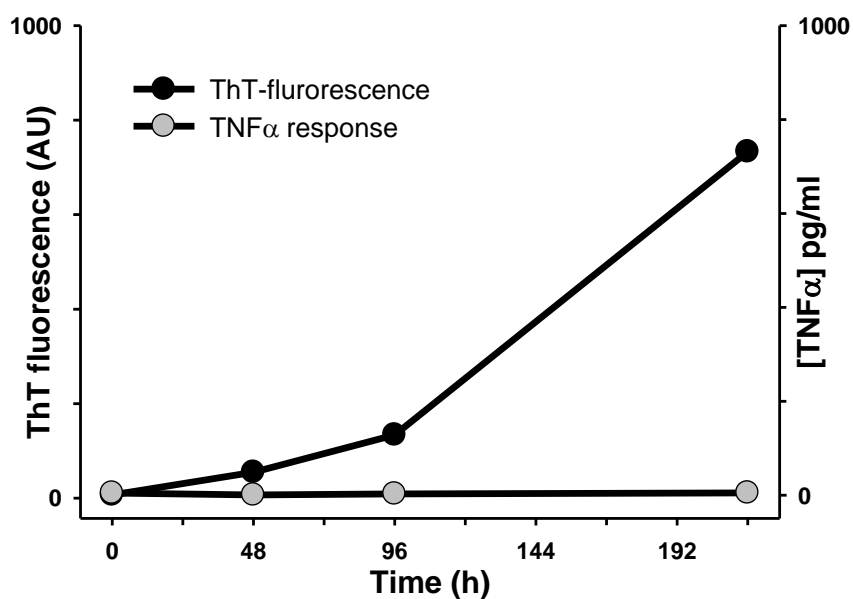
Figure 5.9 Lack of correlation between microglial proinflammatory response and ThT-fluorescence of Aβ(1-42) over the time course of aggregation. Aβ(1-42) monomer (36 μM) was incubated at 37°C for up to 216h and aliquots were drawn at time points shown above. Aliquots were analyzed for ThT binding and proinflammatory activity in primary microglia. Cells were exposed to a final Aβ(1-42) concentration of 11 μM for 6 h.
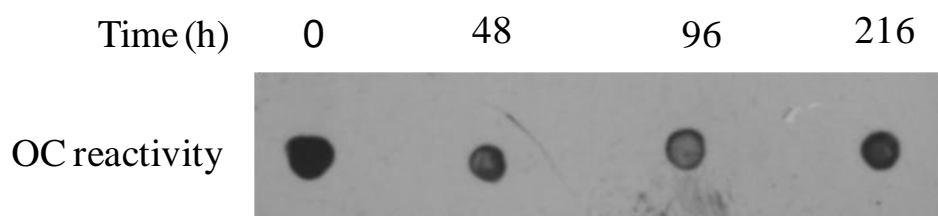
Figure 5.10 Change in OC-immunoreactivity of Aβ(1-42) at 37ºC over time. 2 μl of aggregated Aβ42 (62 μM) at different time points was probed with anti-fibrillar oligomeric OC-antibody in the dot blot assay as described in the methods.

analysis in a similar manner as Western blots. Surprisingly, freshly purified Aβ(1-42) monomer, although showing negligible ThT-fluorescence, was immunoreactive to OC antisera for a wide range of concentrations (data not shown). Furthermore, increasing the time of aggregation had no effect on OC-reactivity. We observed changes in the intensity of dots over the course of aggregation, although no specific trend was obvious (Figure 5.10). OC-reactivity did not seem to correlate with microglial cell stimulation, irrespective of whether we observed a significant TNFα response or not in a particular experiment (data not shown). However, this result does not rule out the possibility that OC-immunoreactivity is essential for microglial stimulation because of several reasons. OC-antibody is known to recognize a wide range of sizes. It is possible that only one or a few OC-positive species, when present at a particular critical concentration, can act as a potent stimulus. Variability in Aβ(1-42) aggregation reactions could be attributed to the concentration of monomer or concentration of seed structures formed rapidly during elution of the peptide.

5.8 Discussion

Understanding microglial activation in response to Aβ has gained a lot of importance particularly since microglia are emerging as one of the cell types displaying a highly dynamic phenotype and versatile functions in the normal brain as well as in the degenerating brain (Nimmerjahn, et al., 2005; Perry, et al., 2010). Recent evidence using multiphoton imaging has shown rapid recruitment of microglia to the nascent plaques in a transgenic mice model of AD (Meyer-Luehmann, et al., 2008) and more recently both

microgliosis and astrocytosis were found to be very well correlated with neuronal loss (Serrano-Pozo, et al., 2011). These and other studies have strongly supported a role for microglia in AD pathogenesis. Aβ acts as a potent proinflammatory stimulus as shown in a number of *in vitro* studies (Meda, et al., 1995; McDonald, et al., 1997; Combs, et al., 2000; Combs, et al., 2001; Klegeris and McGeer, 2001; Stewart, et al., 2010). *In vitro* studies have been useful in studying Aβ-induced stimulation of microglia, since it allows for the flexibility to manipulate not only Aβ aggregation state but also the factors influencing Aβ aggregation. Although, *in vitro* knowledge does not always directly translate to *in vivo* processes, it does provide information which can form a basis for further *in vivo* testing. In the present *in vitro* study, we attempted to investigate an optimal aggregation state of Aβ(1-42) that provokes the maximum proinflammatory response in murine microglia, and it appears that homogeneity and concentration of the Aβ(1-42) aggregation reaction have a substantial role in producing the optimal proinflammatory aggregation state.

In this study, we did not observe a consistent correlation between aggregation of SEC-purified Aβ(1-42) monomer and subsequent microglial TNFα production. In fact, some of our experiments showed that microglial TNFα response increases with increasing time of incubation of Aβ, which correlated with the extent of ThT fluorescence. This observation suggested that fibrils might be the optimal proinflammatory stimulus for murine microglia. But on the other hand, we also observed no specific trend in the microglial TNFα response despite the increase in ThT fluorescence of Aβ(1-42) as a function of time. This observation was surprising because in our previous studies using THP-1 monocytes, we were able to identify an intermediate

aggregation state of Aβ(1-42) (corresponding to 72-96 h incubation) as optimal for producing TNFα response. All the physical factors like temperature, concentration, time of incubation and pH that allowed for more fibril formation, in fact, diminished the TNFα response by THP-1 monocytes. AFM analysis of these aggregation reactions suggested that soluble fibrillar precursors, but not fibrils, are optimal for producing a proinflammatory response in THP-1 monocytes (Ajit, et al., 2009). However, the present study had some differences than the study carried out in THP-1 monocytes. In this study, we prepared Aβ(1-42) in different ways. Firstly, we tried to replicate our preparation of recombinant Aβ(1-42) in water as described in Ajit et al (Ajit, et al., 2009), but it failed to produce any consistent microglial stimulation. One of the potential concerns was the batch to batch variation in the purchased Aβ(1-42) peptide. Previously, we have seen that some batches of purchased Aβ(1-42) produced a significant cellular response while other batches failed to do so, despite using the identical condition for preparation of Aβ (Jan, et al., 2010). Also, in primary and BV-2 microglia, to minimize the cellular variation between different harvests, Aβ(1-42) was aliquoted at different time points, flash frozen using dry ice/ethanol mixture and all the aliquots were thawed on the day of cellular treatment unlike our study in THP-1 monocytes. The effects of flash-freezing on Aβ aggregation were not clear.

To rule out the presence of pre-formed seeds even after HFIP treatment, we took a step further to purify Aβ(1-42) monomer from the pre-existing aggregated Aβ using SEC right after its reconstitution (Jan, et al., 2010). Although, SEC was successful in separating highly purified monomer exhibiting little to no ThT fluorescence from the preformed aggregates, it led to the dilution of Aβ, yielding solutions of Aβ(1-42)

monomer of 36-40 μM (much less than the 100 μM concentration in the Ajit *et al* study) for the subsequent aggregation and cell stimulation studies. Concentration has a profound effect on the aggregation of Aβ as discussed before in section 5.4.3. We were not able to rule out the possibility that the concentration played a major role in both the qualitative and quantitative formation of a particular proinflammatory conformation state. Another important caveat in these studies was that the background TNFα response to the elution buffer, Tris-HCl 50 mM (pH 8.0), differed dramatically from experiment to experiment, making the data difficult to interpret. Overall, Aβ(1-42) failed to induce a reproducible proinflammatory response in murine microglia under identical conditions irrespective of the peptide source being freshly reconstituted peptide or SEC-purified monomer.

In our Aβ(1-42) aggregation studies starting with SEC-purified monomer (as described in section 5.4.3), we observed only weak correlation between concentration and $t_{1/2}$ (time required to achieve half maximal ThT fluorescence). One of the reasons could be that the Aβ(1-42) preparations were less homogenous between different experiments. Aβ follows a nucleation-dependent polymerization kinetics, therefore, the overall rate of Aβ fibrillogenesis is dependent on both the rate of nucleation and rate of elongation (Jarrett and Lansbury, 1992). Moreover, the concentration of Aβ influences both the rate of nucleation as well as the rate of elongation (Lomakin, et al., 1996; Lomakin, et al., 1997). ThT binding measurements have been commonly used to estimate Aβ aggregation. However, this method preferentially detects large polymeric structures and does not provide any information on rate of nucleation and rate of elongation (Lomakin, et al., 1997). The weak correlation between Aβ aggregation as measured by ThT

fluorescence and concentration of Aβ might reflect a lack of sensitivity of ThT measurements for detection of early aggregation events. Also SEC-purifications of Aβ monomer yielded slightly different monomer concentrations between different experiments. Therefore, it is possible that the monomeric solution used to carry out aggregation reactions were less homogenous in the context of nucleation events, which influence the overall aggregation rate. Furthermore, the rate of nucleation and elongation as well as monomer concentration together might influence the qualitative and quantitative formation of oligomeric intermediates responsible for proinflammatory activity. Thus, lack of homogeneity might in turn be responsible for the inconsistency in cellular studies as well. In fact, we were able to prepare and separate Aβ(1-42) protofibrils at high Aβ-concentrations (250 μM) using SEC, which were able to invoke highly reproducible TNFα response in both primary and BV-2 murine microglia. Our own preparations of protofibrils and that described by others (Walsh, et al., 1997; Walsh, et al., 1999; Lashuel, et al., 2003) have also utilized higher concentrations of Aβ (100-200 μM) in order to allow protofibril formation. It is possible that Aβ(1-42) aggregation reactions described in this particular study were limited in the concentration of monomer to produce protofibrils in substantial amounts to evoke an effective proinflammatory response.

Lastly, we took advantage of the conformation-specific OC-antibody that recognizes all Aβ-species that contain elements of fibril structure. In our previous study, we observed that immunodepletion of Aβ(1-42)-aggregation solution with the OC-antibody abrogated the TNFα response by THP-1 monocytes (Ajit, et al., 2009). In our dot-blot assays, we probed solutions of Aβ(1-42) for the presence of OC-

immunoreactivity as a function of time of aggregation. Surprisingly, we did not see any correlation between OC-immunoreactivity and ThT-fluorescence or Aβ-induced TNFα response in murine microglia. In fact, Aβ(1-42) monomer right after its elution from SEC was immunoreactive to OC-antibody although it showed little to no ThT fluorescence. This observation indicates that OC-antibody might be very sensitive in detecting early aggregation events of Aβ even before more common measures like ThT-fluorescence can detect it. Since dot-blot assays are more qualitative in nature, we were not able to investigate the concentration-dependence of Aβ on the OC-reactivity directly. Moreover, OC-antibody can detect Aβ-species of wide range of sizes and structures (Kayed, et al., 2007), making the identification and separation of OC-positive species difficult. Future studies looking at the concentration of OC-positive species using an ELISA will yield more quantitative information regarding Aβ-aggregation.

Together, this study underscores the need to use homogenous Aβ(1-42) solutions in order to study structure-activity relationship in the context of Aβ-induced proinflammatory response in mouse microglia. This study also opens up avenues to utilize conformation-specific OC-antibody to probe early Aβ(1-42) aggregation events.

BIBLIOGRAPHY

Afagh A, Cummings BJ, Cribbs DH, Cotman CW, Tenner AJ.1996.Localization and cell association of C1q in Alzheimer's disease brain. Exp Neurol 138:22-32.

Ajit D, Udan ML, Paranjape G, Nichols MR.2009.Amyloid-beta(1-42) fibrillar precursors are optimal for inducing tumor necrosis factor-alpha production in the THP-1 human monocytic cell line. Biochemistry 48:9011-9021.

Akiyama H, Barger S, Barnum S, Bradt B, Bauer J, Cole GM, Cooper NR, Eikelenboom P, Emmerling M, Fiebich BL, Finch CE, Frautschy S, Griffin WS, Hampel H, Hull M, Landreth G, Lue L, Mrak R, Mackenzie IR, McGeer PL, O'Banion MK, Pachter J, Pasinetti G, Plata-Salaman C, Rogers J, Rydel R, Shen Y, Streit W, Strohmeyer R, Tooyoma I, Van Muiswinkel FL, Veerhuis R, Walker D, Webster S, Wegrzyniak B, Wenk G, Wyss-Coray T.2000.Inflammation and Alzheimer's disease. Neurobiol Aging 21:383-421.

Aloisi F, Care A, Borsellino G, Gallo P, Rosa S, Bassani A, Cabibbo A, Testa U, Levi G, Peschle C.1992.Production of hemolymphopoietic cytokines (IL-6, IL-8, colony-stimulating factors) by normal human astrocytes in response to IL-1 beta and tumor necrosis factor-alpha. J Immunol 149:2358-2366.

Alonso AC, Li B, Grundke-Iqbal I, Iqbal K.2008.Mechanism of tau-induced neurodegeneration in Alzheimer disease and related tauopathies. Curr Alzheimer Res 5:375-384.

Antzutkin ON, Leapman RD, Balbach JJ, Tycko R.2002.Supramolecular structural constraints on Alzheimer's beta-amyloid fibrils from electron microscopy and solid-state nuclear magnetic resonance. Biochemistry 41:15436-15450.

Antzutkin ON, Balbach JJ, Leapman RD, Rizzo NW, Reed J, Tycko R.2000.Multiple quantum solid-state NMR indicates a parallel, not antiparallel, organization of beta-sheets in Alzheimer's beta-amyloid fibrils. Proc Natl Acad Sci U S A 97:13045-13050.

Apelt J, Schliebs R.2001.Beta-amyloid-induced glial expression of both pro- and anti-inflammatory cytokines in cerebral cortex of aged transgenic Tg2576 mice with Alzheimer plaque pathology. Brain Res 894:21-30.

Arai KI, Lee F, Miyajima A, Miyatake S, Arai N, Yokota T.1990.Cytokines: coordinators of immune and inflammatory responses. Annu Rev Biochem 59:783-836.

Arancio O, Zhang HP, Chen X, Lin C, Trinchese F, Puzzo D, Liu S, Hegde A, Yan SF, Stern A, Luddy JS, Lue LF, Walker DG, Roher A, Buttini M, Mucke L, Li W, Schmidt AM, Kindy M, Hyslop PA, Stern DM, Du Yan SS.2004.RAGE potentiates Abeta-induced perturbation of neuronal function in transgenic mice. Embo J 23:4096-4105.

Araque A, Parpura V, Sanzgiri RP, Haydon PG.1999.Tripartite synapses: glia, the unacknowledged partner. Trends Neurosci 22:208-215.

Balbach JJ, Petkova AT, Oyler NA, Antzutkin ON, Gordon DJ, Meredith SC, Tycko R.2002.Supramolecular structure in full-length Alzheimer's beta-amyloid fibrils: evidence for a parallel beta-sheet organization from solid-state nuclear magnetic resonance. Biophys J 83:1205-1216.

Balbach JJ, Ishii Y, Antzutkin ON, Leapman RD, Rizzo NW, Dyda F, Reed J, Tycko R.2000.Amyloid fibril formation by A beta 16-22, a seven-residue fragment of the Alzheimer's beta-amyloid peptide, and structural characterization by solid state NMR. Biochemistry 39:13748-13759.

Bales KR, Du Y, Holtzman D, Cordell B, Paul SM.2000.Neuroinflammation and Alzheimer's disease: critical roles for cytokine/Abeta-induced glial activation, NF-kappaB, and apolipoprotein E. Neurobiol Aging 21:427-432; discussion 451-423.

Bamberger ME, Harris ME, McDonald DR, Husemann J, Landreth GE.2003.A cell surface receptor complex for fibrillar beta-amyloid mediates microglial activation. J Neurosci 23:2665-2674.

Bard F, Cannon C, Barbour R, Burke RL, Games D, Grajeda H, Guido T, Hu K, Huang J, Johnson-Wood K, Khan K, Kholodenko D, Lee M, Lieberburg I, Motter R, Nguyen M, Soriano F, Vasquez N, Weiss K, Welch B, Seubert P, Schenk D, Yednock T.2000.Peripherally administered antibodies against amyloid beta-peptide enter the central nervous system and reduce pathology in a mouse model of Alzheimer disease. Nat Med 6:916-919.

Barger SW, Horster D, Furukawa K, Goodman Y, Krieglstein J, Mattson MP.1995.Tumor necrosis factors alpha and beta protect neurons against amyloid

beta-peptide toxicity: evidence for involvement of a kappa B-binding factor and attenuation of peroxide and Ca2+ accumulation. Proc Natl Acad Sci U S A 92:9328-9332.

Barghorn S, Nimmrich V, Striebinger A, Krantz C, Keller P, Janson B, Bahr M, Schmidt M, Bitner RS, Harlan J, Barlow E, Ebert U, Hillen H.2005.Globular amyloid beta-peptide oligomer - a homogenous and stable neuropathological protein in Alzheimer's disease. J Neurochem 95:834-847.

Barnum SR, Jones JL, Benveniste EN.1993.Interleukin-1 and tumor necrosis factor-mediated regulation of C3 gene expression in human astroglioma cells. Glia 7:225-236.

Barrow CJ, Zagorski MG.1991.Solution structures of beta peptide and its constituent fragments: relation to amyloid deposition. Science 253:179-182.

Beffert U, Poirier J.1996.Apolipoprotein E, plaques, tangles and cholinergic dysfunction in Alzheimer's disease. Ann N Y Acad Sci 777:166-174.

Benzing WC, Wujek JR, Ward EK, Shaffer D, Ashe KH, Younkin SG, Brunden KR.1999.Evidence for glial-mediated inflammation in aged APP(SW) transgenic mice. Neurobiol Aging 20:581-589.

Benzinger TL, Gregory DM, Burkoth TS, Miller-Auer H, Lynn DG, Botto RE, Meredith SC.1998.Propagating structure of Alzheimer's beta-amyloid(10-35) is parallel beta-sheet with residues in exact register. Proc Natl Acad Sci U S A 95:13407-13412.

Binder LI, Guillozet-Bongaarts AL, Garcia-Sierra F, Berry RW.2005.Tau, tangles, and Alzheimer's disease. Biochim Biophys Acta 1739:216-223.

Bitan G, Lomakin A, Teplow DB.2001.Amyloid beta-protein oligomerization: prenucleation interactions revealed by photo-induced cross-linking of unmodified proteins. J Biol Chem 276:35176-35184.

Bitan G, Fradinger EA, Spring SM, Teplow DB.2005.Neurotoxic protein oligomers--what you see is not always what you get. Amyloid 12:88-95.

Bitan G, Kirkitadze MD, Lomakin A, Vollers SS, Benedek GB, Teplow DB.2003.Amyloid beta -protein (Abeta) assembly: Abeta 40 and Abeta 42 oligomerize through distinct pathways. Proc Natl Acad Sci U S A 100:330-335.

Blasko I, Marx F, Steiner E, Hartmann T, Grubeck-Loebenstein B.1999.TNFalpha plus IFNgamma induce the production of Alzheimer beta-amyloid peptides and decrease the secretion of APPs. Faseb J 13:63-68.

Bolmont T, Haiss F, Eicke D, Radde R, Mathis CA, Klunk WE, Kohsaka S, Jucker M, Calhoun ME.2008.Dynamics of the microglial/amyloid interaction indicate a role in plaque maintenance. J Neurosci 28:4283-4292.

Bornemann KD, Wiederhold KH, Pauli C, Ermini F, Stalder M, Schnell L, Sommer B, Jucker M, Staufenbiel M.2001.Abeta-induced inflammatory processes in microglia cells of APP23 transgenic mice. Am J Pathol 158:63-73.

Braak H, Braak E.1991.Neuropathological stageing of Alzheimer-related changes. Acta Neuropathol 82:239-259.

Braak H, Braak E.1995.Staging of Alzheimer's disease-related neurofibrillary changes. Neurobiol Aging 16:271-278; discussion 278-284.

Bradt BM, Kolb WP, Cooper NR.1998.Complement-dependent proinflammatory properties of the Alzheimer's disease beta-peptide. J Exp Med 188:431-438.

Bramblett GT, Goedert M, Jakes R, Merrick SE, Trojanowski JQ, Lee VM.1993.Abnormal tau phosphorylation at Ser396 in Alzheimer's disease recapitulates development and contributes to reduced microtubule binding. Neuron 10:1089-1099.

Brandenburg LO, Konrad M, Wruck CJ, Koch T, Lucius R, Pufe T.2010.Functional and physical interactions between formyl-peptide-receptors and scavenger receptor MARCO and their involvement in amyloid beta 1-42-induced signal transduction in glial cells. J Neurochem 113:749-760.

Broersen K, Jonckheere W, Rozenski J, Vandersteen A, Pauwels K, Pastore A, Rousseau F, Schymkowitz J.2011.A standardized and biocompatible preparation of aggregate-free amyloid beta peptide for biophysical and biological studies of Alzheimer's disease. Protein Eng Des Sel 24:743-750.

Bruce AJ, Boling W, Kindy MS, Peschon J, Kraemer PJ, Carpenter MK, Holtsberg FW, Mattson MP.1996.Altered neuronal and microglial responses to excitotoxic and ischemic brain injury in mice lacking TNF receptors. Nat Med 2:788-794.

Bucciantini M, Giannoni E, Chiti F, Baroni F, Formigli L, Zurdo J, Taddei N, Ramponi G, Dobson CM, Stefani M.2002.Inherent toxicity of aggregates implies a common mechanism for protein misfolding diseases. Nature 416:507-511.

Buck M.1998.Trifluoroethanol and colleagues: cosolvents come of age. Recent studies with peptides and proteins. Q Rev Biophys 31:297-355.

Burdick D, Soreghan B, Kwon M, Kosmoski J, Knauer M, Henschen A, Yates J, Cotman C, Glabe C.1992.Assembly and aggregation properties of synthetic Alzheimer's A4/beta amyloid peptide analogs. J Biol Chem 267:546-554.

Bushong EA, Martone ME, Ellisman MH.2004.Maturation of astrocyte morphology and the establishment of astrocyte domains during postnatal hippocampal development. Int J Dev Neurosci 22:73-86.

Bushong EA, Martone ME, Jones YZ, Ellisman MH.2002.Protoplasmic astrocytes in CA1 stratum radiatum occupy separate anatomical domains. J Neurosci 22:183-192.

Buttini M, Yu GQ, Shockley K, Huang Y, Jones B, Masliah E, Mallory M, Yeo T, Longo FM, Mucke L.2002.Modulation of Alzheimer-like synaptic and cholinergic deficits in transgenic mice by human apolipoprotein E depends on isoform, aging, and overexpression of amyloid beta peptides but not on plaque formation. J Neurosci 22:10539-10548.

Cacquevel M, Lebeurrier N, Cheenne S, Vivien D.2004.Cytokines in neuroinflammation and Alzheimer's disease. Curr Drug Targets 5:529-534.

Cagnin A, Brooks DJ, Kennedy AM, Gunn RN, Myers R, Turkheimer FE, Jones T, Banati RB.2001.In-vivo measurement of activated microglia in dementia. Lancet 358:461-467.

Camacho IE, Serneels L, Spittaels K, Merchiers P, Dominguez D, De Strooper B.2004.Peroxisome-proliferator-activated receptor gamma induces a clearance mechanism for the amyloid-beta peptide. J Neurosci 24:10908-10917.

Cameron B, Landreth GE.2010.Inflammation, microglia, and Alzheimer's disease. Neurobiol Dis 37:503-509.

Canete M, Villanueva A, Juarranz A, Stockert JC.1987.A study of interaction of thioflavine T with DNA: evidence for intercalation. Cell Mol Biol 33:191-199.

Cardona AE, Pioro EP, Sasse ME, Kostenko V, Cardona SM, Dijkstra IM, Huang D, Kidd G, Dombrowski S, Dutta R, Lee JC, Cook DN, Jung S, Lira SA, Littman DR, Ransohoff RM.2006.Control of microglial neurotoxicity by the fractalkine receptor. Nat Neurosci 9:917-924.

Carrell RW, Lomas DA.1997.Conformational disease. Lancet 350:134-138.

Chapman MR, Robinson LS, Pinkner JS, Roth R, Heuser J, Hammar M, Normark S, Hultgren SJ.2002.Role of Escherichia coli curli operons in directing amyloid fiber formation. Science 295:851-855.

Chen G, Chen KS, Knox J, Inglis J, Bernard A, Martin SJ, Justice A, McConlogue L, Games D, Freedman SB, Morris RG.2000.A learning deficit related to age and beta-amyloid plaques in a mouse model of Alzheimer's disease. Nature 408:975-979.

Chen K, Iribarren P, Hu J, Chen J, Gong W, Cho EH, Lockett S, Dunlop NM, Wang JM.2006.Activation of Toll-like receptor 2 on microglia promotes cell uptake of Alzheimer disease-associated amyloid beta peptide. J Biol Chem 281:3651-3659.

Chen K, Iribarren P, Huang J, Zhang L, Gong W, Cho EH, Lockett S, Dunlop NM, Wang JM.2007.Induction of the formyl peptide receptor 2 in microglia by IFN-gamma and synergy with CD40 ligand. J Immunol 178:1759-1766.

Chiti F, Webster P, Taddei N, Clark A, Stefani M, Ramponi G, Dobson CM.1999.Designing conditions for in vitro formation of amyloid protofilaments and fibrils. Proc Natl Acad Sci U S A 96:3590-3594.

Chromy BA, Nowak RJ, Lambert MP, Viola KL, Chang L, Velasco PT, Jones BW, Fernandez SJ, Lacor PN, Horowitz P, Finch CE, Krafft GA, Klein WL.2003.Self-assembly of Abeta(1-42) into globular neurotoxins. Biochemistry 42:12749-12760.

Citron M, Vigo-Pelfrey C, Teplow DB, Miller C, Schenk D, Johnston J, Winblad B, Venizelos N, Lannfelt L, Selkoe DJ.1994.Excessive production of amyloid beta-protein by peripheral cells of symptomatic and presymptomatic patients carrying the Swedish familial Alzheimer disease mutation. Proc Natl Acad Sci U S A 91:11993-11997.

Cleary JP, Walsh DM, Hofmeister JJ, Shankar GM, Kuskowski MA, Selkoe DJ, Ashe KH.2005.Natural oligomers of the amyloid-beta protein specifically disrupt cognitive function. Nat Neurosci 8:79-84.

Colton CA, Wilcock DM.2010.Assessing activation states in microglia. CNS Neurol Disord Drug Targets 9:174-191.

Colton CA, Mott RT, Sharpe H, Xu Q, Van Nostrand WE, Vitek MP.2006.Expression profiles for macrophage alternative activation genes in AD and in mouse models of AD. J Neuroinflammation 3:27.

Combs CK, Karlo JC, Kao SC, Landreth GE.2001.beta-Amyloid stimulation of microglia and monocytes results in TNFalpha-dependent expression of inducible nitric oxide synthase and neuronal apoptosis. J Neurosci 21:1179-1188.

Combs CK, Johnson DE, Karlo JC, Cannady SB, Landreth GE.2000.Inflammatory mechanisms in Alzheimer's disease: inhibition of beta-amyloid-stimulated proinflammatory responses and neurotoxicity by PPARgamma agonists. J Neurosci 20:558-567.

Cooper CL, Jeohn GH, Tobias P, Hong JS.2002.Serum-dependence of LPS-induced neurotoxicity in rat cortical neurons. Ann N Y Acad Sci 962:306-317.

Coraci IS, Husemann J, Berman JW, Hulette C, Dufour JH, Campanella GK, Luster AD, Silverstein SC, El-Khoury JB.2002.CD36, a class B scavenger receptor, is expressed on microglia in Alzheimer's disease brains and can mediate production of reactive oxygen species in response to beta-amyloid fibrils. Am J Pathol 160:101-112.

Corder EH, Saunders AM, Strittmatter WJ, Schmechel DE, Gaskell PC, Small GW, Roses AD, Haines JL, Pericak-Vance MA.1993.Gene dose of apolipoprotein E type 4 allele and the risk of Alzheimer's disease in late onset families. Science 261:921-923.

Cotman CW, Tenner AJ, Cummings BJ.1996.beta-Amyloid converts an acute phase injury response to chronic injury responses. Neurobiol Aging 17:723-731.

Cui S, Xiong F, Hong Y, Jung JU, Li XS, Liu JZ, Yan R, Mei L, Feng X, Xiong WC.2011.APPswe/Abeta regulation of osteoclast activation and RAGE expression in an age-dependent manner. J Bone Miner Res 26:1084-1098.

Cui YH, Le Y, Zhang X, Gong W, Abe K, Sun R, Van Damme J, Proost P, Wang JM.2002.Up-regulation of FPR2, a chemotactic receptor for amyloid beta 1-42 (A beta 42), in murine microglial cells by TNF alpha. Neurobiol Dis 10:366-377.

Dahlgren KN, Manelli AM, Stine WB, Jr., Baker LK, Krafft GA, LaDu MJ.2002.Oligomeric and fibrillar species of amyloid-beta peptides differentially affect neuronal viability. J Biol Chem 277:32046-32053.

DaRocha-Souto B, Scotton TC, Coma M, Serrano-Pozo A, Hashimoto T, Sereno L, Rodriguez M, Sanchez B, Hyman BT, Gomez-Isla T.2011.Brain oligomeric beta-amyloid but not total amyloid plaque burden correlates with neuronal loss and astrocyte inflammatory response in amyloid precursor protein/tau transgenic mice. J Neuropathol Exp Neurol 70:360-376.

Daw EW, Payami H, Nemens EJ, Nochlin D, Bird TD, Schellenberg GD, Wijsman EM.2000.The number of trait loci in late-onset Alzheimer disease. Am J Hum Genet 66:196-204.

Dawson GR, Seabrook GR, Zheng H, Smith DW, Graham S, O'Dowd G, Bowery BJ, Boyce S, Trumbauer ME, Chen HY, Van der Ploeg LH, Sirinathsinghji DJ.1999.Age-related cognitive deficits, impaired long-term potentiation and reduction in synaptic marker density in mice lacking the beta-amyloid precursor protein. Neuroscience 90:1-13.

De Strooper B, Saftig P, Craessaerts K, Vanderstichele H, Guhde G, Annaert W, Von Figura K, Van Leuven F.1998.Deficiency of presenilin-1 inhibits the normal cleavage of amyloid precursor protein. Nature 391:387-390.

Deane R, Du Yan S, Submamaryan RK, LaRue B, Jovanovic S, Hogg E, Welch D, Manness L, Lin C, Yu J, Zhu H, Ghiso J, Frangione B, Stern A, Schmidt AM, Armstrong DL, Arnold B, Liliensiek B, Nawroth P, Hofman F, Kindy M, Stern D, Zlokovic B.2003.RAGE mediates amyloid-beta peptide transport across the blood-brain barrier and accumulation in brain. Nat Med 9:907-913.

Dickson DW.1997.The pathogenesis of senile plaques. J Neuropathol Exp Neurol 56:321-339.

Dickson DW, Lee SC, Mattiace LA, Yen SH, Brosnan C.1993.Microglia and cytokines in neurological disease, with special reference to AIDS and Alzheimer's disease. Glia 7:75-83.

Dickson DW, Farlo J, Davies P, Crystal H, Fuld P, Yen SH.1988.Alzheimer's disease. A double-labeling immunohistochemical study of senile plaques. Am J Pathol 132:86-101.

Dineley KT, Xia X, Bui D, Sweatt JD, Zheng H.2002.Accelerated plaque accumulation, associative learning deficits, and up-regulation of alpha 7 nicotinic receptor protein in transgenic mice co-expressing mutant human presenilin 1 and amyloid precursor proteins. J Biol Chem 277:22768-22780.

Dobson CM.2003.Protein folding and misfolding. Nature 426:884-890.

Duff K, Eckman C, Zehr C, Yu X, Prada CM, Perez-tur J, Hutton M, Buee L, Harigaya Y, Yager D, Morgan D, Gordon MN, Holcomb L, Refolo L, Zenk B, Hardy J, Younkin S.1996.Increased amyloid-beta42(43) in brains of mice expressing mutant presenilin 1. Nature 383:710-713.

Duyckaerts C, Potier MC, Delatour B.2008.Alzheimer disease models and human neuropathology: similarities and differences. Acta Neuropathol 115:5-38.

Eanes ED, Glenner GG.1968.X-ray diffraction studies on amyloid filaments. J Histochem Cytochem 16:673-677.

Edbauer D, Winkler E, Regula JT, Pesold B, Steiner H, Haass C.2003.Reconstitution of gamma-secretase activity. Nat Cell Biol 5:486-488.

Eddleston M, Mucke L.1993.Molecular profile of reactive astrocytes--implications for their role in neurologic disease. Neuroscience 54:15-36.

Edison P, Archer HA, Gerhard A, Hinz R, Pavese N, Turkheimer FE, Hammers A, Tai YF, Fox N, Kennedy A, Rossor M, Brooks DJ.2008.Microglia, amyloid, and cognition in Alzheimer's disease: An [11C](R)PK11195-PET and [11C]PIB-PET study. Neurobiol Dis 32:412-419.

Eikelenboom P, Stam FC.1982.Immunoglobulins and complement factors in senile plaques. An immunoperoxidase study. Acta Neuropathol 57:239-242.

Eikelenboom P, Veerhuis R, van Exel E, Hoozemans JJ, Rozemuller AJ, van Gool WA.2011.The early involvement of the innate immunity in the pathogenesis of late-onset Alzheimer's disease: neuropathological, epidemiological and genetic evidence. Curr Alzheimer Res 8:142-150.

El Khoury J, Hickman SE, Thomas CA, Cao L, Silverstein SC, Loike JD.1996.Scavenger receptor-mediated adhesion of microglia to beta-amyloid fibrils. Nature 382:716-719.

Esen N, Kielian T.2007.Effects of low dose GM-CSF on microglial inflammatory profiles to diverse pathogen-associated molecular patterns (PAMPs). J Neuroinflammation 4:10.

Espuny-Camacho I, Dominguez D, Merchiers P, Van Rompaey L, Selkoe D, De Strooper B.2010.Peroxisome proliferator-activated receptor gamma enhances the activity of an insulin degrading enzyme-like metalloprotease for amyloid-beta clearance. J Alzheimers Dis 20:1119-1132.

Evans KC, Berger EP, Cho CG, Weisgraber KH, Lansbury PT, Jr.1995.Apolipoprotein E is a kinetic but not a thermodynamic inhibitor of amyloid formation: implications for the pathogenesis and treatment of Alzheimer disease. Proc Natl Acad Sci U S A 92:763-767.

Fan R, Tenner AJ.2004.Complement C1q expression induced by Abeta in rat hippocampal organotypic slice cultures. Exp Neurol 185:241-253.

Fang F, Lue LF, Yan S, Xu H, Luddy JS, Chen D, Walker DG, Stern DM, Yan S, Schmidt AM, Chen JX, Yan SS.2010.RAGE-dependent signaling in microglia contributes to neuroinflammation, Abeta accumulation, and impaired learning/memory in a mouse model of Alzheimer's disease. Faseb J 24:1043-1055.

Fassbender K, Walter S, Kuhl S, Landmann R, Ishii K, Bertsch T, Stalder AK, Muehlhauser F, Liu Y, Ulmer AJ, Rivest S, Lentschat A, Gulbins E, Jucker M, Staufenbiel M, Brechtel K, Walter J, Multhaup G, Penke B, Adachi Y, Hartmann T, Beyreuther K.2004.The LPS receptor (CD14) links innate immunity with Alzheimer's disease. Faseb J 18:203-205.

Ferrero-Miliani L, Nielsen OH, Andersen PS, Girardin SE.2007.Chronic inflammation: importance of NOD2 and NALP3 in interleukin-1beta generation. Clin Exp Immunol 147:227-235.

Fields RD, Stevens-Graham B.2002.New insights into neuron-glia communication. Science 298:556-562.

Finch CE, Marchalonis JJ.1996.Evolutionary perspectives on amyloid and inflammatory features of Alzheimer disease. Neurobiol Aging 17:809-815.

Floden AM, Li S, Combs CK.2005.Beta-amyloid-stimulated microglia induce neuron death via synergistic stimulation of tumor necrosis factor alpha and NMDA receptors. J Neurosci 25:2566-2575.

Fonseca MI, Zhou J, Botto M, Tenner AJ.2004.Absence of C1q leads to less neuropathology in transgenic mouse models of Alzheimer's disease. J Neurosci 24:6457-6465.

Fonseca MI, Chu SH, Berci AM, Benoit ME, Peters DG, Kimura Y, Tenner AJ.2011.Contribution of complement activation pathways to neuropathology differs among mouse models of Alzheimer's disease. J Neuroinflammation 8:4.

Fowler DM, Koulov AV, Balch WE, Kelly JW.2007.Functional amyloid--from bacteria to humans. Trends Biochem Sci 32:217-224.

Fowler DM, Koulov AV, Alory-Jost C, Marks MS, Balch WE, Kelly JW.2006.Functional amyloid formation within mammalian tissue. PLoS Biol 4:e6.

Frank S, Burbach GJ, Bonin M, Walter M, Streit W, Bechmann I, Deller T.2008.TREM2 is upregulated in amyloid plaque-associated microglia in aged APP23 transgenic mice. Glia 56:1438-1447.

Frautschy SA, Yang F, Irrizarry M, Hyman B, Saido TC, Hsiao K, Cole GM.1998.Microglial response to amyloid plaques in APPsw transgenic mice. Am J Pathol 152:307-317.

Fukumoto H, Asami-Odaka A, Suzuki N, Iwatsubo T.1996.Association of A beta 40-positive senile plaques with microglial cells in the brains of patients with Alzheimer's disease and in non-demented aged individuals. Neurodegeneration 5:13-17.

Games D, Adams D, Alessandrini R, Barbour R, Berthelette P, Blackwell C, Carr T, Clemens J, Donaldson T, Gillespie F, et al.1995.Alzheimer-type neuropathology in transgenic mice overexpressing V717F beta-amyloid precursor protein. Nature 373:523-527.

Glabe C.2001.Intracellular mechanisms of amyloid accumulation and pathogenesis in Alzheimer's disease. J Mol Neurosci 17:137-145.

Glabe CG.2008.Structural classification of toxic amyloid oligomers. J Biol Chem 283:29639-29643.

Glenner GG, Wong CW.1984.Alzheimer's disease: initial report of the purification and characterization of a novel cerebrovascular amyloid protein. Biochem Biophys Res Commun 120:885-890.

Goate AM, Haynes AR, Owen MJ, Farrall M, James LA, Lai LY, Mullan MJ, Roques P, Rossor MN, Williamson R, et al.1989.Predisposing locus for Alzheimer's disease on chromosome 21. Lancet 1:352-355.

Gong Y, Chang L, Viola KL, Lacor PN, Lambert MP, Finch CE, Krafft GA, Klein WL.2003.Alzheimer's disease-affected brain: presence of oligomeric A beta ligands (ADDLs) suggests a molecular basis for reversible memory loss. Proc Natl Acad Sci U S A 100:10417-10422.

Gonzalez-Scarano F, Baltuch G.1999.Microglia as mediators of inflammatory and degenerative diseases. Annu Rev Neurosci 22:219-240.

Gorevic PD, Castano EM, Sarma R, Frangione B.1987.Ten to fourteen residue peptides of Alzheimer's disease protein are sufficient for amyloid fibril formation and its characteristic x-ray diffraction pattern. Biochem Biophys Res Commun 147:854-862.

Graeber MB.2010.Changing face of microglia. Science 330:783-788.

Graeber MB, Streit WJ.2010.Microglia: biology and pathology. Acta Neuropathol 119:89-105.

Grundke-Iqbal I, Iqbal K, Tung YC, Wang GP, Wisniewski HM.1985.Alzheimer paired helical filaments: cross-reacting polypeptide/s normally present in brain. Acta Neuropathol 66:52-61.

Grundke-Iqbal I, Iqbal K, Quinlan M, Tung YC, Zaidi MS, Wisniewski HM.1986.Microtubule-associated protein tau. A component of Alzheimer paired helical filaments. J Biol Chem 261:6084-6089.

Guillozet-Bongaarts AL, Glajch KE, Libson EG, Cahill ME, Bigio E, Berry RW, Binder LI.2007.Phosphorylation and cleavage of tau in non-AD tauopathies. Acta Neuropathol 113:513-520.

Guo Q, Wang Z, Li H, Wiese M, Zheng H.2011.APP physiological and pathophysiological functions: insights from animal models. Cell Res.

Haass C, Hung AY, Selkoe DJ, Teplow DB.1994.Mutations associated with a locus for familial Alzheimer's disease result in alternative processing of amyloid beta-protein precursor. J Biol Chem 269:17741-17748.

Halle A, Hornung V, Petzold GC, Stewart CR, Monks BG, Reinheckel T, Fitzgerald KA, Latz E, Moore KJ, Golenbock DT.2008.The NALP3 inflammasome is involved in the innate immune response to amyloid-beta. Nat Immunol 9:857-865.

Halverson K, Fraser PE, Kirschner DA, Lansbury PT, Jr.1990.Molecular determinants of amyloid deposition in Alzheimer's disease: conformational studies of synthetic beta-protein fragments. Biochemistry 29:2639-2644.

Hampel H, Shen Y, Walsh DM, Aisen P, Shaw LM, Zetterberg H, Trojanowski JQ, Blennow K.2010.Biological markers of amyloid beta-related mechanisms in Alzheimer's disease. Exp Neurol 223:334-346.

Hardy J, Selkoe DJ.2002.The amyloid hypothesis of Alzheimer's disease: progress and problems on the road to therapeutics. Science 297:353-356.

Hardy J, Duff K, Hardy KG, Perez-Tur J, Hutton M.1998.Genetic dissection of Alzheimer's disease and related dementias: amyloid and its relationship to tau. Nat Neurosci 1:355-358.

Hardy JA, Higgins GA.1992.Alzheimer's disease: the amyloid cascade hypothesis. Science 256:184-185.

Harper JD, Lansbury PT, Jr.1997.Models of amyloid seeding in Alzheimer's disease and scrapie: mechanistic truths and physiological consequences of the time-dependent solubility of amyloid proteins. Annu Rev Biochem 66:385-407.

Harper JD, Wong SS, Lieber CM, Lansbury PT.1997.Observation of metastable Abeta amyloid protofibrils by atomic force microscopy. Chem Biol 4:119-125.

Harper JD, Wong SS, Lieber CM, Lansbury PT, Jr.1999.Assembly of A beta amyloid protofibrils: an in vitro model for a possible early event in Alzheimer's disease. Biochemistry 38:8972-8980.

Harris-White ME, Chu T, Balverde Z, Sigel JJ, Flanders KC, Frautschy SA.1998.Effects of transforming growth factor-beta (isoforms 1-3) on amyloid-beta deposition, inflammation, and cell targeting in organotypic hippocampal slice cultures. J Neurosci 18:10366-10374.

Hartley DM, Zhao C, Speier AC, Woodard GA, Li S, Li Z, Walz T.2008.Transglutaminase induces protofibril-like amyloid beta-protein assemblies that are protease-resistant and inhibit long-term potentiation. J Biol Chem 283:16790-16800.

Hartley DM, Walsh DM, Ye CP, Diehl T, Vasquez S, Vassilev PM, Teplow DB, Selkoe DJ.1999.Protofibrillar intermediates of amyloid beta-protein induce acute electrophysiological changes and progressive neurotoxicity in cortical neurons. J Neurosci 19:8876-8884.

Haydon PG.2001.GLIA: listening and talking to the synapse. Nat Rev Neurosci 2:185-193.

Heber S, Herms J, Gajic V, Hainfellner J, Aguzzi A, Rulicke T, von Kretzschmar H, von Koch C, Sisodia S, Tremml P, Lipp HP, Wolfer DP, Muller U.2000.Mice with combined gene knock-outs reveal essential and partially redundant functions of amyloid precursor protein family members. J Neurosci 20:7951-7963.

Hendriks L, van Duijn CM, Cras P, Cruts M, Van Hul W, van Harskamp F, Warren A, McInnis MG, Antonarakis SE, Martin JJ, et al.1992.Presenile dementia and cerebral haemorrhage linked to a mutation at codon 692 of the beta-amyloid precursor protein gene. Nat Genet 1:218-221.

Heneka MT, Sastre M, Dumitrescu-Ozimek L, Hanke A, Dewachter I, Kuiperi C, O'Banion K, Klockgether T, Van Leuven F, Landreth GE.2005.Acute treatment with the PPARgamma agonist pioglitazone and ibuprofen reduces glial inflammation and Abeta1-42 levels in APPV717I transgenic mice. Brain 128:1442-1453.

Hepler RW, Grimm KM, Nahas DD, Breese R, Dodson EC, Acton P, Keller PM, Yeager M, Wang H, Shughrue P, Kinney G, Joyce JG.2006.Solution state characterization of amyloid beta-derived diffusible ligands. Biochemistry 45:15157-15167.

Herz J, Beffert U.2000.Apolipoprotein E receptors: linking brain development and Alzheimer's disease. Nat Rev Neurosci 1:51-58.

Heurtaux T, Michelucci A, Losciuto S, Gallotti C, Felten P, Dorban G, Grandbarbe L, Morga E, Heuschling P.2010.Microglial activation depends on beta-amyloid conformation: role of the formylpeptide receptor 2. J Neurochem 114:576-586.

Hilbich C, Kisters-Woike B, Reed J, Masters CL, Beyreuther K.1991.Aggregation and secondary structure of synthetic amyloid beta A4 peptides of Alzheimer's disease. J Mol Biol 218:149-163.

Holtzman DM, Fagan AM, Mackey B, Tenkova T, Sartorius L, Paul SM, Bales K, Ashe KH, Irizarry MC, Hyman BT.2000.Apolipoprotein E facilitates neuritic and cerebrovascular plaque formation in an Alzheimer's disease model. Ann Neurol 47:739-747.

Hsiao K, Chapman P, Nilsen S, Eckman C, Harigaya Y, Younkin S, Yang F, Cole G.1996.Correlative memory deficits, Abeta elevation, and amyloid plaques in transgenic mice. Science 274:99-102.

Huang Y.2011.Roles of apolipoprotein E4 (ApoE4) in the pathogenesis of Alzheimer's disease: lessons from ApoE mouse models. Biochem Soc Trans 39:924-932.

Huang Y, Liu XQ, Wyss-Coray T, Brecht WJ, Sanan DA, Mahley RW.2001.Apolipoprotein E fragments present in Alzheimer's disease brains induce neurofibrillary tangle-like intracellular inclusions in neurons. Proc Natl Acad Sci U S A 98:8838-8843.

Husemann J, Loike JD, Anankov R, Febbraio M, Silverstein SC.2002.Scavenger receptors in neurobiology and neuropathology: their role on microglia and other cells of the nervous system. Glia 40:195-205.

Hyman BT.2011.Amyloid-dependent and amyloid-independent stages of Alzheimer disease. Arch Neurol 68:1062-1064.

Ingelsson M, Fukumoto H, Newell KL, Growdon JH, Hedley-Whyte ET, Frosch MP, Albert MS, Hyman BT, Irizarry MC.2004.Early Abeta accumulation and progressive synaptic loss, gliosis, and tangle formation in AD brain. Neurology 62:925-931.

Ishii T, Haga S.1984.Immuno-electron-microscopic localization of complements in amyloid fibrils of senile plaques. Acta Neuropathol 63:296-300.

Itagaki S, McGeer PL, Akiyama H, Zhu S, Selkoe D.1989.Relationship of microglia and astrocytes to amyloid deposits of Alzheimer disease. J Neuroimmunol 24:173-182.

Iwata-Ichikawa E, Kondo Y, Miyazaki I, Asanuma M, Ogawa N.1999.Glial cells protect neurons against oxidative stress via transcriptional up-regulation of the glutathione synthesis. J Neurochem 72:2334-2344.

Iwatsubo T, Odaka A, Suzuki N, Mizusawa H, Nukina N, Ihara Y.1994.Visualization of A beta 42(43) and A beta 40 in senile plaques with end-specific A beta monoclonals: evidence that an initially deposited species is A beta 42(43). Neuron 13:45-53.

Jacobsen JS, Wu CC, Redwine JM, Comery TA, Arias R, Bowlby M, Martone R, Morrison JH, Pangalos MN, Reinhart PH, Bloom FE.2006.Early-onset behavioral and synaptic deficits in a mouse model of Alzheimer's disease. Proc Natl Acad Sci U S A 103:5161-5166.

Jan A, Hartley DM, Lashuel HA.2010.Preparation and characterization of toxic Abeta aggregates for structural and functional studies in Alzheimer's disease research. Nat Protoc 5:1186-1209.

Jana M, Palencia CA, Pahan K.2008.Fibrillar amyloid-beta peptides activate microglia via TLR2: implications for Alzheimer's disease. J Immunol 181:7254-7262.

Janus C, Pearson J, McLaurin J, Mathews PM, Jiang Y, Schmidt SD, Chishti MA, Horne P, Heslin D, French J, Mount HT, Nixon RA, Mercken M, Bergeron C, Fraser PE, St George-Hyslop P, Westaway D.2000.A beta peptide immunization reduces

behavioural impairment and plaques in a model of Alzheimer's disease. Nature 408:979-982.

Jarrett JT, Lansbury PT, Jr.1992.Amyloid fibril formation requires a chemically discriminating nucleation event: studies of an amyloidogenic sequence from the bacterial protein OsmB. Biochemistry 31:12345-12352.

Jarrett JT, Berger EP, Lansbury PT, Jr.1993.The carboxy terminus of the beta amyloid protein is critical for the seeding of amyloid formation: implications for the pathogenesis of Alzheimer's disease. Biochemistry 32:4693-4697.

Jimenez S, Baglietto-Vargas D, Caballero C, Moreno-Gonzalez I, Torres M, Sanchez-Varo R, Ruano D, Vizuete M, Gutierrez A, Vitorica J.2008.Inflammatory response in the hippocampus of PS1M146L/APP751SL mouse model of Alzheimer's disease: age-dependent switch in the microglial phenotype from alternative to classic. J Neurosci 28:11650-11661.

Johnstone M, Gearing AJ, Miller KM.1999.A central role for astrocytes in the inflammatory response to beta-amyloid; chemokines, cytokines and reactive oxygen species are produced. J Neuroimmunol 93:182-193.

Kang J, Lemaire HG, Unterbeck A, Salbaum JM, Masters CL, Grzeschik KH, Multhaup G, Beyreuther K, Muller-Hill B.1987.The precursor of Alzheimer's disease amyloid A4 protein resembles a cell-surface receptor. Nature 325:733-736.

Kayed R, Head E, Thompson JL, McIntire TM, Milton SC, Cotman CW, Glabe CG.2003.Common structure of soluble amyloid oligomers implies common mechanism of pathogenesis. Science 300:486-489.

Kayed R, Pensalfini A, Margol L, Sokolov Y, Sarsoza F, Head E, Hall J, Glabe C.2009.Annular protofibrils are a structurally and functionally distinct type of amyloid oligomer. J Biol Chem 284:4230-4237.

Kayed R, Head E, Sarsoza F, Saing T, Cotman CW, Necula M, Margol L, Wu J, Breydo L, Thompson JL, Rasool S, Gurlo T, Butler P, Glabe CG.2007.Fibril specific, conformation dependent antibodies recognize a generic epitope common to amyloid fibrils and fibrillar oligomers that is absent in prefibrillar oligomers. Mol Neurodegener 2:18.

Kheterpal I, Chen M, Cook KD, Wetzel R.2006.Structural differences in Abeta amyloid protofibrils and fibrils mapped by hydrogen exchange--mass spectrometry with on-line proteolytic fragmentation. J Mol Biol 361:785-795.

Kheterpal I, Lashuel HA, Hartley DM, Walz T, Lansbury PT, Jr., Wetzel R.2003.Abeta protofibrils possess a stable core structure resistant to hydrogen exchange. Biochemistry 42:14092-14098.

Khurana R, Coleman C, Ionescu-Zanetti C, Carter SA, Krishna V, Grover RK, Roy R, Singh S.2005.Mechanism of thioflavin T binding to amyloid fibrils. J Struct Biol 151:229-238.

Kielian T.2006.Toll-like receptors in central nervous system glial inflammation and homeostasis. J Neurosci Res 83:711-730.

Kirschner DA, Inouye H, Duffy LK, Sinclair A, Lind M, Selkoe DJ.1987.Synthetic peptide homologous to beta protein from Alzheimer disease forms amyloid-like fibrils in vitro. Proc Natl Acad Sci U S A 84:6953-6957.

Klegeris A, McGeer PL.2001.Inflammatory cytokine levels are influenced by interactions between THP-1 monocytic, U-373 MG astrocytic, and SH-SY5Y neuronal cell lines of human origin. Neurosci Lett 313:41-44.

Klesney-Tait J, Turnbull IR, Colonna M.2006.The TREM receptor family and signal integration. Nat Immunol 7:1266-1273.

Koenigsknecht-Talboo J, Landreth GE.2005.Microglial phagocytosis induced by fibrillar beta-amyloid and IgGs are differentially regulated by proinflammatory cytokines. J Neurosci 25:8240-8249.

Koffie RM, Hyman BT, Spires-Jones TL.2011.Alzheimer's disease: synapses gone cold. Mol Neurodegener 6:63.

Koffie RM, Meyer-Luehmann M, Hashimoto T, Adams KW, Mielke ML, Garcia-Alloza M, Micheva KD, Smith SJ, Kim ML, Lee VM, Hyman BT, Spires-Jones TL.2009.Oligomeric amyloid beta associates with postsynaptic densities and correlates with excitatory synapse loss near senile plaques. Proc Natl Acad Sci U S A 106:4012-4017.

Kokubo H, Kayed R, Glabe CG, Staufenbiel M, Saido TC, Iwata N, Yamaguchi H.2009.Amyloid Beta annular protofibrils in cell processes and synapses accumulate with aging and Alzheimer-associated genetic modification. Int J Alzheimers Dis 2009.

Kowalska A.2004.Genetic basis of neurodegeneration in familial Alzheimer's disease. Pol J Pharmacol 56:171-178.

Kyle RA.2001.Amyloidosis: a convoluted story. Br J Haematol 114:529-538.

Lacor PN, Buniel MC, Chang L, Fernandez SJ, Gong Y, Viola KL, Lambert MP, Velasco
    PT, Bigio EH, Finch CE, Krafft GA, Klein WL.2004.Synaptic targeting by
    Alzheimer's-related amyloid beta oligomers. J Neurosci 24:10191-10200.

LaDu MJ, Falduto MT, Manelli AM, Reardon CA, Getz GS, Frail DE.1994.Isoform-
    specific binding of apolipoprotein E to beta-amyloid. J Biol Chem 269:23403-
    23406.

LaFerla FM, Green KN, Oddo S.2007.Intracellular amyloid-beta in Alzheimer's disease.
    Nat Rev Neurosci 8:499-509.

Lambert MP, Barlow AK, Chromy BA, Edwards C, Freed R, Liosatos M, Morgan TE,
    Rozovsky I, Trommer B, Viola KL, Wals P, Zhang C, Finch CE, Krafft GA,
    Klein WL.1998.Diffusible, nonfibrillar ligands derived from Abeta1-42 are potent
    central nervous system neurotoxins. Proc Natl Acad Sci U S A 95:6448-6453.

Landreth G, Jiang Q, Mandrekar S, Heneka M.2008.PPARgamma agonists as
    therapeutics for the treatment of Alzheimer's disease. Neurotherapeutics 5:481-
    489.

Lansbury PT, Jr., Costa PR, Griffiths JM, Simon EJ, Auger M, Halverson KJ, Kocisko
    DA, Hendsch ZS, Ashburn TT, Spencer RG, et al.1995.Structural model for the
    beta-amyloid fibril based on interstrand alignment of an antiparallel-sheet
    comprising a C-terminal peptide. Nat Struct Biol 2:990-998.

Lasagna-Reeves CA, Kayed R.2011.Astrocytes contain amyloid-beta annular protofibrils
    in Alzheimer's disease brains. FEBS Lett 585:3052-3057.

Lasagna-Reeves CA, Glabe CG, Kayed R.2011.Amyloid-beta annular protofibrils evade
    fibrillar fate in Alzheimer disease brain. J Biol Chem 286:22122-22130.

Lashuel HA, Hartley D, Petre BM, Walz T, Lansbury PT, Jr.2002.Neurodegenerative
    disease: amyloid pores from pathogenic mutations. Nature 418:291.

Lashuel HA, Hartley DM, Petre BM, Wall JS, Simon MN, Walz T, Lansbury PT,
    Jr.2003.Mixtures of wild-type and a pathogenic (E22G) form of Abeta40 in vitro
    accumulate protofibrils, including amyloid pores. J Mol Biol 332:795-808.

Lazarov O, Morfini GA, Pigino G, Gadadhar A, Chen X, Robinson J, Ho H, Brady ST,
    Sisodia SS.2007.Impairments in fast axonal transport and motor neuron deficits in

transgenic mice expressing familial Alzheimer's disease-linked mutant presenilin 1. J Neurosci 27:7011-7020.

Le Y, Gong W, Tiffany HL, Tumanov A, Nedospasov S, Shen W, Dunlop NM, Gao JL, Murphy PM, Oppenheim JJ, Wang JM.2001.Amyloid (beta)42 activates a G-protein-coupled chemoattractant receptor, FPR-like-1. J Neurosci 21:RC123.

Lehnardt S, Massillon L, Follett P, Jensen FE, Ratan R, Rosenberg PA, Volpe JJ, Vartanian T.2003.Activation of innate immunity in the CNS triggers neurodegeneration through a Toll-like receptor 4-dependent pathway. Proc Natl Acad Sci U S A 100:8514-8519.

Lemere CA, Blusztajn JK, Yamaguchi H, Wisniewski T, Saido TC, Selkoe DJ.1996.Sequence of deposition of heterogeneous amyloid beta-peptides and APO E in Down syndrome: implications for initial events in amyloid plaque formation. Neurobiol Dis 3:16-32.

Lesne S, Koh MT, Kotilinek L, Kayed R, Glabe CG, Yang A, Gallagher M, Ashe KH.2006.A specific amyloid-beta protein assembly in the brain impairs memory. Nature 440:352-357.

LeVine H, 3rd.1993.Thioflavine T interaction with synthetic Alzheimer's disease beta-amyloid peptides: detection of amyloid aggregation in solution. Protein Sci 2:404-410.

Levy E, Carman MD, Fernandez-Madrid IJ, Power MD, Lieberburg I, van Duinen SG, Bots GT, Luyendijk W, Frangione B.1990.Mutation of the Alzheimer's disease amyloid gene in hereditary cerebral hemorrhage, Dutch type. Science 248:1124-1126.

Lewis J, Dickson DW, Lin WL, Chisholm L, Corral A, Jones G, Yen SH, Sahara N, Skipper L, Yager D, Eckman C, Hardy J, Hutton M, McGowan E.2001.Enhanced neurofibrillary degeneration in transgenic mice expressing mutant tau and APP. Science 293:1487-1491.

Li H, Wolfe MS, Selkoe DJ.2009a.Toward structural elucidation of the gamma-secretase complex. Structure 17:326-334.

Li M, Shang DS, Zhao WD, Tian L, Li B, Fang WG, Zhu L, Man SM, Chen YH.2009b.Amyloid beta interaction with receptor for advanced glycation end products up-regulates brain endothelial CCR5 expression and promotes T cells crossing the blood-brain barrier. J Immunol 182:5778-5788.

Liu S, Liu Y, Hao W, Wolf L, Kiliaan AJ, Penke B, Rube CE, Walter J, Heneka MT, Hartmann T, Menger MD, Fassbender K.2011.TLR2 Is a Primary Receptor for Alzheimer's Amyloid beta Peptide To Trigger Neuroinflammatory Activation. J Immunol.

Lomakin A, Teplow DB, Kirschner DA, Benedek GB.1997.Kinetic theory of fibrillogenesis of amyloid beta-protein. Proc Natl Acad Sci U S A 94:7942-7947.

Lomakin A, Chung DS, Benedek GB, Kirschner DA, Teplow DB.1996.On the nucleation and growth of amyloid beta-protein fibrils: detection of nuclei and quantitation of rate constants. Proc Natl Acad Sci U S A 93:1125-1129.

Lord A, Englund H, Soderberg L, Tucker S, Clausen F, Hillered L, Gordon M, Morgan D, Lannfelt L, Pettersson FE, Nilsson LN.2009.Amyloid-beta protofibril levels correlate with spatial learning in Arctic Alzheimer's disease transgenic mice. Febs J 276:995-1006.

Lorenzo A, Yankner BA.1994.Beta-amyloid neurotoxicity requires fibril formation and is inhibited by congo red. Proc Natl Acad Sci U S A 91:12243-12247.

Lorton D.1997.beta-Amyloid-induced IL-1 beta release from an activated human monocyte cell line is calcium- and G-protein-dependent. Mech Ageing Dev 94:199-211.

Lotz M, Ebert S, Esselmann H, Iliev AI, Prinz M, Wiazewicz N, Wiltfang J, Gerber J, Nau R.2005.Amyloid beta peptide 1-40 enhances the action of Toll-like receptor-2 and -4 agonists but antagonizes Toll-like receptor-9-induced inflammation in primary mouse microglial cell cultures. J Neurochem 94:289-298.

Lue LF, Walker DG, Brachova L, Beach TG, Rogers J, Schmidt AM, Stern DM, Yan SD.2001.Involvement of microglial receptor for advanced glycation endproducts (RAGE) in Alzheimer's disease: identification of a cellular activation mechanism. Exp Neurol 171:29-45.

Lue LF, Kuo YM, Roher AE, Brachova L, Shen Y, Sue L, Beach T, Kurth JH, Rydel RE, Rogers J.1999.Soluble amyloid beta peptide concentration as a predictor of synaptic change in Alzheimer's disease. Am J Pathol 155:853-862.

Luterman JD, Haroutunian V, Yemul S, Ho L, Purohit D, Aisen PS, Mohs R, Pasinetti GM.2000.Cytokine gene expression as a function of the clinical progression of Alzheimer disease dementia. Arch Neurol 57:1153-1160.

Mackenzie IR.2000.Anti-inflammatory drugs and Alzheimer-type pathology in aging. Neurology 54:732-734.

Mackenzie IR, Hao C, Munoz DG.1995.Role of microglia in senile plaque formation. Neurobiol Aging 16:797-804.

Maeda S, Sahara N, Saito Y, Murayama S, Ikai A, Takashima A.2006.Increased levels of granular tau oligomers: an early sign of brain aging and Alzheimer's disease. Neurosci Res 54:197-201.

Maeda S, Sahara N, Saito Y, Murayama M, Yoshiike Y, Kim H, Miyasaka T, Murayama S, Ikai A, Takashima A.2007.Granular tau oligomers as intermediates of tau filaments. Biochemistry 46:3856-3861.

Mahley RW.1988.Apolipoprotein E: cholesterol transport protein with expanding role in cell biology. Science 240:622-630.

Malm TM, Koistinaho M, Parepalo M, Vatanen T, Ooka A, Karlsson S, Koistinaho J.2005.Bone-marrow-derived cells contribute to the recruitment of microglial cells in response to beta-amyloid deposition in APP/PS1 double transgenic Alzheimer mice. Neurobiol Dis 18:134-142.

Martinez FO, Helming L, Gordon S.2009.Alternative activation of macrophages: an immunologic functional perspective. Annu Rev Immunol 27:451-483.

Martins IC, Kuperstein I, Wilkinson H, Maes E, Vanbrabant M, Jonckheere W, Van Gelder P, Hartmann D, D'Hooge R, De Strooper B, Schymkowitz J, Rousseau F.2008.Lipids revert inert Abeta amyloid fibrils to neurotoxic protofibrils that affect learning in mice. Embo J 27:224-233.

Masliah E, Sisk A, Mallory M, Mucke L, Schenk D, Games D.1996.Comparison of neurodegenerative pathology in transgenic mice overexpressing V717F beta-amyloid precursor protein and Alzheimer's disease. J Neurosci 16:5795-5811.

Masters CL, Simms G, Weinman NA, Multhaup G, McDonald BL, Beyreuther K.1985a.Amyloid plaque core protein in Alzheimer disease and Down syndrome. Proc Natl Acad Sci U S A 82:4245-4249.

Masters CL, Multhaup G, Simms G, Pottgiesser J, Martins RN, Beyreuther K.1985b.Neuronal origin of a cerebral amyloid: neurofibrillary tangles of Alzheimer's disease contain the same protein as the amyloid of plaque cores and blood vessels. Embo J 4:2757-2763.

Masters SL, O'Neill LA.2011.Disease-associated amyloid and misfolded protein aggregates activate the inflammasome. Trends Mol Med 17:276-282.

Mattson MP, Rychlik B.1990.Glia protect hippocampal neurons against excitatory amino acid-induced degeneration: involvement of fibroblast growth factor. Int J Dev Neurosci 8:399-415.

Mattson MP, Tomaselli KJ, Rydel RE.1993.Calcium-destabilizing and neurodegenerative effects of aggregated beta-amyloid peptide are attenuated by basic FGF. Brain Res 621:35-49.

Mattson MP, Gary DS, Chan SL, Duan W.2001.Perturbed endoplasmic reticulum function, synaptic apoptosis and the pathogenesis of Alzheimer's disease. Biochem Soc Symp:151-162.

Mattson MP, Cheng B, Davis D, Bryant K, Lieberburg I, Rydel RE.1992.beta-Amyloid peptides destabilize calcium homeostasis and render human cortical neurons vulnerable to excitotoxicity. J Neurosci 12:376-389.

Mayeux R, Tang MX, Jacobs DM, Manly J, Bell K, Merchant C, Small SA, Stern Y, Wisniewski HM, Mehta PD.1999.Plasma amyloid beta-peptide 1-42 and incipient Alzheimer's disease. Ann Neurol 46:412-416.

McDonald DR, Brunden KR, Landreth GE.1997.Amyloid fibrils activate tyrosine kinase-dependent signaling and superoxide production in microglia. J Neurosci 17:2284-2294.

McGeer EG, McGeer PL.1998.The importance of inflammatory mechanisms in Alzheimer disease. Exp Gerontol 33:371-378.

McGeer PL, McGeer EG.2007.NSAIDs and Alzheimer disease: epidemiological, animal model and clinical studies. Neurobiol Aging 28:639-647.

McGeer PL, Schulzer M, McGeer EG.1996.Arthritis and anti-inflammatory agents as possible protective factors for Alzheimer's disease: a review of 17 epidemiologic studies. Neurology 47:425-432.

McKenna MC.2007.The glutamate-glutamine cycle is not stoichiometric: fates of glutamate in brain. J Neurosci Res 85:3347-3358.

Meda L, Cassatella MA, Szendrei GI, Otvos L, Jr., Baron P, Villalba M, Ferrari D, Rossi F.1995.Activation of microglial cells by beta-amyloid protein and interferon-gamma. Nature 374:647-650.

Medeiros R, Prediger RD, Passos GF, Pandolfo P, Duarte FS, Franco JL, Dafre AL, Di
Giunta G, Figueiredo CP, Takahashi RN, Campos MM, Calixto
JB.2007.Connecting TNF-alpha signaling pathways to iNOS expression in a
mouse model of Alzheimer's disease: relevance for the behavioral and synaptic
deficits induced by amyloid beta protein. J Neurosci 27:5394-5404.

Meyer-Luehmann M, Spires-Jones TL, Prada C, Garcia-Alloza M, de Calignon A,
Rozkalne A, Koenigsknecht-Talboo J, Holtzman DM, Bacskai BJ, Hyman
BT.2008.Rapid appearance and local toxicity of amyloid-beta plaques in a mouse
model of Alzheimer's disease. Nature 451:720-724.

Moechars D, Lorent K, Van Leuven F.1999.Premature death in transgenic mice that
overexpress a mutant amyloid precursor protein is preceded by severe
neurodegeneration and apoptosis. Neuroscience 91:819-830.

Moore KJ, El Khoury J, Medeiros LA, Terada K, Geula C, Luster AD, Freeman
MW.2002.A CD36-initiated signaling cascade mediates inflammatory effects of
beta-amyloid. J Biol Chem 277:47373-47379.

Morris JC, Roe CM, Grant EA, Head D, Storandt M, Goate AM, Fagan AM, Holtzman
DM, Mintun MA.2009.Pittsburgh compound B imaging and prediction of
progression from cognitive normality to symptomatic Alzheimer disease. Arch
Neurol 66:1469-1475.

Mucke L, Masliah E, Yu GQ, Mallory M, Rockenstein EM, Tatsuno G, Hu K,
Kholodenko D, Johnson-Wood K, McConlogue L.2000.High-level neuronal
expression of abeta 1-42 in wild-type human amyloid protein precursor transgenic
mice: synaptotoxicity without plaque formation. J Neurosci 20:4050-4058.

Mullan M, Crawford F, Axelman K, Houlden H, Lilius L, Winblad B, Lannfelt L.1992.A
pathogenic mutation for probable Alzheimer's disease in the APP gene at the N-
terminus of beta-amyloid. Nat Genet 1:345-347.

Nagele RG, Wegiel J, Venkataraman V, Imaki H, Wang KC, Wegiel J.2004.Contribution
of glial cells to the development of amyloid plaques in Alzheimer's disease.
Neurobiol Aging 25:663-674.

Naslund J, Haroutunian V, Mohs R, Davis KL, Davies P, Greengard P, Buxbaum
JD.2000.Correlation between elevated levels of amyloid beta-peptide in the brain
and cognitive decline. Jama 283:1571-1577.

Nichols MR, Moss MA, Reed DK, Cratic-McDaniel S, Hoh JH, Rosenberry
TL.2005.Amyloid-beta protofibrils differ from amyloid-beta aggregates induced

in dilute hexafluoroisopropanol in stability and morphology. J Biol Chem 280:2471-2480.

Nichols MR, Moss MA, Reed DK, Lin WL, Mukhopadhyay R, Hoh JH, Rosenberry TL.2002.Growth of beta-amyloid(1-40) protofibrils by monomer elongation and lateral association. Characterization of distinct products by light scattering and atomic force microscopy. Biochemistry 41:6115-6127.

Nilsberth C, Westlind-Danielsson A, Eckman CB, Condron MM, Axelman K, Forsell C, Stenh C, Luthman J, Teplow DB, Younkin SG, Naslund J, Lannfelt L.2001.The 'Arctic' APP mutation (E693G) causes Alzheimer's disease by enhanced Abeta protofibril formation. Nat Neurosci 4:887-893.

Nimmerjahn A, Kirchhoff F, Helmchen F.2005.Resting microglial cells are highly dynamic surveillants of brain parenchyma in vivo. Science 308:1314-1318.

O'Nuallain B, Freir DB, Nicoll AJ, Risse E, Ferguson N, Herron CE, Collinge J, Walsh DM.2010.Amyloid beta-protein dimers rapidly form stable synaptotoxic protofibrils. J Neurosci 30:14411-14419.

Oda T, Wals P, Osterburg HH, Johnson SA, Pasinetti GM, Morgan TE, Rozovsky I, Stine WB, Snyder SW, Holzman TF, et al.1995.Clusterin (apoJ) alters the aggregation of amyloid beta-peptide (A beta 1-42) and forms slowly sedimenting A beta complexes that cause oxidative stress. Exp Neurol 136:22-31.

Paresce DM, Ghosh RN, Maxfield FR.1996.Microglial cells internalize aggregates of the Alzheimer's disease amyloid beta-protein via a scavenger receptor. Neuron 17:553-565.

Parvathy S, Rajadas J, Ryan H, Vaziri S, Anderson L, Murphy GM, Jr.2009.Abeta peptide conformation determines uptake and interleukin-1alpha expression by primary microglial cells. Neurobiol Aging 30:1792-1804.

Perea G, Navarrete M, Araque A.2009.Tripartite synapses: astrocytes process and control synaptic information. Trends Neurosci 32:421-431.

Perlmutter LS, Barron E, Chui HC.1990.Morphologic association between microglia and senile plaque amyloid in Alzheimer's disease. Neurosci Lett 119:32-36.

Perry RT, Collins JS, Wiener H, Acton R, Go RC.2001.The role of TNF and its receptors in Alzheimer's disease. Neurobiol Aging 22:873-883.

Perry VH, Nicoll JA, Holmes C.2010.Microglia in neurodegenerative disease. Nat Rev Neurol 6:193-201.

Petkova AT, Buntkowsky G, Dyda F, Leapman RD, Yau WM, Tycko R.2004.Solid state NMR reveals a pH-dependent antiparallel beta-sheet registry in fibrils formed by a beta-amyloid peptide. J Mol Biol 335:247-260.

Petkova AT, Leapman RD, Guo Z, Yau WM, Mattson MP, Tycko R.2005.Self-propagating, molecular-level polymorphism in Alzheimer's beta-amyloid fibrils. Science 307:262-265.

Petkova AT, Ishii Y, Balbach JJ, Antzutkin ON, Leapman RD, Delaglio F, Tycko R.2002.A structural model for Alzheimer's beta -amyloid fibrils based on experimental constraints from solid state NMR. Proc Natl Acad Sci U S A 99:16742-16747.

Phinney AL, Calhoun ME, Wolfer DP, Lipp HP, Zheng H, Jucker M.1999.No hippocampal neuron or synaptic bouton loss in learning-impaired aged beta-amyloid precursor protein-null mice. Neuroscience 90:1207-1216.

Pike CJ, Burdick D, Walencewicz AJ, Glabe CG, Cotman CW.1993.Neurodegeneration induced by beta-amyloid peptides in vitro: the role of peptide assembly state. J Neurosci 13:1676-1687.

Podlisny MB, Ostaszewski BL, Squazzo SL, Koo EH, Rydell RE, Teplow DB, Selkoe DJ.1995.Aggregation of secreted amyloid beta-protein into sodium dodecyl sulfate-stable oligomers in cell culture. J Biol Chem 270:9564-9570.

Podlisny MB, Walsh DM, Amarante P, Ostaszewski BL, Stimson ER, Maggio JE, Teplow DB, Selkoe DJ.1998.Oligomerization of endogenous and synthetic amyloid beta-protein at nanomolar levels in cell culture and stabilization of monomer by Congo red. Biochemistry 37:3602-3611.

Potter H, Nelson RB, Das S, Siman R, Kayyali US, Dressler D.1992.The involvement of proteases, protease inhibitors, and an acute phase response in Alzheimer's disease. Ann N Y Acad Sci 674:161-173.

Qiao X, Cummins DJ, Paul SM.2001.Neuroinflammation-induced acceleration of amyloid deposition in the APPV717F transgenic mouse. Eur J Neurosci 14:474-482.

Raber J, Wong D, Yu GQ, Buttini M, Mahley RW, Pitas RE, Mucke L.2000.Apolipoprotein E and cognitive performance. Nature 404:352-354.

Rahimi F, Shanmugam A, Bitan G.2008.Structure-function relationships of pre-fibrillar
protein assemblies in Alzheimer's disease and related disorders. Curr Alzheimer
Res 5:319-341.

Rapoport M, Dawson HN, Binder LI, Vitek MP, Ferreira A.2002.Tau is essential to beta -
amyloid-induced neurotoxicity. Proc Natl Acad Sci U S A 99:6364-6369.

Reed-Geaghan EG, Savage JC, Hise AG, Landreth GE.2009.CD14 and toll-like receptors
2 and 4 are required for fibrillar A{beta}-stimulated microglial activation. J
Neurosci 29:11982-11992.

Reed-Geaghan EG, Reed QW, Cramer PE, Landreth GE.2010.Deletion of CD14
attenuates Alzheimer's disease pathology by influencing the brain's inflammatory
milieu. J Neurosci 30:15369-15373.

Reed MN, Hofmeister JJ, Jungbauer L, Welzel AT, Yu C, Sherman MA, Lesne S, LaDu
MJ, Walsh DM, Ashe KH, Cleary JP.2011.Cognitive effects of cell-derived and
synthetically derived Abeta oligomers. Neurobiol Aging 32:1784-1794.

Rentz DM, Locascio JJ, Becker JA, Moran EK, Eng E, Buckner RL, Sperling RA,
Johnson KA.2010.Cognition, reserve, and amyloid deposition in normal aging.
Ann Neurol 67:353-364.

Rogers J, Webster S, Lue LF, Brachova L, Civin WH, Emmerling M, Shivers B, Walker
D, McGeer P.1996.Inflammation and Alzheimer's disease pathogenesis.
Neurobiol Aging 17:681-686.

Rogers J, Cooper NR, Webster S, Schultz J, McGeer PL, Styren SD, Civin WH,
Brachova L, Bradt B, Ward P, et al.1992.Complement activation by beta-amyloid
in Alzheimer disease. Proc Natl Acad Sci U S A 89:10016-10020.

Rogers JT, Leiter LM, McPhee J, Cahill CM, Zhan SS, Potter H, Nilsson
LN.1999.Translation of the alzheimer amyloid precursor protein mRNA is up-
regulated by interleukin-1 through 5'-untranslated region sequences. J Biol Chem
274:6421-6431.

Salminen A, Ojala J, Kauppinen A, Kaarniranta K, Suuronen T.2009.Inflammation in
Alzheimer's disease: amyloid-beta oligomers trigger innate immunity defence via
pattern recognition receptors. Prog Neurobiol 87:181-194.

Sanchez MP, Alvarez-Tallada V, Avila J.2001.[The microtubule-associated protein tau in
neurodegenerative diseases. Tauopathies]. Rev Neurol 33:169-177.

Sasaki A, Yamaguchi H, Ogawa A, Sugihara S, Nakazato Y.1997.Microglial activation in early stages of amyloid beta protein deposition. Acta Neuropathol 94:316-322.

Saunders AM, Schmader K, Breitner JC, Benson MD, Brown WT, Goldfarb L, Goldgaber D, Manwaring MG, Szymanski MH, McCown N, et al.1993.Apolipoprotein E epsilon 4 allele distributions in late-onset Alzheimer's disease and in other amyloid-forming diseases. Lancet 342:710-711.

Schenk D, Barbour R, Dunn W, Gordon G, Grajeda H, Guido T, Hu K, Huang J, Johnson-Wood K, Khan K, Kholodenko D, Lee M, Liao Z, Lieberburg I, Motter R, Mutter L, Soriano F, Shopp G, Vasquez N, Vandevert C, Walker S, Wogulis M, Yednock T, Games D, Seubert P.1999.Immunization with amyloid-beta attenuates Alzheimer-disease-like pathology in the PDAPP mouse. Nature 400:173-177.

Scheuner D, Eckman C, Jensen M, Song X, Citron M, Suzuki N, Bird TD, Hardy J, Hutton M, Kukull W, Larson E, Levy-Lahad E, Viitanen M, Peskind E, Poorkaj P, Schellenberg G, Tanzi R, Wasco W, Lannfelt L, Selkoe D, Younkin S.1996.Secreted amyloid beta-protein similar to that in the senile plaques of Alzheimer's disease is increased in vivo by the presenilin 1 and 2 and APP mutations linked to familial Alzheimer's disease. Nat Med 2:864-870.

Schmidt AM, Yan SD, Yan SF, Stern DM.2000.The biology of the receptor for advanced glycation end products and its ligands. Biochim Biophys Acta 1498:99-111.

Schummers J, Yu H, Sur M.2008.Tuned responses of astrocytes and their influence on hemodynamic signals in the visual cortex. Science 320:1638-1643.

Scudiero DA, Shoemaker RH, Paull KD, Monks A, Tierney S, Nofziger TH, Currens MJ, Seniff D, Boyd MR.1988.Evaluation of a soluble tetrazolium/formazan assay for cell growth and drug sensitivity in culture using human and other tumor cell lines. Cancer Res 48:4827-4833.

Seabrook GR, Smith DW, Bowery BJ, Easter A, Reynolds T, Fitzjohn SM, Morton RA, Zheng H, Dawson GR, Sirinathsinghji DJ, Davies CH, Collingridge GL, Hill RG.1999.Mechanisms contributing to the deficits in hippocampal synaptic plasticity in mice lacking amyloid precursor protein. Neuropharmacology 38:349-359.

Selkoe DJ.1994.Cell biology of the amyloid beta-protein precursor and the mechanism of Alzheimer's disease. Annu Rev Cell Biol 10:373-403.

Selkoe DJ.2000.Toward a comprehensive theory for Alzheimer's disease. Hypothesis: Alzheimer's disease is caused by the cerebral accumulation and cytotoxicity of amyloid beta-protein. Ann N Y Acad Sci 924:17-25.

Selkoe DJ.2003.Folding proteins in fatal ways. Nature 426:900-904.

Selkoe DJ.2004.Alzheimer disease: mechanistic understanding predicts novel therapies. Ann Intern Med 140:627-638.

Selkoe DJ.2011.Alzheimer's disease. Cold Spring Harb Perspect Biol 3.

Selkoe DJ, Podlisny MB.2002.Deciphering the genetic basis of Alzheimer's disease. Annu Rev Genomics Hum Genet 3:67-99.

Senechal Y, Kelly PH, Dev KK.2008.Amyloid precursor protein knockout mice show age-dependent deficits in passive avoidance learning. Behav Brain Res 186:126-132.

Serpell LC, Smith JM.2000.Direct visualisation of the beta-sheet structure of synthetic Alzheimer's amyloid. J Mol Biol 299:225-231.

Serpell LC, Blake CC, Fraser PE.2000.Molecular structure of a fibrillar Alzheimer's A beta fragment. Biochemistry 39:13269-13275.

Serrano-Pozo A, Mielke ML, Gomez-Isla T, Betensky RA, Growdon JH, Frosch MP, Hyman BT.2011.Reactive Glia not only Associates with Plaques but also Parallels Tangles in Alzheimer's Disease. Am J Pathol.

Seubert P, Vigo-Pelfrey C, Esch F, Lee M, Dovey H, Davis D, Sinha S, Schlossmacher M, Whaley J, Swindlehurst C, et al.1992.Isolation and quantification of soluble Alzheimer's beta-peptide from biological fluids. Nature 359:325-327.

Seubert P, Oltersdorf T, Lee MG, Barbour R, Blomquist C, Davis DL, Bryant K, Fritz LC, Galasko D, Thal LJ, et al.1993.Secretion of beta-amyloid precursor protein cleaved at the amino terminus of the beta-amyloid peptide. Nature 361:260-263.

Shankar GM, Bloodgood BL, Townsend M, Walsh DM, Selkoe DJ, Sabatini BL.2007.Natural oligomers of the Alzheimer amyloid-beta protein induce reversible synapse loss by modulating an NMDA-type glutamate receptor-dependent signaling pathway. J Neurosci 27:2866-2875.

Shankar GM, Li S, Mehta TH, Garcia-Munoz A, Shepardson NE, Smith I, Brett FM, Farrell MA, Rowan MJ, Lemere CA, Regan CM, Walsh DM, Sabatini BL, Selkoe

DJ.2008.Amyloid-beta protein dimers isolated directly from Alzheimer's brains impair synaptic plasticity and memory. Nat Med 14:837-842.

Sherman MY, Goldberg AL.2001.Cellular defenses against unfolded proteins: a cell biologist thinks about neurodegenerative diseases. Neuron 29:15-32.

Shimizu E, Kawahara K, Kajizono M, Sawada M, Nakayama H.2008.IL-4-induced selective clearance of oligomeric beta-amyloid peptide(1-42) by rat primary type 2 microglia. J Immunol 181:6503-6513.

Shivaprasad S, Wetzel R.2006.Analysis of amyloid fibril structure by scanning cysteine mutagenesis. Methods Enzymol 413:182-198.

Shoji M, Golde TE, Ghiso J, Cheung TT, Estus S, Shaffer LM, Cai XD, McKay DM, Tintner R, Frangione B, et al.1992.Production of the Alzheimer amyloid beta protein by normal proteolytic processing. Science 258:126-129.

Simard AR, Rivest S.2004.Bone marrow stem cells have the ability to populate the entire central nervous system into fully differentiated parenchymal microglia. Faseb J 18:998-1000.

Simard AR, Soulet D, Gowing G, Julien JP, Rivest S.2006.Bone marrow-derived microglia play a critical role in restricting senile plaque formation in Alzheimer's disease. Neuron 49:489-502.

Sisodia SS, Koo EH, Beyreuther K, Unterbeck A, Price DL.1990.Evidence that beta-amyloid protein in Alzheimer's disease is not derived by normal processing. Science 248:492-495.

Sondag CM, Dhawan G, Combs CK.2009.Beta amyloid oligomers and fibrils stimulate differential activation of primary microglia. J Neuroinflammation 6:1.

Soreghan B, Kosmoski J, Glabe C.1994.Surfactant properties of Alzheimer's A beta peptides and the mechanism of amyloid aggregation. J Biol Chem 269:28551-28554.

Spillantini MG, Crowther RA, Kamphorst W, Heutink P, van Swieten JC.1998.Tau pathology in two Dutch families with mutations in the microtubule-binding region of tau. Am J Pathol 153:1359-1363.

Stalder M, Phinney A, Probst A, Sommer B, Staufenbiel M, Jucker M.1999.Association of microglia with amyloid plaques in brains of APP23 transgenic mice. Am J Pathol 154:1673-1684.

Stewart CR, Stuart LM, Wilkinson K, van Gils JM, Deng J, Halle A, Rayner KJ, Boyer L, Zhong R, Frazier WA, Lacy-Hulbert A, El Khoury J, Golenbock DT, Moore KJ.2010.CD36 ligands promote sterile inflammation through assembly of a Toll-like receptor 4 and 6 heterodimer. Nat Immunol 11:155-161.

Stine WB, Jr., Dahlgren KN, Krafft GA, LaDu MJ.2003.In vitro characterization of conditions for amyloid-beta peptide oligomerization and fibrillogenesis. J Biol Chem 278:11612-11622.

Stoltzner SE, Grenfell TJ, Mori C, Wisniewski KE, Wisniewski TM, Selkoe DJ, Lemere CA.2000.Temporal accrual of complement proteins in amyloid plaques in Down's syndrome with Alzheimer's disease. Am J Pathol 156:489-499.

Storm DR, Rosenthal KS, Swanson PE.1977.Polymyxin and related peptide antibiotics. Annu Rev Biochem 46:723-763.

Strittmatter WJ, Weisgraber KH, Huang DY, Dong LM, Salvesen GS, Pericak-Vance M, Schmechel D, Saunders AM, Goldgaber D, Roses AD.1993.Binding of human apolipoprotein E to synthetic amyloid beta peptide: isoform-specific effects and implications for late-onset Alzheimer disease. Proc Natl Acad Sci U S A 90:8098-8102.

Strohmeyer R, Shen Y, Rogers J.2000.Detection of complement alternative pathway mRNA and proteins in the Alzheimer's disease brain. Brain Res Mol Brain Res 81:7-18.

Sunde M, Blake C.1997.The structure of amyloid fibrils by electron microscopy and X-ray diffraction. Adv Protein Chem 50:123-159.

Suzuki N, Cheung TT, Cai XD, Odaka A, Otvos L, Jr., Eckman C, Golde TE, Younkin SG.1994.An increased percentage of long amyloid beta protein secreted by familial amyloid beta protein precursor (beta APP717) mutants. Science 264:1336-1340.

Tagliavini F, Giaccone G, Frangione B, Bugiani O.1988.Preamyloid deposits in the cerebral cortex of patients with Alzheimer's disease and nondemented individuals. Neurosci Lett 93:191-196.

Tarkowski E, Blennow K, Wallin A, Tarkowski A.1999.Intracerebral production of tumor necrosis factor-alpha, a local neuroprotective agent, in Alzheimer disease and vascular dementia. J Clin Immunol 19:223-230.

Tesseur I, Zou K, Esposito L, Bard F, Berber E, Can JV, Lin AH, Crews L, Tremblay P, Mathews P, Mucke L, Masliah E, Wyss-Coray T.2006.Deficiency in neuronal TGF-beta signaling promotes neurodegeneration and Alzheimer's pathology. J Clin Invest 116:3060-3069.

Thies W, Bleiler L.2011.2011 Alzheimer's disease facts and figures. Alzheimers Dement 7:208-244.

Tiffany HL, Lavigne MC, Cui YH, Wang JM, Leto TL, Gao JL, Murphy PM.2001.Amyloid-beta induces chemotaxis and oxidant stress by acting at formylpeptide receptor 2, a G protein-coupled receptor expressed in phagocytes and brain. J Biol Chem 276:23645-23652.

Tjernberg LO, Naslund J, Lindqvist F, Johansson J, Karlstrom AR, Thyberg J, Terenius L, Nordstedt C.1996.Arrest of beta-amyloid fibril formation by a pentapeptide ligand. J Biol Chem 271:8545-8548.

Tsai J, Grutzendler J, Duff K, Gan WB.2004.Fibrillar amyloid deposition leads to local synaptic abnormalities and breakage of neuronal branches. Nat Neurosci 7:1181-1183.

Tycko R.2011.Solid-state NMR studies of amyloid fibril structure. Annu Rev Phys Chem 62:279-299.

Tycko R, Sciarretta KL, Orgel JP, Meredith SC.2009.Evidence for novel beta-sheet structures in Iowa mutant beta-amyloid fibrils. Biochemistry 48:6072-6084.

Tzounopoulos T, Kim Y, Oertel D, Trussell LO.2004.Cell-specific, spike timing-dependent plasticities in the dorsal cochlear nucleus. Nat Neurosci 7:719-725.

Udan ML, Ajit D, Crouse NR, Nichols MR.2008.Toll-like receptors 2 and 4 mediate Abeta(1-42) activation of the innate immune response in a human monocytic cell line. J Neurochem 104:524-533.

Veerhuis R, Janssen I, De Groot CJ, Van Muiswinkel FL, Hack CE, Eikelenboom P.1999.Cytokines associated with amyloid plaques in Alzheimer's disease brain stimulate human glial and neuronal cell cultures to secrete early complement proteins, but not C1-inhibitor. Exp Neurol 160:289-299.

Vitek MP, Bhattacharya K, Glendening JM, Stopa E, Vlassara H, Bucala R, Manogue K, Cerami A.1994.Advanced glycation end products contribute to amyloidosis in Alzheimer disease. Proc Natl Acad Sci U S A 91:4766-4770.

von Koch CS, Zheng H, Chen H, Trumbauer M, Thinakaran G, van der Ploeg LH, Price DL, Sisodia SS.1997.Generation of APLP2 KO mice and early postnatal lethality in APLP2/APP double KO mice. Neurobiol Aging 18:661-669.

Wajant H, Pfizenmaier K, Scheurich P.2003.Tumor necrosis factor signaling. Cell Death Differ 10:45-65.

Wake H, Moorhouse AJ, Jinno S, Kohsaka S, Nabekura J.2009.Resting microglia directly monitor the functional state of synapses in vivo and determine the fate of ischemic terminals. J Neurosci 29:3974-3980.

Walker DG, Dalsing-Hernandez JE, Campbell NA, Lue LF.2009.Decreased expression of CD200 and CD200 receptor in Alzheimer's disease: a potential mechanism leading to chronic inflammation. Exp Neurol 215:5-19.

Walsh DM, Selkoe DJ.2007.A beta oligomers - a decade of discovery. J Neurochem 101:1172-1184.

Walsh DM, Lomakin A, Benedek GB, Condron MM, Teplow DB.1997.Amyloid beta-protein fibrillogenesis. Detection of a protofibrillar intermediate. J Biol Chem 272:22364-22372.

Walsh DM, Tseng BP, Rydel RE, Podlisny MB, Selkoe DJ.2000.The oligomerization of amyloid beta-protein begins intracellularly in cells derived from human brain. Biochemistry 39:10831-10839.

Walsh DM, Klyubin I, Fadeeva JV, Cullen WK, Anwyl R, Wolfe MS, Rowan MJ, Selkoe DJ.2002.Naturally secreted oligomers of amyloid beta protein potently inhibit hippocampal long-term potentiation in vivo. Nature 416:535-539.

Walsh DM, Townsend M, Podlisny MB, Shankar GM, Fadeeva JV, El Agnaf O, Hartley DM, Selkoe DJ.2005.Certain inhibitors of synthetic amyloid beta-peptide (Abeta) fibrillogenesis block oligomerization of natural Abeta and thereby rescue long-term potentiation. J Neurosci 25:2455-2462.

Walsh DM, Hartley DM, Kusumoto Y, Fezoui Y, Condron MM, Lomakin A, Benedek GB, Selkoe DJ, Teplow DB.1999.Amyloid beta-protein fibrillogenesis. Structure and biological activity of protofibrillar intermediates. J Biol Chem 274:25945-25952.

Walter S, Letiembre M, Liu Y, Heine H, Penke B, Hao W, Bode B, Manietta N, Walter J, Schulz-Schuffer W, Fassbender K.2007.Role of the toll-like receptor 4 in neuroinflammation in Alzheimer's disease. Cell Physiol Biochem 20:947-956.

Wang Q, Wu J, Rowan MJ, Anwyl R.2005.Beta-amyloid inhibition of long-term potentiation is mediated via tumor necrosis factor. Eur J Neurosci 22:2827-2832.

Weggen S, Eriksen JL, Das P, Sagi SA, Wang R, Pietrzik CU, Findlay KA, Smith TE, Murphy MP, Bulter T, Kang DE, Marquez-Sterling N, Golde TE, Koo EH.2001.A subset of NSAIDs lower amyloidogenic Abeta42 independently of cyclooxygenase activity. Nature 414:212-216.

Weingarten MD, Lockwood AH, Hwo SY, Kirschner MW.1975.A protein factor essential for microtubule assembly. Proc Natl Acad Sci U S A 72:1858-1862.

Westlind-Danielsson A, Arnerup G.2001.Spontaneous in vitro formation of supramolecular beta-amyloid structures, "betaamy balls", by beta-amyloid 1-40 peptide. Biochemistry 40:14736-14743.

White JA, Manelli AM, Holmberg KH, Van Eldik LJ, Ladu MJ.2005.Differential effects of oligomeric and fibrillar amyloid-beta 1-42 on astrocyte-mediated inflammation. Neurobiol Dis 18:459-465.

Winship IR, Plaa N, Murphy TH.2007.Rapid astrocyte calcium signals correlate with neuronal activity and onset of the hemodynamic response in vivo. J Neurosci 27:6268-6272.

Wisniewski HM, Wegiel J, Wang KC, Kujawa M, Lach B.1989.Ultrastructural studies of the cells forming amyloid fibers in classical plaques. Can J Neurol Sci 16:535-542.

Wogulis M, Wright S, Cunningham D, Chilcote T, Powell K, Rydel RE.2005.Nucleation-dependent polymerization is an essential component of amyloid-mediated neuronal cell death. J Neurosci 25:1071-1080.

Wong PC, Cai H, Borchelt DR, Price DL.2002.Genetically engineered mouse models of neurodegenerative diseases. Nat Neurosci 5:633-639.

Wyss-Coray T, Masliah E, Mallory M, McConlogue L, Johnson-Wood K, Lin C, Mucke L.1997.Amyloidogenic role of cytokine TGF-beta1 in transgenic mice and in Alzheimer's disease. Nature 389:603-606.

Wyss-Coray T, Lin C, Yan F, Yu GQ, Rohde M, McConlogue L, Masliah E, Mucke L.2001.TGF-beta1 promotes microglial amyloid-beta clearance and reduces plaque burden in transgenic mice. Nat Med 7:612-618.

Yan SD, Chen X, Fu J, Chen M, Zhu H, Roher A, Slattery T, Zhao L, Nagashima M, Morser J, Migheli A, Nawroth P, Stern D, Schmidt AM.1996.RAGE and amyloid-beta peptide neurotoxicity in Alzheimer's disease. Nature 382:685-691.

Yao J, Harvath L, Gilbert DL, Colton CA.1990.Chemotaxis by a CNS macrophage, the microglia. J Neurosci Res 27:36-42.

Yates SL, Burgess LH, Kocsis-Angle J, Antal JM, Dority MD, Embury PB, Piotrkowski AM, Brunden KR.2000.Amyloid beta and amylin fibrils induce increases in proinflammatory cytokine and chemokine production by THP-1 cells and murine microglia. J Neurochem 74:1017-1025.

Yazawa H, Yu ZX, Takeda, Le Y, Gong W, Ferrans VJ, Oppenheim JJ, Li CC, Wang JM.2001.Beta amyloid peptide (Abeta42) is internalized via the G-protein-coupled receptor FPRL1 and forms fibrillar aggregates in macrophages. Faseb J 15:2454-2462.

Yoshiyama Y, Higuchi M, Zhang B, Huang SM, Iwata N, Saido TC, Maeda J, Suhara T, Trojanowski JQ, Lee VM.2007.Synapse loss and microglial activation precede tangles in a P301S tauopathy mouse model. Neuron 53:337-351.

Zempel H, Thies E, Mandelkow E, Mandelkow EM.2011.Abeta oligomers cause localized Ca(2+) elevation, missorting of endogenous Tau into dendrites, Tau phosphorylation, and destruction of microtubules and spines. J Neurosci 30:11938-11950.

Zheng WH, Bastianetto S, Mennicken F, Ma W, Kar S.2002.Amyloid beta peptide induces tau phosphorylation and loss of cholinergic neurons in rat primary septal cultures. Neuroscience 115:201-211.

VITA

Geeta S. Paranjape is the daughter of Subhash and Smita Paranjape. She was born in Dombivli, India, on October 19, 1982. She obtained her Bachelor's degree in Biochemistry from Ramanarain Ruia College, Mumbai, India in 2003. She obtained her Master's degree in Biotechnology from University of Mumbai, Mumbai, India in 2005. She joined Changu Kana Thakur College of Arts, Science and Commerce, New Panvel, India as a Lecturer in November 2005. In 2006, she was accepted into the graduate program of Department of Chemistry and Biochemistry in University of Missouri-St Louis (UMSL). She joined the laboratory of Dr Michael R. Nichols for her PhD research. In 2008, she earned MS in Chemistry from UMSL.